

This is to certify that the

thesis entitled

CRUSTAL THICKNESS OF NORTHEAST RUSSIA presented by

KEVIN G. MACKEY

has been accepted towa	ards fulfillment		
of the requirements for			
M.S.	GEOLOGICAL	SCIENCES	
degree ir	1		

Date____FEB. 29, 1996

MSU is an Affirmative Action/Equal Opportunity Institution

O-7639



PLACE IN RETURN BOX to remove this checkout from your record. TO AVOID FINES return on or before date due.

DATE DUE	DATE DUE	DATE DUE

MSU is An Affirmative Action/Equal Opportunity Institution

CRUSTAL THICKNESS OF NORTHEAST RUSSIA

Ву

Kevin George Mackey

A THESIS

Submitted to
Michigan State University
in partial fulfillment of the requirements
for the degree of

MASTER OF SCIENCE

Department of Geological sciences

1996

ABSTRACT

CRUSTAL THICKNESS OF NORTHEAST RUSSIA

By

Kevin G. Mackey

The first order crustal structure of the Magadan region and northeast Sakha Republic (Yakutia), northeast Russia, is obtained by simultaneously inverting for origin times and travel time curves. As an average, a 37 km thick, 5.992±0.007 km/sec crust overlying an 7.961±0.015 km/sec mantle provides an excellent fit to phase data listed in the *Materialy po Seismichnosti Sibiri* bulletin. Travel-time curves for individual stations are very close to this average, though there are some variations in both crustal thickness and velocities; upper mantle velocities and crustal thickness appear to increase along the southern edge of the Okhotsk-Chukotka volcanic belt and decrease in the upper Kolyma River basin and along the trace of the proposed Moma Rift. Crustal thickness is greatest at Khandyga, on the Siberian platform, and lowest at Yubileniya, which may lie within the currently active Laptev Sea rift system.

ACKNOWLEDGEMENTS

First, I would like to thank Kaz Fujita for all the support and guidance over the past two years, without which this project would not have seen completion. Secondly, I would like to thank my parents for their love, support, and understanding during the past several years. A million thanks to Trent Faust who slaved for weeks typing and checking phase data used in this study (I'm glad I did not have to do all of it). Dr. Larry Ruff deserves credit and thanks for the use of, and assistance with 'SOUINT', his traveltime inversion program. The University of Michigan Seismological Observatory provided the computer resources for running 'SQUINT'. I thank Boris Koz'min and Dima Gunbin for station information and discussions of data processing methods used in the former Soviet Union. I also thank the Yakut Science Center and World Data Center B for providing seismological bulletins. Thanks to Boris Koz'min from Yakutsk, and Valentin Kovalev from Magadan, who provided earthquake data and helpful comments on their respective regions. Thanks to David Stone, Pavel Minyuk, Valentin Kovalev, the Gunbin family, and the Koz'min family who made my stay in Russia educational, eventful, and fun. Larun Izmailov was especially helpful in Magadan with Russian Customs, and in getting me the nicest hotel room in the city (sorry Kaz). I thank Bill Cambray and Hugh Bennett for stimulating discussions and serving on my guidance committee. I also thank Tom Vogel for discussion on some of my ideas. Diane Baclawski, the librarian has been most helpful in finding sources for research. I thank Steve Riegel and all those before me for building the foundation for this study. Many thanks to Diane and Cliff Gray, who

provided transportation and a different perspective of Fairbanks. Thanks to Michelle, who has done a great job of keeping me sane. This work is part of an ongoing cooperative research program between the University of Alaska Fairbanks, Michigan State University, the Yakut Institute of Geological Sciences, and the Magadan Experimental Methodological Seismological Division to study the tectonics and seismicity of northeast Russia. This project was funded by the Incorporated Research Institutions for Seismology Joint Seismic Program (IRIS-JSP), and by National Science Foundation (NSF) grants OPP #92-24193 and OPP #94-24139. Additional funding and support for this project and myself was provided by a Michigan State University teaching assistantship, the Michigan State University College of Natural Sciences, the University of Alaska Geophysical Institute, and the Scottish Rite Masons.

TABLE OF CONTENTS

LIST OF TABLES	vi
LIST OF FIGURES	vii
INTRODUCTION	1
PREVIOUS STUDIES	8
METHODOLOGY AND REGIONAL CRUSTAL MODEL	14
INDIVIDUAL STATIONS	41
DISCUSSION	79
CONCLUSIONS	85
APPENDIX A	87
APPENDIX B	95
BIBLIOGRAPHY	98

LIST OF TABLES

Table 1.	New origin times and time shifts from inversion for best 75 events	36
Table 2.	Comparison of crustal thicknesses determined in this and other studies	42
Table 3.	Comparison of seismic velocities determined in this and other studies	43

LIST OF TABLES

Table 1.	New origin times and time shifts from inversion for best 75 events	36
Table 2.	Comparison of crustal thicknesses determined in this and other studies	42
Table 3.	Comparison of seismic velocities determined in this and other studies	43

LIST OF FIGURES

Figure 1.	Tectonic setting of northeast Russia and boundaries of	
	study area	2
Figure 2.	Seismic activity of northeast Russia	3
Figure 3.	Moma rift system map	5
Figure 4.	Laptev Sea rift system map	6
Figure 5.	Magadan-Kolyma DSS profile	9
Figure 6.	Crustal structure map from study by Suvorov and Kornilova (1986)	11
Figure 7.	Seismic stations and epicenters of earthquakes used in the study	15
Figure 8.	Change in relocated epicenters vs. year	17
Figure 9.	Change in Pg phase relocated epicenters vs. azimuth	19
Figure 10.	Change in Pn phase relocated epicenters vs. azimuth	20
Figure 11	Simplified fault map of the central and southern portions of the study area.	21
Figure 12.	Distribution of selected 75 events used in the study	23
Figure 13.	Pg, and Pn data plotted using Materialy reported epicenters	25
Figure 14.	Pg, and Pn data plotted using relocated epicenters	26
Figure 15.	Sg, and Sn data plotted using Materialy reported epicenters	27
Figure 16.	Sg, and Sn data plotted using relocated epicenters	28
Figure 17.	Change in Pg phase relocated epicenters vs. azimuth for best 75 events	30

LIST OF FIGURES

Figure 1.	Tectonic setting of northeast Russia and boundaries of study area	2
Figure 2.	Seismic activity of northeast Russia	3
Figure 3.	Moma rift system map	5
Figure 4.	Laptev Sea rift system map	6
Figure 5.	Magadan-Kolyma DSS profile	9
Figure 6.	Crustal structure map from study by Suvorov and Kornilova (1986)	11
Figure 7.	Seismic stations and epicenters of earthquakes used in the study	15
Figure 8.	Change in relocated epicenters vs. year	17
Figure 9.	Change in Pg phase relocated epicenters vs. azimuth	19
Figure 10.	Change in Pn phase relocated epicenters vs. azimuth	20
Figure 11	Simplified fault map of the central and southern portions of the study area.	21
Figure 12.	Distribution of selected 75 events used in the study	23
Figure 13.	Pg, and Pn data plotted using Materialy reported epicenters	25
Figure 14.	Pg, and Pn data plotted using relocated epicenters	26
Figure 15.	Sg, and Sn data plotted using Materialy reported epicenters	27
Figure 16.	Sg, and Sn data plotted using relocated epicenters	28
Figure 17.	Change in Pg phase relocated epicenters vs. azimuth for best 75 events	30

LIST OF FIGURES (continued)

Figure 18.	Movement of relocated epicenters away from bulk of receiving stations	31
Figure 19.	Pg, and Pn data after initial inversion	33
Figure 20.	PG, and Pn data inverted after removal of erroneous arrivals	34
Figure 21.	Regional travel time curve	39
Figure 22.	Station Magadan data	44
Figure 23.	Station Takhtoyamsk data	45
Figure 24.	Station Stekolnyi data	48
Figure 25.	Station Debin data	49
Figure 26.	Station Myakit data	50
Figure 27.	Station Omsukchan data	51
Figure 28.	Station Seimchan data	52
Figure 29.	Station Sinegor'e data	53
Figure 30.	Station Talaya data	55
Figure 31.	Station Kulu data	56
Figure 32.	Station Susuman data	57
Figure 33.	Station Nelkoba data	58
Figure 34.	Station Ust' Omchug data	59
Figure 35.	Station Ust' Nera data	61
Figure 36.	Station Moma data	61
Figure 37.	Station Sasyr data	64

LIST OF FIGURES (continued)

Figure 38.	Station Zyryanka data	65
Figure 39.	Station Tabalakh data	66
Figure 40.	Station Batagai data	67
Figure 41.	Station Saidy data	68
Figure 42.	Station Naiba data	69
Figure 43.	Station Yubileniya data	71
Figure 44.	Station Tenkeli data	72
Figure 45.	Station Yakutsk data	73
Figure 46.	Station Khandyga data	74
Figure 47.	Station Nezhdaninskoe data	75
Figure 48.	Station Evensk data	77
Figure 49.	Station Omolon data	78
Figure 50.	Distribution of crustal thickness	80
Figure 51.	Gravity anomaly map	83
Figure 52.	Heat flow level map	84

Introduction

In this study the first order variations in crustal structure in northeast Russia are investigated using seismic wave travel time data from regional seismic events published in Russian seismic bulletins. Northeastern Russia is a region presently under compression and uplift as a result of the convergence of the North American and Eurasian plates (e.g., Naimark, 1976; Cook et al., 1986; Riegel et al., 1993). This region is composed of a series of exotic terranes which accreted in the Mesozoic (e.g., Parfenov, 1991) and then participated in an apparently extensional episode in the Pliocene which resulted in the formation of the Moma rift system (Grachev, 1973; Fujita et al., 1990a). This study is confined to the areas best covered by the Magadan and northern Yakut regional seismic networks from the late 1970s to early 1990s. This region lies approximately between 57-70°N and 125-163°E and includes the Chersky seismic belt (CSB), the eastern portion of the Siberian Platform, the Kolyma gold mining belt and the region around Magadan (Fig. 1; q.v., Koz'min, 1984; Parfenov et al., 1988; Fujita et al., 1990b). The study area is centered approximately at the junction between the North American plate, the Eurasian plate, and Okhotsk microplate or block. In the southern region, the Okhotsk microplate is undergoing deformation as it is compressed and extruded as a result of the convergence of the North American and Eurasian plates (Riegel et al., 1993; Riegel, 1994). The deformation within the Okhotsk block results in a geographically large area of seismic activity. Figure 2 shows the trends of microseismic activity within the study area. Microseismicity within the CSB is heaviest in the vicinity of Susuman; but levels may

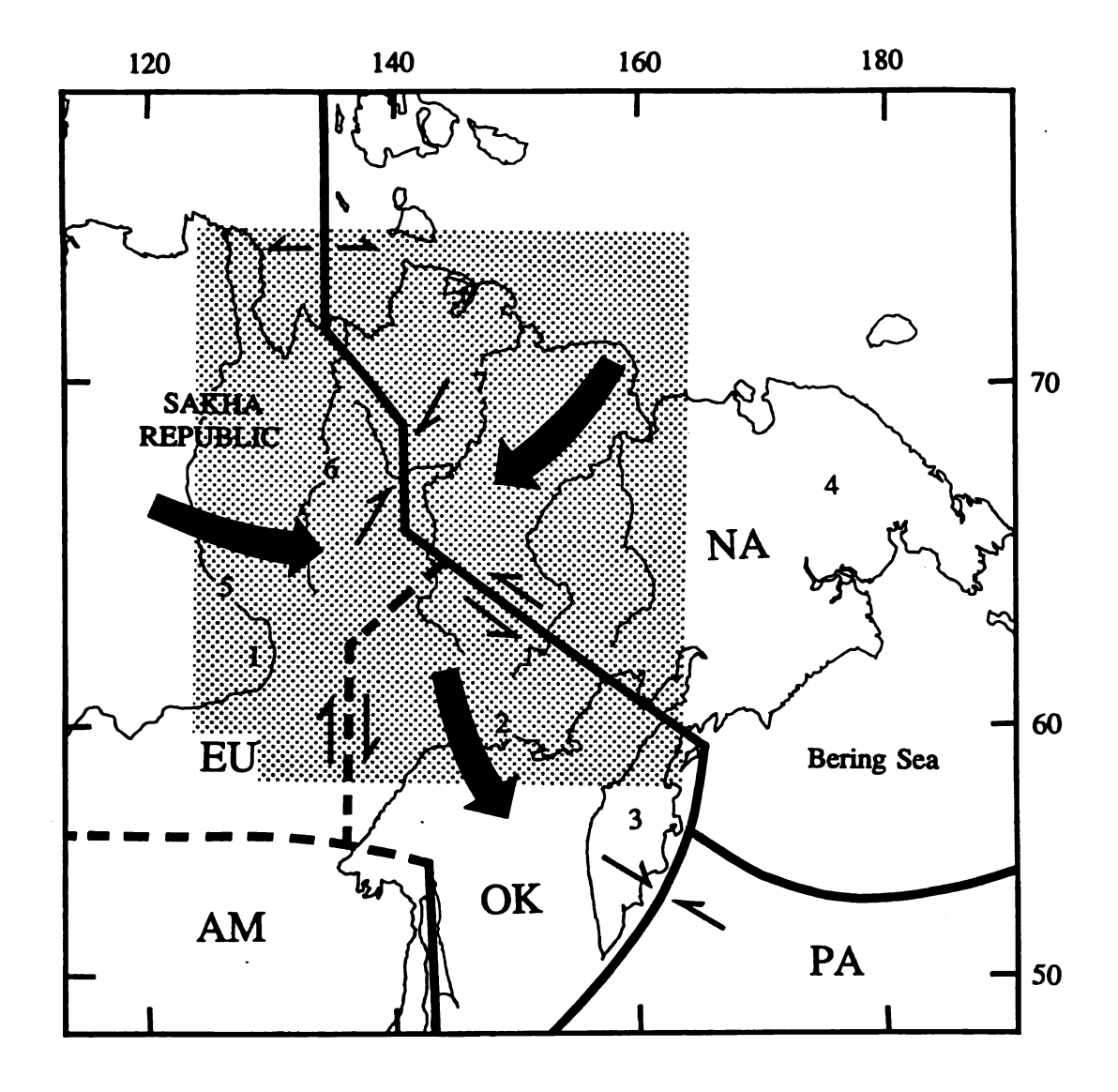


Figure 1. Plate configuration of northeast Russia, showing boundaries between the Eurasian (EU), North American (NA), Okhotsk (OK), Pacific (PA), and Amur (AM) plates. Solid lines denote established boundaries, while dashed represent diffuse or inferred. Large arrows represent relative motions between plates, and small show relative motion along individual boundaries. Stippled area covers the region considered in this study. 1 = Yakutsk, 2 = Magadan, 3 = Kamchatka Peninsula, 4 = Chukotka 5 = Lena River, 6 = Yana River. Adapted from Riegel (1994).

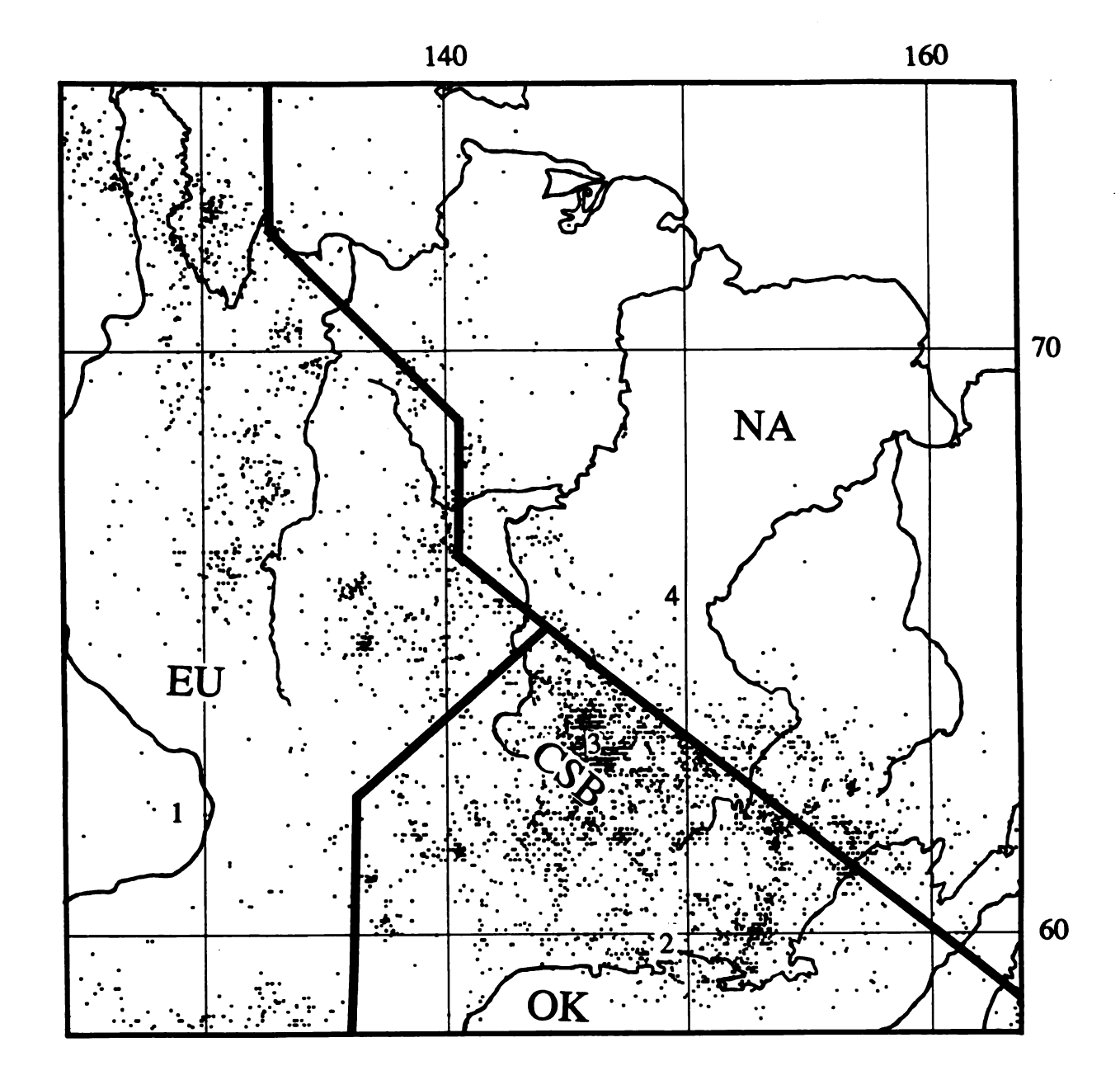


Figure 2. All known locatable seismicity within the study area. Seismicity shown ranges from approximately Mb = 2.0 to greater than 6.0. Seismicity is due to interaction between the North American (NA), Eurasian (EU), and Okhotsk (OK) plates. Highly seismic area represents the Cherskii Seismic Belt (CSB). 1 = Yakutsk, 2 = Magadan, 3 = Susuman, 4 = Zyryanka. Data from *Materialy Po Seismichnosti Sibiri*, years 1976-1991, and *Zemletryaseniya V SSSR*, years 1962-1989. Additional data supplied by B. Koz'min for Sakha Republic (Yakutia; personal communication, 1994), and L. Gunbina for Magadan (personal communication, 1995).

be inflated due to mining. Since the mid 1960s, when seismic networks were first opened in the area, approximately 5,000 CSB earthquakes have been catalogued and located. North of the CSB, microseismicity declines rapidly. This may be partially due to station distribution, but Riegel (1994) notes that the installation of a station at Zyryanka (Fig. 2) has not altered the microseismicity distribution.

The central portion of the study area is currently under transpression along the North American and Eurasian plate boundaries. However, in the Pliocene this region apparently underwent extension, forming the Moma rift system (Fig. 3). Within the past 0.5 m.y., the pole of rotation for the NA-EU plate is suggested to have moved north and extensional activity along the Moma rift cease (Cook et al., 1986). The northern portion of the study area includes the Laptev Sea rift system. The Laptev Sea rift system is the extension of the Arctic Mid-Ocean Ridge onto the Siberian continental shelf, expressed as a system of grabens (Fig. 4; Kim, 1986; Fujita et al., 1990a). Within the Laptev Sea rift system, Kim (1986) suggests the Omoloi graben is the presently active zone of extension. Drachev (1994) indicates extensional features throughout the southern portions of the Laptev Sea. Microseismicity levels are highest along the southern edge of the South Laptev basin (Fig. 4), although larger events are located both here and along the Omoloi graben. Fewer microseismic locations in the Omoloi graben is likely a result of seismic station distribution. The western portion of the study area contains the eastern portions of the Siberian platform. The Siberian platform generally consists of a flat lying Precambrian basement overlain by a few kilometers of Riphean, Cambrian, and Jurassic sedimentary materials (Parfenov, 1991). Topographically, the Siberian platform is

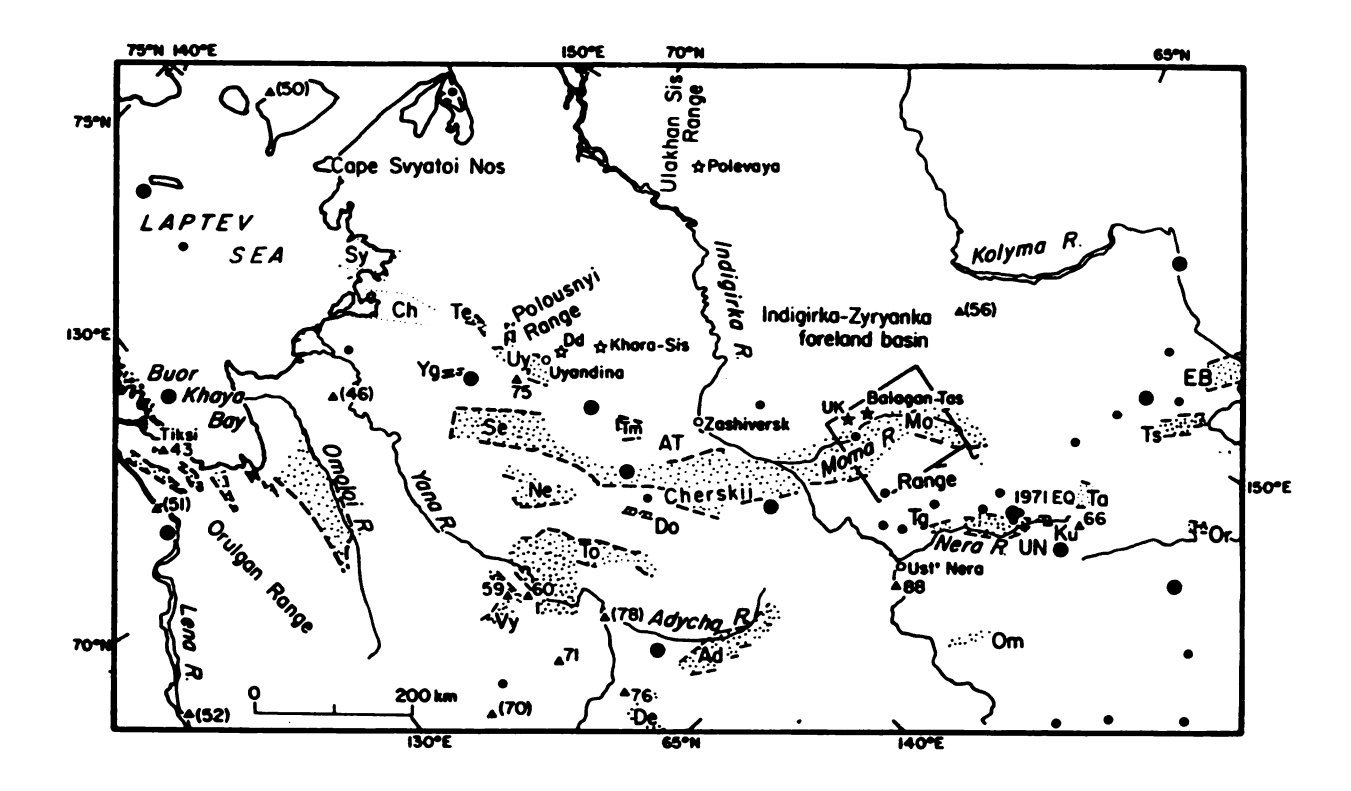


Figure 3. Map of the Moma rift system. Dashed lines show faults bounding grabens and half grabens, dotted where based on geophysical data. Cenozoic basins are stippled. AT denotes the Andrei Tas Range; UK the Uraga-Khaya dome and Dd the D'akhtardaakh volcano. Other letter pairs label grabens: Ad=Adycha; Ch=Chondon; De=Derbeke; Do=Dogdo (Darpir); EB=El'gen (Seimchan) - Buyunda; Ku=Khudzakh; Mo=Moma; Ne=Nenneli; Om=Oimyakon; Or=Orotuk; Se=Selennyakh; Sy=Sellyakh Gulf; Ta=Talon; Te=Tenkeli; Tg=Tagyn'ya; Tm=Tommot; To=Toustakh; Ts=Taskan; UN=Upper Nera; Uy=Uyandina; Vy=Verkhoyansk (Upper Yana). Dots denote teleseismic earthquakes. Triangles represent heat flow measurements in mW/m². Stars indicate volcanoes: white for Late Cenozoic, black for Quaternary. From Fujita et al. (1990a).

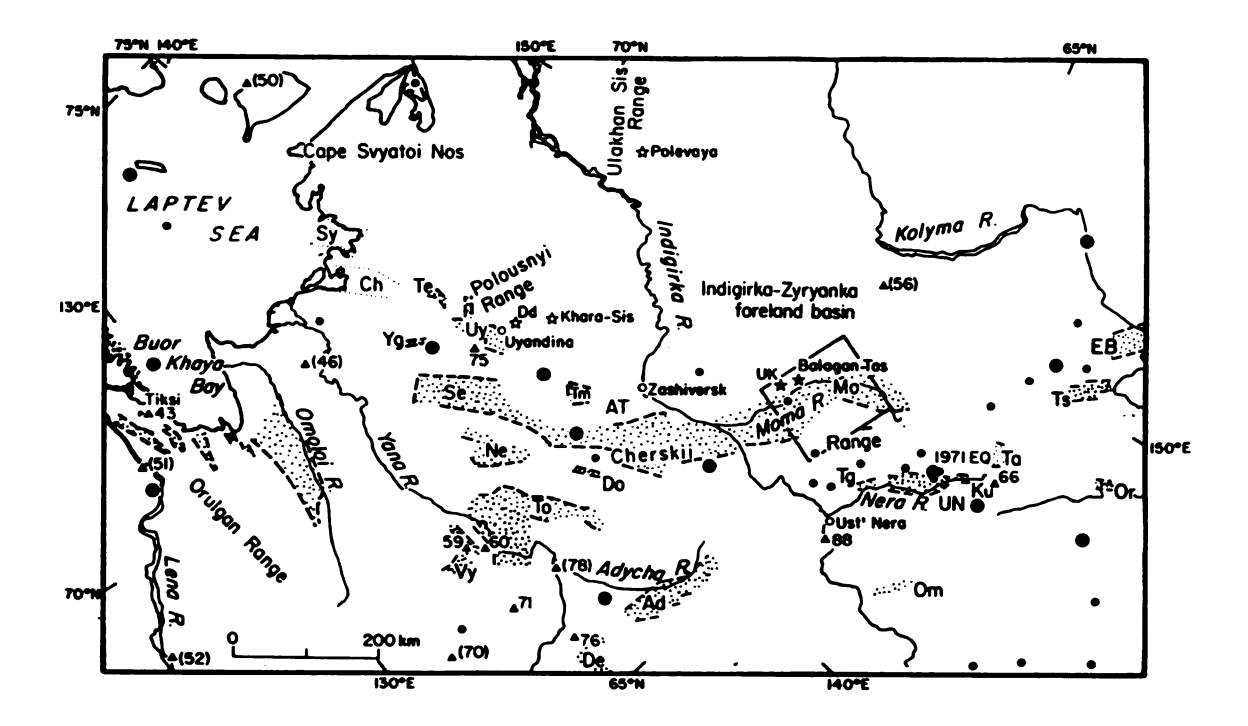


Figure 3. Map of the Moma rift system. Dashed lines show faults bounding grabens and half grabens, dotted where based on geophysical data. Cenozoic basins are stippled. AT denotes the Andrei Tas Range; UK the Uraga-Khaya dome and Dd the D'akhtardaakh volcano. Other letter pairs label grabens: Ad=Adycha; Ch=Chondon; De=Derbeke; Do=Dogdo (Darpir); EB=El'gen (Seimchan) - Buyunda; Ku=Khudzakh; Mo=Moma; Ne=Nenneli; Om=Oimyakon; Or=Orotuk; Se=Selennyakh; Sy=Sellyakh Gulf; Ta=Talon; Te=Tenkeli; Tg=Tagyn'ya; Tm=Tommot; To=Toustakh; Ts=Taskan; UN=Upper Nera; Uy=Uyandina; Vy=Verkhoyansk (Upper Yana). Dots denote teleseismic earthquakes. Triangles represent heat flow measurements in mW/m². Stars indicate volcanoes: white for Late Cenozoic, black for Quaternary. From Fujita et al. (1990a).

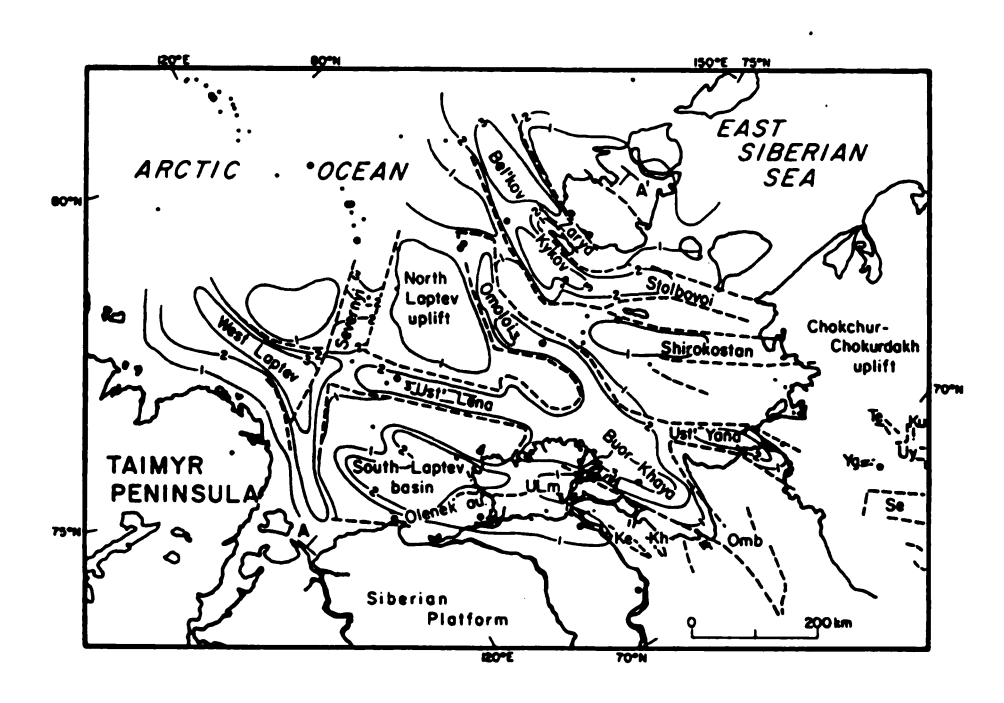


Figure 4. Map of the Laptev Sea rift system. Dashed lines indicate faults, primarily geophysically determined, and contours are for sediment thickness in km. Two letter abbreviations denote Cenozoic grabens: Ke=Kengdei; Kh=Khopto; Ku=Keranak; Se=Selennyakh; Te=Tenkeli; Uy=Uyandina; Yg=Yglan. Omb identifies the Omoloi basin. From Fujita et al. (1990a).

....

relatively flat.

Considering the regional tectonics, the crustal structure of the study area is expected to be very complex. Due to its general inaccessibility, however, few seismic studies have been conducted in northeast Russia; the few available studies are based on isolated seismic refraction profiles, converted phases, and differential travel-times. None of the long-distance refraction lines conducted throughout the Siberian platform reached (Razinkova, 1987) this area. Thus, the crustal structure is poorly known and some of the studies have resulted in contradictory results. The resolution of crustal thickness in this area contributes to the understanding of the present-day tectonics of the area, the extent of rifting during the development of the Pliocene Moma rift, and on the nature of the North America-Eurasia plate boundary.

In addition to the resolution of crustal thickness in northeast Russia, this study was also used to test the 'SQUINT' traveltime inversion program with application to a wide network. The 'SQUINT' program was originally developed for use with a small local network, and has never been applied to a large area with a regional network (Ruff et al., 1994).

The Chersky seismic belt region was selected for study because of the relatively dense network of seismic stations, which should result in better focal parameters, the great number of earthquakes, and the presence of a 350 km long, deep-seismic sounding (DSS; refraction) line conducted in 1959 between Magadan and Ust' Srednikan on the Kolyma River (Magadan-Kolyma DSS profile; Davydova et al., 1968; Ansimov et al., 1967). This line can be used to calibrate crustal studies.

PREVIOUS STUDIES

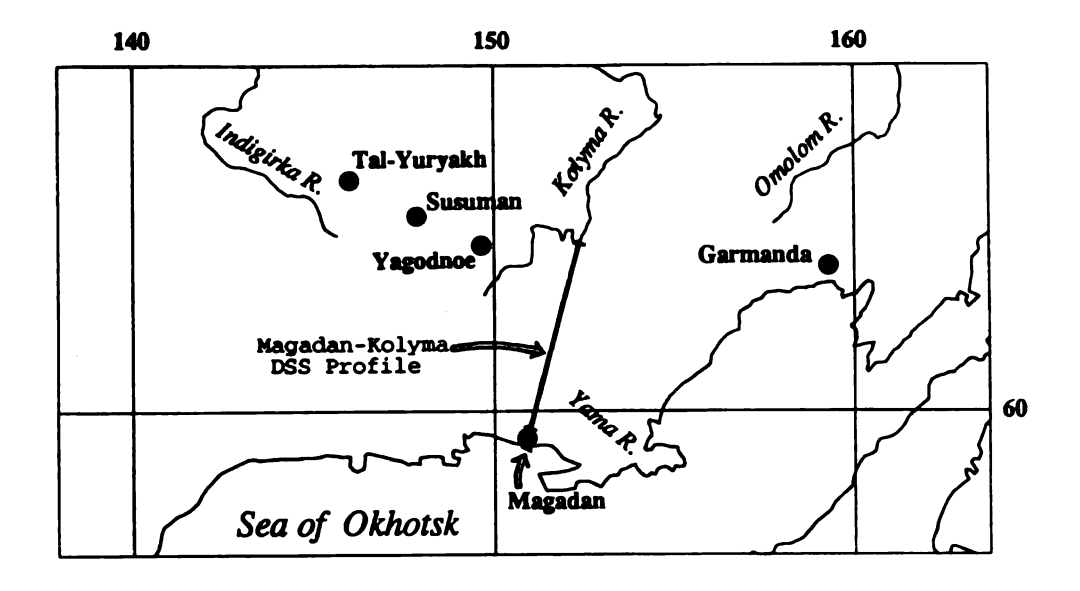
Several previous studies have considered this region. The earliest study of large scale crustal structure in this region was the Magadan-Kolyma Deep Seismic Sounding (DSS) profile conducted in 1959. This profile was conducted along the Magadan - Ust' Srednikan highway for a total distance of 350 km between end shot points with observations covering 156 km (Fig. 5). The profile indicates a crustal thickness of 31 km near Stekolnyi increasing to 38 km in the north (Davydova et al., 1968; Ansimov et al., 1967). According to Ansimov et al. (1967), the profile shows a 15 km thick granitic layer with velocities ranging from 6.0 km/sec to 6.5 km/sec. Beneath the granitic layer lies a 15-16 km thick basaltic layer where velocities are between 6.5 km/sec and 7.0 km/sec (Ansimov et al., 1967). The Moho, with a velocity of 8.1 km/sec underlies the basaltic layer (Ansimov et al., 1967). Velocities shown on figure 5, also from Ansimov et al. (1967) are not consistent with his text. Unfortunately, no direct data is available beneath Magadan; however, by extrapolation with an offshore refraction line, a depth of 29-30 km is inferred (Fig. 5: Ansimov et al., 1967).

The most comprehensive crustal structure study in the area was by Suvorov and Kornilova (1986). This study used Russian bulletin data and travel time differences between seismic stations for common events to study crustal thickness and crustal and mantle velocities. Their method initially assumes a homogeneous crustal strata and that the refracted phase for individual events travels along a flat underlying boundary (Suvorov and Kornilova, 1985). Consistent changes in travel times for certain regions

PREVIOUS STUDIES

Several previous studies have considered this region. The earliest study of large scale crustal structure in this region was the Magadan-Kolyma Deep Seismic Sounding (DSS) profile conducted in 1959. This profile was conducted along the Magadan - Ust' Srednikan highway for a total distance of 350 km between end shot points with observations covering 156 km (Fig. 5). The profile indicates a crustal thickness of 31 km near Stekolnyi increasing to 38 km in the north (Davydova et al., 1968; Ansimov et al., 1967). According to Ansimov et al. (1967), the profile shows a 15 km thick granitic layer with velocities ranging from 6.0 km/sec to 6.5 km/sec. Beneath the granitic layer lies a 15-16 km thick basaltic layer where velocities are between 6.5 km/sec and 7.0 km/sec (Ansimov et al., 1967). The Moho, with a velocity of 8.1 km/sec underlies the basaltic layer (Ansimov et al., 1967). Velocities shown on figure 5, also from Ansimov et al. (1967) are not consistent with his text. Unfortunately, no direct data is available beneath Magadan; however, by extrapolation with an offshore refraction line, a depth of 29-30 km is inferred (Fig. 5: Ansimov et al., 1967).

The most comprehensive crustal structure study in the area was by Suvorov and Kornilova (1986). This study used Russian bulletin data and travel time differences between seismic stations for common events to study crustal thickness and crustal and mantle velocities. Their method initially assumes a homogeneous crustal strata and that the refracted phase for individual events travels along a flat underlying boundary (Suvorov and Kornilova, 1985). Consistent changes in travel times for certain regions



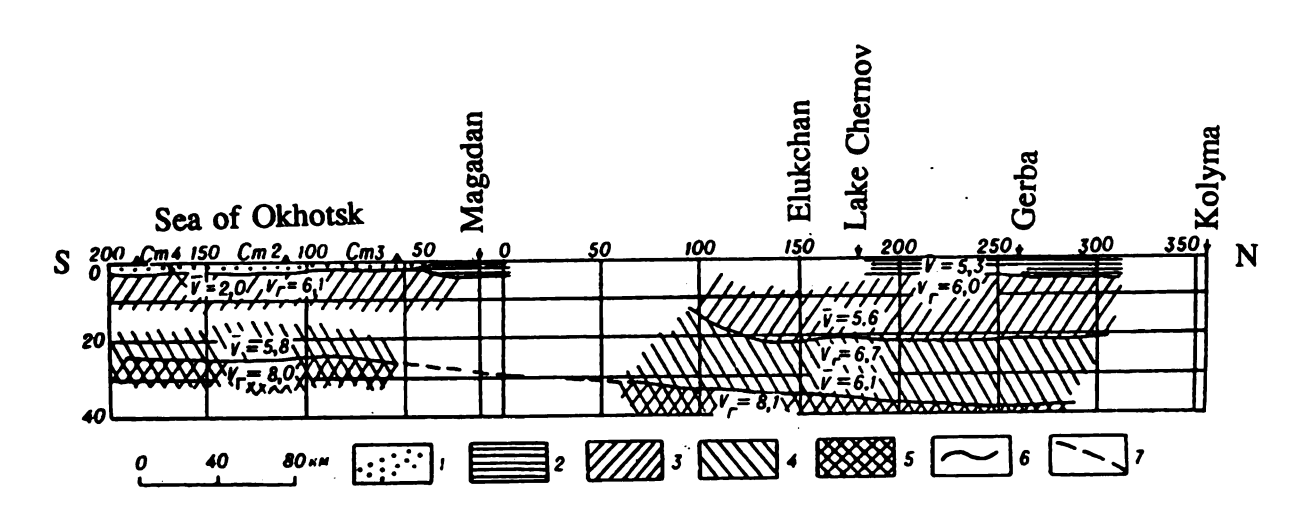


Figure 5. The Magadan-Kolyma Deep Seismic Sounding (DSS) profile and location map. Left portion of figure shows a portion of a DSS profile from the sea of Okhotsk. Magadan is located at the 0 km point. 1 - sediments with velocities up to 2.5 km/sec; 2 - sediments with velocities from 2.5 km/sec to 6.0 km/sec; 3 - granitic layer with velocities from 6.0 km/sec to 6.5 km/sec; basaltic layer with velocities from 6.5 km/sec to 7.0 km/sec; 5 - subcrustal layer with velocities above 8.0 km/sec; 6 - deep boundaries according to DSS data; 7 - deep boundaries in region of interpolation. From Ansimov et al. (1967).

1

Si

ar

te

S

fo

Si

in

5).

indicate variations in crustal thickness and seismic velocities. Their results suggest crustal thicknesses increasing toward the east and west edges of this study area (24 km at Ust' Nera to 38 km at Omsukchan in the east, and 44 km at Khandyga in the west), and upper mantle velocities of 7.9 to 8.1 km/sec, with the higher values predominantly in the east and west (Fig. 6). Their results are consistent with a significant Pliocene rifting episode resulting in an elevated and lower velocity upper mantle; this result is supported by the surface wave polarization study of Lander (1984) which concludes that there is anomalous mantle under the Chersky Range. Suvorov and Kornilova (1986) also conclude that crustal (Pg) velocities are between 5.8 and 6.2 km/sec.

Crustal studies using P to Ps conversions were first utilized for this area by Mishin and Dareshkina (1966). For the study, the crustal velocity structure used was that determined by the Magadan-Kolyma DSS profile. For consistency, only earthquakes at teleseismic distances were utilized (Mishin and Dareshkina, 1966). The original Mishin and Dareshkina (1966) study calculated depths for only four of the stations used in this study. It should be noted that only 6 earthquakes per station were used for the Mishin and Dareshkina (1966) study. A later paper by Mishin et al. (1979) adds additional data for stations Seimchan and Susuman. Their studies yield a generally thin crust in the Kolyma gold belt, between 30 and 34 km, which increases in the north to 50 km at Susuman. Belyaevsky (1974) attributes data identical to that of Mishin to Nikolaevsky. Belyaevsky (1974) includes data beyond the Mishin and Dareshkina (1966) paper, including a Moho depth of 43 km for Debin and 34 km for Garmanda (near Evensk; Fig. 5). A P-Ps converted wave study by Belyaevsky and Borisov (1974) report generally

indicate variations in crustal thickness and seismic velocities. Their results suggest crustal thicknesses increasing toward the east and west edges of this study area (24 km at Ust' Nera to 38 km at Omsukchan in the east, and 44 km at Khandyga in the west), and upper mantle velocities of 7.9 to 8.1 km/sec, with the higher values predominantly in the east and west (Fig. 6). Their results are consistent with a significant Pliocene rifting episode resulting in an elevated and lower velocity upper mantle; this result is supported by the surface wave polarization study of Lander (1984) which concludes that there is anomalous mantle under the Chersky Range. Suvorov and Kornilova (1986) also conclude that crustal (Pg) velocities are between 5.8 and 6.2 km/sec.

Crustal studies using P to Ps conversions were first utilized for this area by Mishin and Dareshkina (1966). For the study, the crustal velocity structure used was that determined by the Magadan-Kolyma DSS profile. For consistency, only earthquakes at teleseismic distances were utilized (Mishin and Dareshkina, 1966). The original Mishin and Dareshkina (1966) study calculated depths for only four of the stations used in this study. It should be noted that only 6 earthquakes per station were used for the Mishin and Dareshkina (1966) study. A later paper by Mishin et al. (1979) adds additional data for stations Seimchan and Susuman. Their studies yield a generally thin crust in the Kolyma gold belt, between 30 and 34 km, which increases in the north to 50 km at Susuman. Belyaevsky (1974) attributes data identical to that of Mishin to Nikolaevsky. Belyaevsky (1974) includes data beyond the Mishin and Dareshkina (1966) paper, including a Moho depth of 43 km for Debin and 34 km for Garmanda (near Evensk; Fig. 5). A P-Ps converted wave study by Belyaevsky and Borisov (1974) report generally

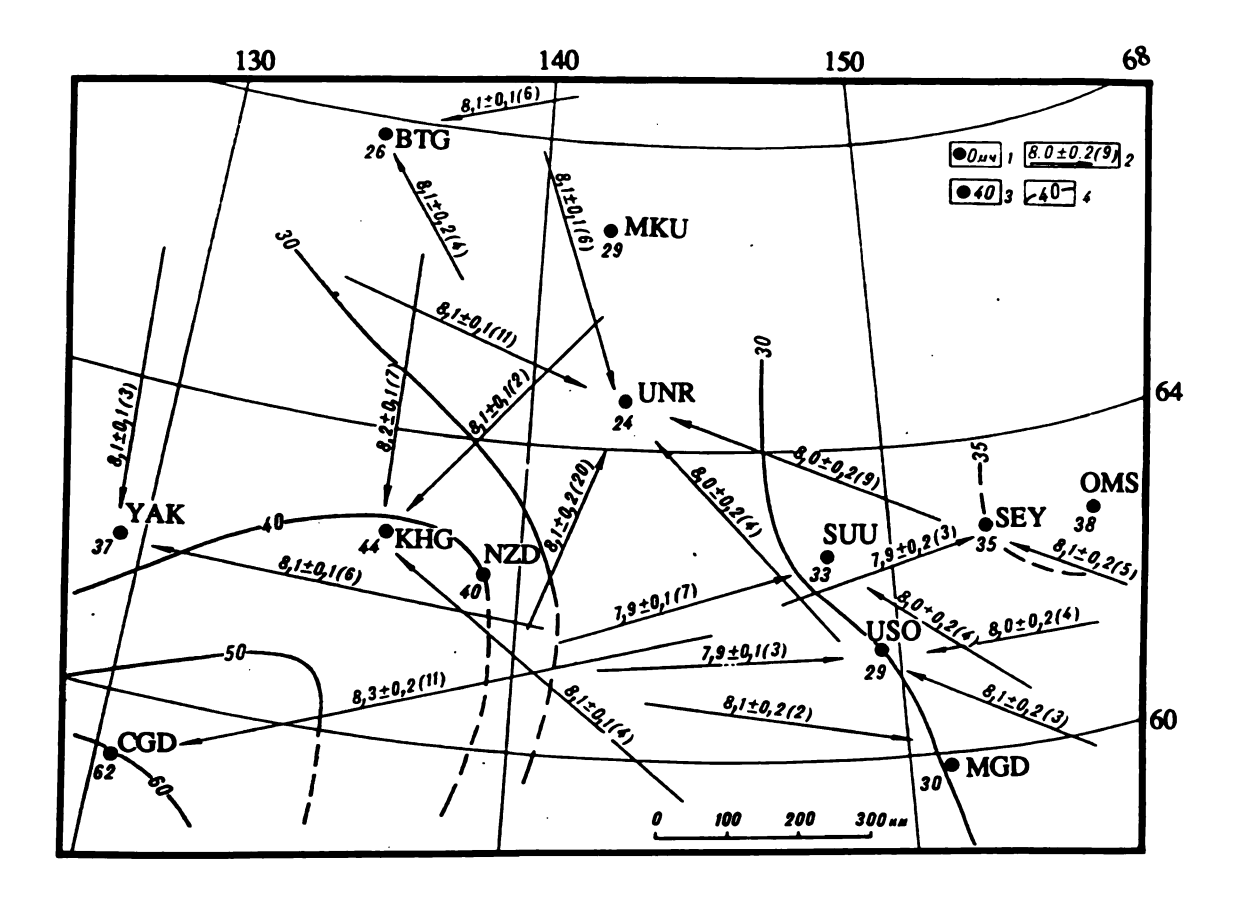


Figure 6. Results from Suvorov and Kornilova (1986) crustal structure study. Dots represent seismic stations (1) and associated numbers are depths in kilometers (3). Arrows indicate trends of Moho velocity, in km/sec (2). Numbers in brackets indicate the number of events used in the determination of velocity (2). Contours show general trend of crustal thickness (4). From Suvorov and Kornilova (1986).

g

is

ch

de

kn

do

and obt

ирр

higher values of crustal thickness approaching 40 km. Vaschilov (1979) cites data from Mishin and Dareshkina (1966), including a depth for Garmanda identical to that cited in Belyaevsky (1974) (this station does not appear in Mishin and Dareshkina (1966)). Vaschilov (1979) recalculates the crustal depths using a different formula. Crustal depths generally increase about 2 km from the Mishin and Dareshkina (1966) values (Vaschilov, 1979).

The most recent study using P-Ps converted waves computes crustal thicknesses at 43 permanent and temporary seismic stations throughout eastern Siberia (Bulin, 1989). The velocity structure used in the study was also from the Magadan - Kolyma DSS profile and other DSS profiles in adjacent areas. In addition, the regional near surface geology was taken into account for individual stations (Bulin, 1989). Values computed by Bulin (1989) are consistently 1.5-3.0 km thinner than those computed by Mishin. This is generally due to increasing the V_p/V_s ratio from 1.73 used by Mishin to greater than or equal to 1.8 (Bulin, 1989), which seems a bit high. The justification for this ratio change is not clear. In direct contrast to Suvorov and Kornilova (1986), Bulin has determined a thick crust reaching 40 km at Ust' Nera, under the Chersky Range, and 40+km in the Okhotsk-Chukotka volcanic belt (Bulin, 1989). Unfortunately, Bulin (1989) does not list data for all the seismic stations used in his study.

Sedov and Luchnina (1988) used mine blasts along a profile between Tal-Yuryakh and Susuman to determine seismic velocities and layer thicknesses. The velocities obtained are somewhat different from the other studies cited above; a 5.5-5.6 km/sec upper crust overlying a 6.5-7.3 km/sec lower crust and an apparent Moho refraction of

Ċ

СТ

19

\$0

19

thi

Ear pro

ano grav

map

to th

and.

10.6 km/sec. The high Moho velocity is attributed by them to a thinning of the crust in the direction of the profile; this end of the profile was not reversed. In a continuation of this study, Sedov (1993) conducted DSS profiling along the central Kolyma Highway including the Susuman - Maisky - Myaudzha and Susuman - Neksikan - Kadykchan branches. This DSS profile indicates a crustal thickness of 41.5 km at Susuman, decreasing to 37.1 km at Yagodnoe in the east and increasing to 43 km in the northwest at Tal-Yuryakh (Sedov, 1993; Fig. 5).

In the northern portion of the study area, Avetisov and Guseva (1991) used the Method of Reflected Wave Sounding (MRWS) to construct seismic profiles of the Earth's crust in the Omoloi graben. A crustal thickness of 29 - 31 km was established for the southern portion of the graben, in the vicinity of station Naiba (Avetisov and Guseva, 1991). This thickness is supported by a DSS profile in the southern Laptev sea (Kogan 1974) and a compilation of previous work (Avetisov, 1983) which indicate a crustal thickness of 29 - 30 km overlying a mantle with a velocity of 7.5 km/sec.

Neustroev and Parfenov (1985) have found a correlation between thickness of the Earth's crust and thickness of platform cover deposits from deep seismic sounding profiles. From this correlation, correction factors were introduced into the Bouger anomalies to remove the effect of the platform cover. Using several DSS profiles, gravimetric maps, and a 1:2,500,000 map of topography of the crystalline basement, a map of crustal thickness was produced for the eastern Siberian platform. Of relevance to this study, the crustal thickness was determined to be 42 km at Yakutsk and Khandyga, and 40 km at Nezhdaninskoe (Neustroev and Parfenov, 1985). Neustroev and Parfenov

(1985) indicate anomalies due to thick platform cover are sufficient to mask any anomaly resulting from variations in crustal thickness. This calls into question previous methods which have determined crustal thicknesses in the Siberian platform using gravity.

Intracrustal structure, based on gravity variations, has been extensively studied using the method of Vashchilov (1984) for the entire region. Bobrobnikov and Izmailov (1989) use gravity data to suggest 30-35 km crustal thicknesses for the study area, increasing to as high as 60 km southwest of the study area. Deep seismic sounding is reported to have obtained a crustal thickness of 38 km in the upper Yama River valley (Bobrobnikov and Izmailov, 1989; Fig. 5).

Methodology and Regional Crustal Model

For this study, a data base of travel time data from over 850 regional events occurring in the Magadan region, Sakha Republic (Yakutia), and the Laptev Sea was created. Data from 1976 to 1990 are taken from Materialy po Seismichnosti Sibiri and covers both the Magadan region and Sakha Republic (Yakutia). From 1991 to 1994, additional unpublished data was provided by B. M. Koz'min for the Yakut network (Personal communication, 1994) and by L. Gunbina for the Magadan network (Personal communication, 1995). These data were supplemented by phase data for approximately 50 events reported in the International Seismological Center Bulletin and the Obninsk Seismological Bulletin for stations in northeast Russia. The study area was selected based on the distribution of the regional seismicity and the location of seismic stations. Figure

Figure the OM Nell Kular = K. TLI = Sto

ī

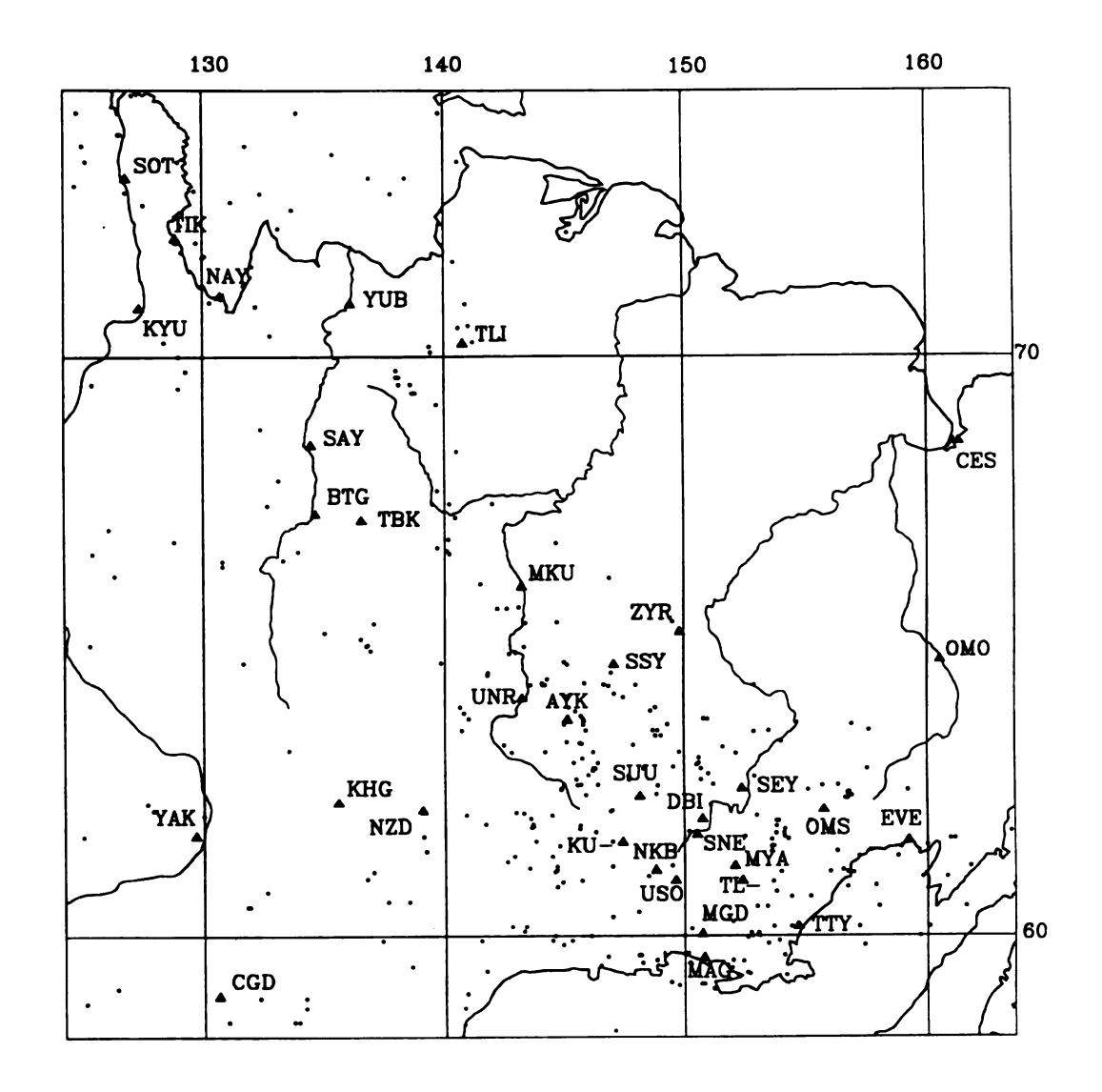


Figure 7. Study area showing seismic stations and epicenters of earthquakes used in the study. MAG = Magadan, TTY = Takhtoyamsk, MGD = Stekolnyi, EVE = Evensk, OMS = Omsukchan, TL- = Talaya, MYA = Myakit, USO = Ust' Omchug, NKB = Nelkoba, SNE = Sinegor'e, DBI = Debin, SEY = Seimchan, OMO = Omolon, KU- = Kulu, Suu = Susuman, CGD = Chagda, YAK = Yakutsk, NZD = Nezhdaninskoe, KHG = Khandyga, AYK = Artyk, UNR = Ust' Nera, SSY = Sasyr', ZYR = Zyryanka, MKU = Moma (Khonou), CES = Cherskii, TBK = Tabalakh, BTG = Batagai, SAY = Saidy, TLI = Tenkeli, YUB = Yubileniya, KYU = Kyusyur, NAY = Naiba, TIK = Tiksi, SOT = Stolb.

7 sh

ever

the

laye

Ever proc

as a

arriv

resid

For

misic

Duri

an ac

are e

most reloca

1:200

comn

Russia

chang(

7 shows the boundaries of the study area as well as seismic stations and epicenters of events considered in the study. In total, 441 events from the original data set fall within the study area.

All events were relocated using Pg arrivals only, assuming a 6.00 km/sec crustal layer, as well as first arrivals (Pg or Pn) using Jeffreys-Bullen travel-times (Appendix A). Events with fewer than four arrivals were not possible to locate. In the relocation process, many misidentified phase arrivals were discovered. A Pn arrival misidentified as a Pg arrival stands out in a Pg location with a large negative residual. Likewise, a Pg arrival misidentified as a Pn arrival shows clearly in a Pn location with a large positive residual. In such cases, the phase of the arrival was corrected, and the event relocated. For events with large residual arrivals which did not correspond to any possible misidentified phases, the anomalous arrival was removed from the relocation process. During the 1980s, most of the stations in this region used the "Mayak" timing system with an accuracy of about 0.3 sec; combined with reading uncertainties, errors of 0.4-0.5 sec are expected; no attempt was made to reduce statistical residuals below this level. The most recent determinations of station coordinates and their elevations were used in the relocations. For Yakutian stations, new coordinates and elevations were determined from 1:200,000 topographic maps with assistance from B. M. Koz'min (Appendix B; Personal communication, 1994).

In the relocations, most epicenters moved only 1-20 km relative to those given in Russian bulletins. For events in which five or more arrivals were used in the relocation, change in epicenter vs. year was plotted (Fig. 8). There is no evidence that the Russian

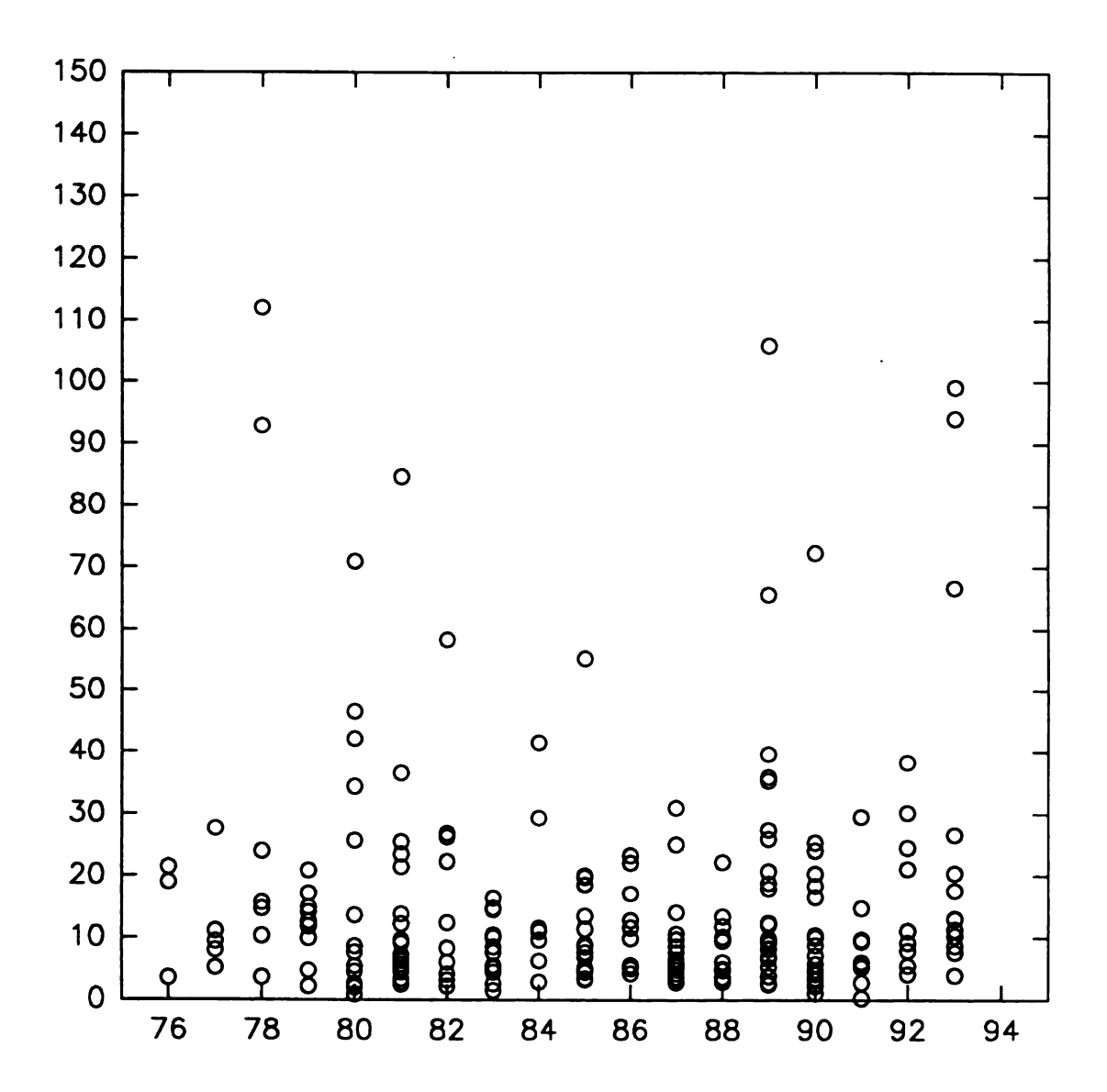


Figure 8. Year vs. change in kilometers of relocated epicenters for events shown in Fig. 7. Relocations computed with Pg phase only, assuming a single layer crust of velocity 6.00 km/sec. Lack of systematic trend through time indicates that the quality of original locations has remained consistant. Original epicenters taken from *Materialy Po Seismichnosti Sibiri*.

ep

m

to

lik di:

M

I v

dej

COI

det rel

are on

tho

to t

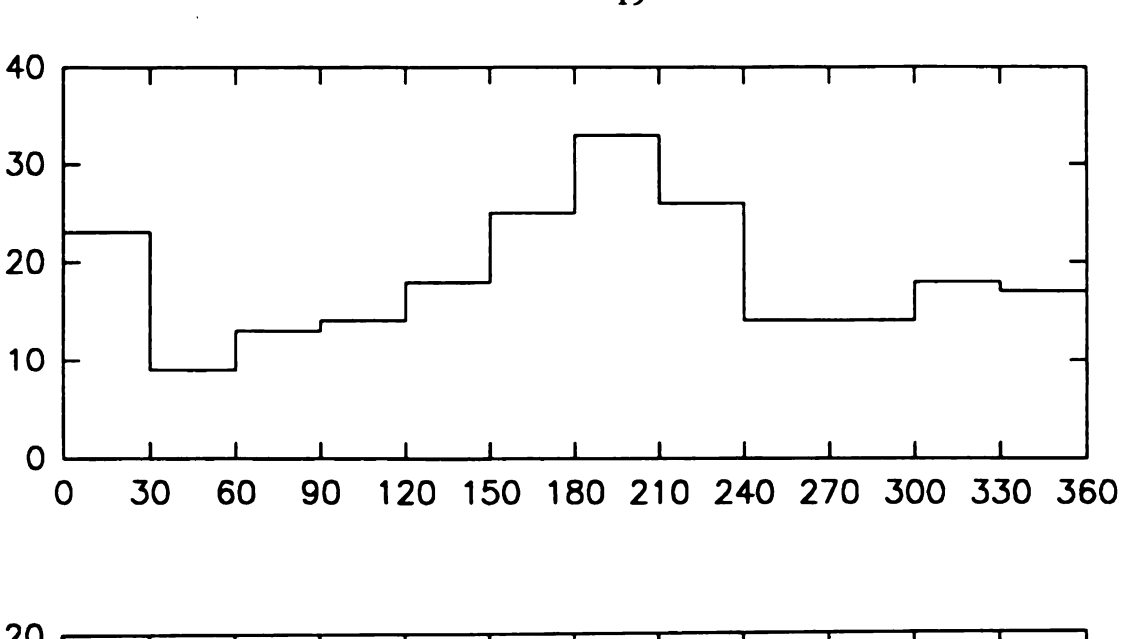
For

rel₀

dete

epicenters improve in later years, even with better station distribution and presumably more accurate timing. There is evidence for systematic mislocations in the Russian data set. Relocations computed with Pg arrivals show a strong tendency to move south, and to a lesser extent north, relative to the *Materialy* reported epicenter (Fig. 9). This is likely due to a difference in the crustal velocity used in the different locations, and is discussed below. Relocations using first arrivals show no systematic trend (Fig. 10). Many events reported in the Russian bulletins report a calculated depth. In most cases, I was unable to calculate depths in the relocation process. For events where a shallow depth was determined, there is no consistent correlation with the Russian bulletin reported depths. Thus, for this study, most depths were confined to 10 or 15 km. Relocations computed early in the study used a confining depth of 15 km, while more recent determinations use 10 km. In general, this change seems to have little effect in the relocation process.

The Pg relocated epicenters were plotted on a simplified fault map of the study area (Fig. 11). Fault locations are from Imaev et al. (1994), as well as lineaments visible on landsat images. Activity on many of these faults is restricted to smaller events than those locatable with phase data in *Materialy po Seismichnosti Sibiri*, thus faults known to be active may not show activity on this map. Relocated epicenters correspond well to several of the mapped faults, such as the left-lateral Ulakhan fault (Imaev et al., 1994). For events believed associated with the Ulakhan fault, the bulletin epicenters and relocated epicenters were plotted on 1:500,000 scale topographic maps in an attempt to determine whether or not the relocated epicenters show an improved correlation with the



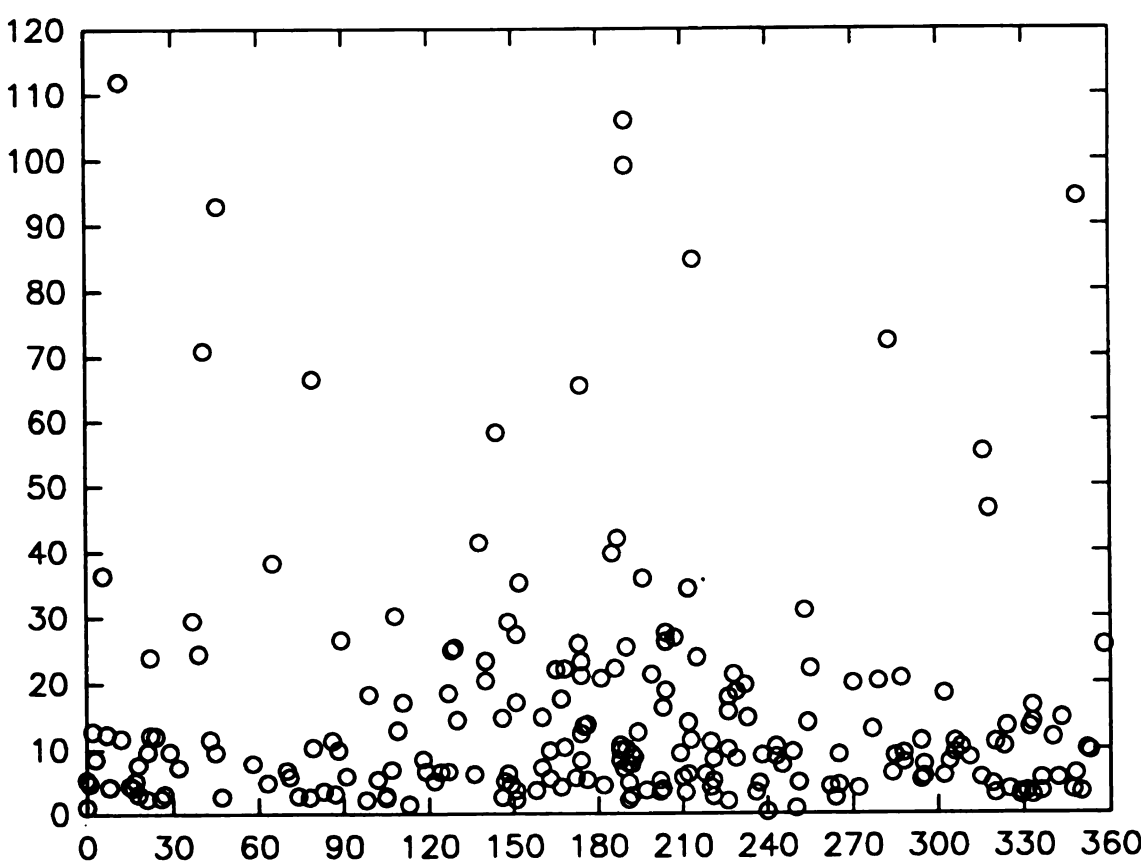


Figure 9. Azimuth from original to Pg data relocated epicenter vs distance of epicenter change (in km). As shown in the upper portion of the figure, epicenters tend to move south, indicating a systematic error in the original locations. Original epicenters taken from *Materialy Po Seismichnosti Sibiri*.

'50

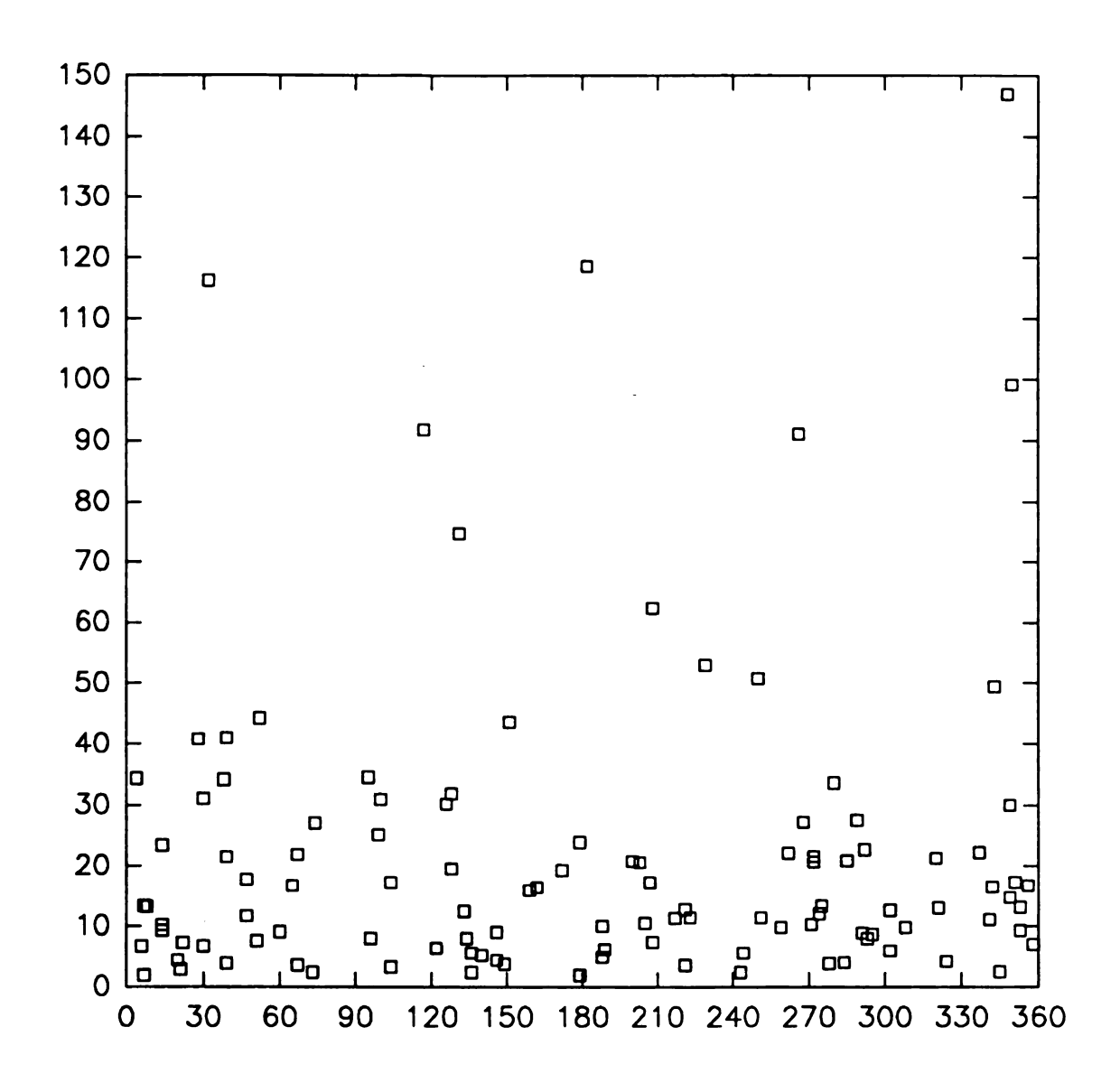


Figure 10. Azimuth from original to Pn data relocated epicenter vs distance of epicenter change (in km). Epicenters show no systematic direction of change. Original epicenters taken from *Materialy Po Seismichnosti Sibiri*.

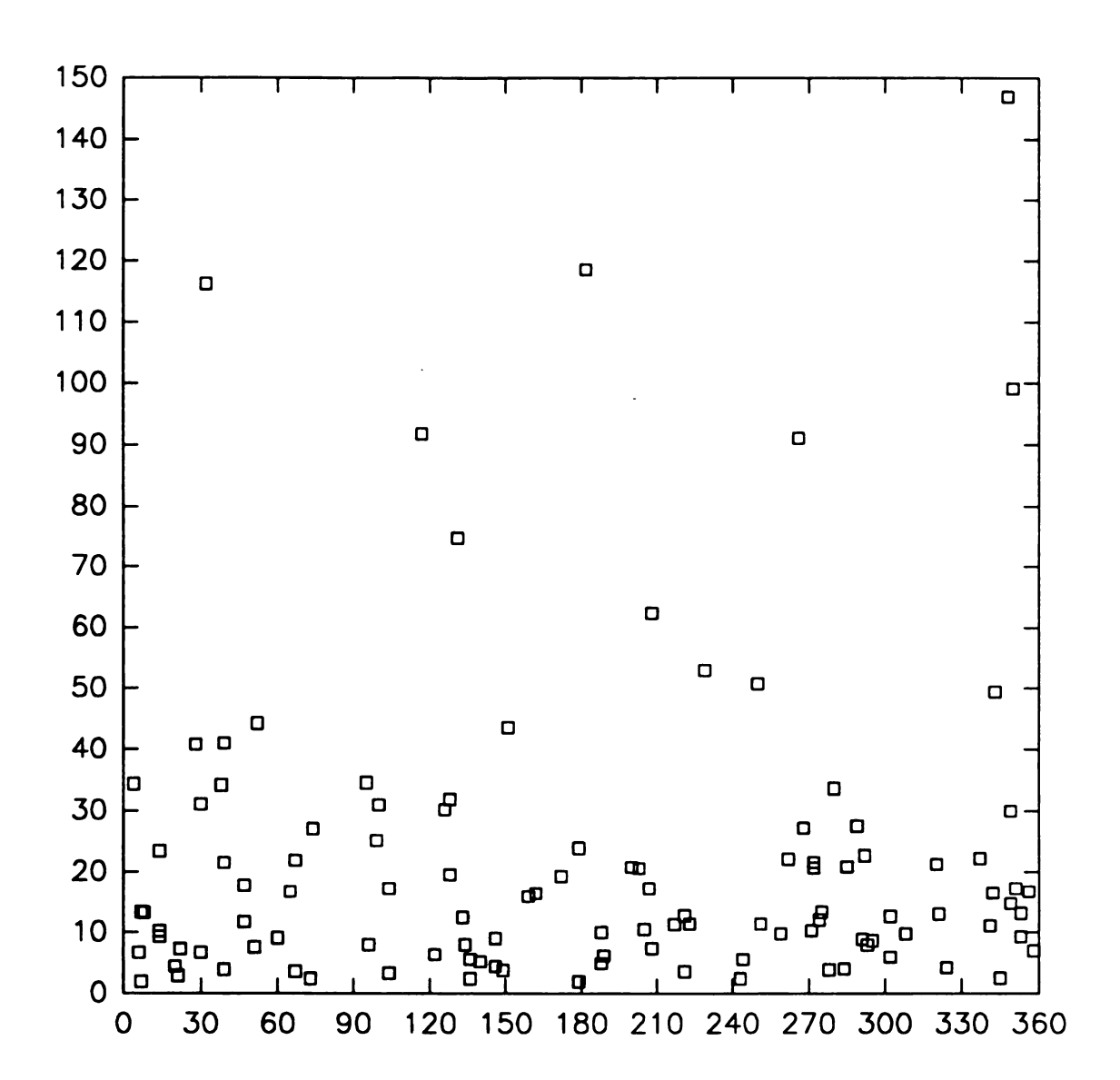


Figure 10. Azimuth from original to Pn data relocated epicenter vs distance of epicenter change (in km). Epicenters show no systematic direction of change. Original epicenters taken from *Materialy Po Seismichnosti Sibiri*.

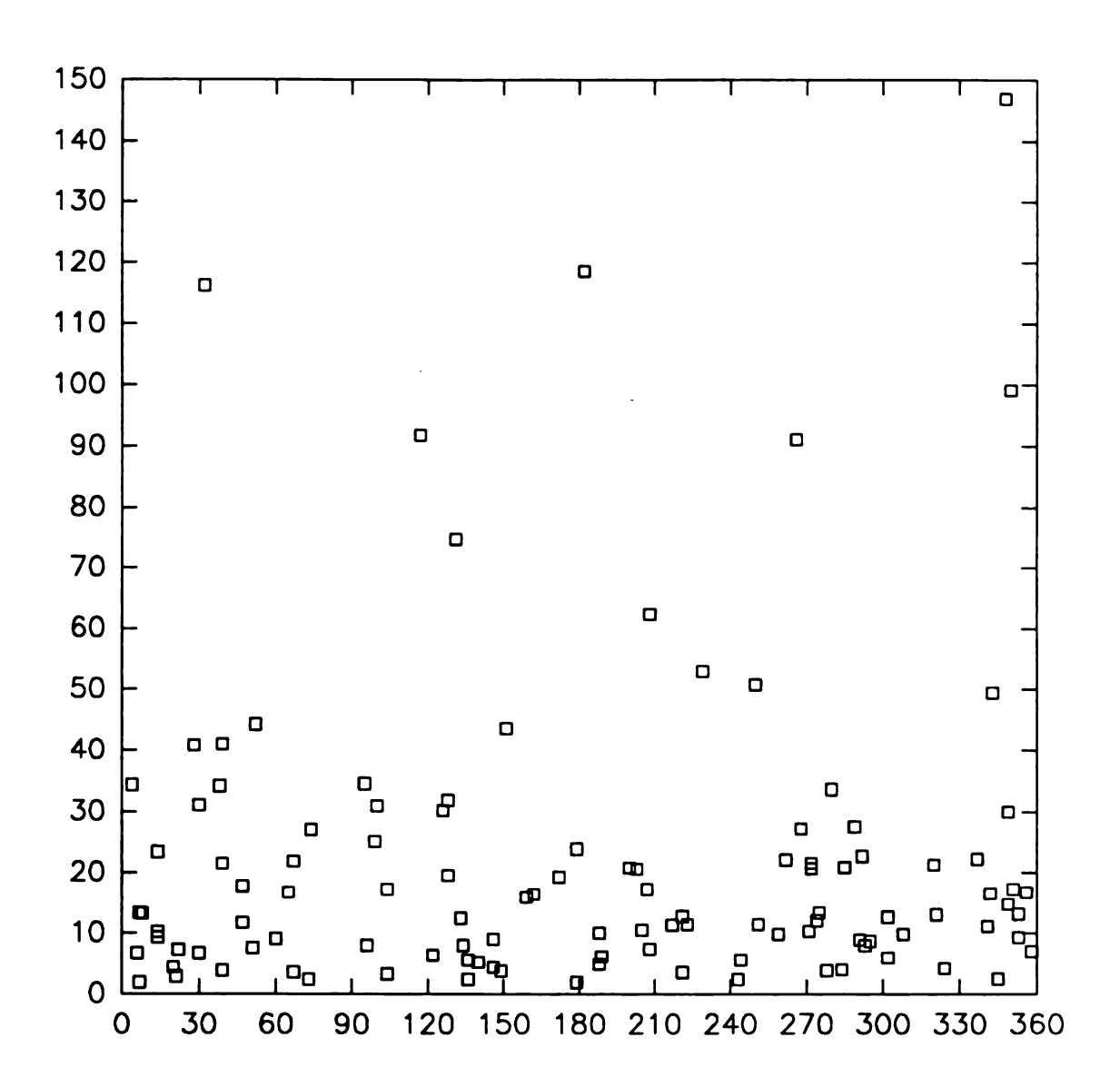


Figure 10. Azimuth from original to Pn data relocated epicenter vs distance of epicenter change (in km). Epicenters show no systematic direction of change. Original epicenters taken from *Materialy Po Seismichnosti Sibiri*.

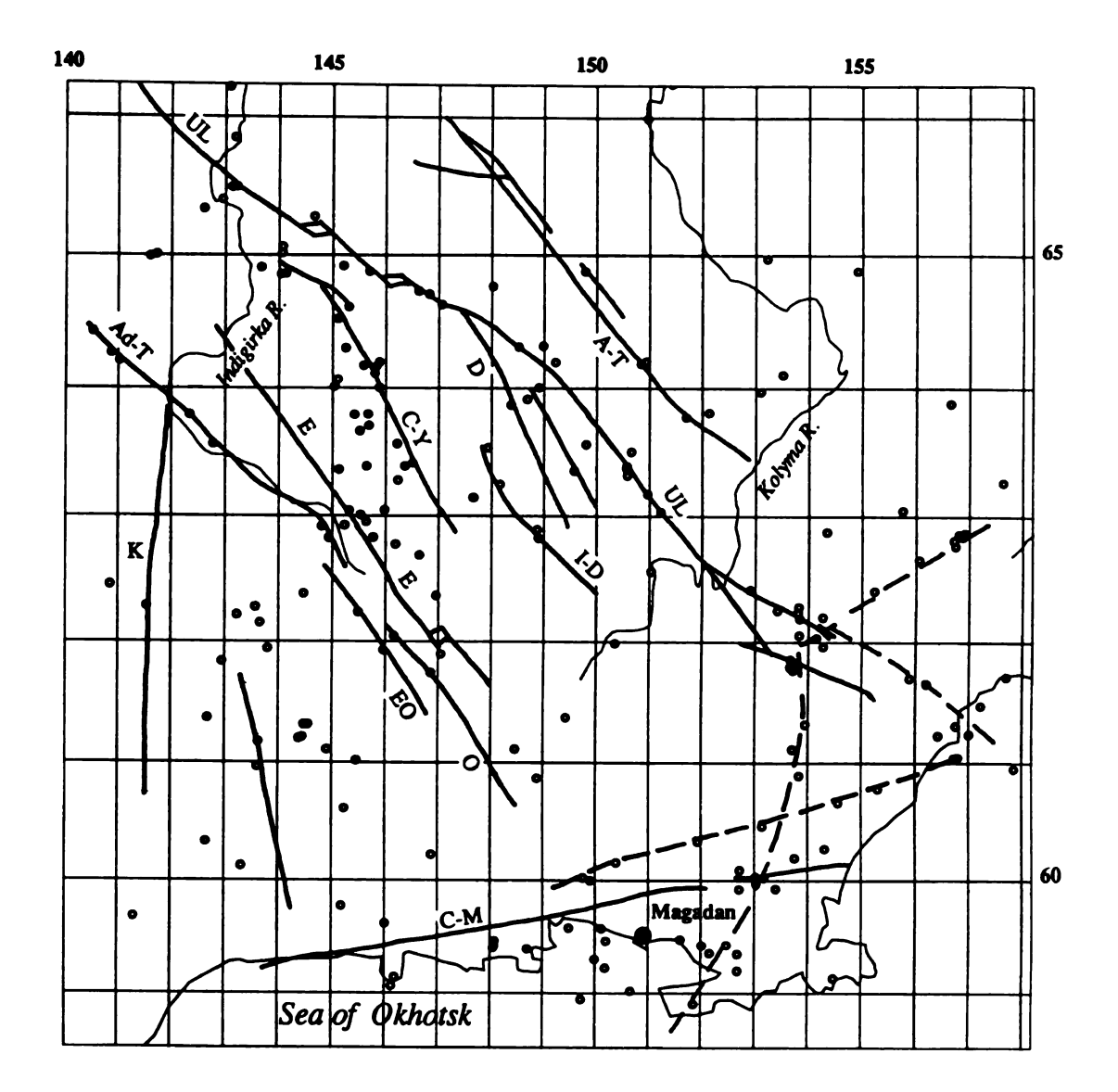


Figure 11. Map of major faults in the southern portion of the study area and their relations to relocated epicenters. Solid lines represent faults mapped in Imaev (1994), as well as those visible as lineaments on satellite images. Dashed lines represent faults inferred from linear trends in relocated epicenters. UL denotes the Ulakhan fault; A-T the Arga-Tas; D the Darpir; I-D the In'yali-Debin; E the Elgin; O the Oimyakon; EO the Eastern Okhotsk; C-Y the Chia-Yureya; C-M the Chelomdzha-Yama; K the Ketanda; Ad-T the Adycha-Taryn.

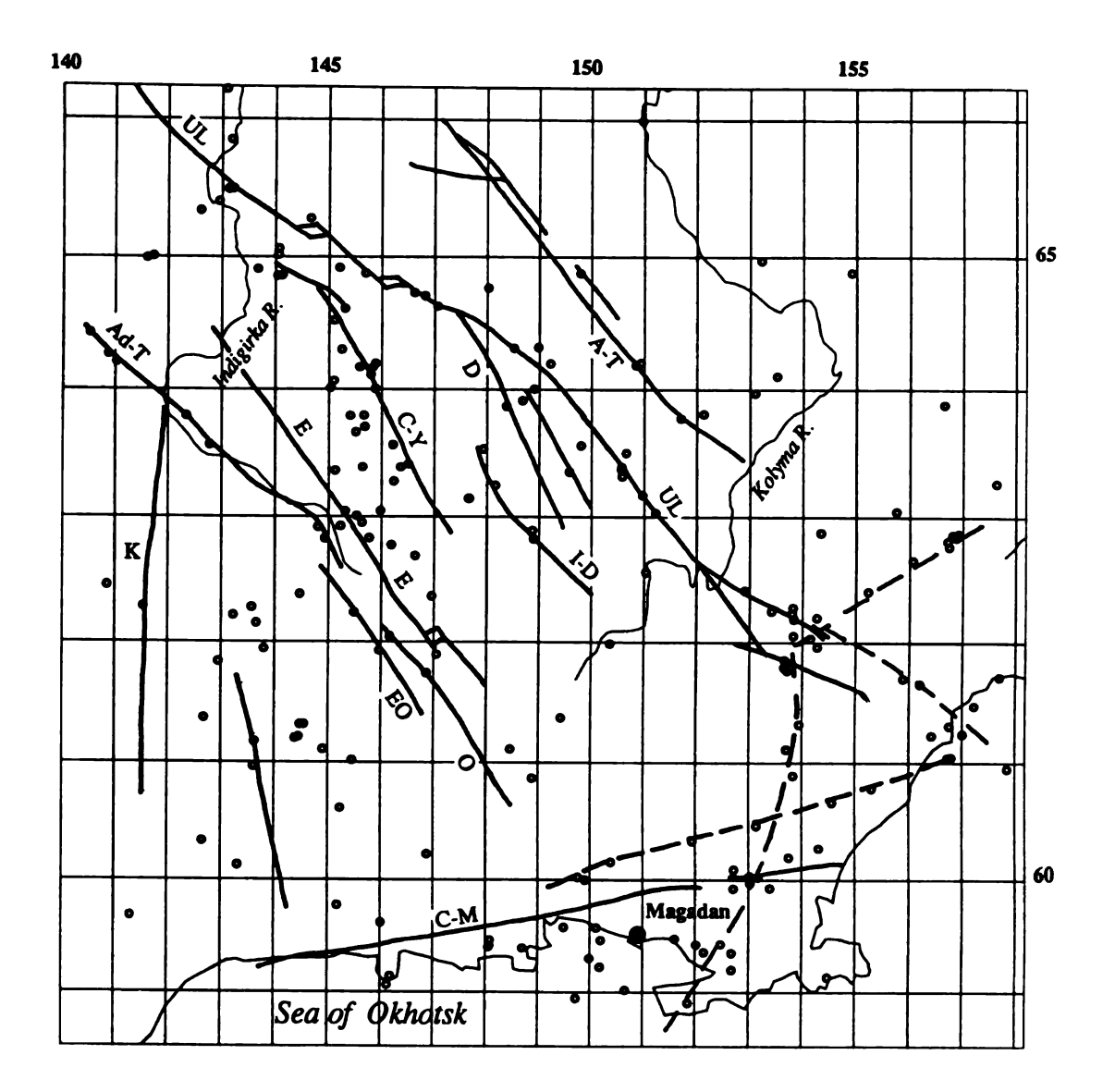


Figure 11. Map of major faults in the southern portion of the study area and their relations to relocated epicenters. Solid lines represent faults mapped in Imaev (1994), as well as those visible as lineaments on satellite images. Dashed lines represent faults inferred from linear trends in relocated epicenters. UL denotes the Ulakhan fault; A-T the Arga-Tas; D the Darpir; I-D the In'yali-Debin; E the Elgin; O the Oimyakon; EO the Eastern Okhotsk; C-Y the Chia-Yureya; C-M the Chelomdzha-Yama; K the Ketanda; Ad-T the Adycha-Taryn.

fault trace. There is no apparent improvement in the correlation between relocated epicenters and the Ulakhan fault trace relative to the Russian determined epicenters. This may be a result of the lack of knowledge regarding the structure of the Ulakhan fault at depth, and poor depth control for both the relocated and bulletin reported epicenters. Some of the events plotted may actually occur on unrecognized faults in the vicinity of the Ulakhan. For many of the events, the Ulakhan fault trace is within the location errors as discussed below.

The best located 75 events were selected for the determination of crustal structure. Several criteria were established for selecting these events (Fig. 12). First, events were required to contain seven or more arrivals used in the Pg relocation. Fewer arrivals than seven causes individual stations to be weighted heavily, thus one mispicked arrival could result in considerable error in the relocation. Secondly, the azimuthal coverage had to exceed 130°. For events where the range of azimuths was less than 130°, the event could simply be moved towards or away from the recording stations, trading off only with origin time, and having little effect on the residuals. Lastly, the difference in epicenters between the Pg relocation and the first arrival relocation should not exceed 15 km, and the difference in origin times should be less than 2.0 sec. These criteria were intended to select events where the first arrival times were compatible with the Pg relocated epicenter, thus increasing the likelihood of good data. Because of the poor distribution of recording stations, the first two criteria were difficult to meet for events near the edge of the study area, or away from the network. This was particularly true for events in the Laptev Sea. In an effort to use a widely distributed data base, these criteria were

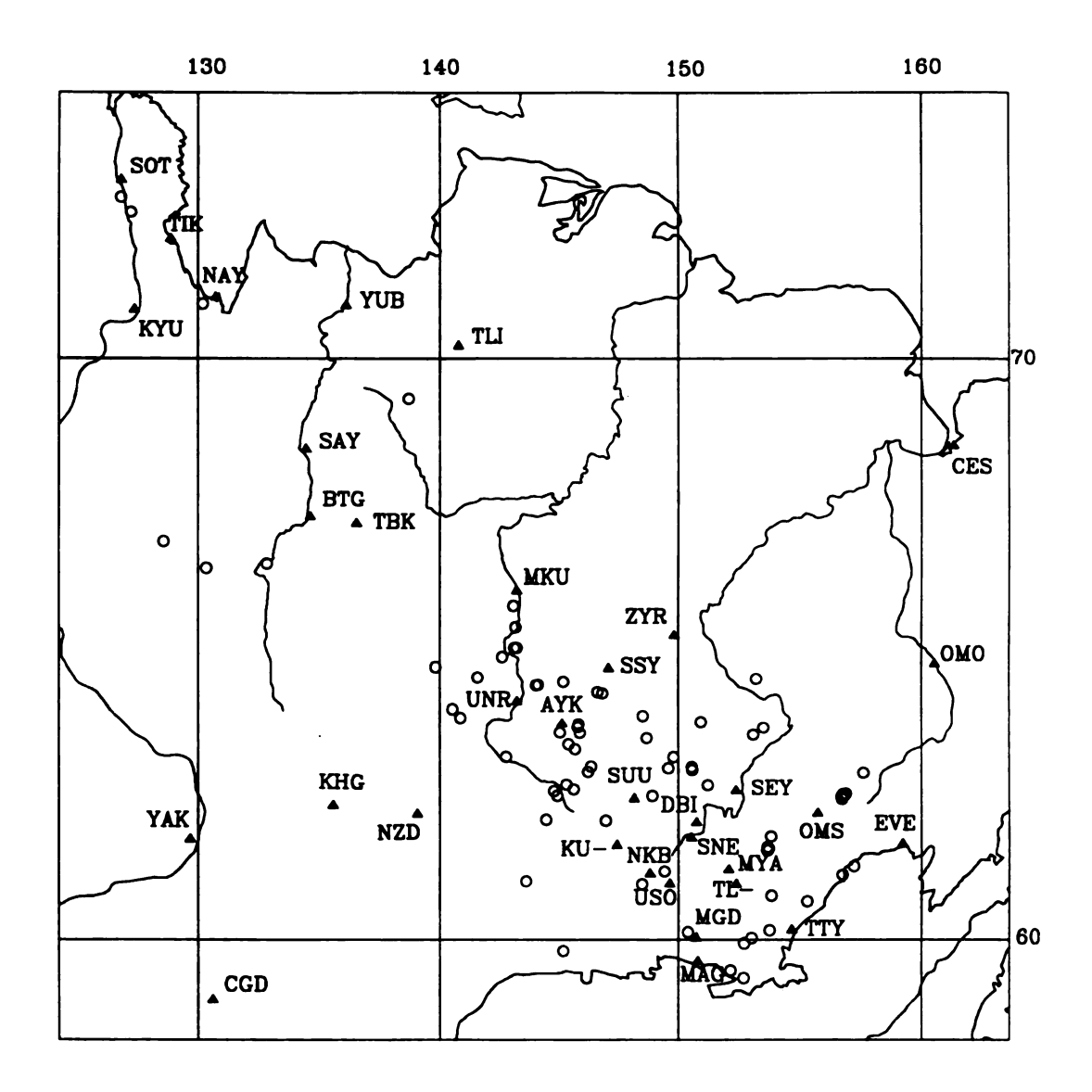


Figure 12. Relocated epicenters of the selected best 75 events in the study area. These events used in the determination of crustal thicknesses. Seismic station codes as noted in Fig. 7.

somewhat lessened for outlying events.

For the best 75 events, relocated epicenter errors range from ± 1 to ± 8 km, averaging ± 3 km. It was noted that for events occurring from 1991 to 1993, average errors for the relocations increased slightly to ± 4 km. The calculated errors on the relocated epicenters are less than the location errors reported in the *Materialy* bulletin. Bulletin reported epicentral errors average about ± 10 km for these 75 events.

To assess the precision of the epicenters reported in *Materialy* and compare them with the Pg relocations, the travel-time data for the 75 selected events was plotted. Looking at the Pg data, there is a significant reduction in scatter of the arrival times using the Pg relocation epicenter and origin time compared to those reported in *Materialy* (Figs. 13 and 14). This suggests problems with the reported epicenters.

A significant reduction in scatter of the Pn data is also observed when plotted with the Pg relocation parameters and compared with the plot using the *Materialy* parameters (Figs. 13 and 14). Sg and Sn data are also plotted using Pg location parameters, though they show a lesser reduction in scatter when compared to the data plotted with the *Materialy* epicenter and origin time (Figs. 15 and 16). For all phases, the use of the Pg phase relocated epicenter and origin time in place of those from *Materialy* results in a reduction of scatter in the plotted travel time curves. Therefore, my relocations using only Pg data are most certainly an improvement on the Russian locations.

Comparing the Pg travel time curves, it is apparent that the Russian locations are determined with a higher Pg velocity. A velocity of 6.10 km/sec fits the Pg travel time curve derived from the original Russian locations (Fig. 13). This is consistent with the

some

avera

error

reloc

Bulle

with Look

the P

13 an

the Pg

they s

Materi

phase reducti

only P

determi

curve d

somewhat lessened for outlying events.

For the best 75 events, relocated epicenter errors range from ± 1 to ± 8 km, averaging ± 3 km. It was noted that for events occurring from 1991 to 1993, average errors for the relocations increased slightly to ± 4 km. The calculated errors on the relocated epicenters are less than the location errors reported in the *Materialy* bulletin. Bulletin reported epicentral errors average about ± 10 km for these 75 events.

To assess the precision of the epicenters reported in *Materialy* and compare them with the Pg relocations, the travel-time data for the 75 selected events was plotted. Looking at the Pg data, there is a significant reduction in scatter of the arrival times using the Pg relocation epicenter and origin time compared to those reported in *Materialy* (Figs. 13 and 14). This suggests problems with the reported epicenters.

A significant reduction in scatter of the Pn data is also observed when plotted with the Pg relocation parameters and compared with the plot using the *Materialy* parameters (Figs. 13 and 14). Sg and Sn data are also plotted using Pg location parameters, though they show a lesser reduction in scatter when compared to the data plotted with the *Materialy* epicenter and origin time (Figs. 15 and 16). For all phases, the use of the Pg phase relocated epicenter and origin time in place of those from *Materialy* results in a reduction of scatter in the plotted travel time curves. Therefore, my relocations using only Pg data are most certainly an improvement on the Russian locations.

Comparing the Pg travel time curves, it is apparent that the Russian locations are determined with a higher Pg velocity. A velocity of 6.10 km/sec fits the Pg travel time curve derived from the original Russian locations (Fig. 13). This is consistent with the

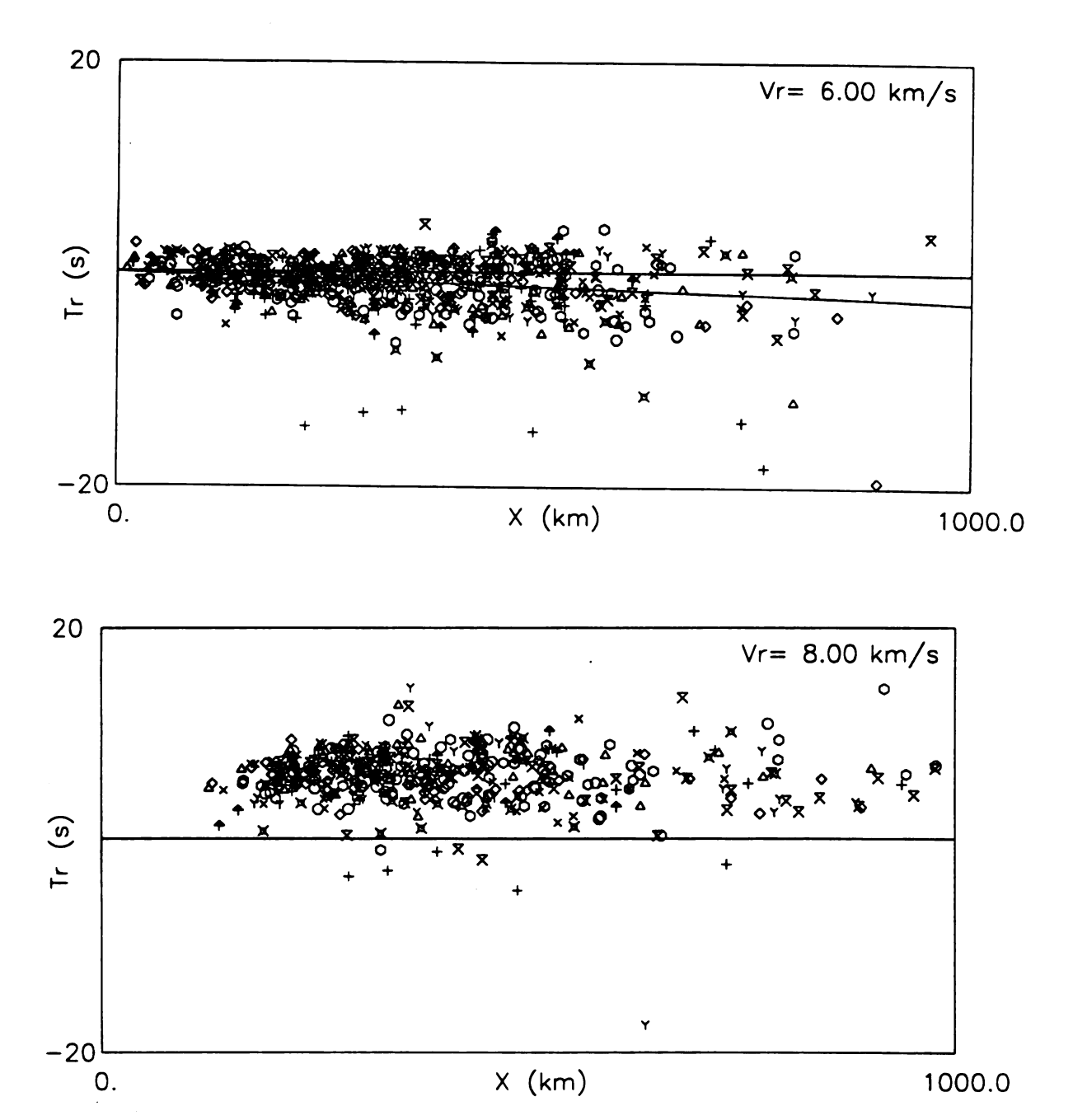


Figure 13. Reduced traveltime curves for Pg (A) and Pn (B) data of selected best 75 events using epicenters and origin times reported in *Materialy po Seismichnosti Sibiri*. Reduction velocities are noted on figures. For Pg data, the best fit velocity is 6.10 km/sec (optically determined). Individual events are represented by different symbols.

-20¹— 0.

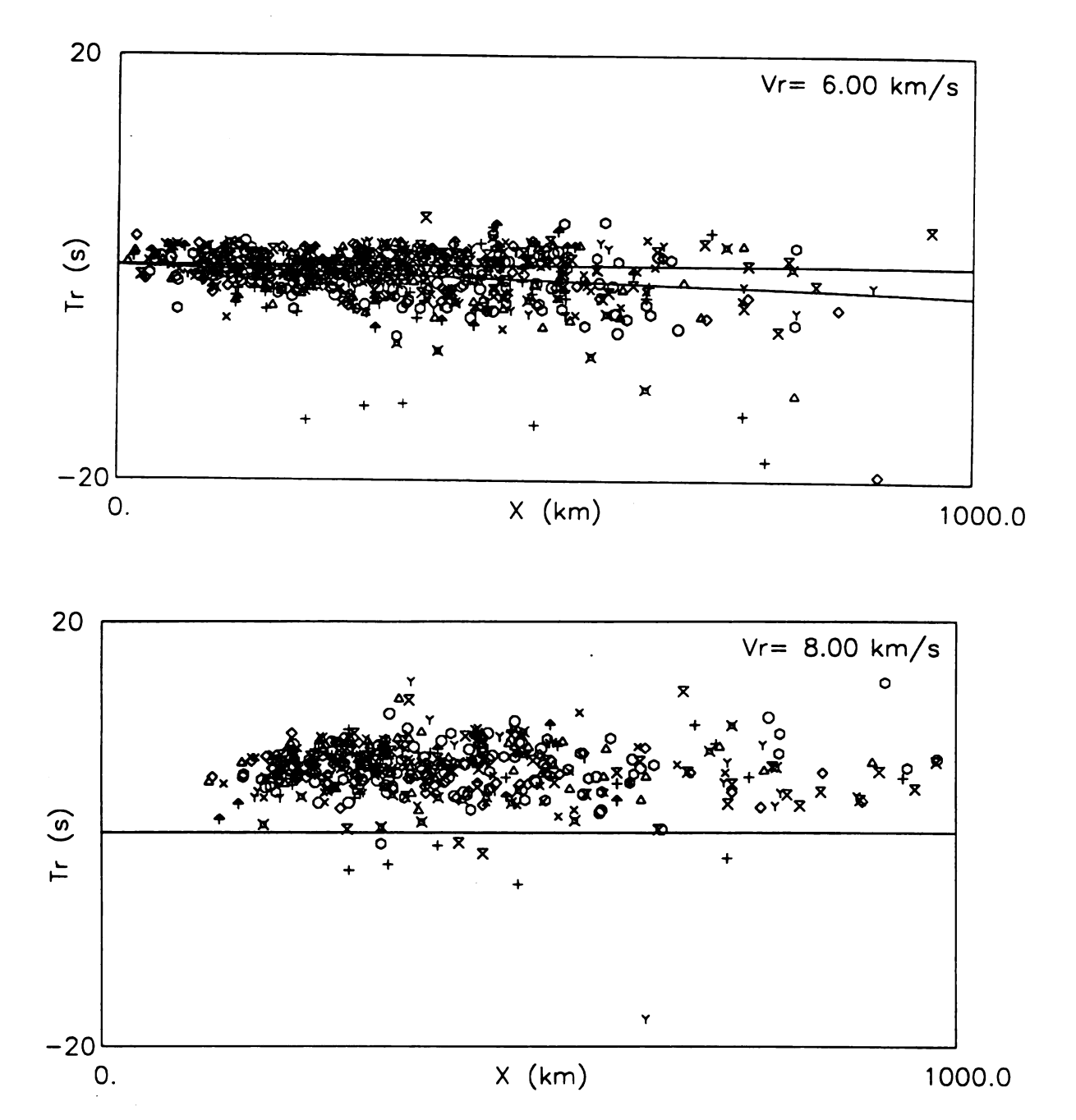


Figure 13. Reduced traveltime curves for Pg (A) and Pn (B) data of selected best 75 events using epicenters and origin times reported in *Materialy po Seismichnosti Sibiri*. Reduction velocities are noted on figures. For Pg data, the best fit velocity is 6.10 km/sec (optically determined). Individual events are represented by different symbols.

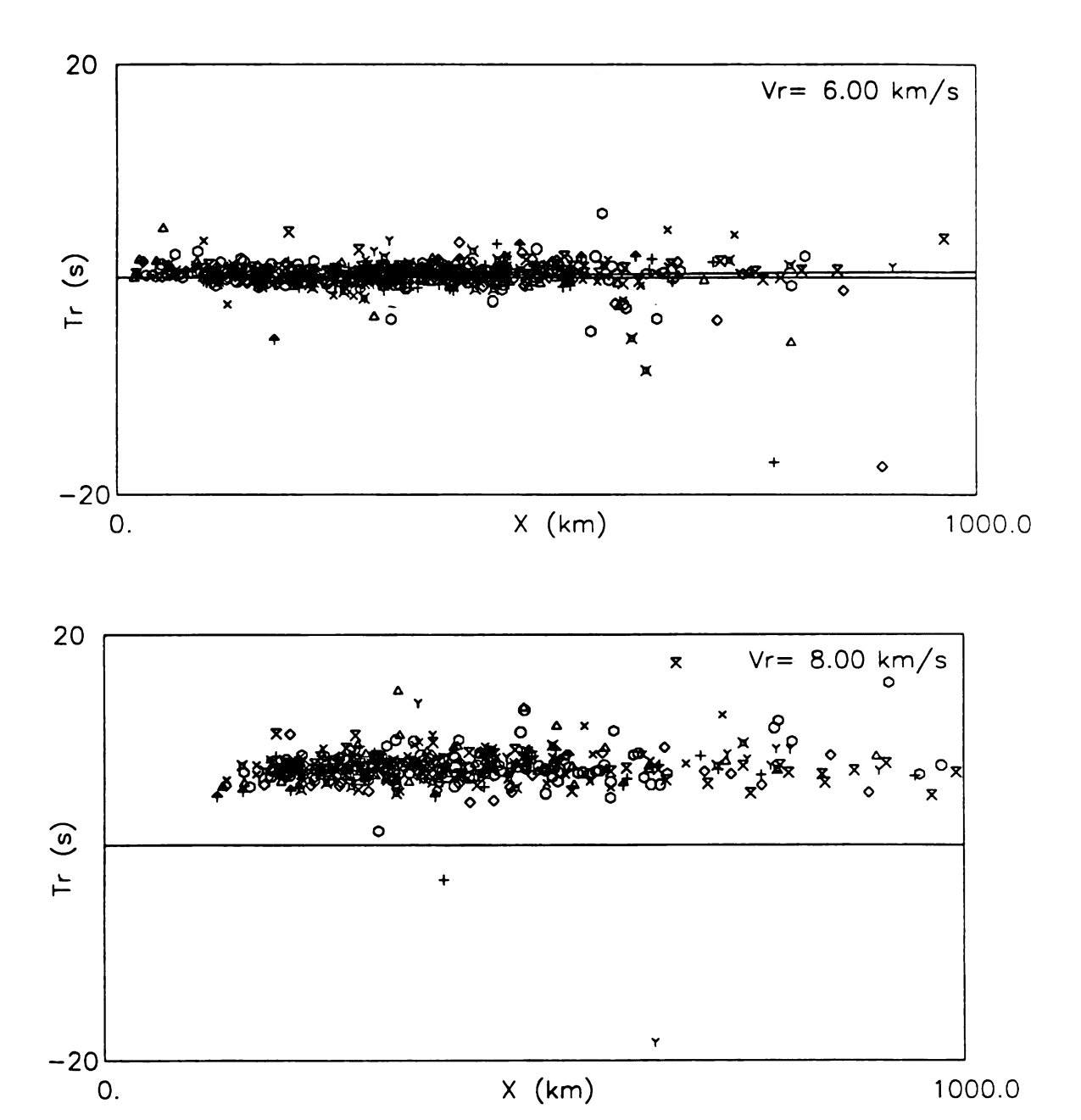


Figure 14. Reduced traveltime curves for Pg (A) and Pn (B) data of selected best 75 events using epicenters and origin times determined from relocations using Pg data. Reduction velocities are noted on figures. Individual events are represented by different symbols.

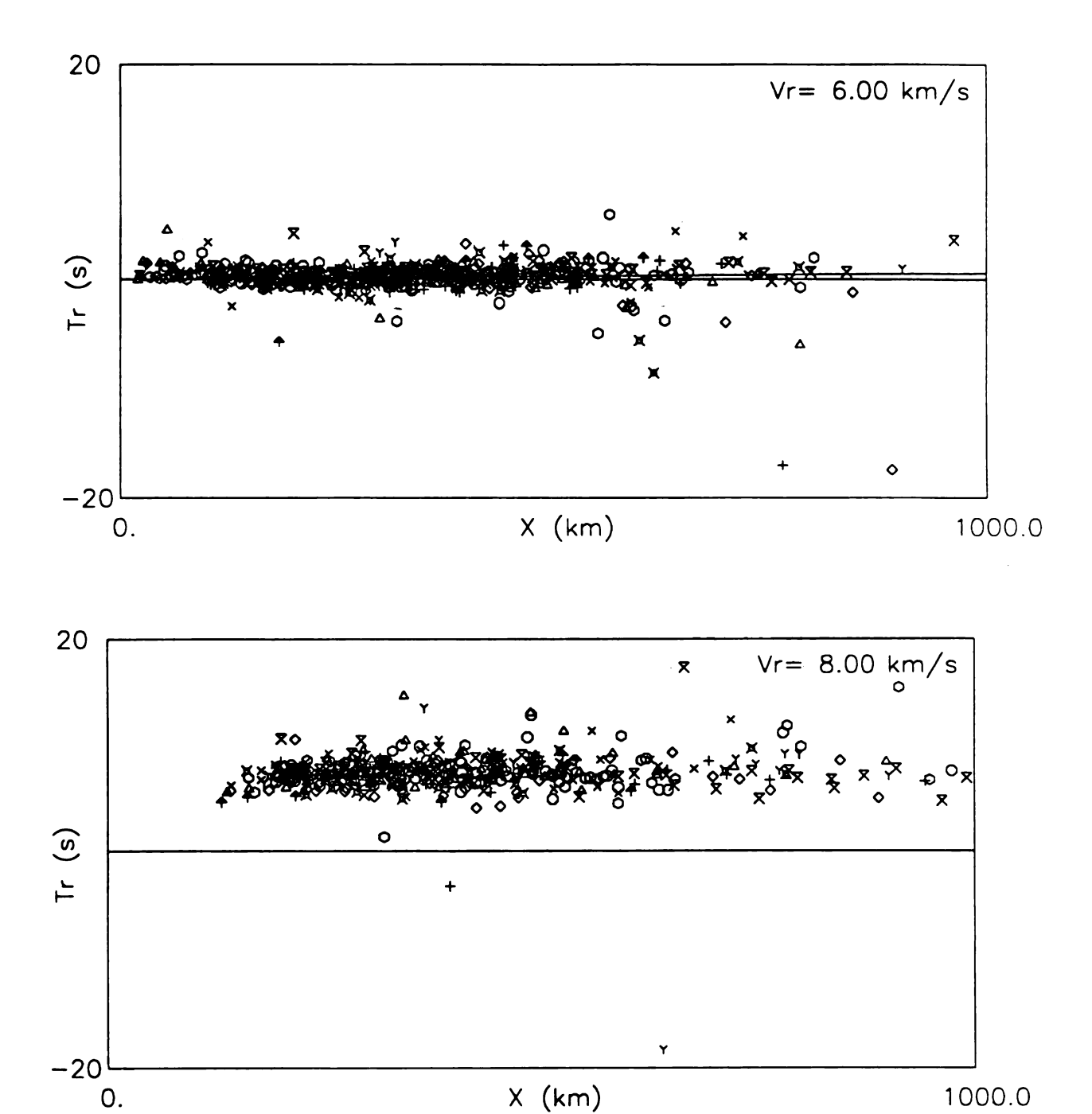


Figure 14. Reduced traveltime curves for Pg (A) and Pn (B) data of selected best 75 events using epicenters and origin times determined from relocations using Pg data. Reduction velocities are noted on figures. Individual events are represented by different symbols.

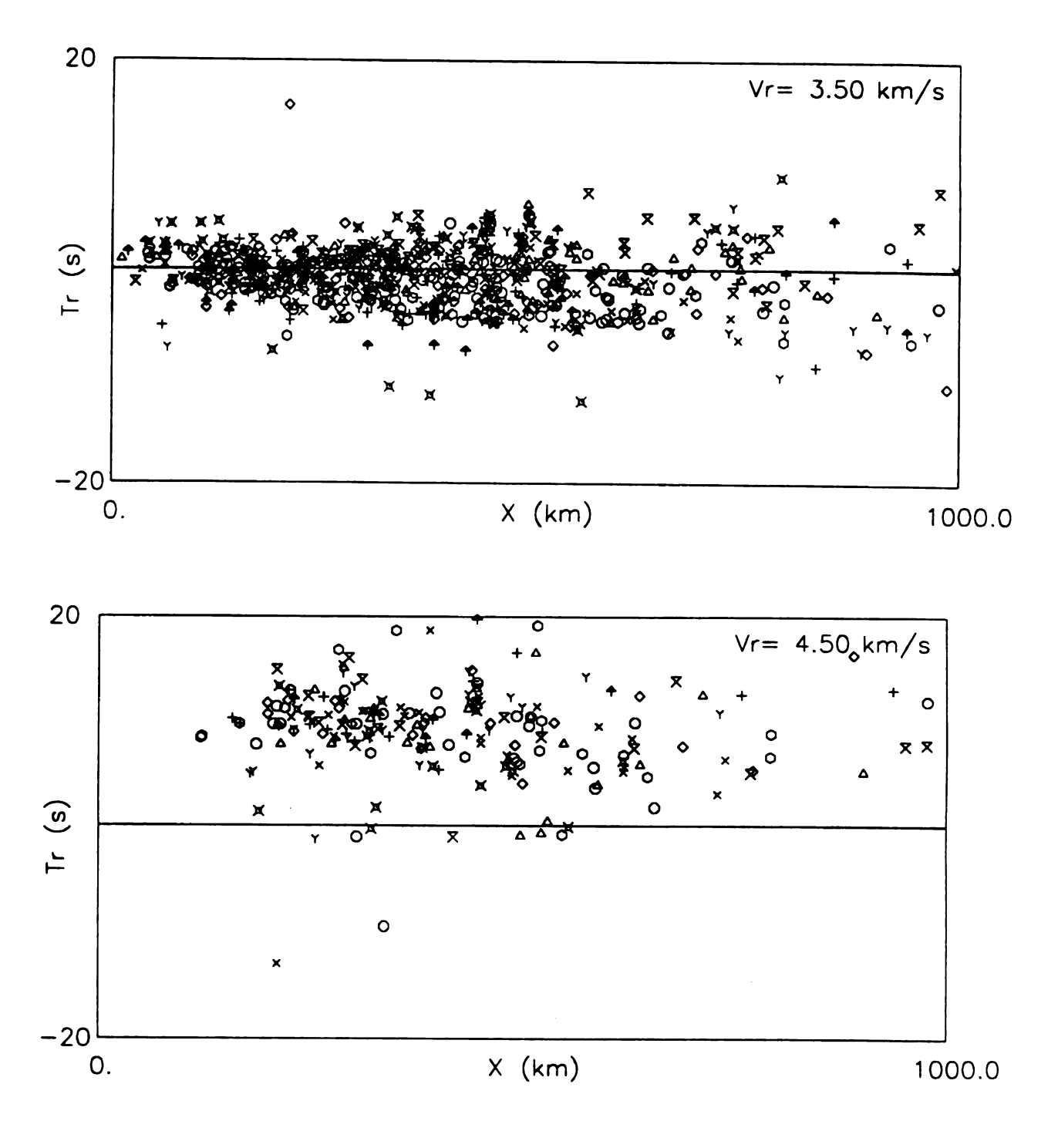


Figure 15. Reduced traveltime curves for Sg (A) and Sn (B) data of selected best 75 events using epicenters and origin times reported in *Materialy po Seismichnosti Sibiri*. Reduction velocities are noted on figures. Individual events are represented by different symbols.

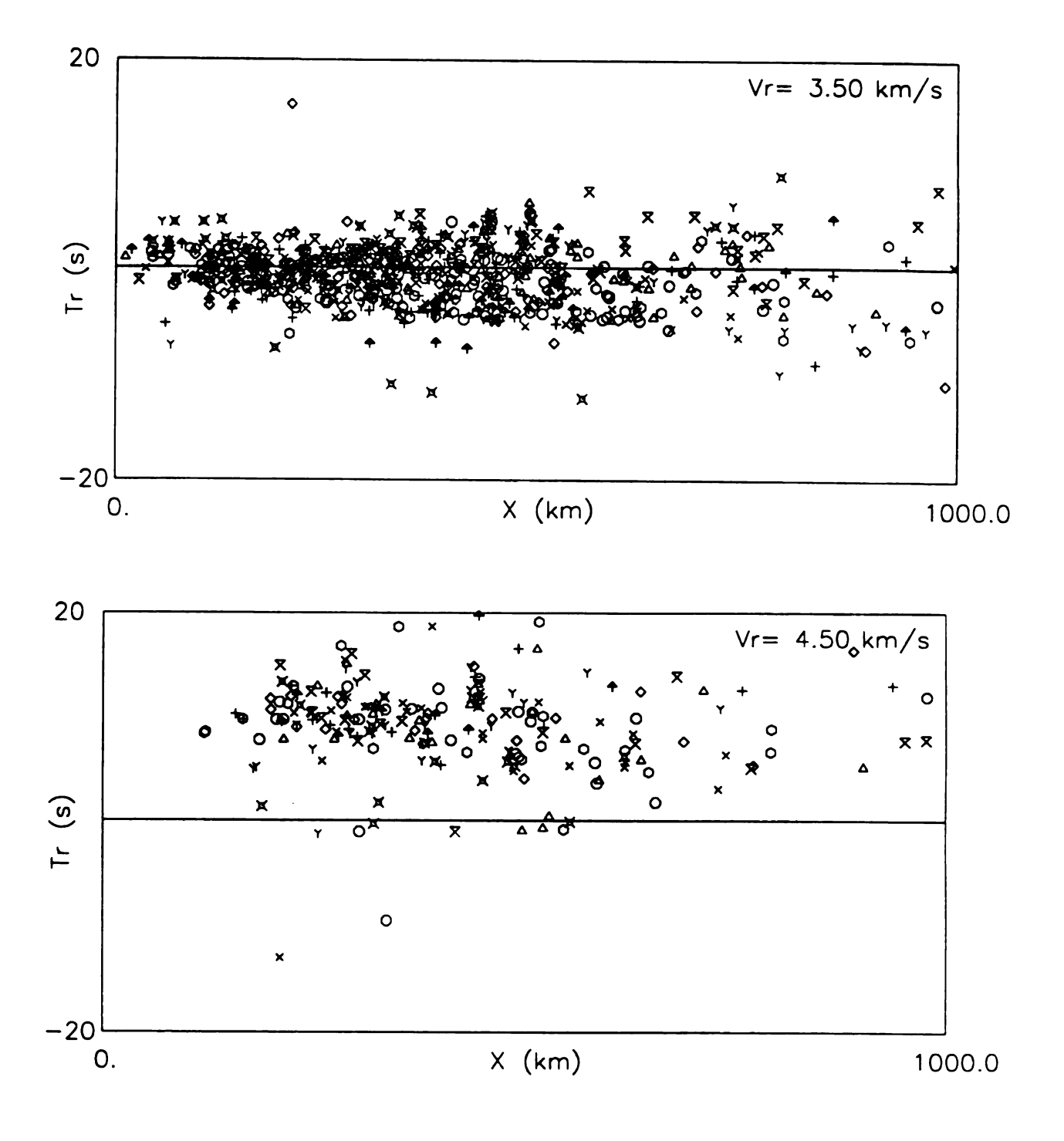


Figure 15. Reduced traveltime curves for Sg (A) and Sn (B) data of selected best 75 events using epicenters and origin times reported in *Materialy po Seismichnosti Sibiri*. Reduction velocities are noted on figures. Individual events are represented by different symbols.

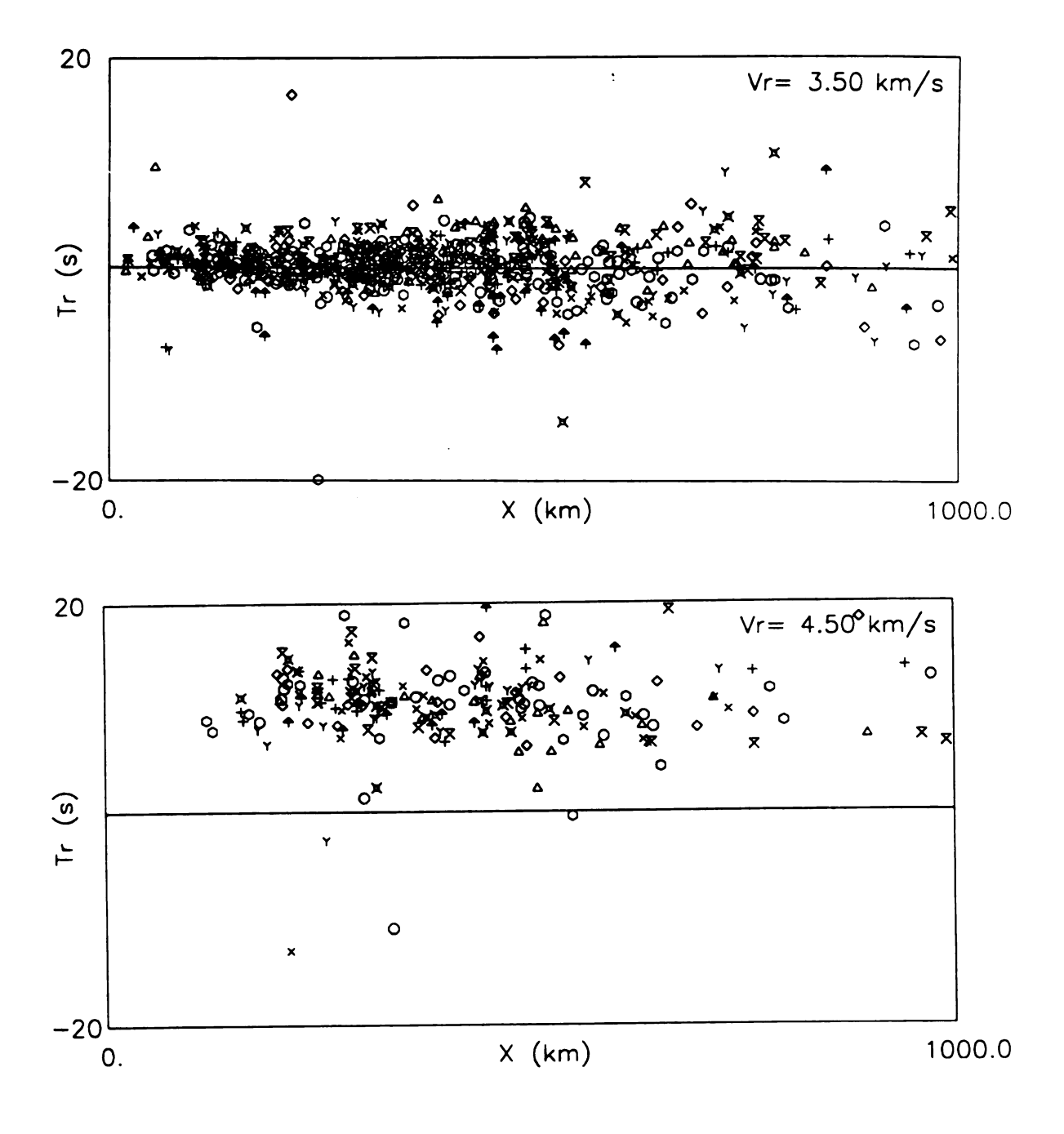


Figure 16. Reduced travel time curves for Sg (A) and Sn (B) data of selected best 75 events using epicenters and origin times determined from relocations using Pg data. Reduction velocities are noted on figures. Individual events are represented by different symbols. Note reduced scatter in data when compared Fig. 15.

travel time curve used in Magadan, which assumes a 6.1 km/sec crustal layer, according to D. Gunbin (Personal communication, 1995), and Andreev, (1984). The different Pg velocities used can account for the systematic change in epicenters that are apparent in the relocations (Fig. 9). The tendency for epicenters to move south is also evident when looking only at the selected events, although to a lesser degree (Fig. 17). In locating earthquakes, if one uses too high a velocity for Pg, but a correct velocity for Sg, the Pg-Sg time interval will be increased for any given distance. Thus, when using such a travel time curve, the apparent distance between epicenter and station will be decreased, and the origin time will be late. Note on figures 15 and 16 that a velocity of 3.50 km/sec fits the Sg data equally well using the bulletin or relocated epicenters. If the station distribution around the epicenter is not symmetric about 360° (which is the case for virtually all events in the study area), the epicenter will move toward the majority of the recording stations. Using a slower Pg velocity, the Pg-Sg time intervals will decrease for a given distance. In this case, the epicenter will move away from the recording stations, and origin time will be earlier. This occurs with the Pg arrival relocated epicenters. Figure 18 shows the azimuth from epicenter to station, relative to azimuthal change in epicenter for the relocation, using 26 events randomly selected from the best 75. For these events, there are a total of 230 Pg arrivals. I found that the epicenters moved away from the recording station in 142 of the arrivals (61.7%) and moved towards the recording station in 88 arrivals (38.3%). For the best 75 events, the origin times shifted an average of 1.16 sec earlier. In total, 56 events shifted to an earlier time, 19 shifted later, and one remained constant. With the above evidence, and considering the reduction of scatter of

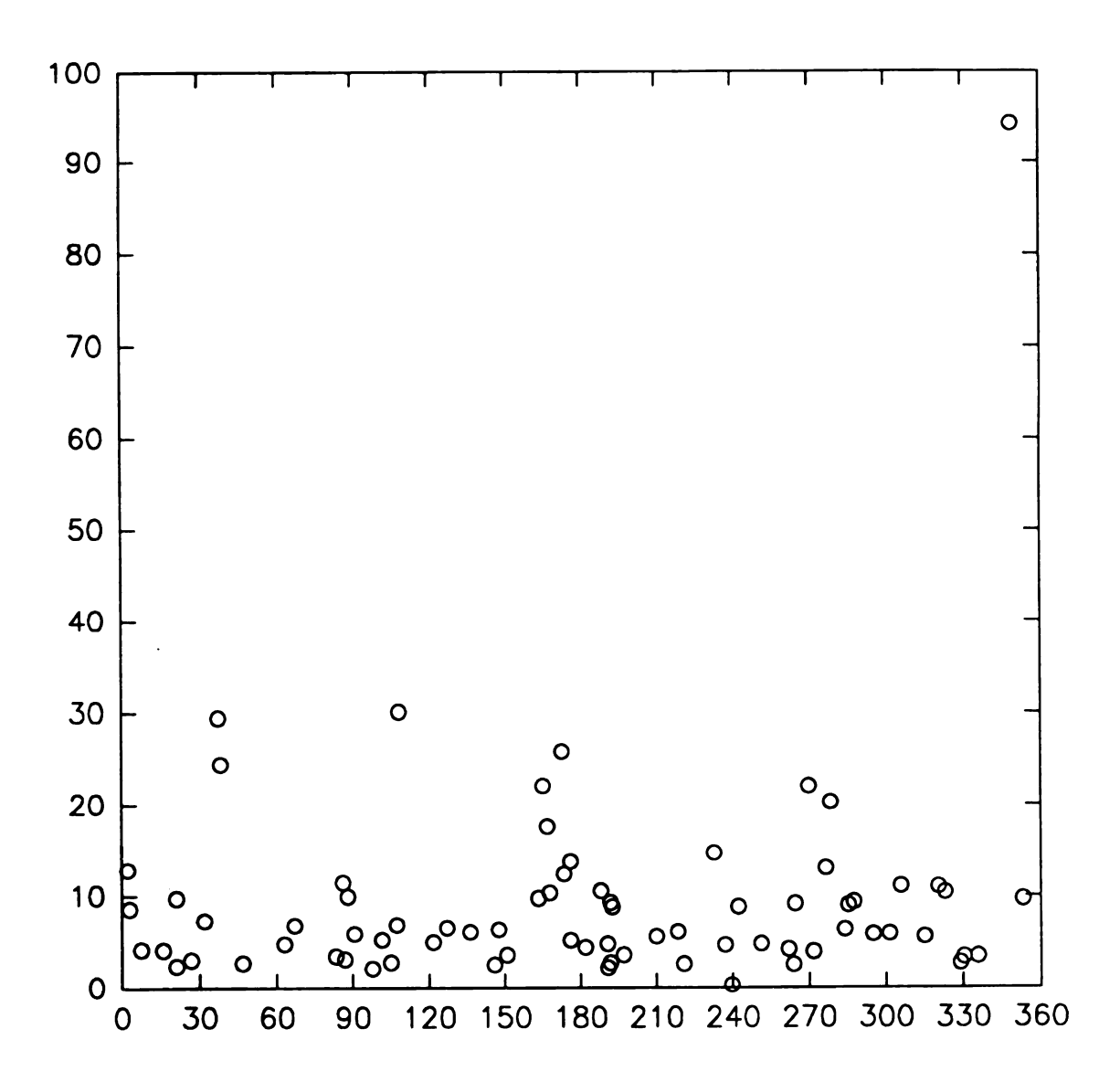


Figure 17. For selected best 75 events, azimuth from original to Pg data relocated epicenter vs. distance of epicenter change (in km). Epicenters tend to move south, indicating a systematic error in the original locations. Original epicenters taken from *Materialy Po Seismichnosti Sibiri*.

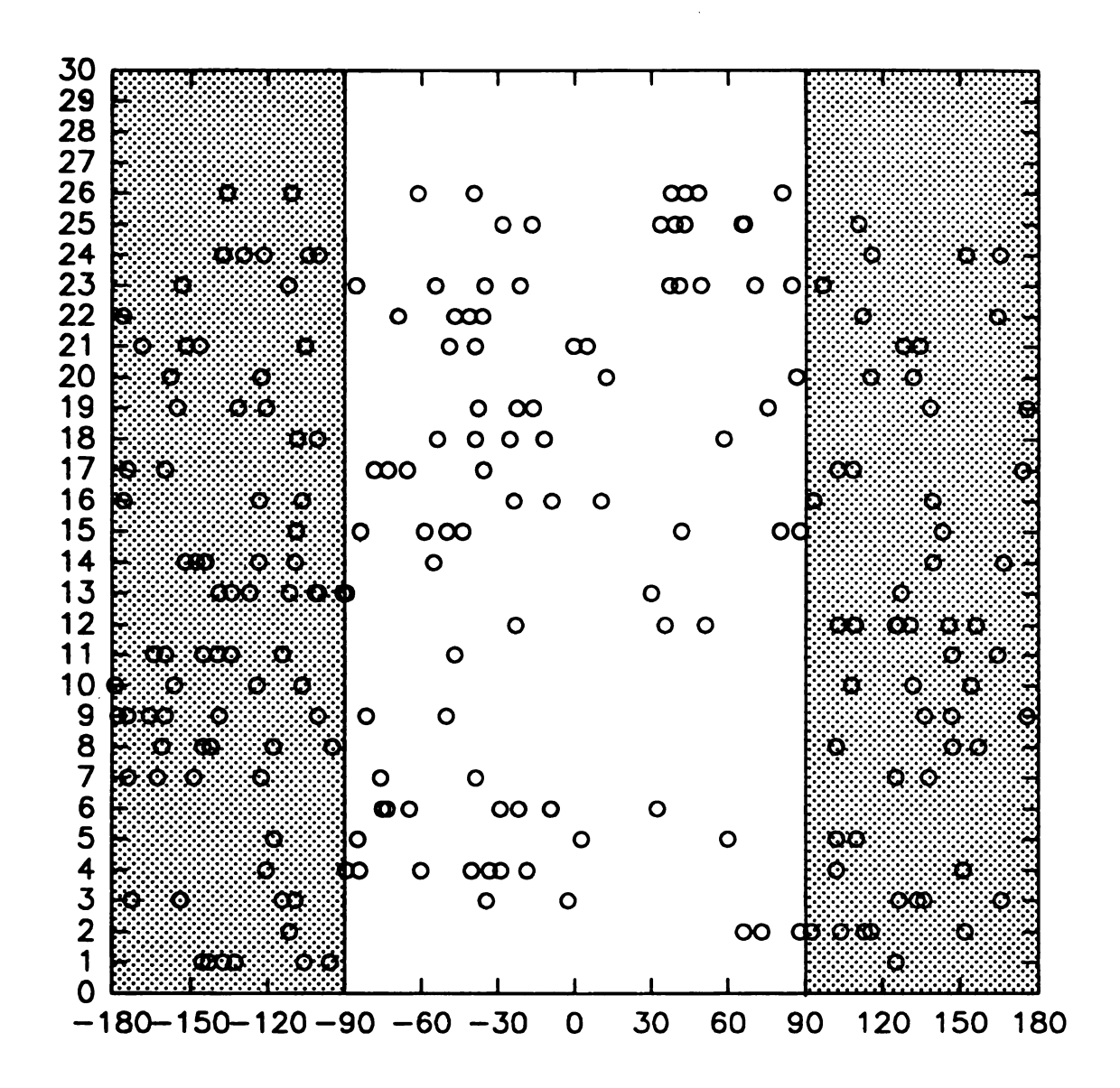


Figure 18. Angle between azimuth from relocated epicenter to station and azimuth from original epicenter to relocated epicenter for 26 of the selected best 75 events. This figure illustrates that the relocated epicenters tend to move away from the bulk of the receiving stations. Relocation moved the epicenter away from the recording stations in 142 out of 230 arrivals, denoted by the shaded regions of the plot.

Pg velocity used to determine locations listed in the Materialy catalog is too high.

Research by D. Gunbin (Personal communication, 1995) also indicates improved locations when a slower crustal velocity of 6.0 km/sec is used for the Magadan region.

The method of earthquake location used for most of the epicenters reported in *Materialy* may also contribute to errors in the epicenters. Earthquakes in the Sakha Republic (Yakutia) are still located by drawing arcs on large scale (approximately 1:8,000,000) paper maps. Considering the scale of the maps and thickness of the pencil line being drawn, errors of several kilometers may be introduced into the location process. These errors would probably be random with respect to azimuth.

In order to determine the first-order crustal structure, the method of Ruff et al., (1994) 'SQUINT' is used. This method assumes that regional travel time curves for multiple earthquakes can be approximated with a regional average crustal model. Given a set of earthquakes, the Pg travel time data are simultaneously inverted, solving for the best fit velocity for the set of events, and new origin times for individual events, assuming fixed hypocenters. For a given station, any systematic variation from the regional average should be a result of local variations in crustal structure. The Pg data was initially inverted with all spurious arrivals included (Fig. 19). Although this results in an increase in data scatter compared with the non-inverted data, it allows easy identification of dubious arrivals, which are then removed. Following the removal of spurious data, the data were again inverted for the determination of new origin times and regional crustal velocity (Fig. 20). The origin times of most events were moved 0.2-0.3

data for all phases when plotted with the Pg relocations, I conclude that the 6.1 km/sec Pg velocity used to determine locations listed in the *Materialy* catalog is too high. Research by D. Gunbin (Personal communication, 1995) also indicates improved locations when a slower crustal velocity of 6.0 km/sec is used for the Magadan region.

The method of earthquake location used for most of the epicenters reported in *Materialy* may also contribute to errors in the epicenters. Earthquakes in the Sakha Republic (Yakutia) are still located by drawing arcs on large scale (approximately 1:8,000,000) paper maps. Considering the scale of the maps and thickness of the pencil line being drawn, errors of several kilometers may be introduced into the location process. These errors would probably be random with respect to azimuth.

In order to determine the first-order crustal structure, the method of Ruff et al., (1994) 'SQUINT' is used. This method assumes that regional travel time curves for multiple earthquakes can be approximated with a regional average crustal model. Given a set of earthquakes, the Pg travel time data are simultaneously inverted, solving for the best fit velocity for the set of events, and new origin times for individual events, assuming fixed hypocenters. For a given station, any systematic variation from the regional average should be a result of local variations in crustal structure. The Pg data was initially inverted with all spurious arrivals included (Fig. 19). Although this results in an increase in data scatter compared with the non-inverted data, it allows easy identification of dubious arrivals, which are then removed. Following the removal of spurious data, the data were again inverted for the determination of new origin times and regional crustal velocity (Fig. 20). The origin times of most events were moved 0.2-0.3

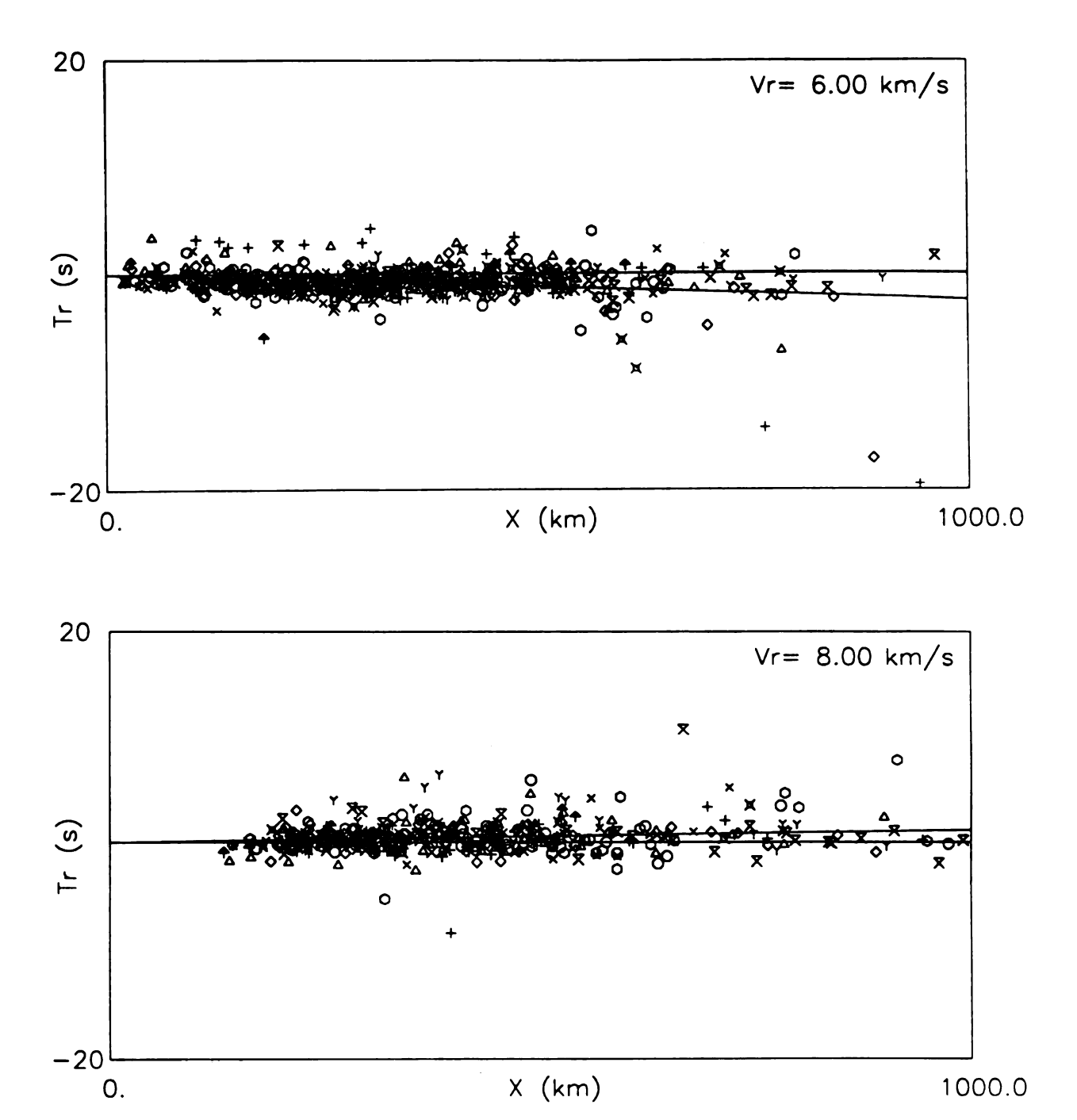
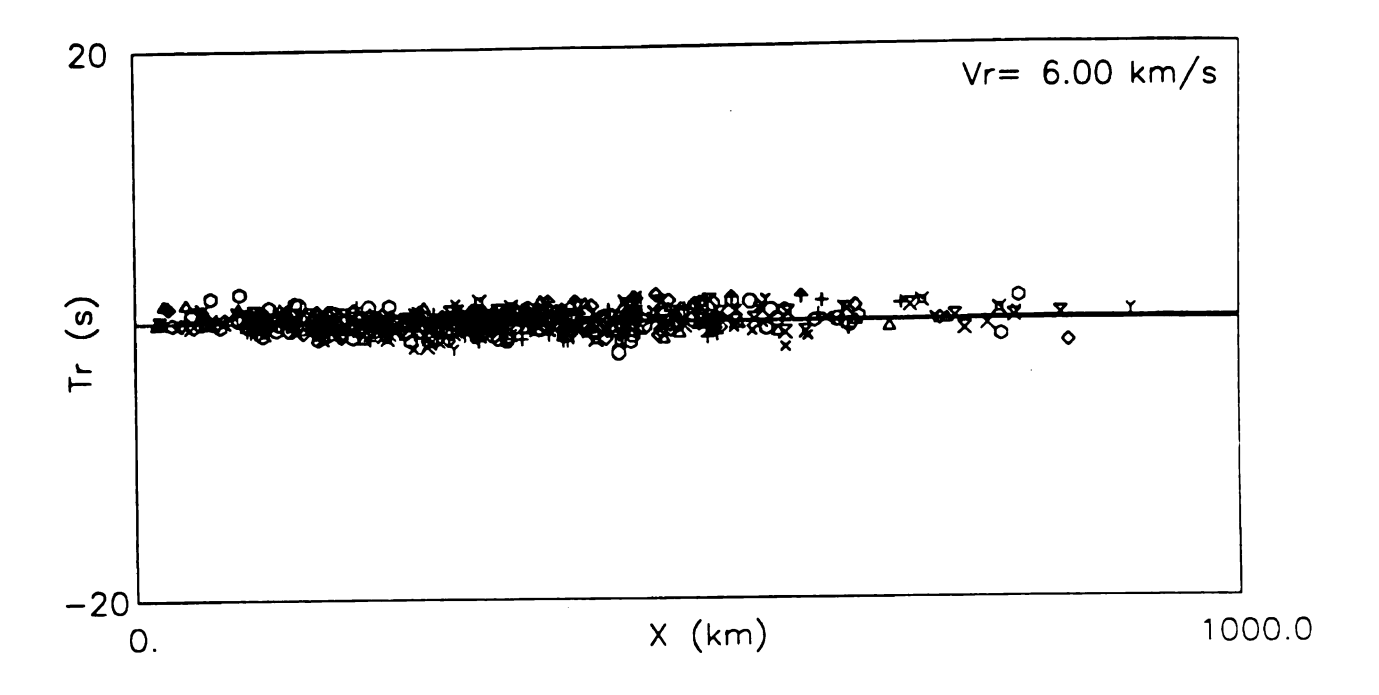


Figure 19. Reduced traveltime curves for Pg (A) and Pn (B) data of selected best 75 events using relocated epicenters and origin times determined from the 'SQUINT' inversion program. All data was included for this inversion trial. Individual events are represented by different symbols.



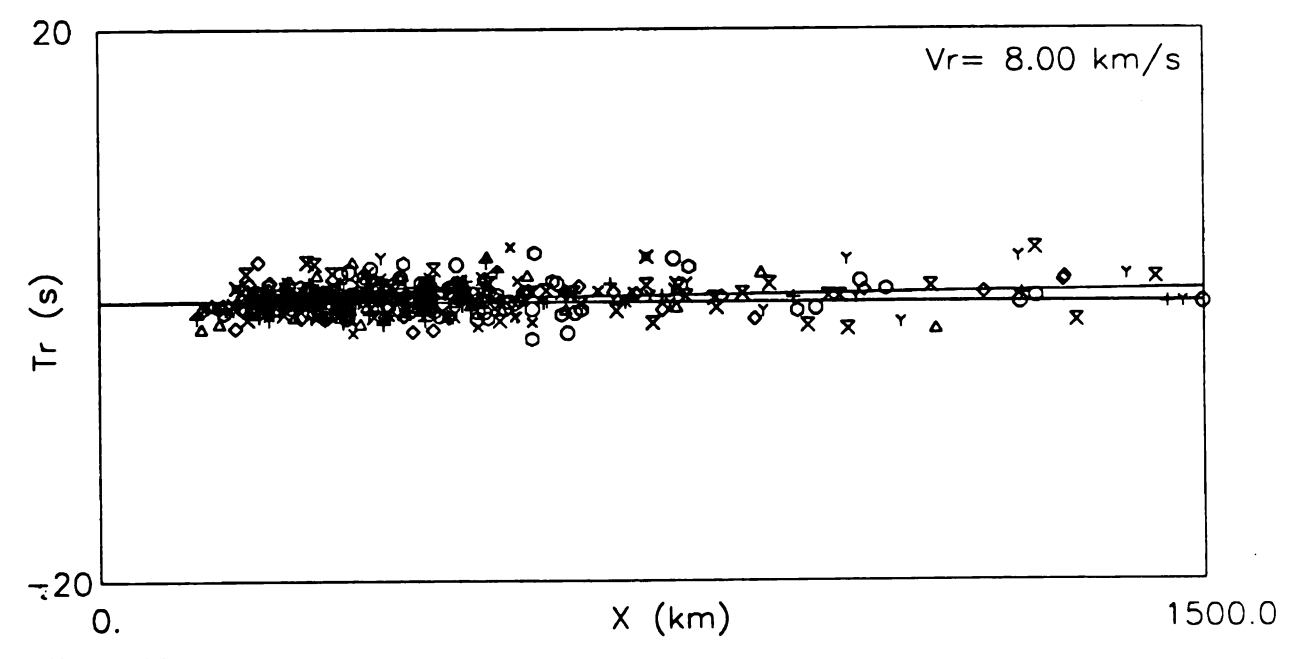


Figure 20. Reduced traveltime curves for Pg (A) and Pn (B) data of selected best 75 events. Epicenter relocations used are computed with Pg data, while origin times determined from the 'SQUINT' inversion program after high residual arrivals were removed. These traveltime curves indicate a Pg velocity of 5.992 ± 0.007 km/sec and a Pn velocity of 7.961 ± 0.015 km/sec. Reduction velocities are noted on figures. Individual events are represented by different symbols.

seconds later from the origin time determined in the Pg relocation (Table 1). The reason for the consistent shifts in origin times is not clear, though may be related to incorrect assumptions about source depth. Using the Pg relocation epicenter, the Pn data were also inverted, first for identification of spurious arrivals (Fig. 19), which were subsequently removed. The Pn data were again inverted to determine the regional Pn velocity. Although inversion of the Pn data reveals nothing with respect to origin time, it does allow the best determination of the regional Pn velocity. Knowledge of the regional Pn velocity is necessary for the interpretation of the regional crustal structure.

As a result of this inversion the apparent velocities and crossover distance, and thus approximate crustal thickness are obtained for the study area as a whole (Fig. 21). Results for the Magadan region and Sakha Republic (Yakutia) indicate a simple structure with a 5.992 ± 0.007 km/sec layer overlying a 7.961 ± 0.015 km/sec layer. Average thickness is about 37 km. Data at shorter epicentral distances (< 260 km) suggest a slightly higher Pg velocity; the reason for this is likely related to misidentification of phases at the crossover distance. This apparent slightly higher crustal velocity is visible on the regional crustal travel time curve as a slight downwarp in the data (Fig. 20). I do not believe this downwarp to be caused from a 6.7 km/sec intermediate layer as reported by Ansimov et al. (1967). The existence of a 6.7 km/sec refracting intermediate layer should cause a significant number of mispicked Pg and Pn phases at distances greater than the crossover, which is not evident on any plotted traveltime curve.

seconds later from the origin time determined in the Pg relocation (Table 1). The reason for the consistent shifts in origin times is not clear, though may be related to incorrect assumptions about source depth. Using the Pg relocation epicenter, the Pn data were also inverted, first for identification of spurious arrivals (Fig. 19), which were subsequently removed. The Pn data were again inverted to determine the regional Pn velocity. Although inversion of the Pn data reveals nothing with respect to origin time, it does allow the best determination of the regional Pn velocity. Knowledge of the regional Pn velocity is necessary for the interpretation of the regional crustal structure.

As a result of this inversion the apparent velocities and crossover distance, and thus approximate crustal thickness are obtained for the study area as a whole (Fig. 21). Results for the Magadan region and Sakha Republic (Yakutia) indicate a simple structure with a 5.992 ± 0.007 km/sec layer overlying a 7.961 ± 0.015 km/sec layer. Average thickness is about 37 km. Data at shorter epicentral distances (< 260 km) suggest a slightly higher Pg velocity; the reason for this is likely related to misidentification of phases at the crossover distance. This apparent slightly higher crustal velocity is visible on the regional crustal travel time curve as a slight downwarp in the data (Fig. 20). I do not believe this downwarp to be caused from a 6.7 km/sec intermediate layer as reported by Ansimov et al. (1967). The existence of a 6.7 km/sec refracting intermediate layer should cause a significant number of mispicked Pg and Pn phases at distances greater than the crossover, which is not evident on any plotted traveltime curve.

Table 1. New origin times for the selected best 75 events, computed by 'SQUINT'. Relocation origin times from Pg phase relocations.

37

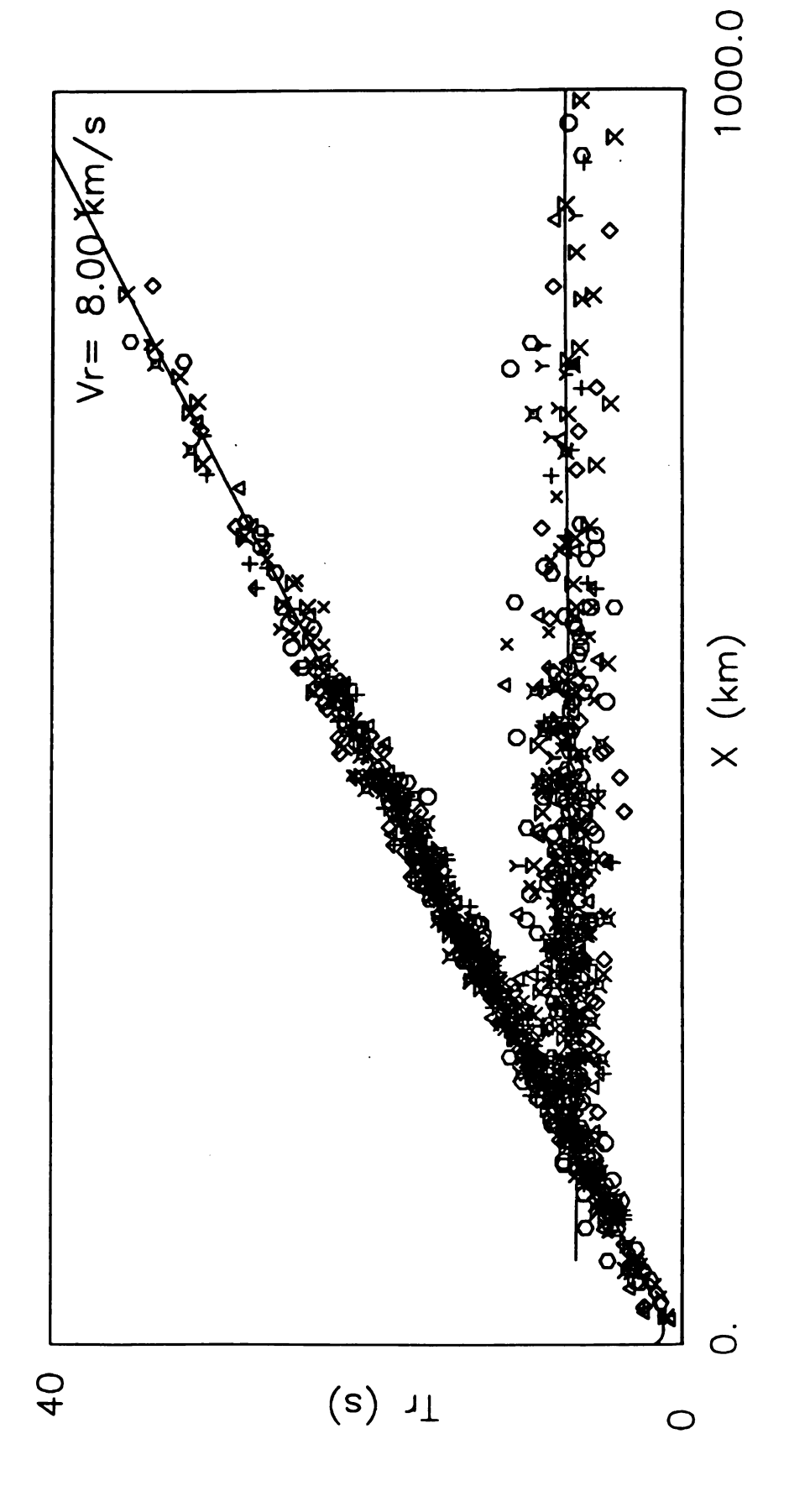
TABLE 1

DATE	RELOCATION	TIME	NEW O.T.
	O.T.	SHIFT (S)	
81-02-02	19:15:15.5	+0.19	19:15:15.69
81-05-10	18:08:25.8	+0.28	18:08:26.08
81-11-08	21:56:08.9	+0.28	21:56:09.19
81-11-10	10:54:15.5	+0.20	10:54:15.70
81-11-11	14:22:18.5	+0.22	14:22:18.72
81-12-08	10:57:20.6	+0.26	10:57:20.86
82-04-06	14:41:13.9	-0.38	14:41:13.52
82-08-04	20:17:03.5	+0.27	20:17:03.77
82-12-22	15:47:03.6	+0.22	15:47:03.82
83-03-12	11:55:11.7	+0.09	11:55:11.79
83-03-25	10:36:55.1	+0.19	10:36:55.29
83-05-09	16:48:05.3	+0.29	16:48:05.59
83-10-25	19:44:59.9	+0.17	19:45:00.07
84-08-21	17:41:02.7	-0.23	17:41:02.47
84-12-02	08:35:45.1	+0.35	08:35:45.45
84-12-02	18:17:54.9	+0.23	18:17:55.13
85-01-21	18:03:50.4	+0.25	18:03:50.65
85-01-24	20:26:33.2	+0.28	20:26:33.48
85-01-29	00:36:06.2	+0.02	00:36:06.22
85-03-08	22:24:37.8	+0.32	22:24:38.12
85-06-02	04:08:08.8	+0.31	04:08:09.11
85-11-28	08:38:20.5	+0.20	08:38:20.70
86-01-18	13:13:22.0	+0.28	13:13:22.28
86-02-15	20:30:26.3	+0.20	20:30:26.50
86-03-07	23:28:08.2	+0.23	23:28:08.43
86-04-06	01:27:20.5	+0.22	01:27:20.72
86-12-18	18:04:11.2	+0.27	18:04:11.47
86-12-26	03:21:04.5	+0.31	03:21:04.81
87-02-11	00:58:19.8	+0.26	00:58:20.06
87-02-11	01:03:08.0	+0.19	01:03:08.19
87-02-11	01:09:50.8	+0.28	01:09:51.08
87-02-11	06:19:16.3	+0.40	06:19:16.70
87-02-11 87-02-11	07:28:17.5	+0.17 +0.19	07:28:17.67 11:36:16.29
	11:36:16.1	+0.19	00:09:28.39
87-03-04 87-04-13	00:09:28.0 21:20:12.8	+0.39	21:20:12.98
87-04-13 87-09-09	04:43:22.8	+0.18	04:43:23.10
88-02-19	00:04:04.0	+0.30	00:04:04.23
88-02-19 88-02-19	23:50:24.9	+0.23	23:50:25.08
88-04-03	02:01:28.6	+0.16	02:01:28.76
88-05-25	16:55:43.7	+0.16	16:55:43.75
88-06-09	13:37:32.9	+0.05	13:37:33.07
88-06-14	13:37:32.9	+0.17	13:37:33:07 14:44:44.34
88-10-17	00:27:59.2	+0.24	00:27:59.46
88-10-17 89-01-29	23:23:01.6	+0.26	23:23:01.83
89-01-29 89-03-21	10:53:05.1	+0.23	10:53:05.26
07-U3-21	10:55:05.1	+0.10	10.55.05.20

Table 1 (continued)

89-04-09	04:16:23.0	+0.43	04:16:23.43
89-06-16	07:36:08.5	+0.16	07:36:08.66
89-07-07	10:51:43.1	+0.14	10:51:43.24
89-07-09	18:11:49.0	+0.21	18:11:49.22
89-10-04	20:56:47.2	+0.52	20:56:47.72
90-03-29	20:47:29.7	+0.11	20:47:29.81
90-05-30	11:56:45.1	+0.27	11:56:45.37
90-06-25	07:33:51.7	+0.21	07:33:51.91
90-07-12	02:22:50.5	+0.18	02:22:50.68
90-08-24	01:04:44.6	+0.28	01:04:44.88
90-11-01	13:42:06.1	+0.27	13:42:06.37
90-11-02	21:54:03.2	+0.31	21:54:03.51
90-11-22	19:36:25.1	+0.28	19:36:25.38
90-12-13	21:34:39.1	+0.26	21:34:39.36
91-02-10	18:16:32.3	+0.13	18:16:32.43
91-03-01	01:57:04.1	+0.38	01:57:04.48
91-07-02	13:43:45.0	+0.27	13:43:45.27
91-07-31	01:44:02.7	+0.32	01:44:03.02
91-08-04	10:08:05.9	+0.25	10:08:06.15
91-08-04	19:14:40.6	+0.17	19:14:40.77
91-08-26	09:35:49.0	+0.40	09:35:49.40
92-01-22	06:29:16.1	+0.33	06:29:16.43
92-02-12	17:14:51.2	+0.28	17:14:51.48
92-06-28	23:53:17.4	+0.23	23:53:17.63
92-11-17	07:55:13.8	+0.22	07:55:14.02
93-03-05	04:21:05.1	+0.20	04:21:05.30
93-03-22	18:14:06.8	+0.21	18:14:07.01
93-03-24	16:18:05.9	+0.27	16:18:06.17
93-08-30	07:56:34.9	+0.37	07:56:35.27

Figure 21. Reduced traveltime curve for combined Pg and Pn data. All data plotted use the Pg data relocated epicenter and origin times from the 'SQUINT' inversion program after high residual arrivals were removed. The Pg-Pn crossover point is consistant with a regional crustal thickness of 37 km (optically determined). Pg velocity plotted is 5.99 km/sec, and Pn velocity is 7.96 km/sec. Reduction velocities are noted on figures. Individual events are represented by different symbols.



Individual Stations

I next examined the travel time data for individual stations. A best-fit crustal structure was estimated based on travel time curves derived from relocated epicenters and inverted origin times. Best-fit lines to the data were determined optically. The use of seventy five events in the analysis results in a lack of data at some outlying stations, and thus poorer determinations of velocities and crustal thickness. This primarily affects the stations in northern Yakutia. This problem is more serious for the mantle refraction, Pn. Sufficient data were available for 27 stations, and present data suggests that structural variations between stations in the study area are resolvable with this method. Based on final results, the errors in determining crustal thickness appear to be ±4-5 km, Pg velocities, ±0.03 km/sec, and Pn velocities, ±0.1 km/sec. In general, Sg velocities appear to be 3.5 ±0.04 km/sec, while Sn velocities are generally unobtainable. There is some trade off between Pn velocity and crustal thickness; higher velocities usually result in greater thicknesses. The use of a computer data-fitting routine will improve these determinations. The use of additional data, particularly from outlying regions would also improve the crustal parameter determinations.

The results (Tables 2 and 3) suggest that velocities and thicknesses are very close to those determined to be the regional average. Most stations are fit well with a 6.00 km/sec Pg velocity, a 7.99 km/sec Pn velocity, and a 37 km depth. Magadan (Fig. 22) and Takhtoyamsk (Fig. 23) appear to have greater thicknesses of 40 km, although both are constrained by a small number of observations. Significantly, both of these stations

Table 2

COMPARISON OF CRUSTAL THICKNESSES

This Study	K F F 4 8 8 K F 8 8 8 F 8 8 E F F F 8 8 8 8 8 5 4
Neustroev and Parfenov (1985)	5 4 5
Bulin (1989)	37 04 4 4
Mishin and Dareshkins (1966)	38.9 38.9 30.2 40 31.0
Vaschilov (1979) ⁵	33.8 (36.0) 38.9 (41.2) 38.9 (40.1) 30.2 (31.8) 31.0 (32.9)
Suvorov and Komikva (1986)	26±3 30±2* 29±7 33±13 33±3 37±6
Bobrobnikov and Emailov (1989) ²	43.0 38.9 34.0 31.0 50.0
Belyaevsky and Bonisov (1974)	46 46 38 46 46 37 45 (7)
Belyaevsky (1974)	£ 8 8 E
Station	Batagai Debin Evensk Khandyga Kulu Magadan Moma Moma Myakii Naiba Neikoba Nezhdaninskoe Omolon Omsukchan Saidy Saidy Saidy Saidy Saidy Saidy Saidy Saidy Saidy Saidy Saidy Suchan Tablakh Talakh Talakh Usi' Nena Usi' Omchug Yakutsk Yubileinaya Zyryanka
Code	BTG DBI EVE KHG KHG KU- MAGG MACO MYA NAY NAY NAY NAY NAY NAY NAGD SAY SSY SSY SSY SSY SSY STU TTY TTY TTY TTY TTY TTY TTY TTY TTY T

³Values reported by Bobrobnikov and Izmailov (1989) attributed to Mishin and Dareshkina (1966). Bobrobnikov and Izmailov (1989) consider the value for Debin to be an error.

³Data from Belyaevsky (1974) and Belyaevsky and Borisov (1974) for Garmanda, about 20 km north of Evensk.

⁴Suvorov and Komilova (1986) used Magadan as a calibration point based on the 1959 deep seismic sounding line.

⁵First column is attributed to Mishin and Dareshkina (1966), while values in brackets are from P-S conversions determined with a different formula. Attributed to work by Nikolaevsky.

Table 3
PN AND PG VELOCITIES

Station	Pg This Study	Pn This Study	Pn Suvorov and Kornilova (1986)
Batagai	5.97	7.94	8.1
Debin	5.99	7.97	
Evensk	6.01	8.07	
Khandyga	6.00	8.10	8.1-8.2
Kulu	5.98	7.73	
Magadan	6.01	8.00	
Moma	6.03	7.98	8.1
Myakit	5.99	7.90	
Naiba	5.96	7.70	
Nelkoba	5.97	7.87	
Nezhdaninskoe	5.98	7.98	
Omolon	5.98	7.98	
Omsukchan ¹	5.99	8.00	
Saidy	6.01	8.04	
Sasyr	5.98	8.00	
Seimchan	5.98	8.00	7.9-8.1
Sinegore	6.00	8.00	
Stekolnyi	5.98	8.04	
Susuman	6.00	7.96	7.9-8.0
Tabalakh	6.01	7.94	
Takhtoyamsk	6.02	8.10	
Talaya	5.96	8.10	
Tenkeli	5.98		
Ust' Nera	5.99	7.95	8.0-8.1
Ust' Omchug	6.05	7.90	7.9-8.1
Yakutsk	6.03	8.00	
Yubileinaya	5.96	7.49	
Zyryanka	5.98	8.22	
REGIONAL	5.99	8.00	

¹ Mishin and Dareshkina (1966) calculated a Pg velocity for Omsukchan of 6.02 km/sec by the method of Gaiskii.

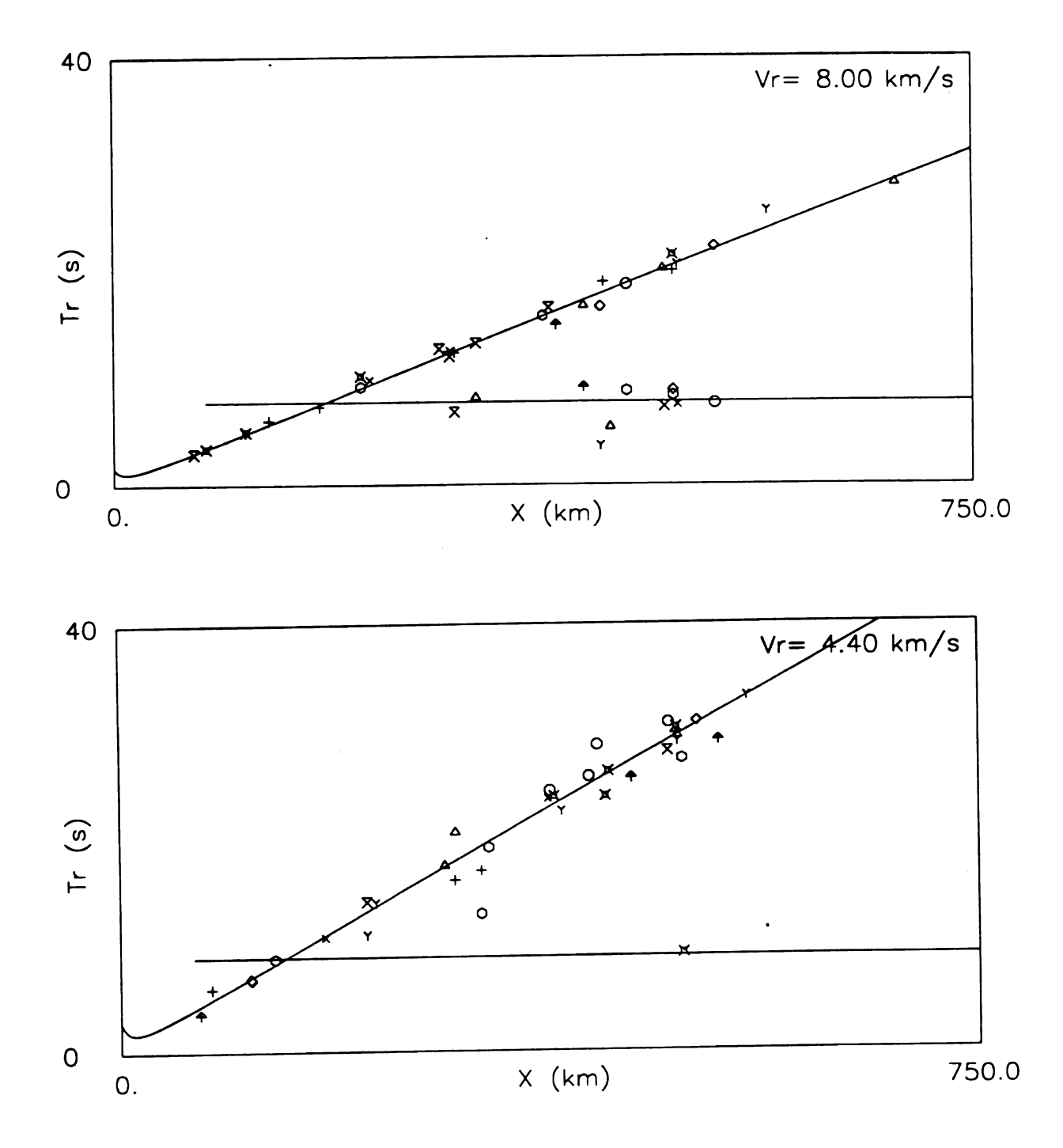
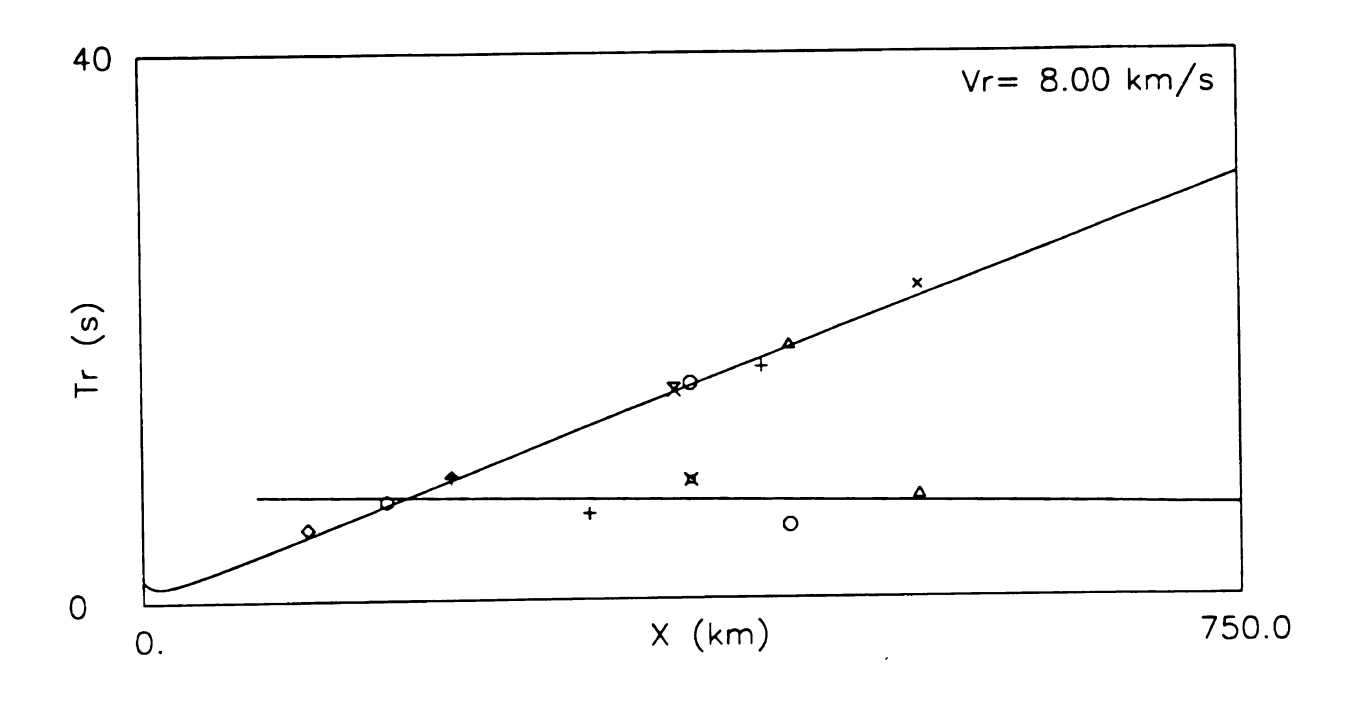


Figure 22. Magadan station traveltime curves and crustal model. Upper plot shows Pg and Pn data with velocities of 6.01 km/sec and 8.00 km/sec respectively. The Pg-Pn crossover point is consistent with a crustal thickness of 40 km. Lower plot shows Sg and Sn data. Sg data is best fit with a velocity of 3.50 km/sec. No attempt was made to fit Sn data. All velocities and crustal thickness were fit optically. Reduction velocities are noted on figures. Individual events are represented by different symbols.



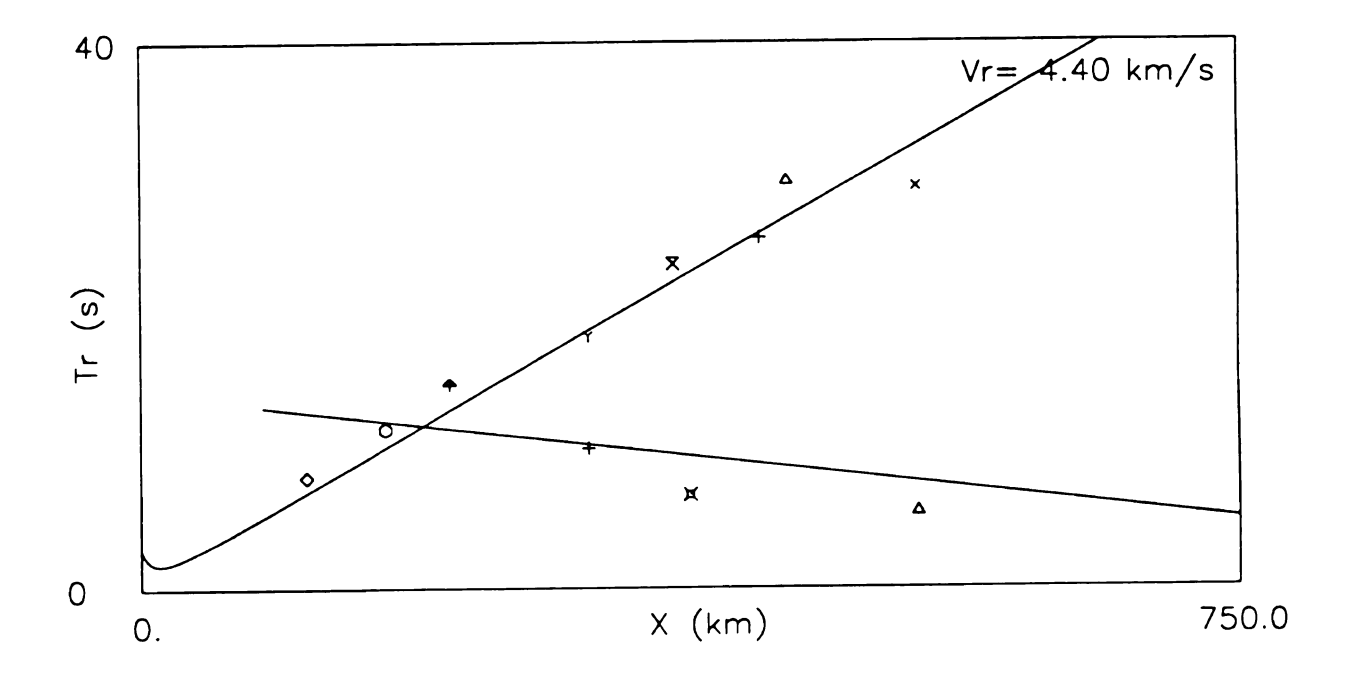


Figure 23. Takhtoyamsk station reduced traveltime curves and crustal model. Pg velocity 6.02 km/sec, Pn velocity 8.10 km/sec, and crustal thickness 40 km. Sg velocity 3.47 km/sec. Conventions as in Figure 22.

are located on the southern edge of the Okhotsk-Chukotka volcanic belt. In the region of Magadan and Takhtoyamsk, the Okhotsk-Chukotka volcanic belt overlies the Kony-Murgal terrane. The Kony-Murgal terrane is composed primarily of an accreted sequence of island are volcanic, plutonic, and related sedimentary rocks dating from Late Jurassic to Early Cretaceous (Nokleberg et al., 1994; Watson and Fujita, 1985). Results are also in good agreement with the deep seismic sounding results from the upper Yama River valley, also near this suture, reported by Bobrobnikov and Izmailov (1989). extrapolation of the Magadan-Ust' Srednikan DSS profile, the crustal thickness at Magadan is estimated to be approximately 30 km (Davydova et al., 1968; Ansimov et el. 1967; Suvorov and Kornilova, 1986). However, Magadan is located on a separate terrane from the area actually covered by DSS profiles, and no data is available directly under Magadan. Therefore, it may not be a valid assumption to extrapolate for crustal thickness and velocities. It should be noted that for both Magadan and Takhtoyamsk, the Pn data are sparse or scattered, with only one or two points controlling Pn velocity and crustal thickness. Both crustal thickness and Pn velocity could be affected significantly by alteration of only one data point in each plot. The Pg data for Magadan and Takhtoyamsk fit well with velocities of 6.01 km/sec and 6.02 km/sec respectively. There is no clear evidence in the data to support a 6.7 km/sec lower crust as observed along the Magadan - Ust' Srednikan profile (Ansimov et al., 1967).

Stekolnyi is located approximately 70 km north of Magadan within the Viliga terrane. This terrane consists primarily of a thick section of Carboniferous, Permian, Triassic, and Jurassic marine clastic rocks with some intermixed volcanics (Nokleberg et

al., 1994). This study derives a crustal thickness of 37 km for Stekolnyi, with Pg and Pn velocities of 5.98 km/sec, and 8.04 km/sec respectively (Fig 24). S wave data are fit well with Sg and Sn velocities of 3.48 km/sec and 4.6 km/sec, with a crustal thickness of 38 km. The Sn data show considerable scatter, thus the Sn velocity and thickness are unreliable. The crustal thickness here is in good agreement with the P-Ps conversion study by Belyaevsky and Borisov (1974), which indicates a 37 km thick crust. The thickness determined in this study is a bit higher than the 31-32 km indicated by the DSS line. The data for Stekolnyi are considered good, as the velocities are constrained by many points.

To the north of Stekolnyi, within the Viliga terrane, are the stations Debin, Myakit, Omsukchan, Seimchan, and Sinegor'e. These stations are all within a 200 km radius, and are fit well with a thickness of 37 km and Pg velocity of 5.98-6.00 km/sec (Figs 25-29). Mishin and Dareshkina (1966) calculated a Pg velocity for Omsukchan of 6.02 km/sec using the "method of Gaiskii". Pn velocity is 8.00 km/sec for these stations, with the exception of Myakit and Debin, where velocities are 7.90 km/sec and 7.97 km/sec respectively. Sg velocities are also well constrained at 3.52 km/sec for Seimchan and Omsukchan and 3.50 km/sec for Debin. The scatter in the Debin Pn data are considerable, while Myakit and Sinegor'e have Pn data over a short epicentral distance, thus Pn velocities have large error bars. For both Seimchan and Omsukchan, the velocities and thickness are well constrained. There are no previous velocities or thickness reported for Sinegor'e or Myakit, and only Belyaevsky (1974) reports a thickness for Debin, at 43 km. Bobrobnikov and Izmailov (1979) believe the 43 km figure for Debin to be in error. Previous determinations for crustal thickness at

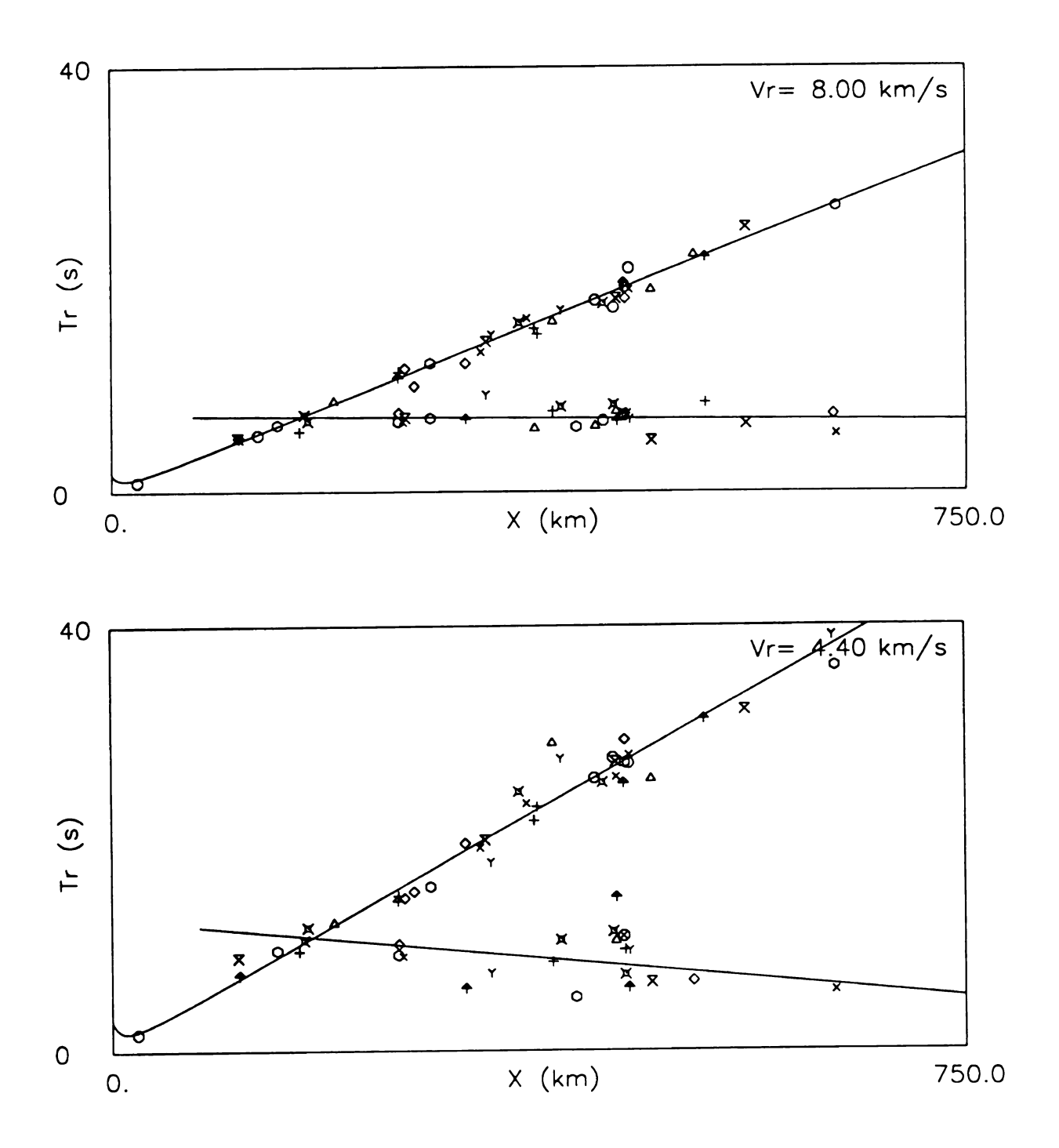
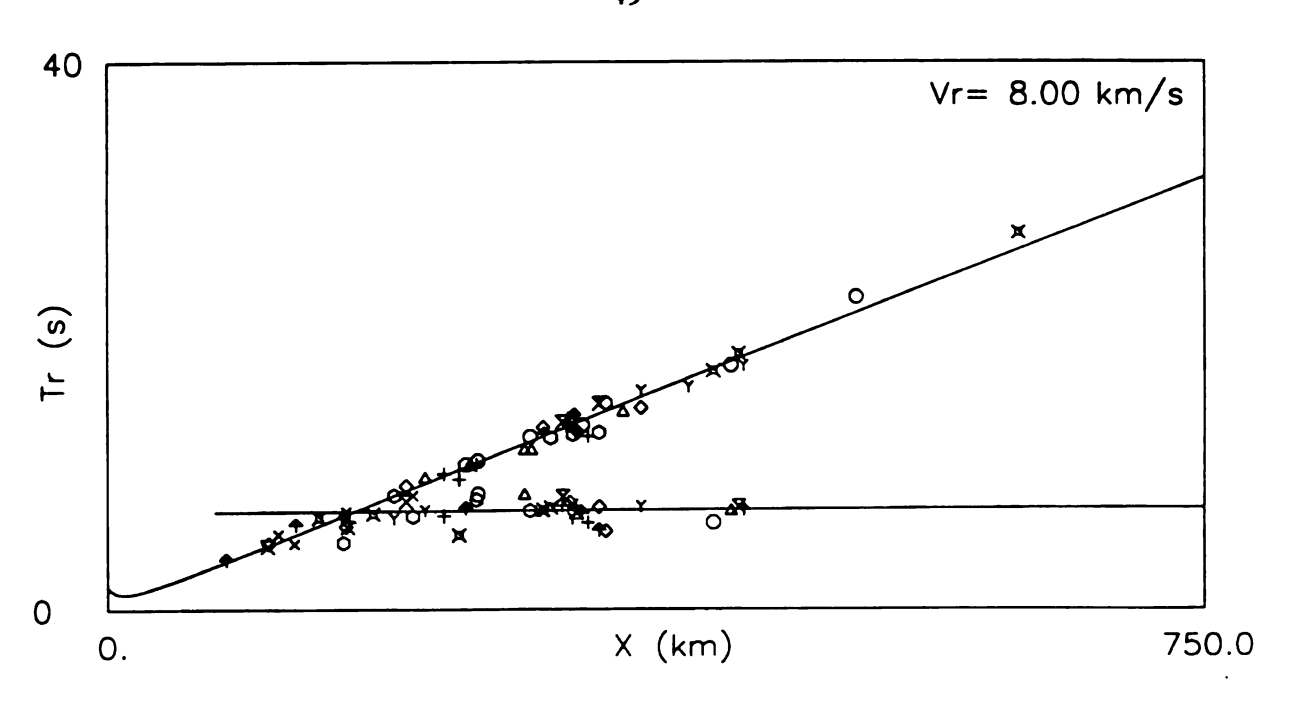


Figure 24. Stekolnyi station reduced traveltime curves and crustal model. Pg velocity 5.98 km/sec, Pn velocity 8.04 km/sec, and crustal thickness 37 km. Sg velocity 3.48 km/sec. Conventions as in Figure 22.



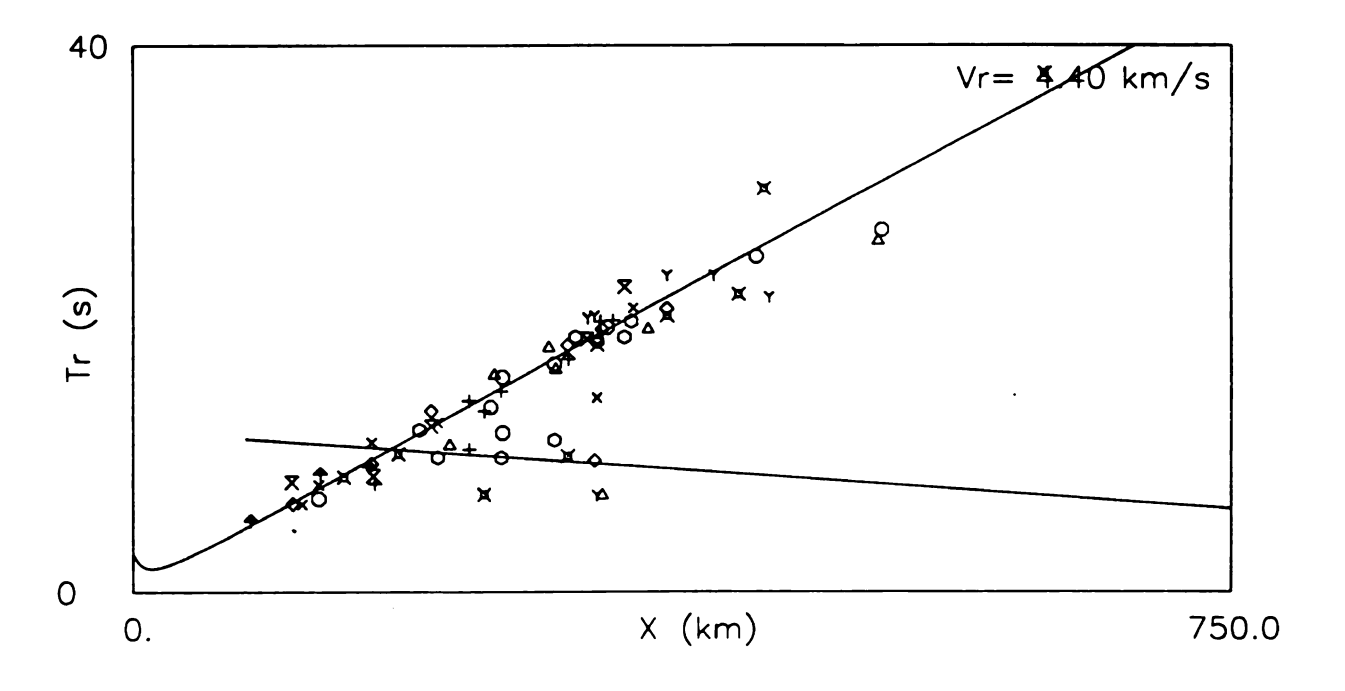
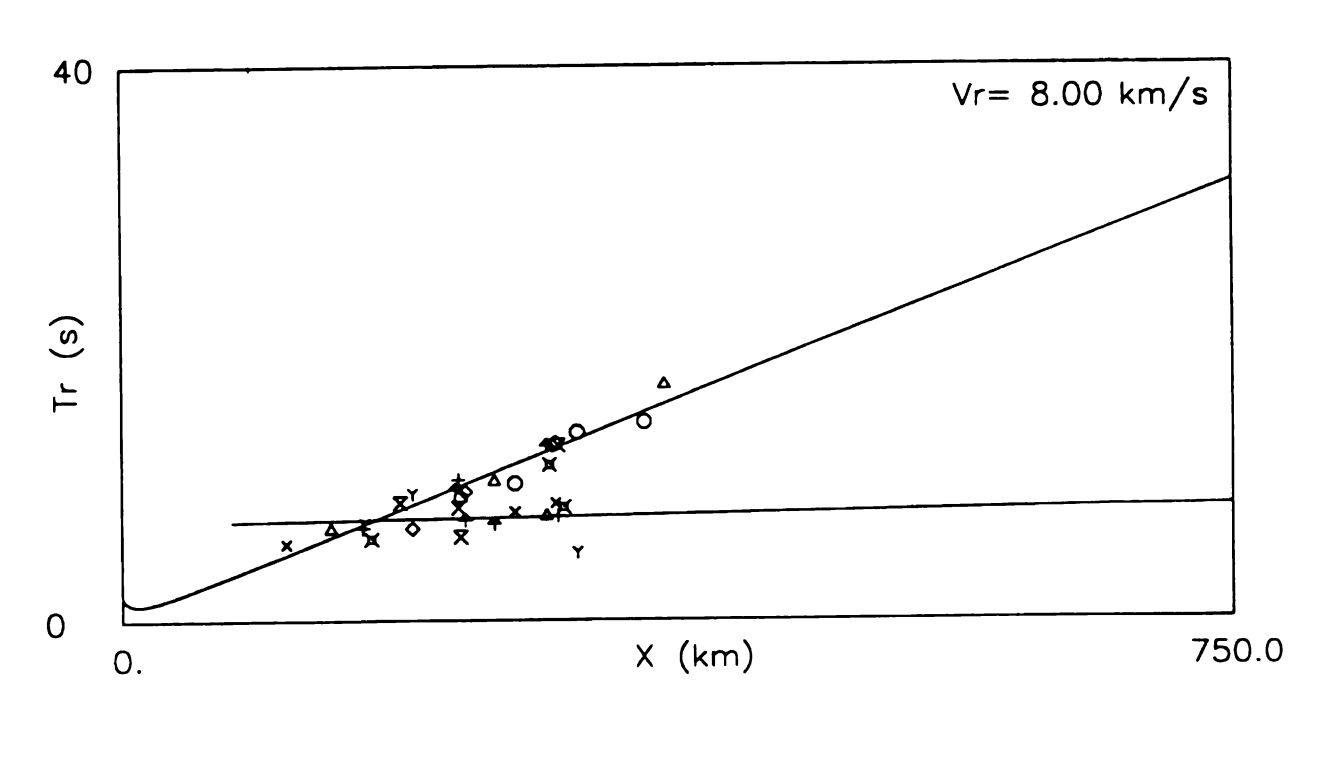


Figure 25. Debin station reduced traveltime curves and crustal model. Pg velocity 5.99 km/sec, Pn velocity 7.97 km/sec, and crustal thickness 37 km. Sg velocity 3.50 km/sec. Conventions as in Figure 22.



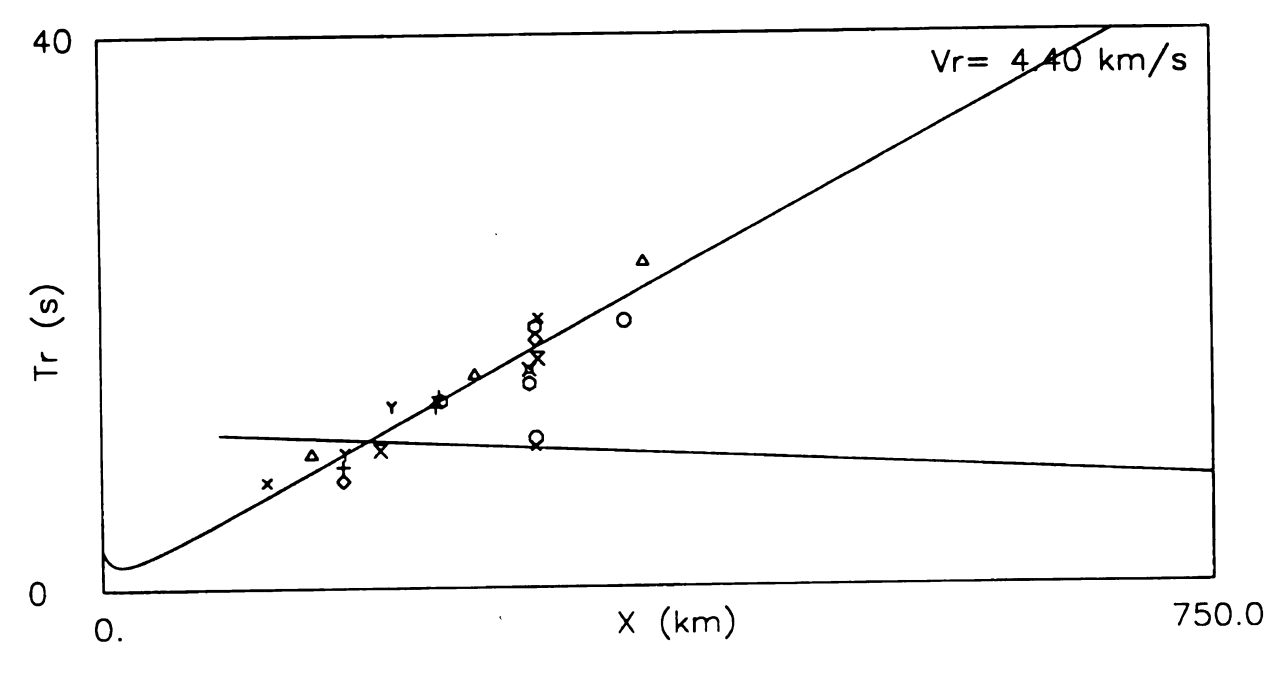


Figure 26. Myakit station reduced traveltime curves and crustal model. Pg velocity 5.99 km/sec, Pn velocity 7.90 km/sec, and crustal thickness 37 km. Sg velocity 3.50 km/sec. Conventions as in Figure 22.

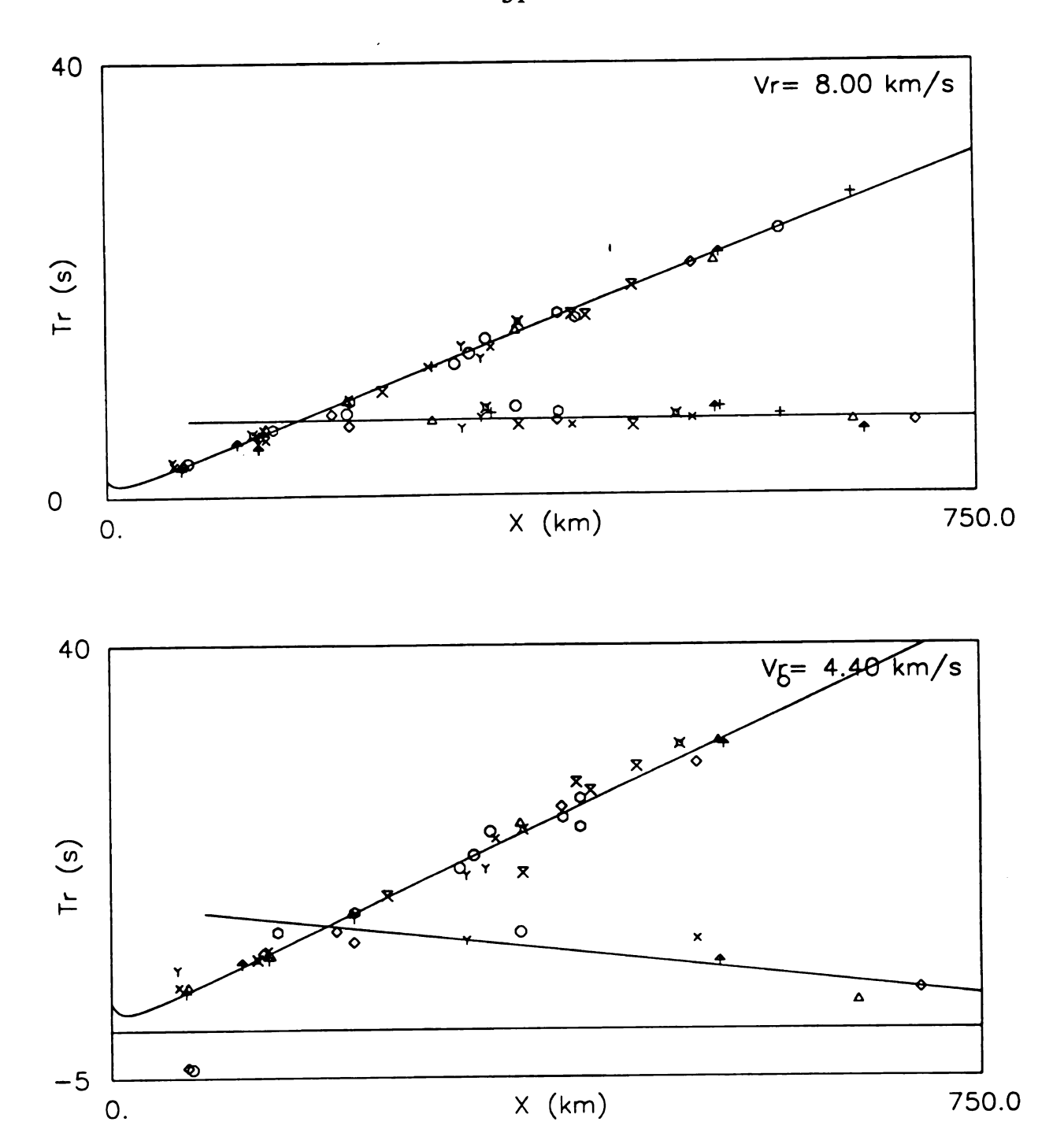


Figure 27. Omsukchan station reduced traveltime curves and crustal model. Pg velocity 5.99 km/sec, Pn velocity 8.00 km/sec, and crustal thickness 36.5 km. Sg velocity 3.52 km/sec. Conventions as in Figure 22.

15 (5)

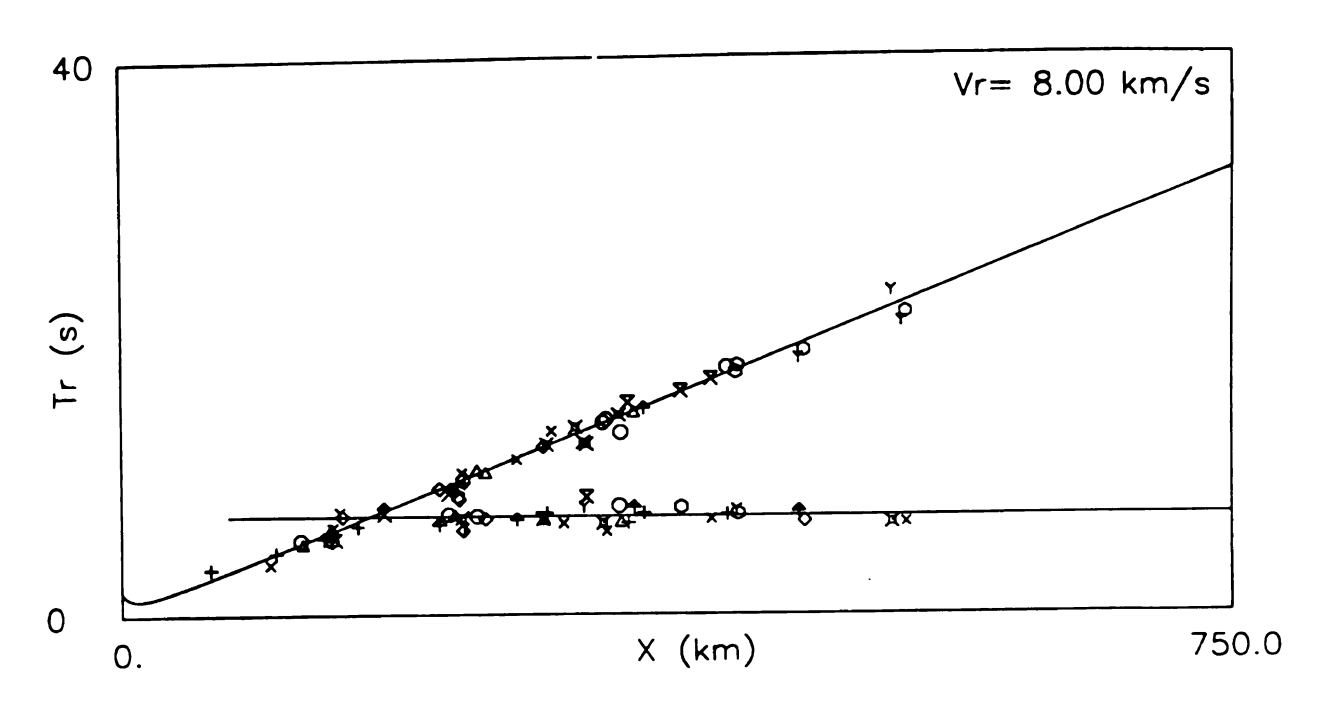
0

4

(2)

_

Fig 5.9 km



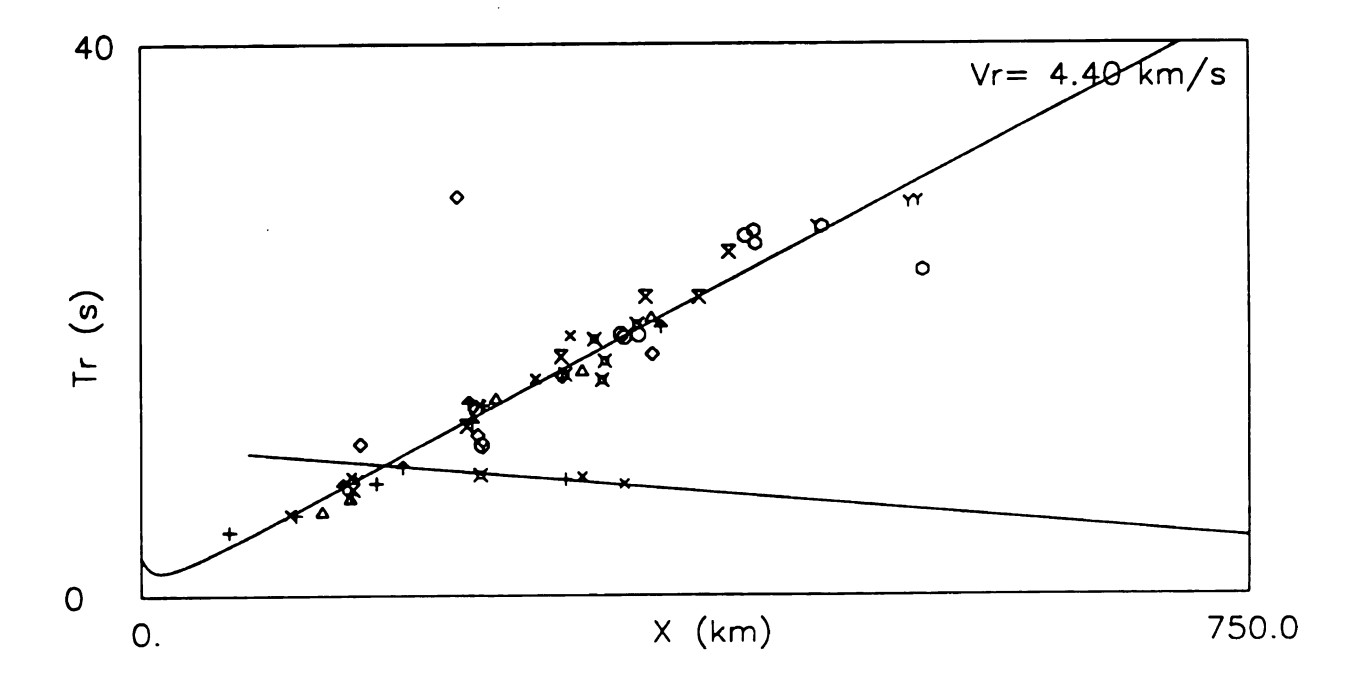


Figure 28. Seimchan station reduced traveltime curves and crustal model. Pg velocity 5.98 km/sec, Pn velocity 8.00 km/sec, and crustal thickness 37 km. Sg velocity 3.52 km/sec. Conventions as in Figure 22.

(s) L

0

40

Ir (s)

C

Figu 6.00 km/s

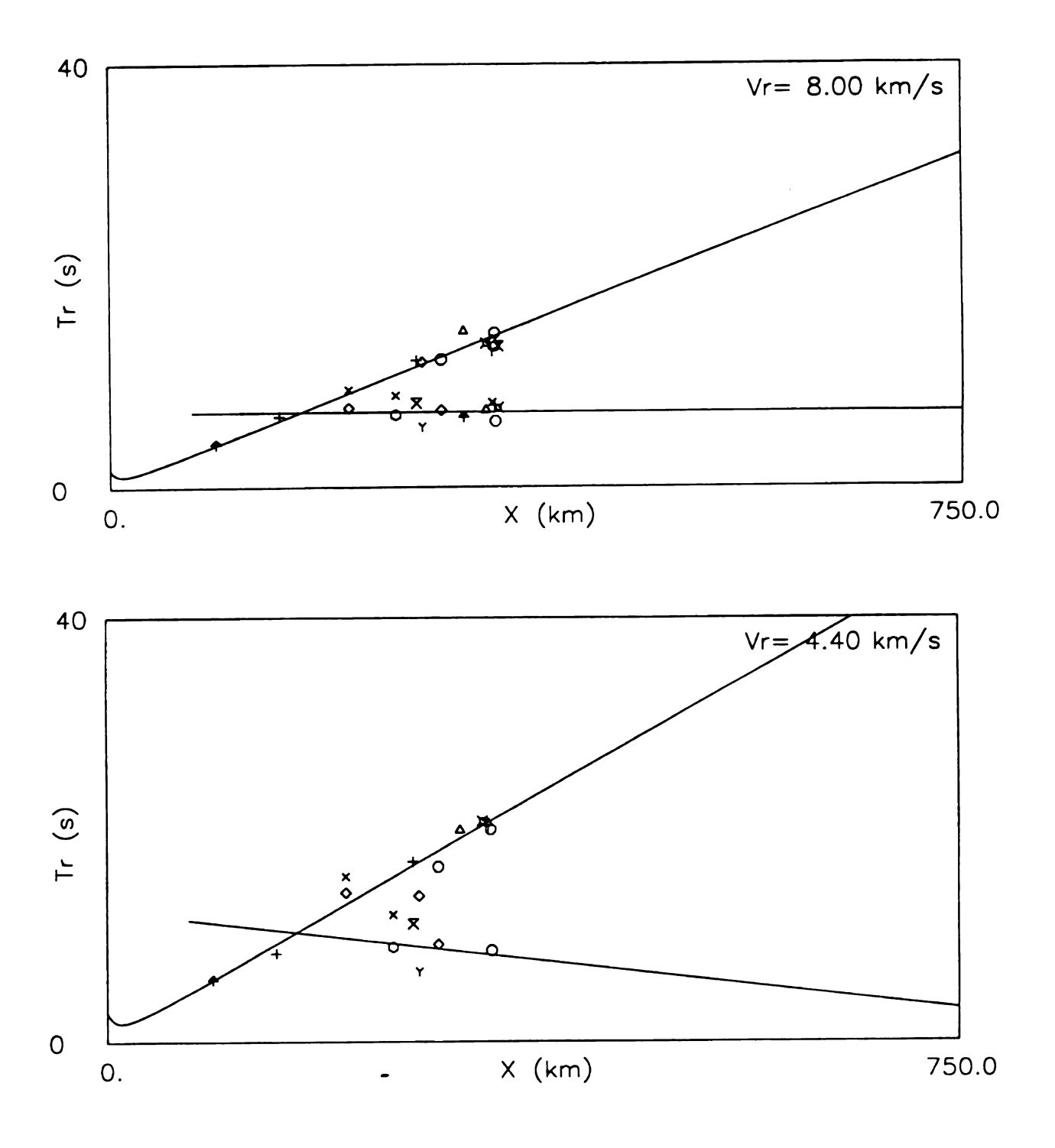


Figure 29. Sinegor'e station reduced traveltime curves and crustal model. Pg velocity 6.00 km/sec, Pn velocity 8.00 km/sec, and crustal thickness 37 km. Sg velocity 3.53 km/sec. Conventions as in Figure 22.

Omsukchan range from 30 km (Belyaevsky, 1974) to 38 km (Suvorov and Kornilova, 1986). The thickness determination for Omsukchan in this study falls in between at 36.5 km. For Seimchan, this study determines the thickness to be 2-3 km greater than previous studies. For this study, I estimate crustal thickness errors for Seimchan and Omsukchan to be 2 km. Bulin (1989) has also determined this region of the study area to have a homogeneous crustal structure, which is consistent with my results.

Talaya may also fit within this homogeneous region, although Pg and Sg velocities for Talaya are lower than the above discussed region at 5.96 km/sec and 3.48 km/sec, respectively, both being fairly well constrained (Fig. 30). A crustal thickness of 38 km is calculated for Talaya, although Pn data are sparse. This crustal thickness would be consistent with a thickening of the crust toward the south, as indicated by Magadan and Takhtoyamsk.

The area immediately east of the homogeneous region discussed above contains Kulu, Susuman, Nelkoba, and Ust' Omchug stations, all showing a slightly reduced crustal thickness (Figs. 31-34). Crustal thicknesses range from 30 km at Susumam to 35 km at the other stations. In addition, all stations indicate reduced Pn velocities ranging from 7.73 km/sec at Kulu to 7.96 km/sec at Susuman. For these stations, there is no consistent velocity change for either Pg or Sg phases. It should be noted that values for Ust' Omchug have large error bars due to limited data. The previous estimates of crustal thickness for Ust' Omchug are 29 km by Suvorov and Kornilova (1986), and an estimate of 36 km from the Magadan-Ust' Srednikan profile. Previous estimates for Susuman are inconsistent, with values ranging from 33 km (Suvorov and Kornilova, 1986) to 50 km

10

C

F 5 k

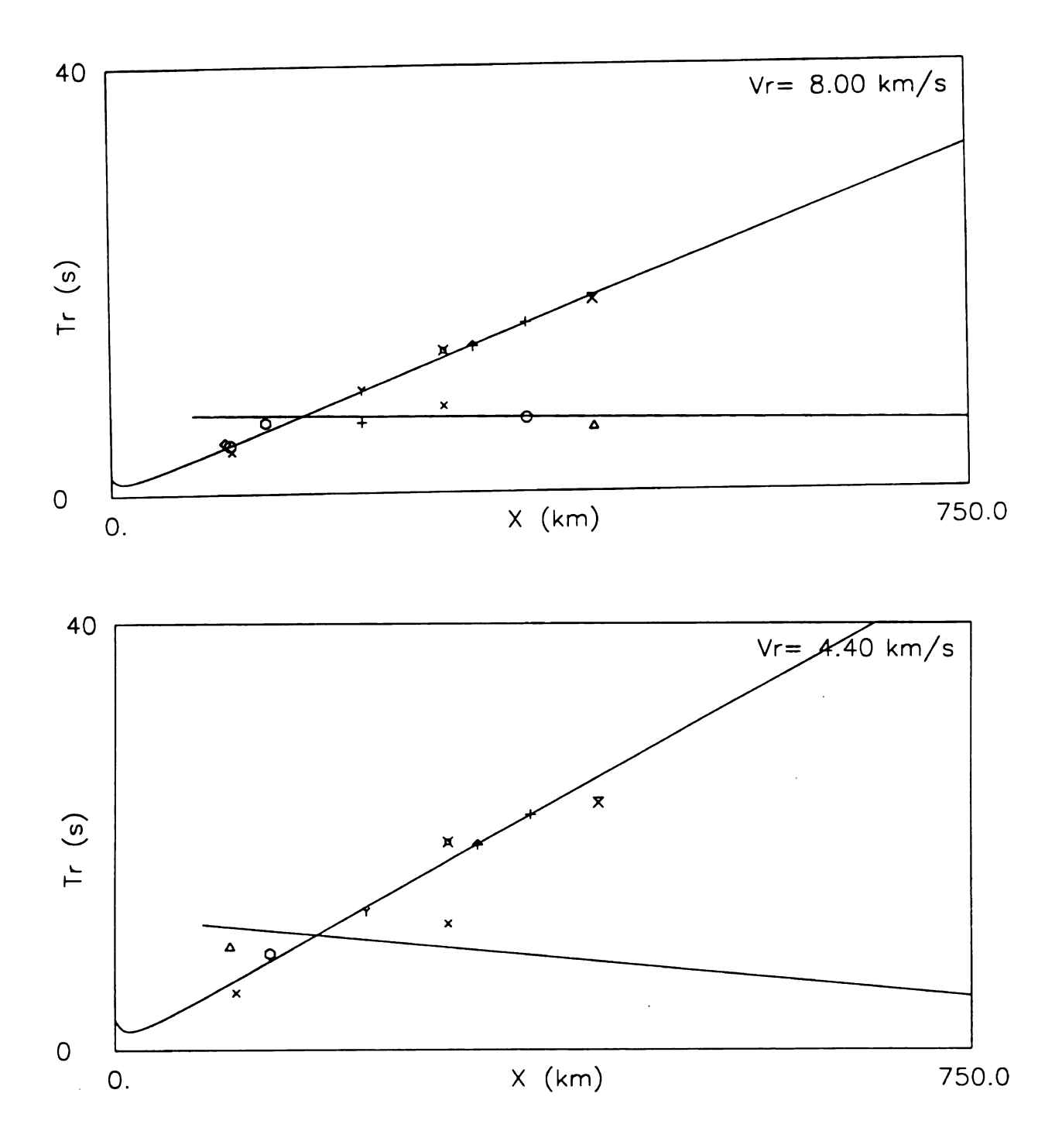


Figure 30. Talaya station reduced traveltime curves and crustal model. Pg velocity 5.96 km/sec, Pn velocity 8.10 km/sec, and crustal thickness 38 km. Sg velocity 3.48 km/sec. Conventions as in Figure 22.

F 5 k

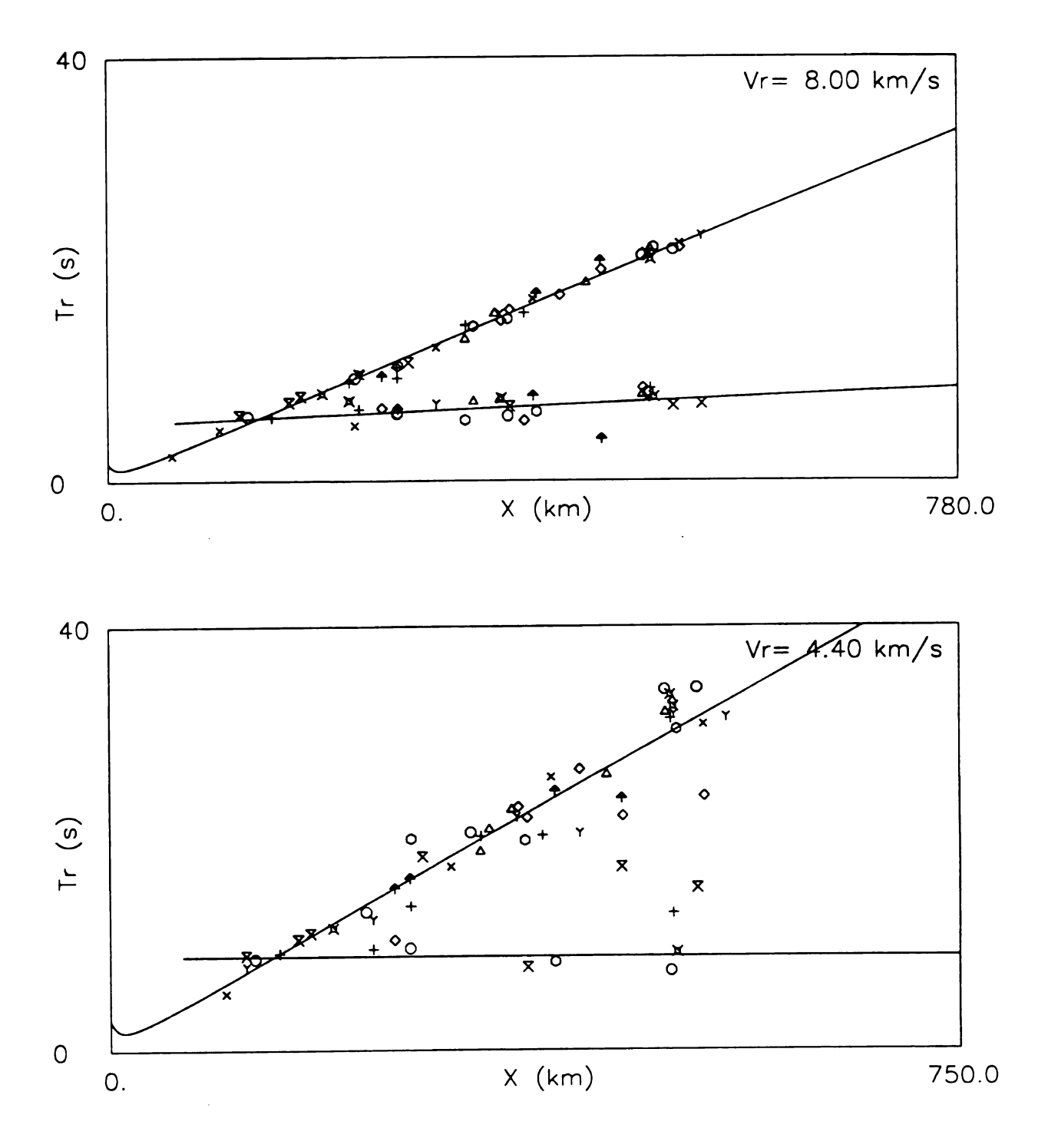
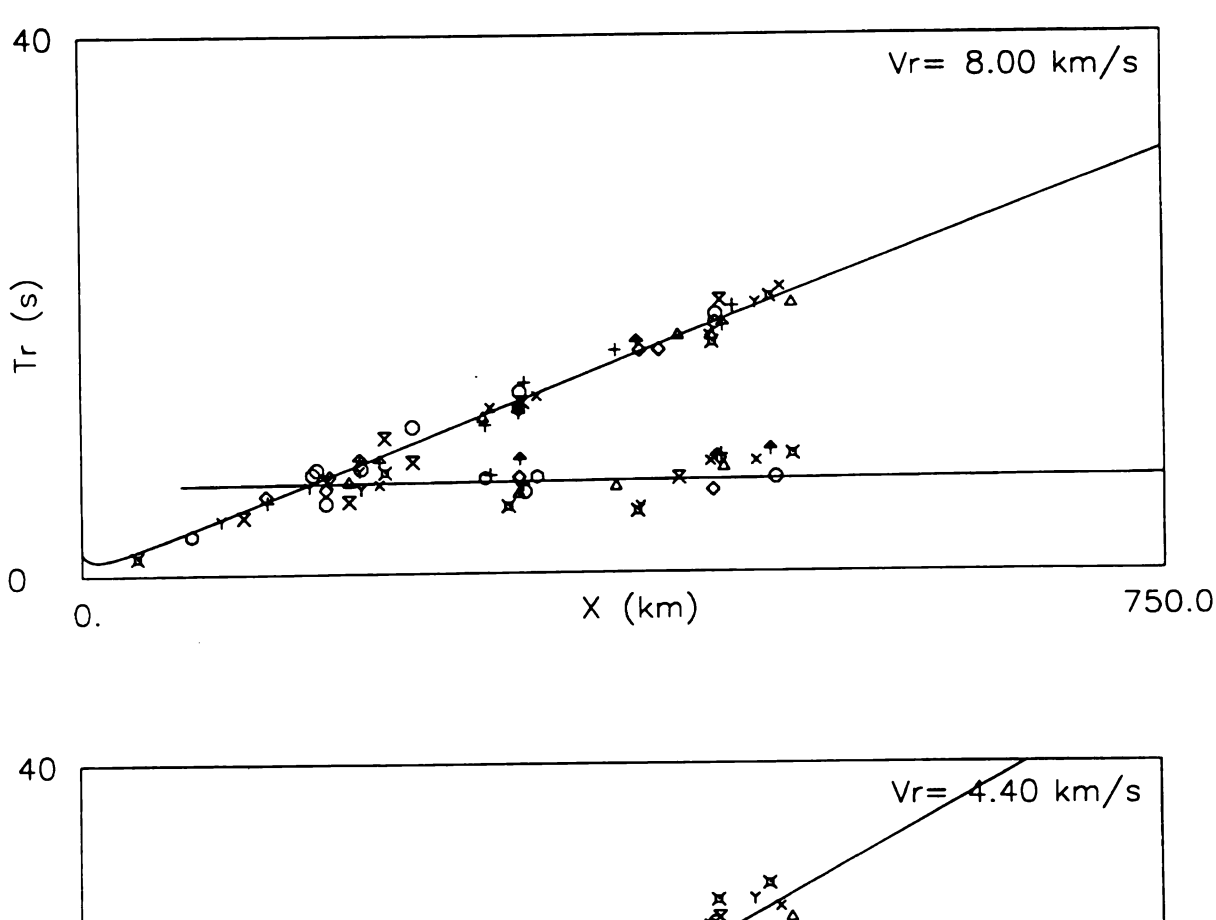


Figure 31. Kulu station reduced traveltime curves and crustal model. Pg velocity 5.98 km/sec, Pn velocity 7.73 km/sec, and crustal thickness 30 km. Sg velocity 3.48 km/sec. Conventions as in Figure 22.



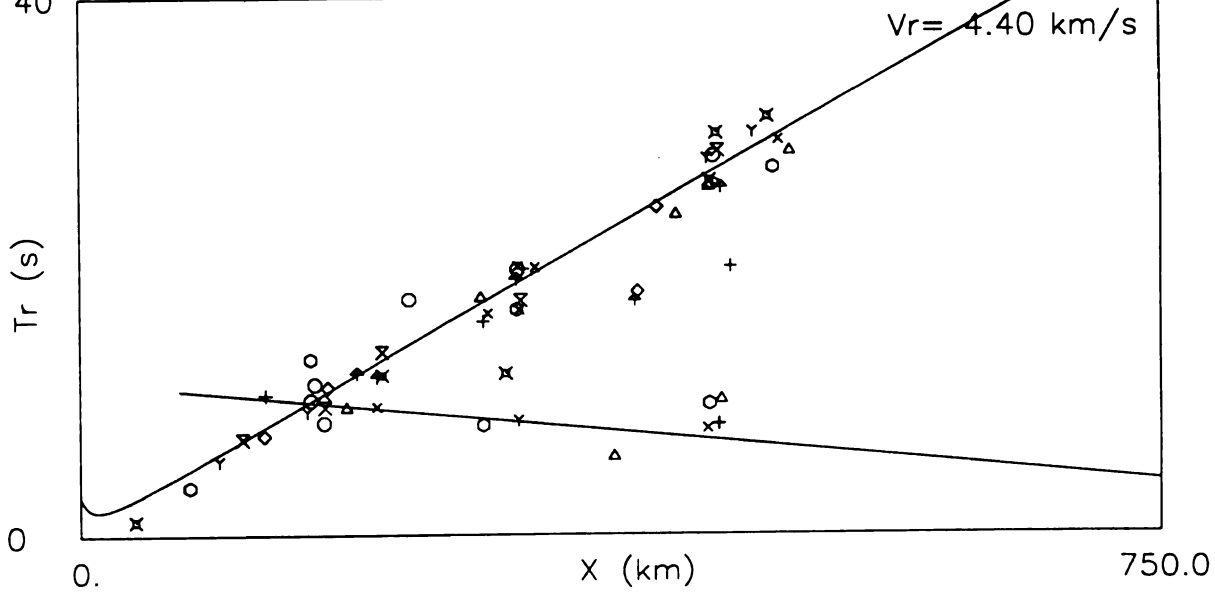


Figure 32. Susuman station reduced traveltime curves and crustal model. Pg velocity 6.00 km/sec, Pn velocity 7.96 km/sec, and crustal thickness 35 km. Sg velocity 3.47 km/sec. Conventions as in Figure 22.

(8) 1

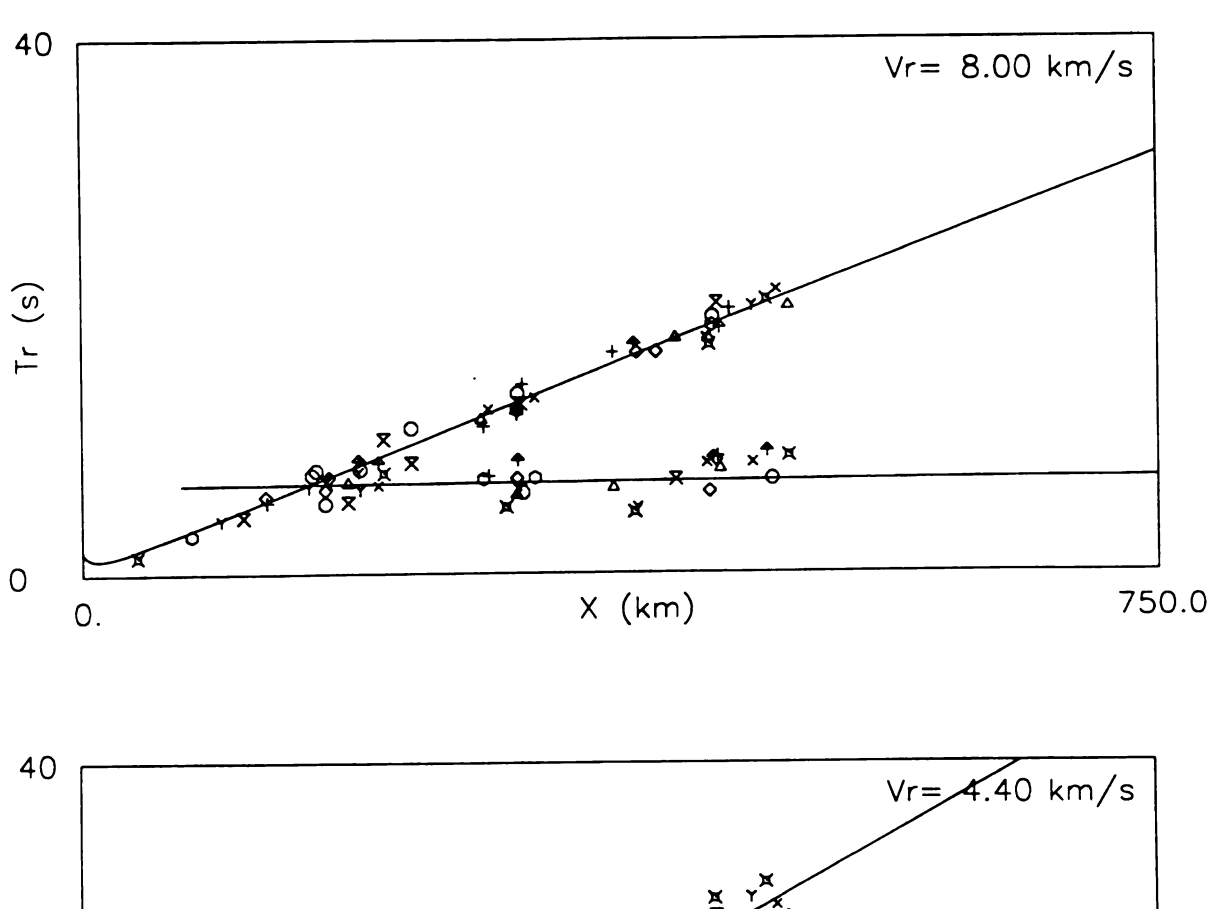
0

40

(s)

0

Figur 6.00 km/sc



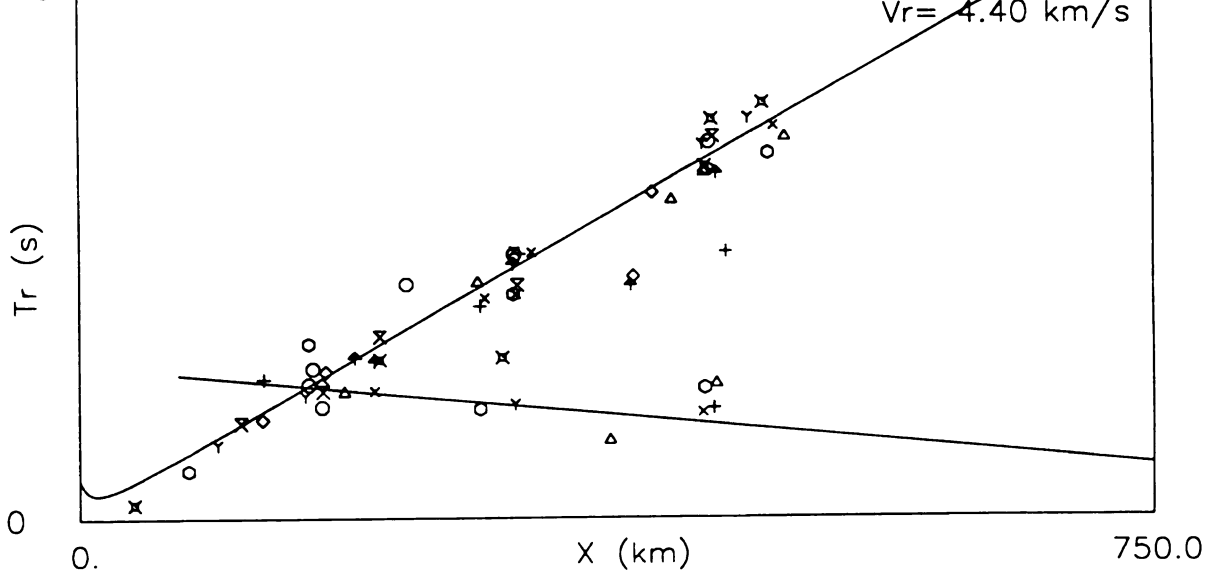


Figure 32. Susuman station reduced traveltime curves and crustal model. Pg velocity 6.00 km/sec, Pn velocity 7.96 km/sec, and crustal thickness 35 km. Sg velocity 3.47 km/sec. Conventions as in Figure 22.

7, (2)

C

4

` `

Fi 5. kr

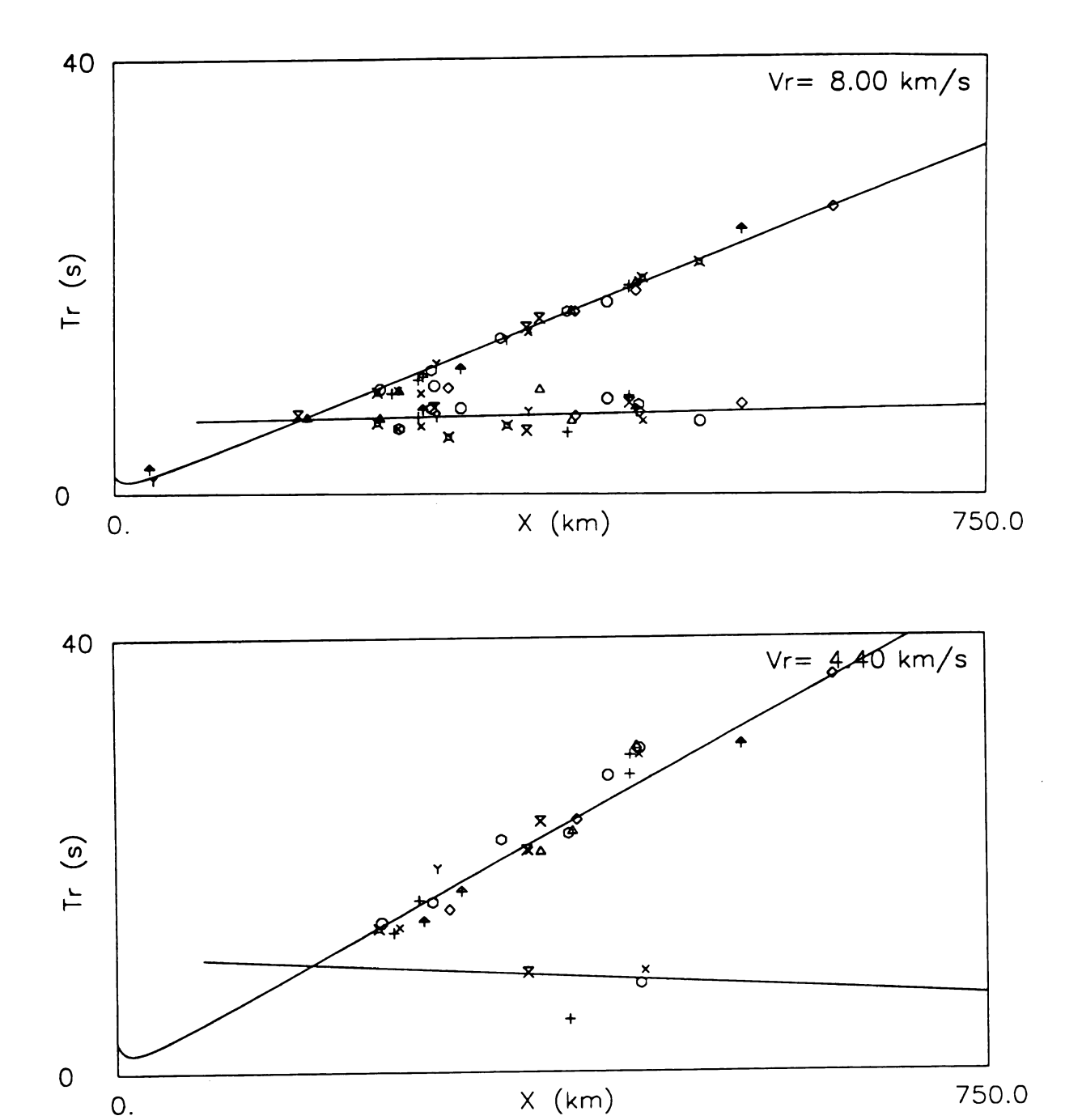


Figure 33. Nelkoba station reduced traveltime curves and crustal model. Pg velocity 5.97 km/sec, Pn velocity 7.87 km/sec, and crustal thickness 35 km. Sg velocity 3.50 km/sec. Conventions as in Figure 22.

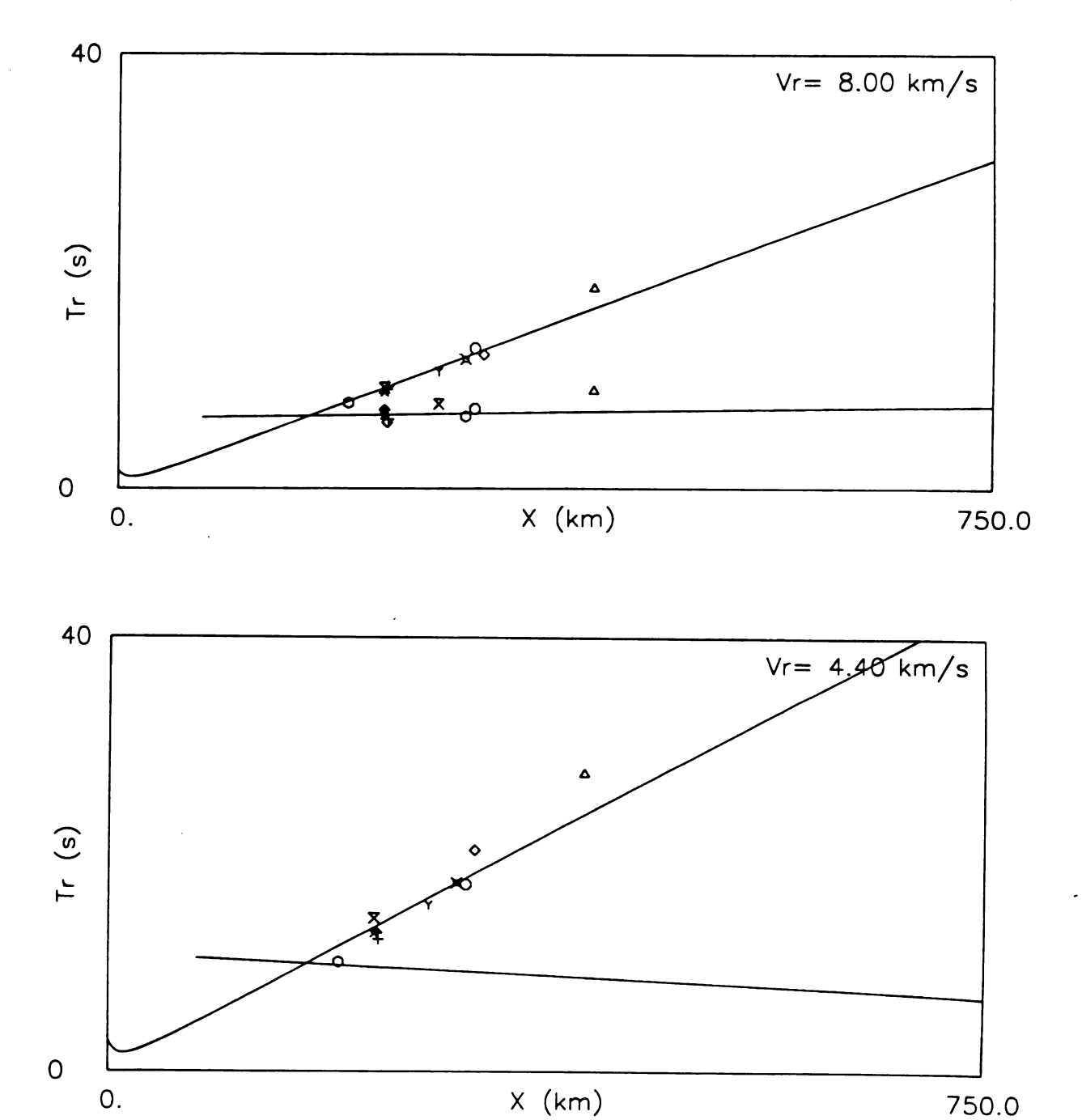


Figure 34. Ust' Omchug station reduced traveltime curves and crustal model. Pg velocity 6.05 km/sec, Pn velocity 7.90 km/sec, and crustal thickness 35 km. Sg velocity 3.51 km/sec. Conventions as in Figure 22.

(Bel

estin

Prev

to in

igno

Stru

the 36).

at 3

6.03

Ner set

of (

no :

thic unc

The

Alt

blo

The

N₀₁

(Belyaevsky, 1974). Given the 2 km difference between the Suvorov and Kornilova estimate and my estimate, I believe the Belyaevsky (1974) estimate to be in error. Previous studies on Nelkoba indicate a thickness of 39-40 km. It is not possible for me to increase crustal thickness by the required 4-5 km to agree with previous studies without ignoring a significant portion of my data. No previous studies have considered the crustal structure at Kulu.

Ust' Nera and Moma (Khonu) are located to the northwest of Susuman, continuing the trend of a slightly elevated Moho at 35 km and reduced Pn velocities (Figs. 35 and 36). For Ust' Nera, Pn velocity is 7.95 km/sec, with Pg velocity at 5.99 km/sec and Sg at 3.53 km/sec. For Moma, Pn velocity is 7.87 km/sec, while Pg and Sg velocities are 6.03 km/sec and 3.55 km/sec respectively. Previous estimates of crustal thickness at Ust' Nera range from 24 km (Suvorov and Kornilova, 1986) to 40 km (Bulin, 1989). The data set for Ust' Nera is one of the best in terms of epicentral distance coverage, and scatter of data are acceptable, thus I feel the 35 km crustal thickness is reasonable. There are no previous velocity or thickness determinations for Moma. The slightly reduced crustal thickness and reduced Pn velocity are consistent with a region which has recently undergone an extensional event, and thus may represent a relic of the Moma rift system. The station at Moma is within the Moma rift proper, as defined by Fujita et al. (1990a). Although this region is presently under compression, caused by extrusion of the Okhotsk block (Riegel et al., 1993; Cook et al., 1986) the region was recently under extension. The transition from extension to compression occurred as a result of the migration of the North American-Eurasian pole to the north as recently as 0.5 Ma (Cook et al., 1986).

(s)

0

45

(s)

C

Figu 5.99 km/s

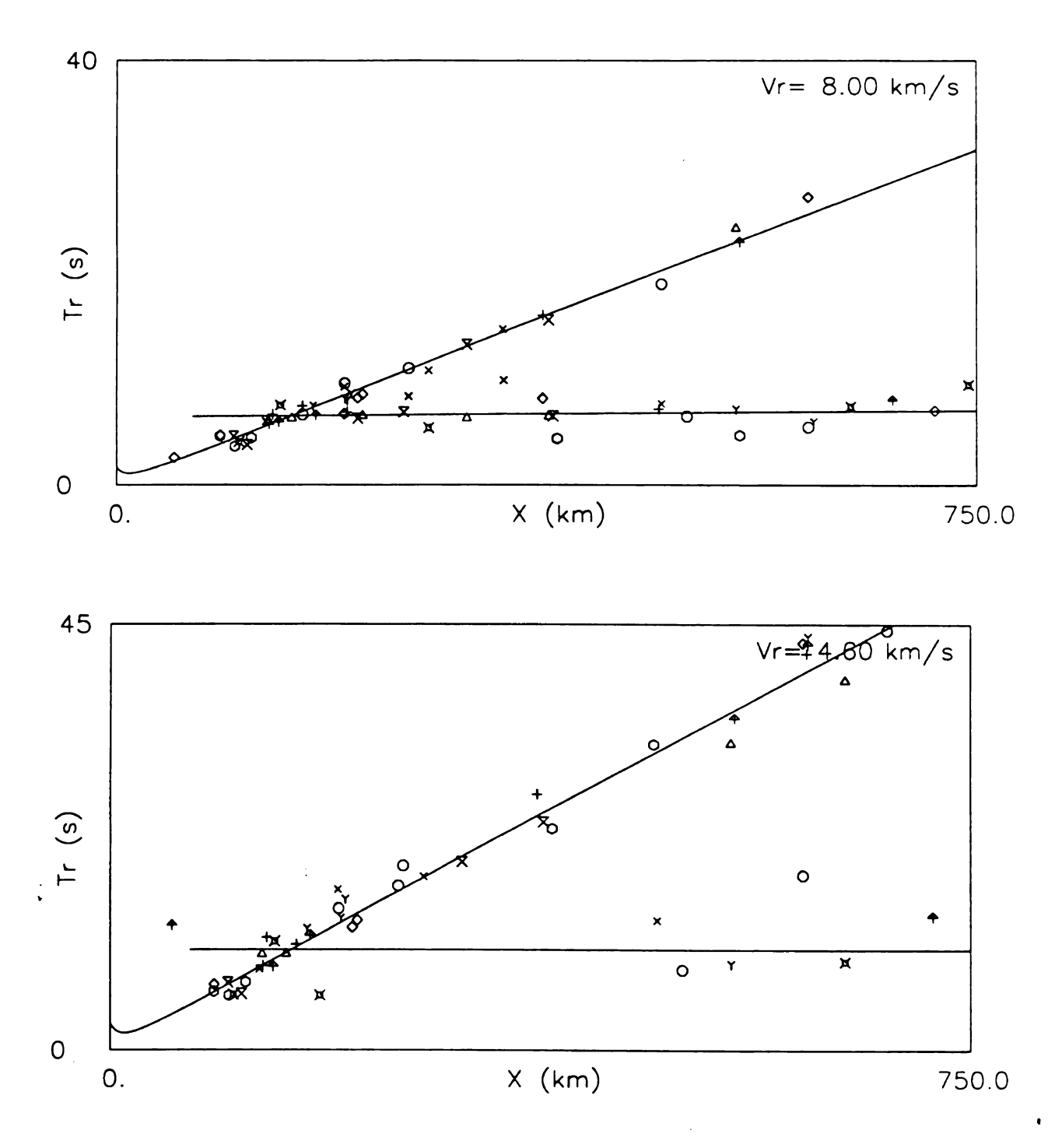


Figure 35. Ust' Nera station reduced traveltime curves and crustal model. Pg velocity 5.99 km/sec, Pn velocity 7.95 km/sec, and crustal thickness 34 km. Sg velocity 34 km/sec. Conventions as in Figure 22.

7r (s

C

40

1r (s)

C

Figure 6.03 k km/sec

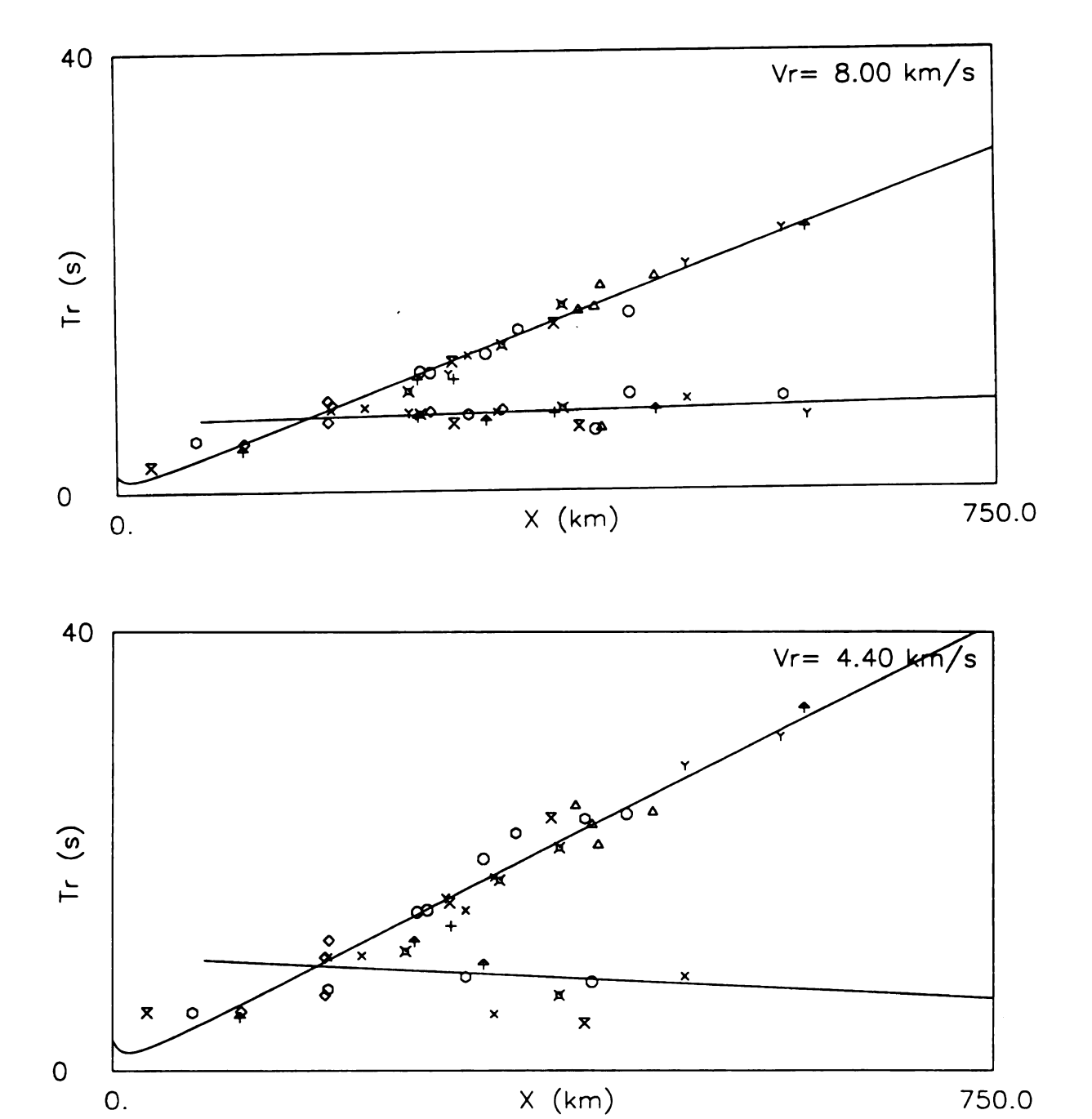


Figure 36. Moma station reduced traveltime curves and crustal model. Pg velocity 6.03 km/sec, Pn velocity 7.87 km/sec, and crustal thickness 35 km. Sg velocity 3.55 km/sec. Conventions as in Figure 22.

Giver

reflec

an inc

38).

veloc

(1989

Zyry

porti

Bata

et al.

by T

show

km/s

sligh

is lo

km s

for t a thi

Naib

Given the recent transition to compression, the former extensional regions may still be reflected in an elevated Moho and reduced Pn velocity.

Northeast from Ust' Nera are stations Sasyr' and Zyryanka. Both stations show an increased crustal thickness, at 37 km for Sasyr', and 47 km for Zyryanka (Figs. 37 and 38). Velocities are close to regional averages with the exception of an 8.22 km/sec Pn velocity at Zyryanka. Station Sasyr' has been considered in previous studies. Bulin (1989) reports a thickness of 41 km for Ugol'naya (Zyryanka), and a thickness at Zyryanka of 35-45 km is possible (Suvorov and Kornilova, 1986).

Continuing northwest along the trend of thinner crust, are the stations Tabalakh, Batagai, and Saidy. Saidy is within the region encompassed by the Toustakh graben, a portion of the Moma rift, while Batagai and Tabalakh lie immediately to the south (Fujita et al., 1990a). Of the three stations, Batagai shows the thinnest crust at 32 km, followed by Tabalakh at 34 km and Saidy at 35 km (Figs. 39-41). Both Batagai and Tabalakh show reduced Pn velocities of 7.94 km/sec while Saidy has an elevated velocity of 8.04 km/sec. Compared to Batagai and Tabalakh, Saidy shows a higher Pn velocity and slightly thicker crust.

Stations Naiba and Yubileniya are in the northern portion of the study area. Naiba is located on Buor Khaya Bay, off the Laptev Sea, and Yubileniya is approximately 100 km south of the Laptev sea along the Yana river. The crustal thickness determinations for these stations are among this study's most interesting results. The Naiba data indicate a thin crust at 29 km, with a reduced Pn velocity of 7.70 km/sec (Fig. 42). Geologically, Naiba is located on the western edge of the Omoloi basin, the southern extension of the

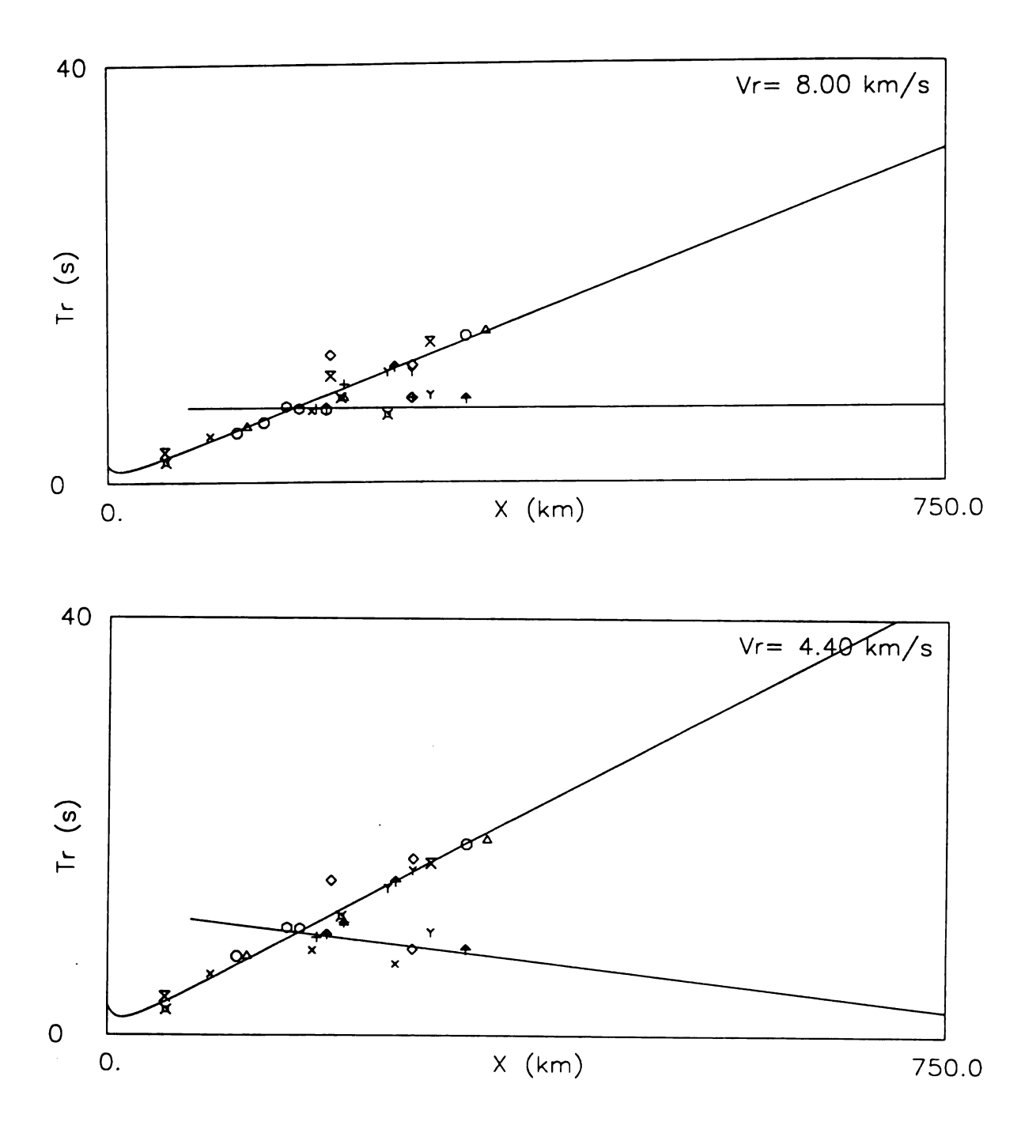


Figure 37. Sasyr' station reduced traveltime curves and crustal model. Pg velocity 5.98 km/sec, Pn velocity 8.00 km/sec, and crustal thickness 37 km. Sg velocity 3.52 km/sec. Conventions as in Figure 22.

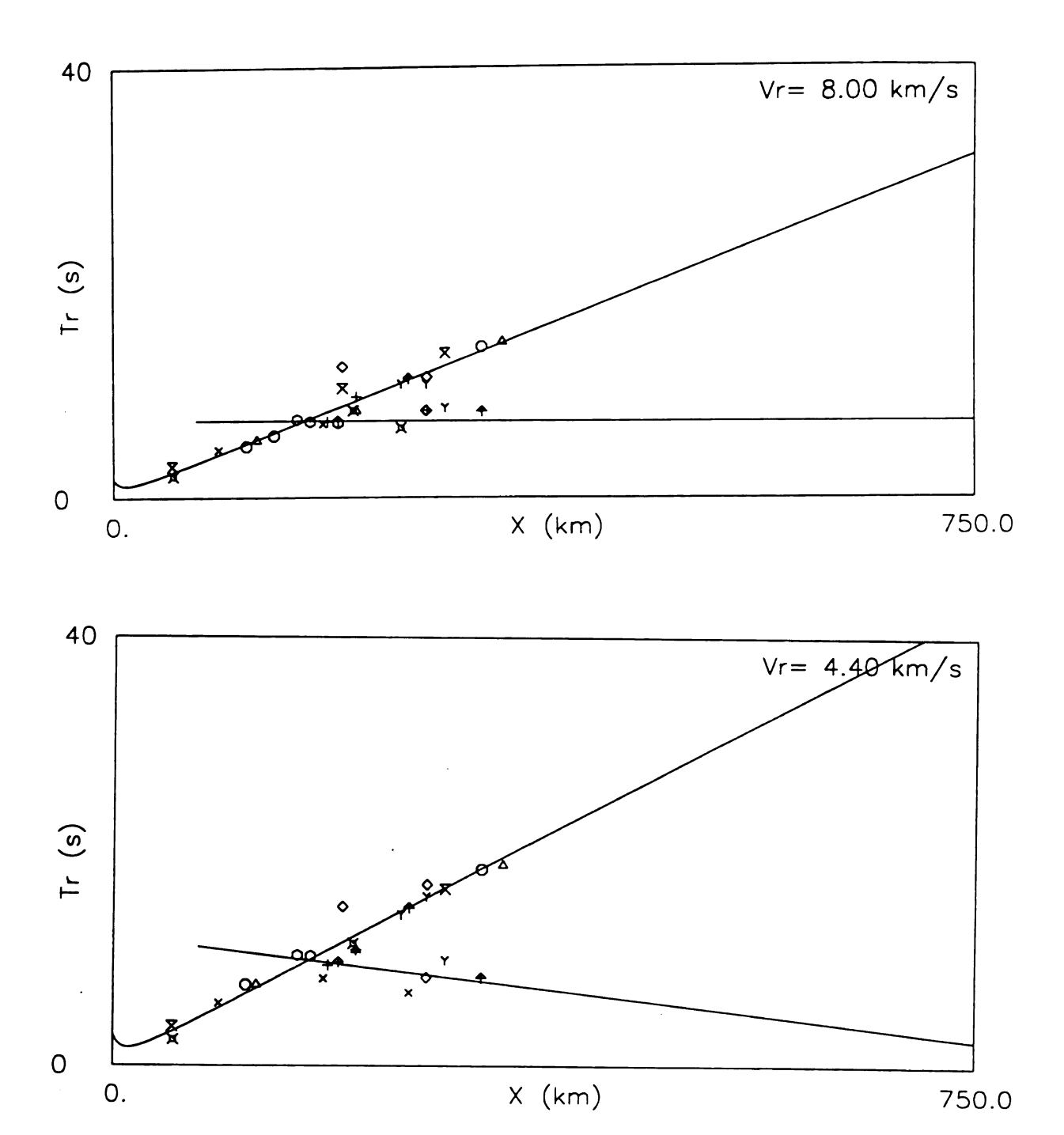


Figure 37. Sasyr' station reduced traveltime curves and crustal model. Pg velocity 5.98 km/sec, Pn velocity 8.00 km/sec, and crustal thickness 37 km. Sg velocity 3.52 km/sec. Conventions as in Figure 22.

Tr (s)

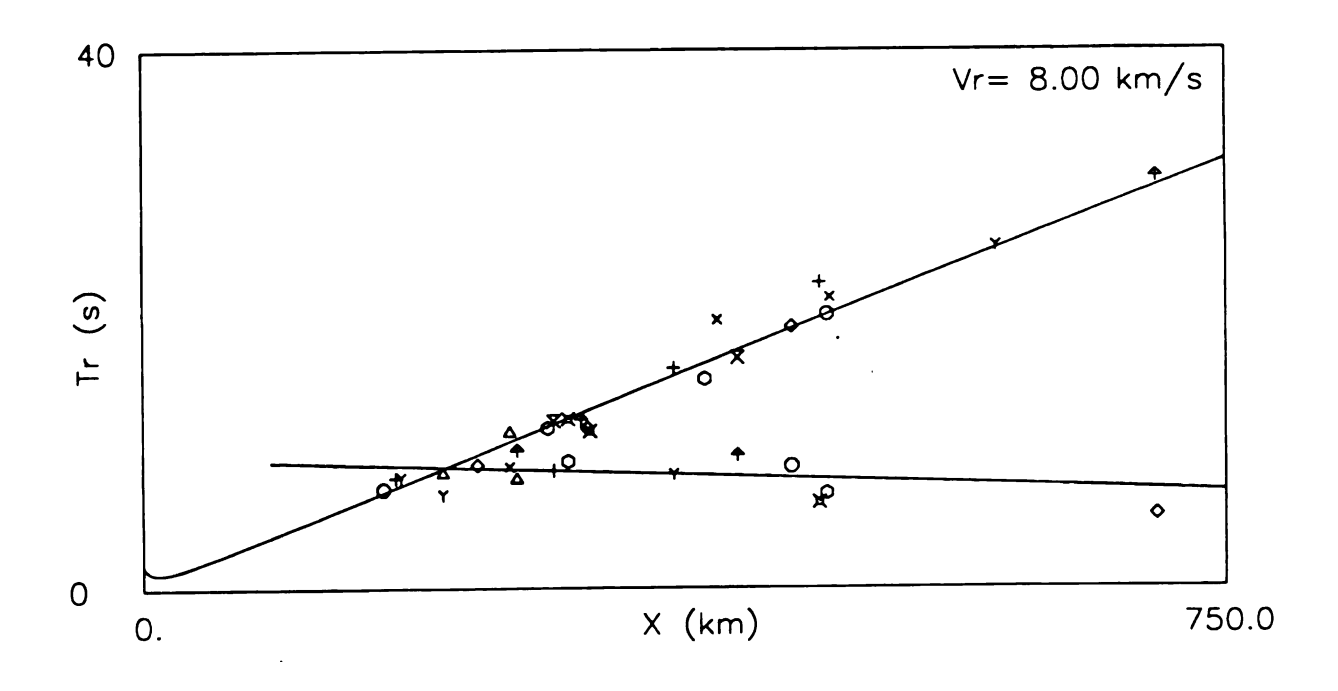
0

40

Ir (s)

0

Figu 5.98 km/s



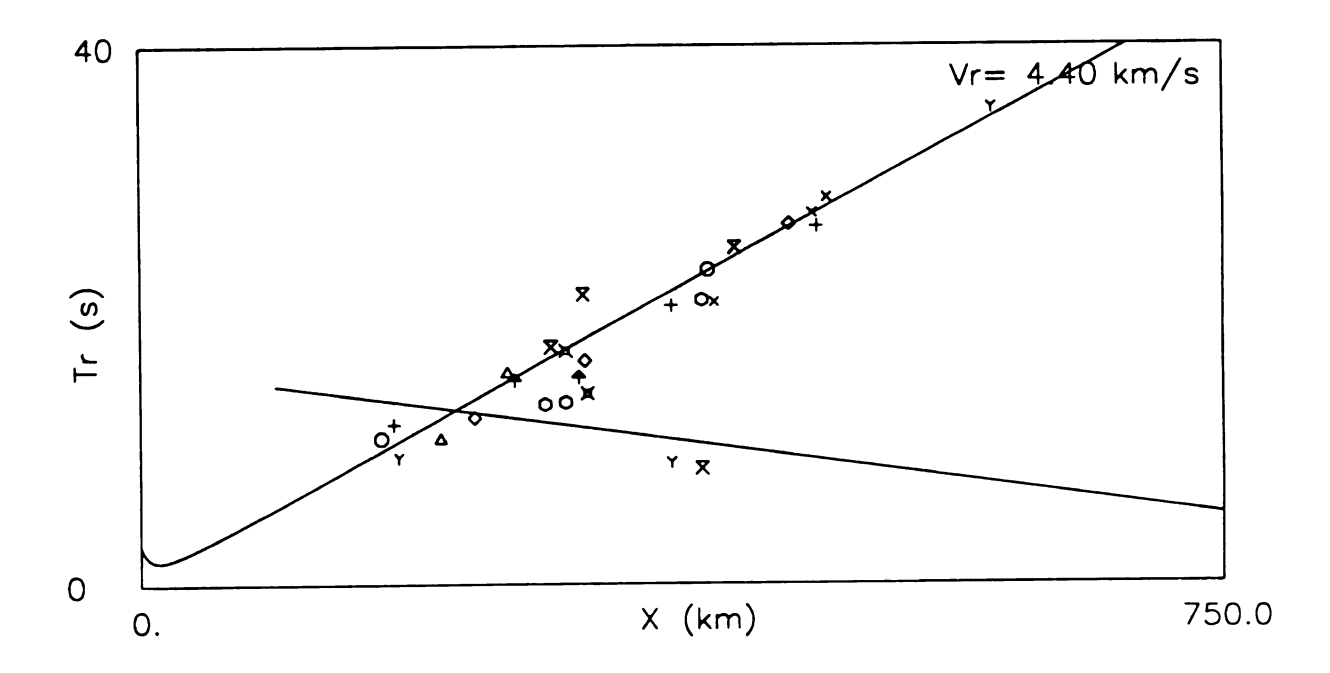


Figure 38. Zyryznka station reduced traveltime curves and crustal model. Pg velocity 5.98 km/sec, Pn velocity 8.22 km/sec, and crustal thickness 47 km. Sg velocity 3.50 km/sec. Conventions as in Figure 22.

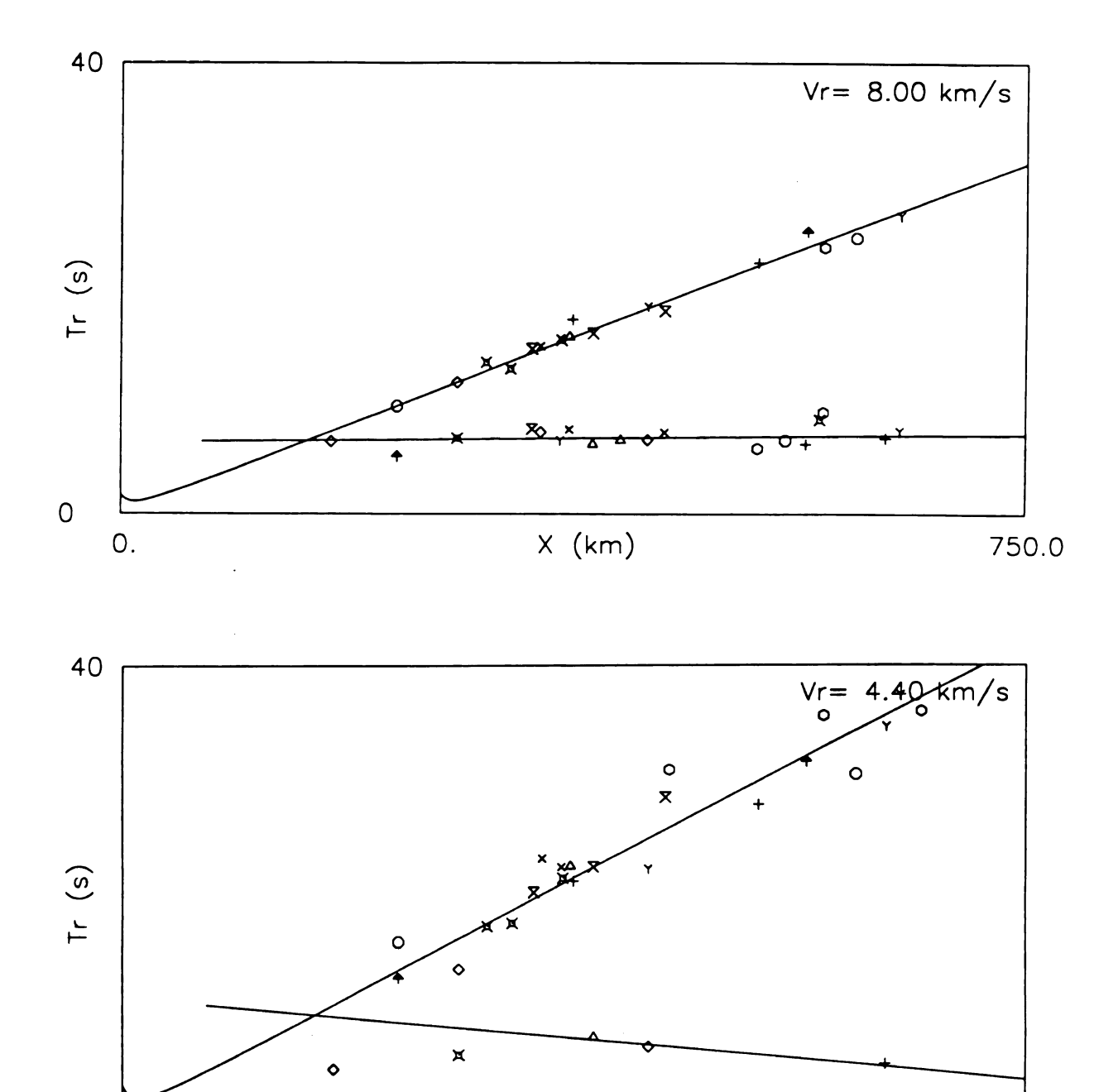


Figure 39. Tabalakh station reduced traveltime curves and crustal model. Pg velocity 6.01 km/sec, Pn velocity 7.94 km/sec, and crustal thickness 34 km. Sg velocity 3.53 km/sec. Conventions as in Figure 22.

X (km)

750.0

0

0.

1r (s)

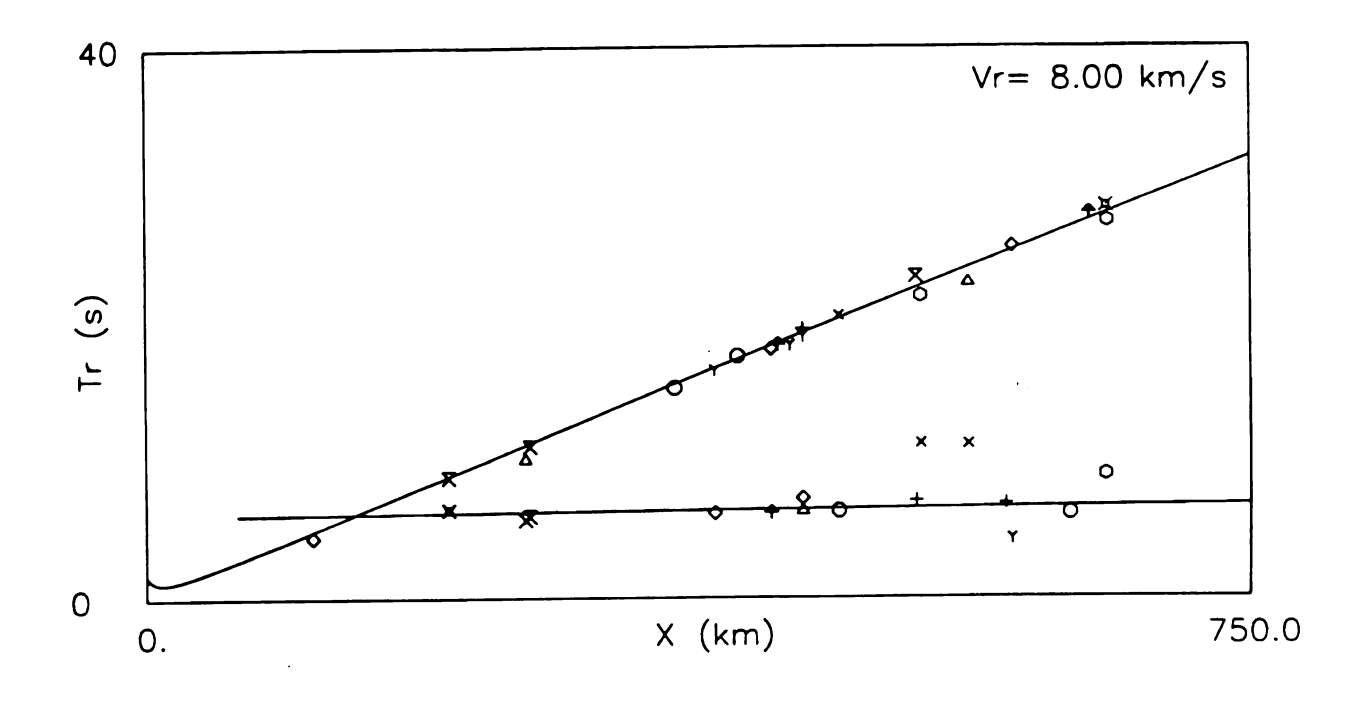
0

40

Tr (s)

C

Figu 5.97 km/s



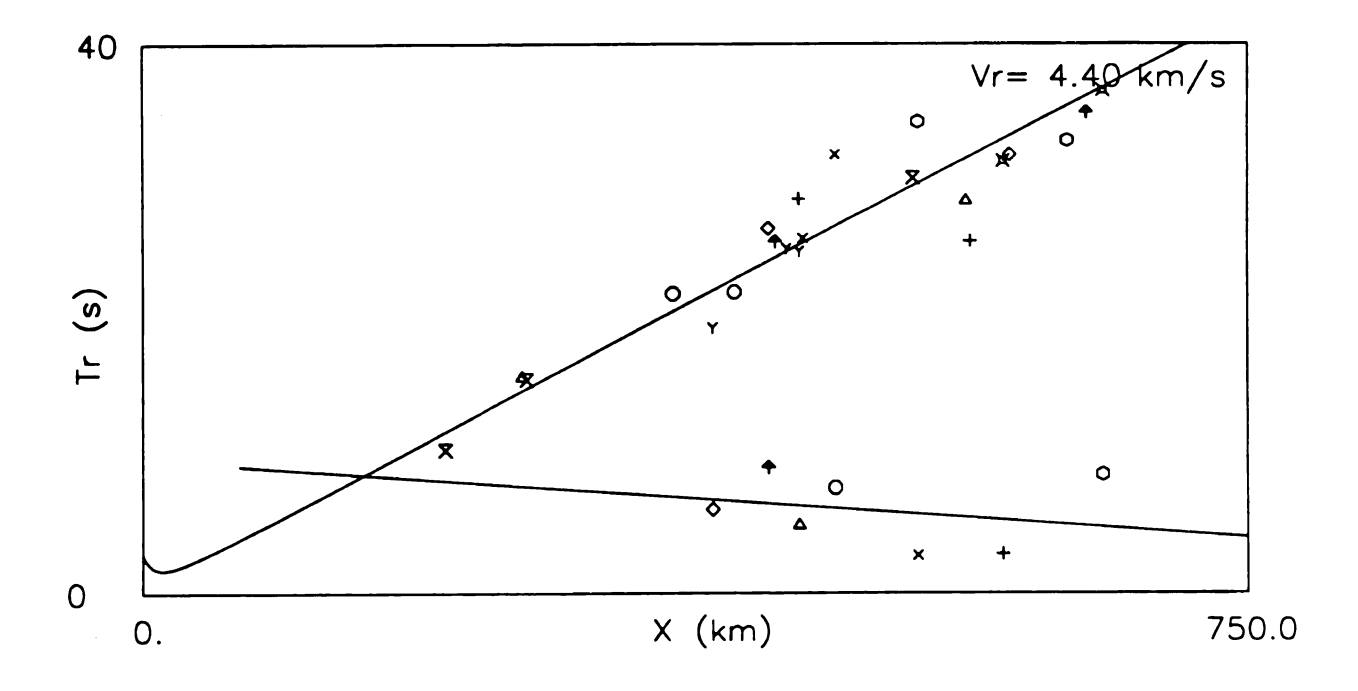


Figure 40. Batagai station reduced traveltime curves and crustal model. Pg velocity 5.97 km/sec, Pn velocity 7.94 km/sec, and crustal thickness 32 km. Sg velocity 3.53 km/sec. Conventions as in Figure 22.

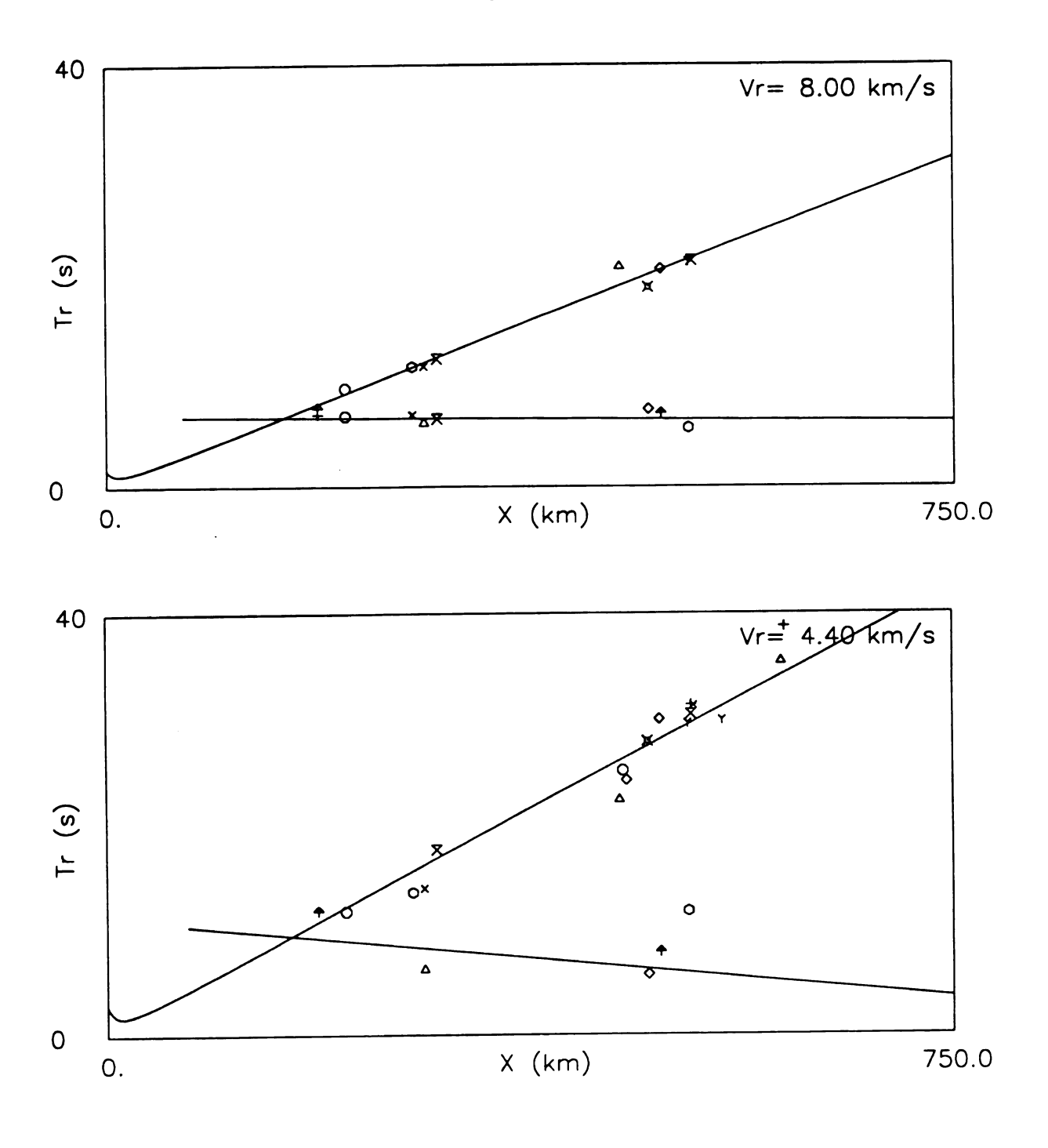


Figure 41. Saidy station reduced traveltime curves and crustal model. Pg velocity 6.01 km/sec, Pn velocity 8.04 km/sec, and crustal thickness 35 km. Sg velocity 3.52 km/sec. Conventions as in Figure 22.

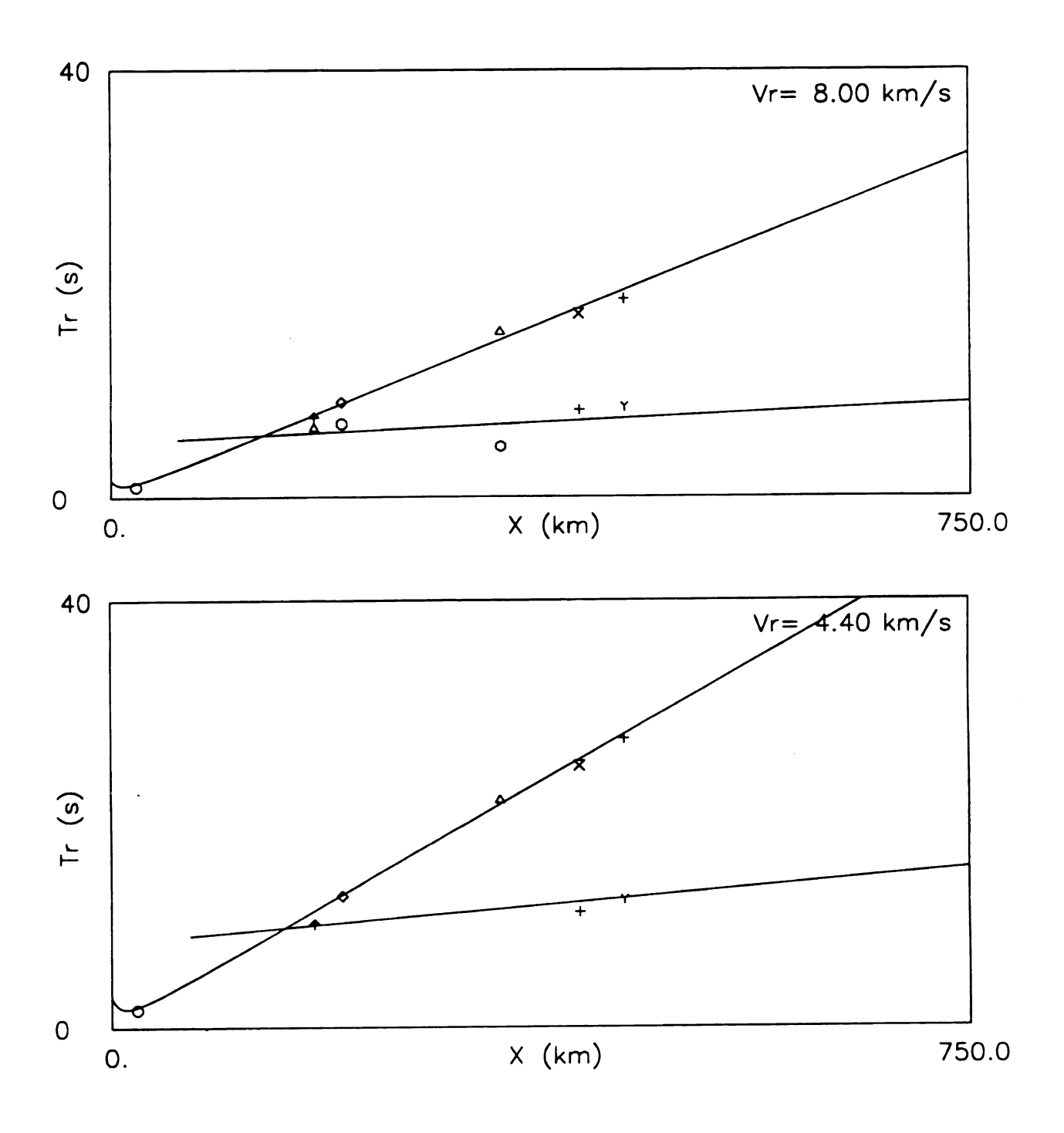


Figure 42. Naiba station reduced traveltime curves and crustal model. Pg velocity 5.96 km/sec, Pn velocity 7.70 km/sec, and crustal thickness 29 km. Sg velocity 3.47 km/sec. Conventions as in Figure 22.

Omoloi graben (Fig. 4). This study shows Yubileniya to be located above a zone of anomalously thin crust at 19 km (Fig. 43). For Yubileniya, Pn velocities are significantly reduced at 7.49 km/sec, while Pg velocities are near normal at 5.96 km/sec. Note that the data supporting such a thin crust contains minimal scatter, and is not constrained by any single point. Yubileniya is located in the southern end of the Ust' Yana graben (Fig. 4). For both stations, local grabens from regional extension seem to be the controlling factor in thinning of the crust. These stations indicate clear evidence of anomalously thin continental crust in the southern portion of the Laptev rift system. Thin crust and low Pn velocities are supported by DSS profiles in the south Laptev sea (Avetisov and Guseva, 1991; Avetisov, 1983; Kogan, 1974). A reflection profile 30 km east of Naiba indicates a crustal thickness of approximately 28km (Avetisov and Guseva, 1991).

Located east of Yubileniya, station Tenkeli is located in the vicinity of Tenkeli basin (Fig. 4), where an elevated Moho and reduced Pn velocity could be expected. Unfortunately, Tenkeli results are inconclusive due to Pn data scatter and lack of close in data. For Tenkeli, acceptance or rejection of a single datum can vary crustal thickness from 24 km to 42 km (Fig. 44). Crustal velocity is constrained at 5.98 km/sec.

The southwest portion of the study area contains stations Yakutsk, Khandyga, and Nezhdaninskoe. These stations are located within the eastern Siberian platform. These stations evidence a generally thickened crust of 44 km at Khandyga, 39 km at Nezhdaninskoe, and 38 at Yakutsk (Figs. 45-47). Pn velocities are near average, except Khandyga where the Pn velocity is 8.10 km/sec. Pn velocity and crustal thickness are poorly constrained for Yakutsk. Previous studies are in good agreement with these

(s)

C

45

Ir (s)

0

Figur veloc 3.54

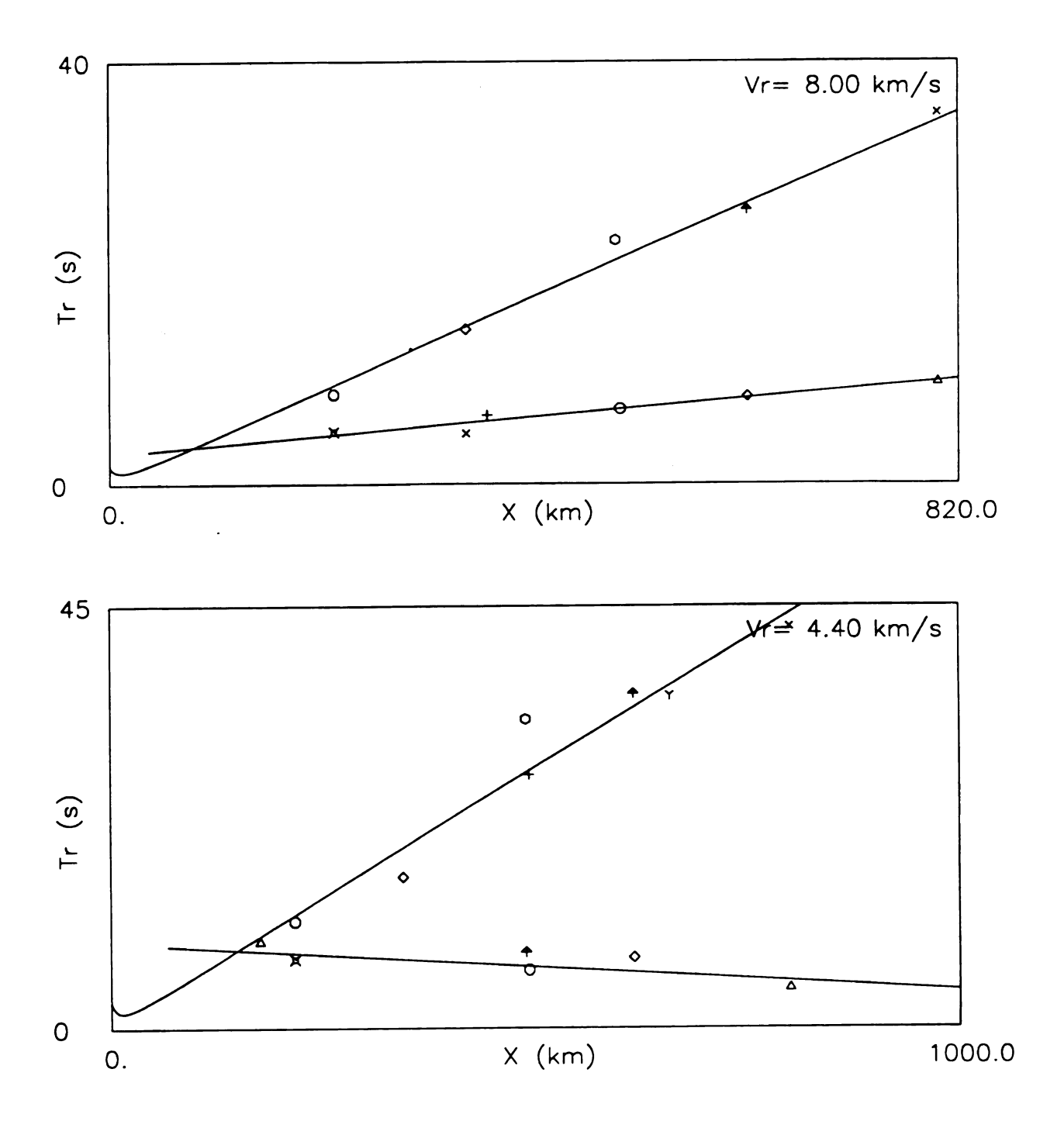


Figure 43. Yubileniya station reduced traveltime curves and crustal model. Pg velocity 5.96 km/sec, Pn velocity 7.49 km/sec, and crustal thickness 19 km. Sg velocity 3.54 km/sec. Conventions as in Figure 22.

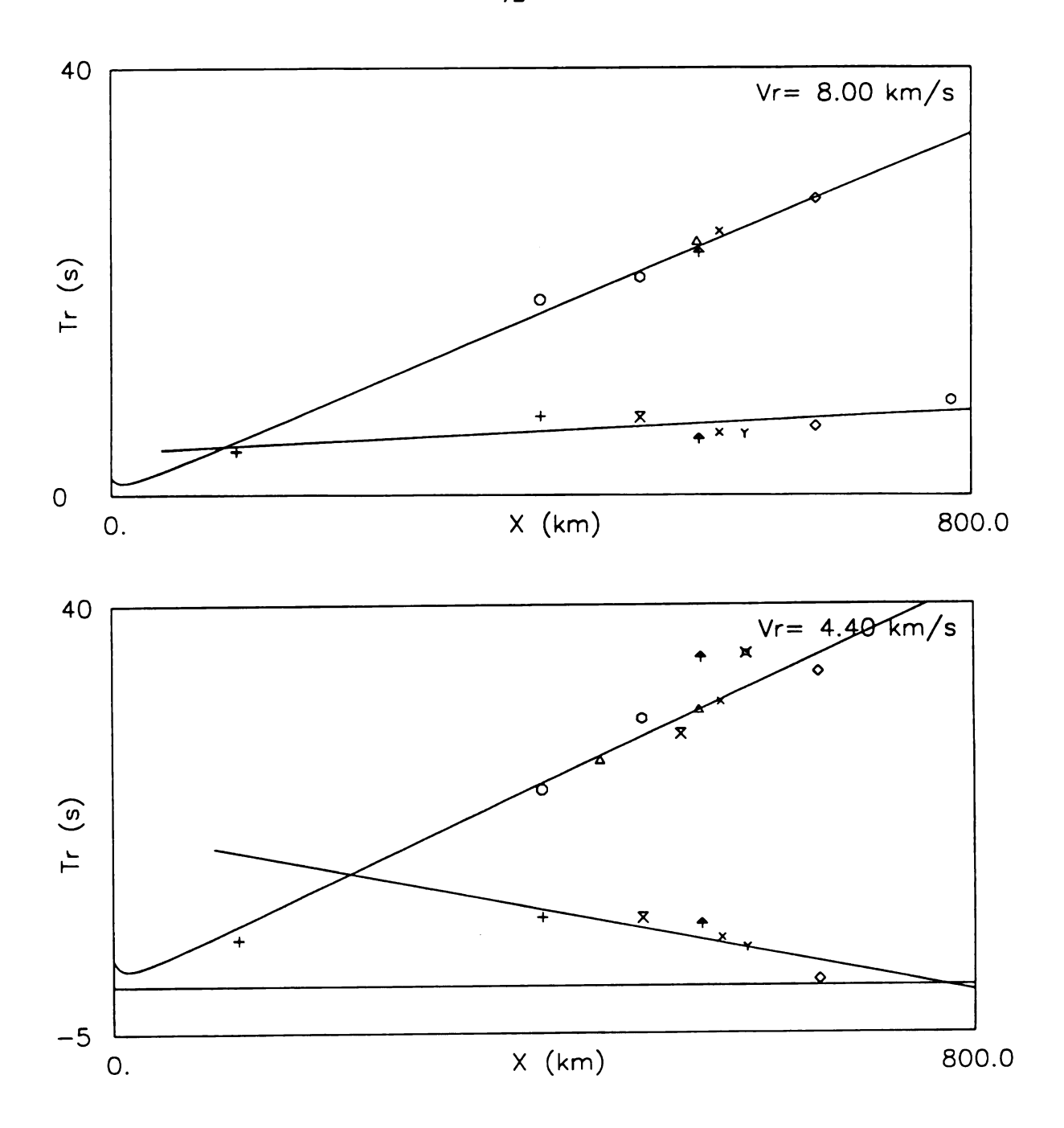


Figure 44. Tenkeli station reduced traveltime curves and crustal model. Pg velocity 5.98 km/sec, Pn velocity 7.70 km/sec, and crustal thickness 24 km. Sg velocity 3.57 km/sec. Conventions as in Figure 22.

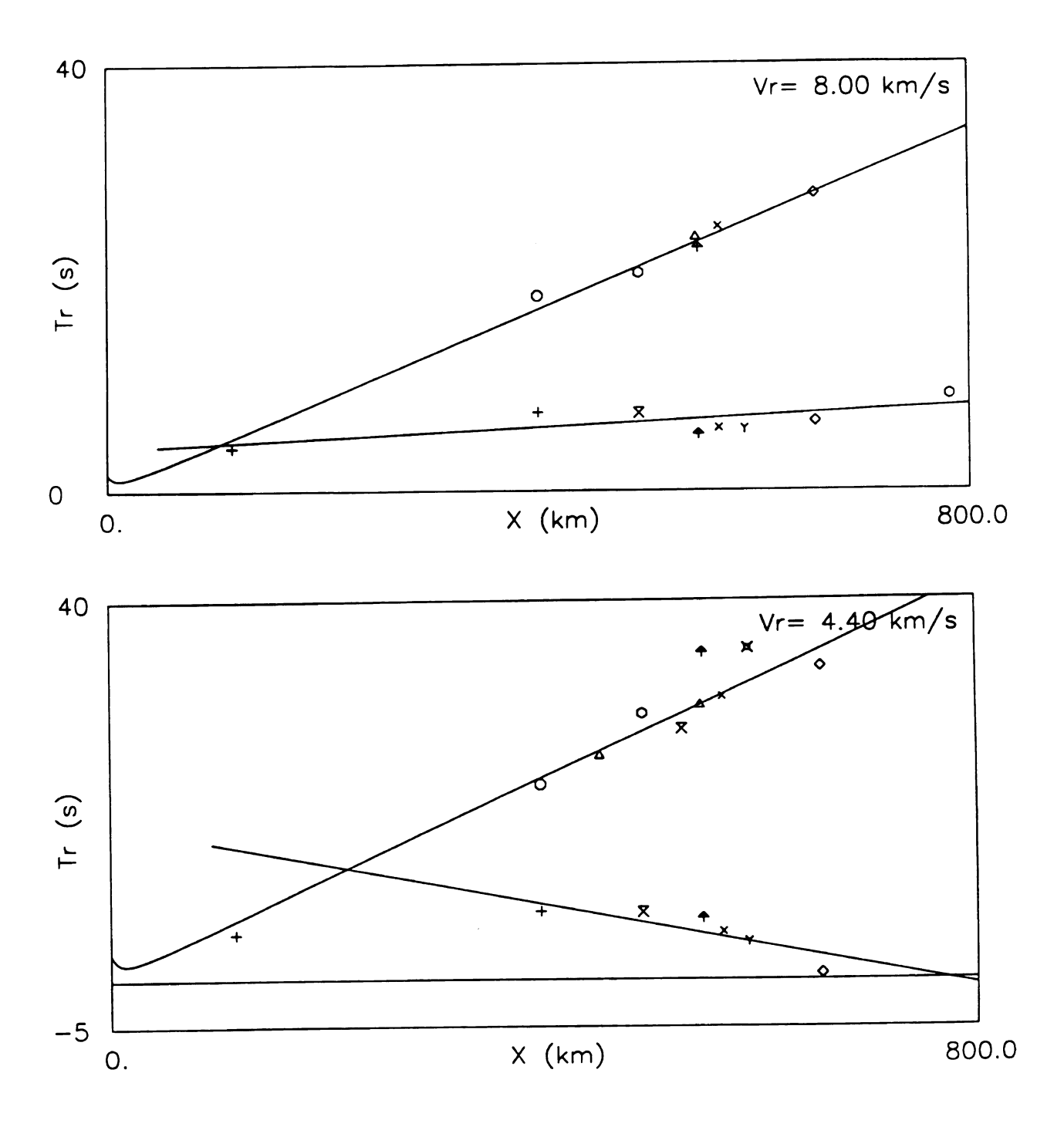


Figure 44. Tenkeli station reduced traveltime curves and crustal model. Pg velocity 5.98 km/sec, Pn velocity 7.70 km/sec, and crustal thickness 24 km. Sg velocity 3.57 km/sec. Conventions as in Figure 22.

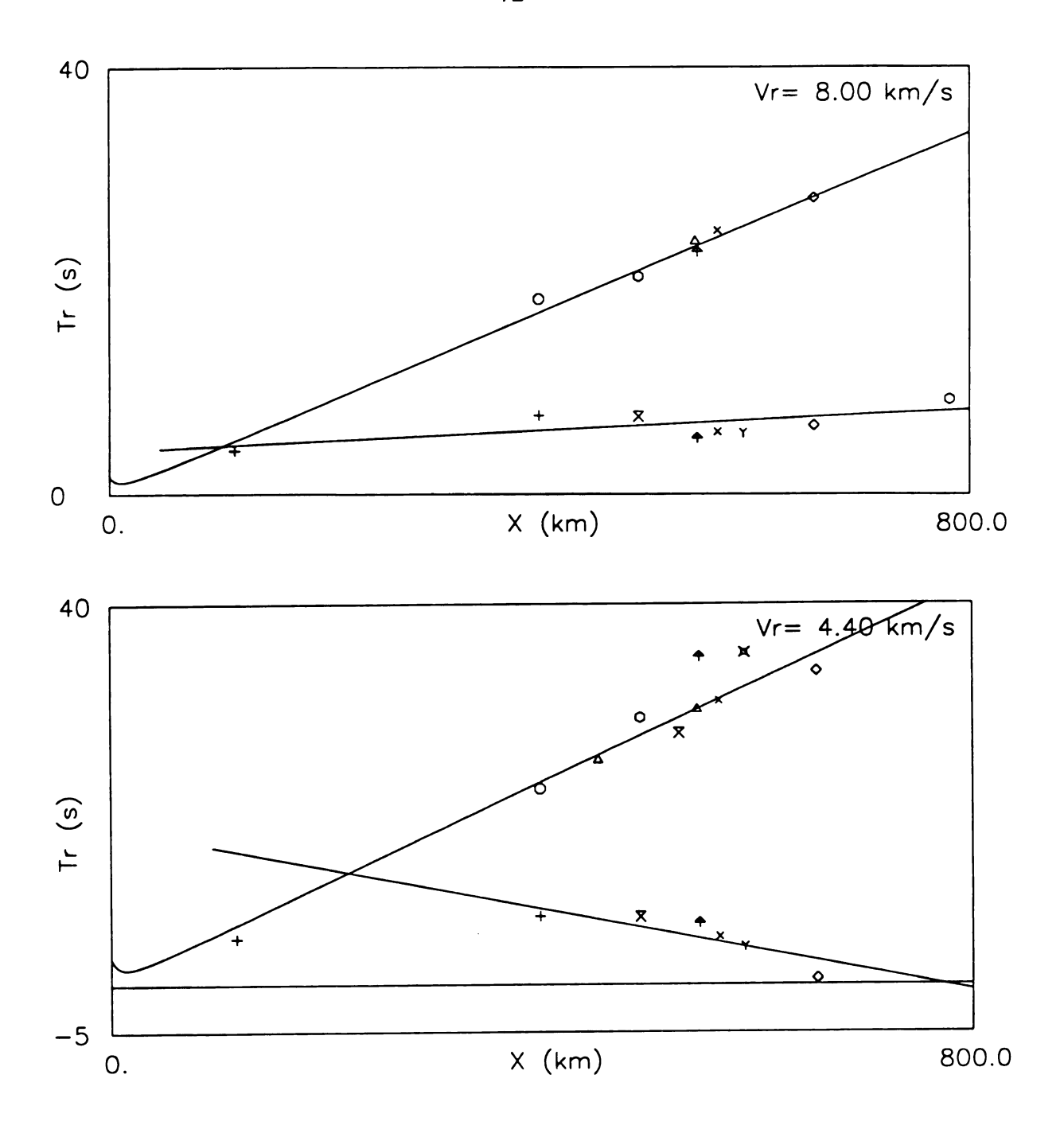


Figure 44. Tenkeli station reduced traveltime curves and crustal model. Pg velocity 5.98 km/sec, Pn velocity 7.70 km/sec, and crustal thickness 24 km. Sg velocity 3.57 km/sec. Conventions as in Figure 22.

F k

.

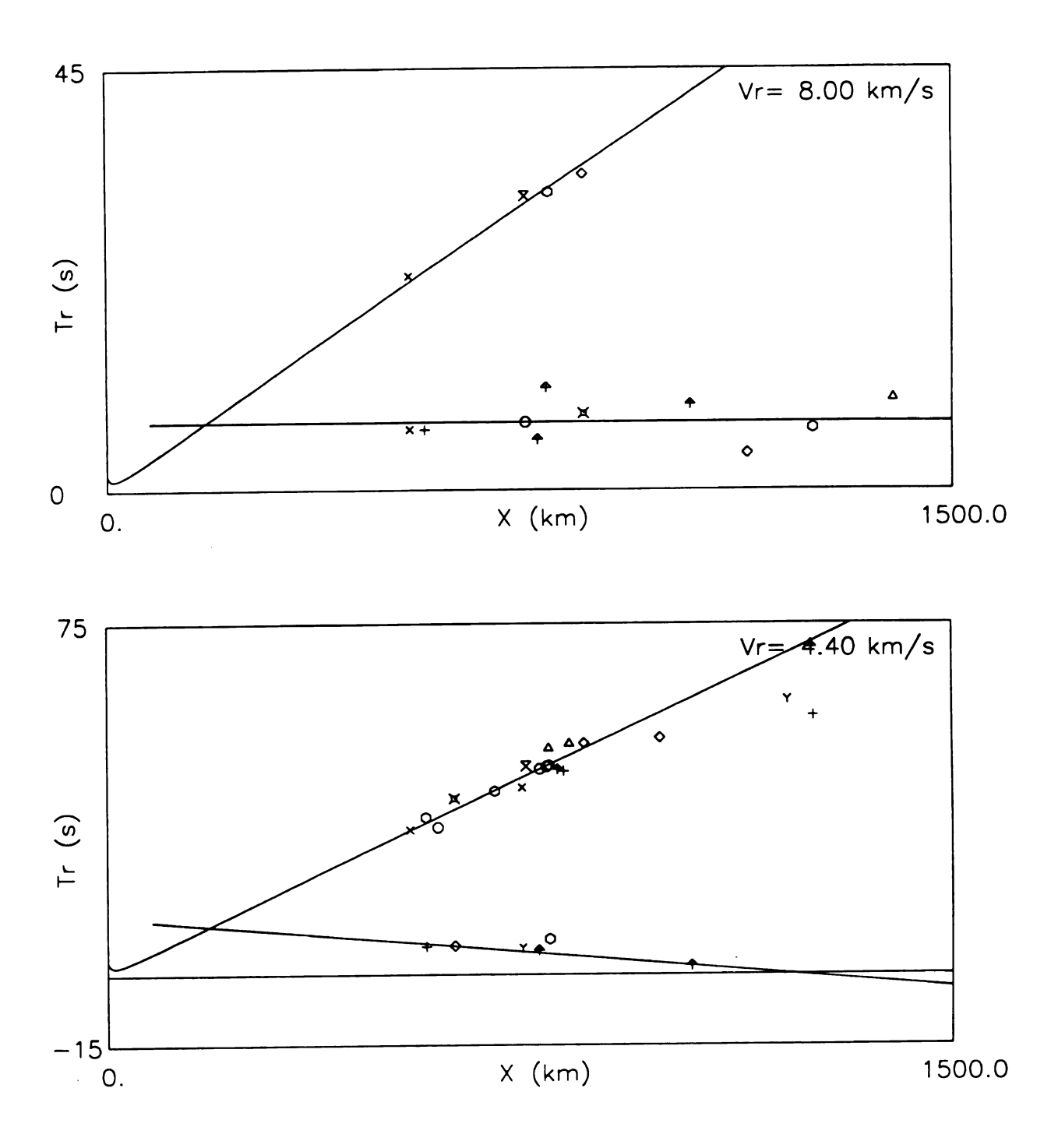


Figure 45. Yakutsk station reduced traveltime curves and crustal model. Pg velocity 6.03 km/sec, Pn velocity 8.00 km/sec, and crustal thickness 38 km. Sg velocity 3.52 km/sec. Conventions as in Figure 22.

Fig km Co

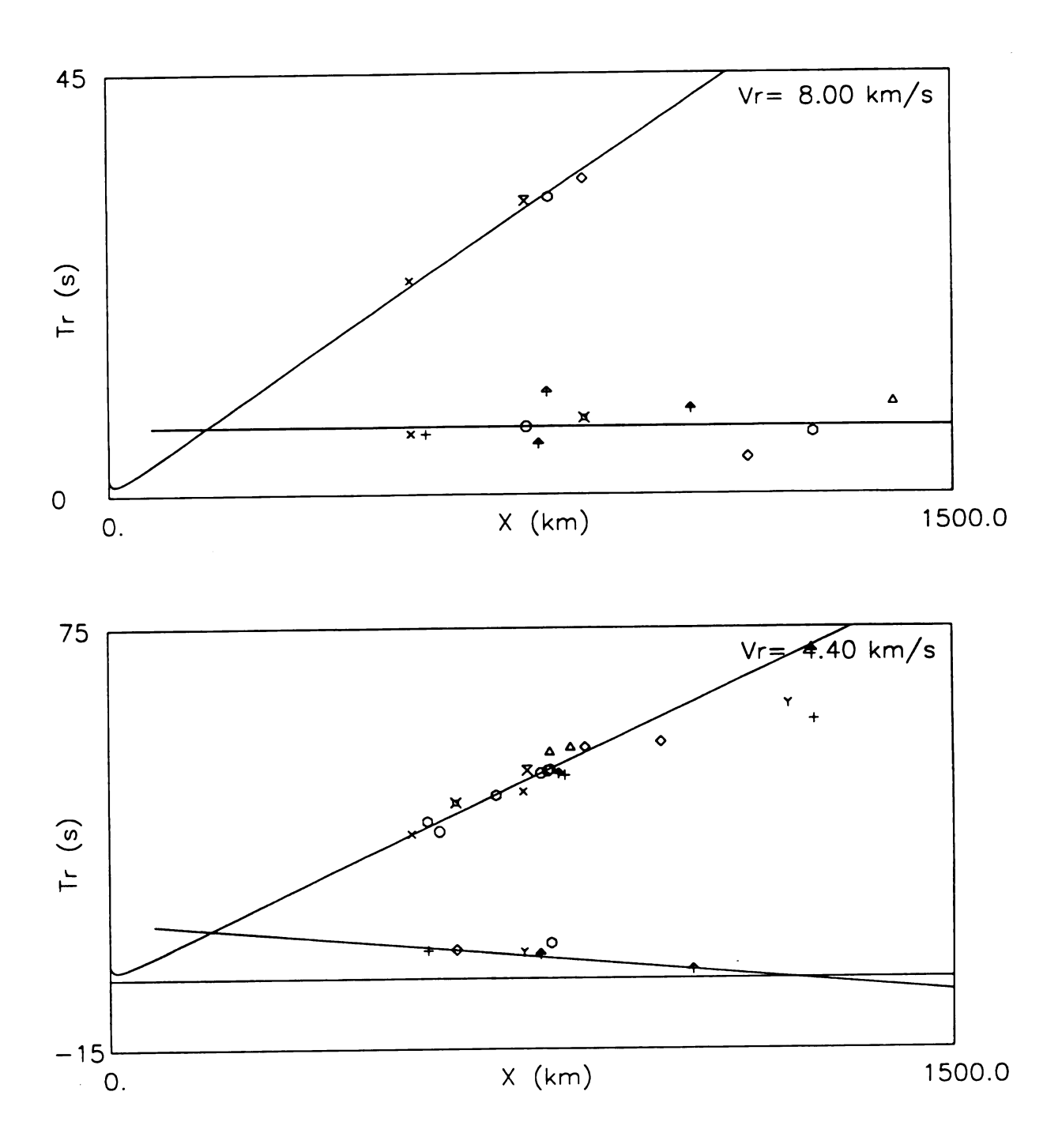


Figure 45. Yakutsk station reduced traveltime curves and crustal model. Pg velocity 6.03 km/sec, Pn velocity 8.00 km/sec, and crustal thickness 38 km. Sg velocity 3.52 km/sec. Conventions as in Figure 22.

С

4

(8)

0

Figu 6.00 km/

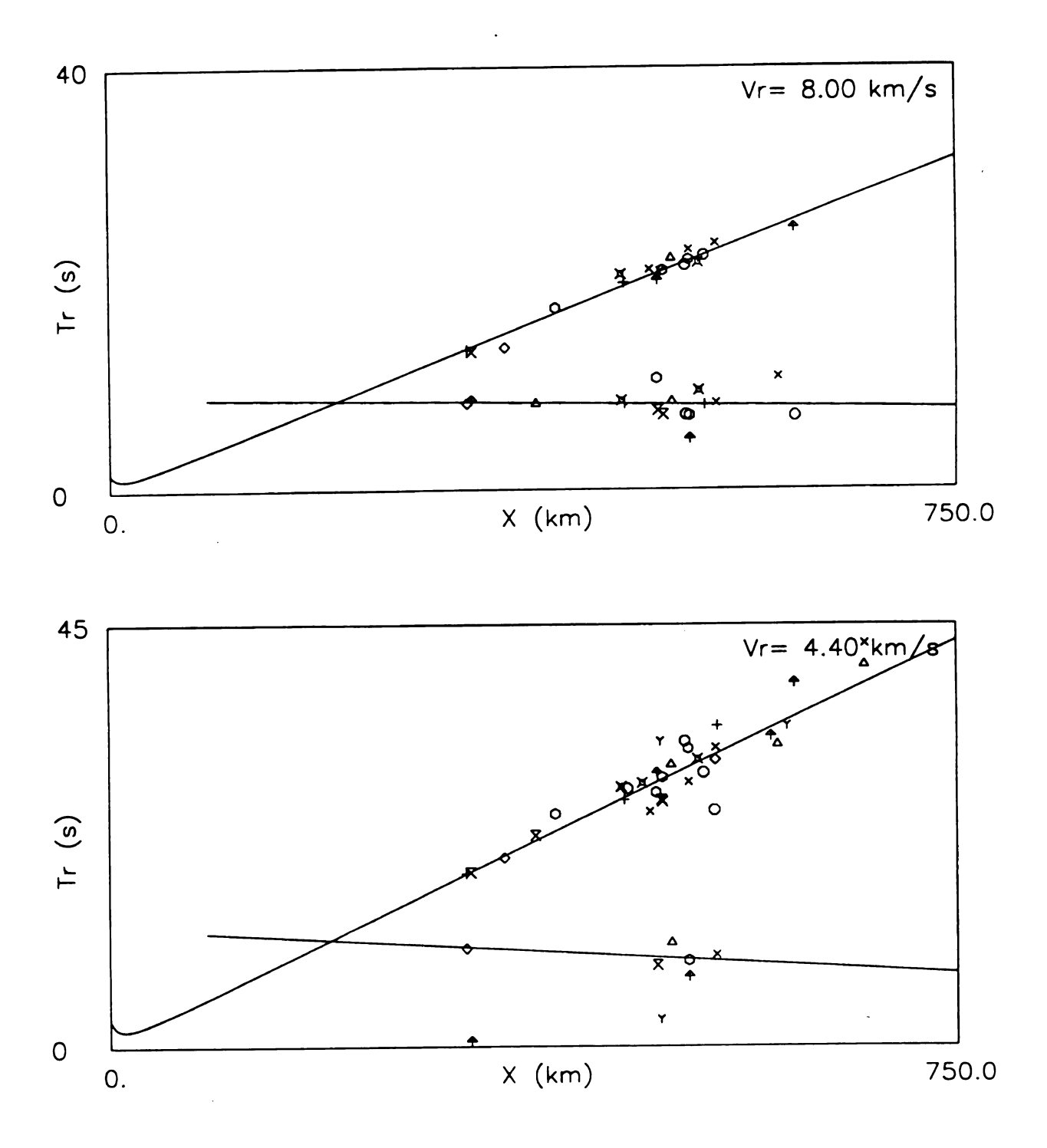


Figure 46. Khandyga station reduced traveltime curves and crustal model. Pg velocity 6.00 km/sec, Pn velocity 8.10 km/sec, and crustal thickness 44 km. Sg velocity 3.51 km/sec. Conventions as in Figure 22.

Tr (s)

С

50

Fig vel 3.5

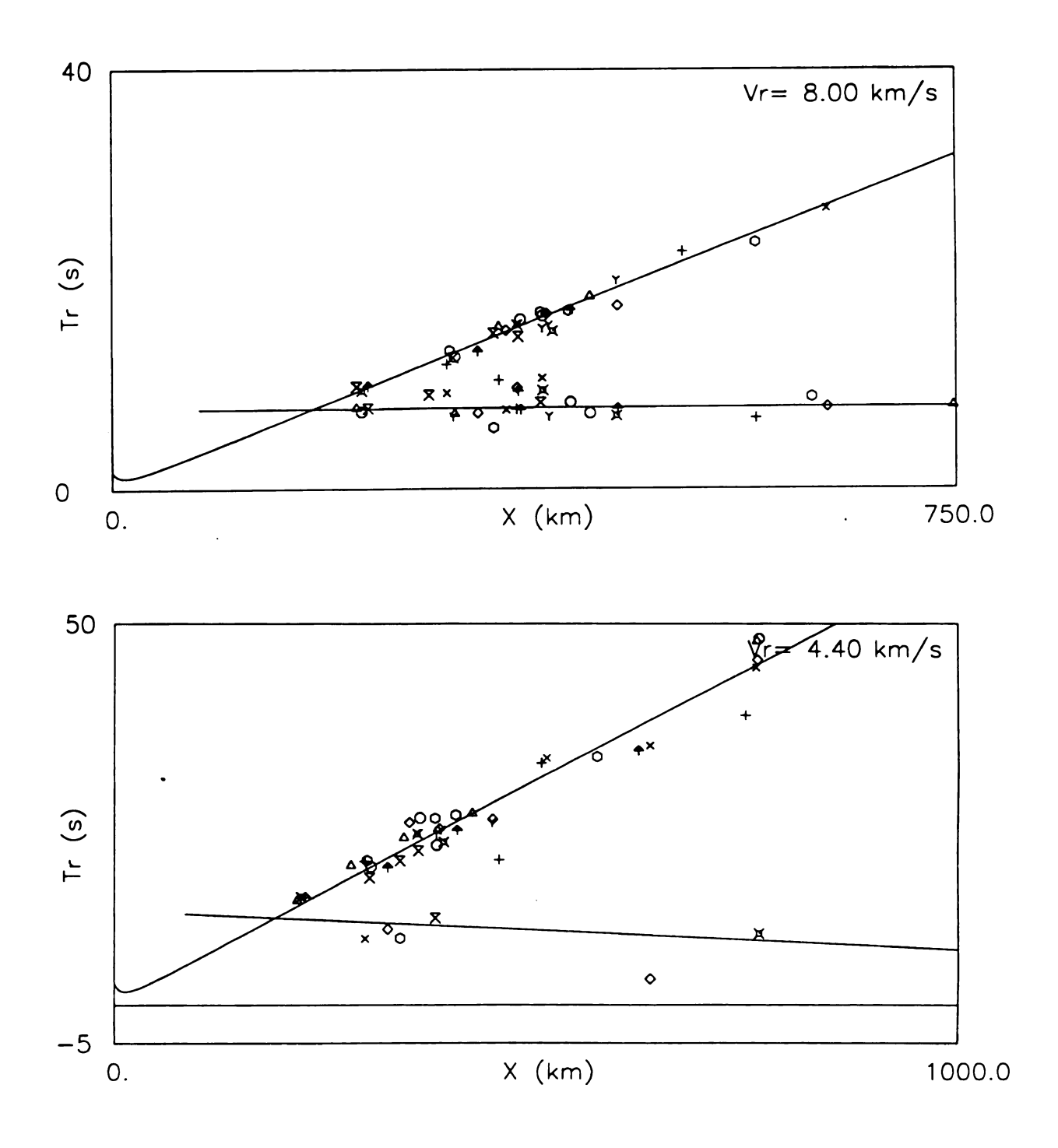


Figure 47. Nezhdaninskoe station reduced traveltime curves and crustal model. Pg velocity 5.98 km/sec, Pn velocity 7.98 km/sec, and crustal thickness 39 km. Sg velocity 3.50 km/sec. Conventions as in Figure 22.

1r (s)

С

5

(0)

Fig vel 3.5

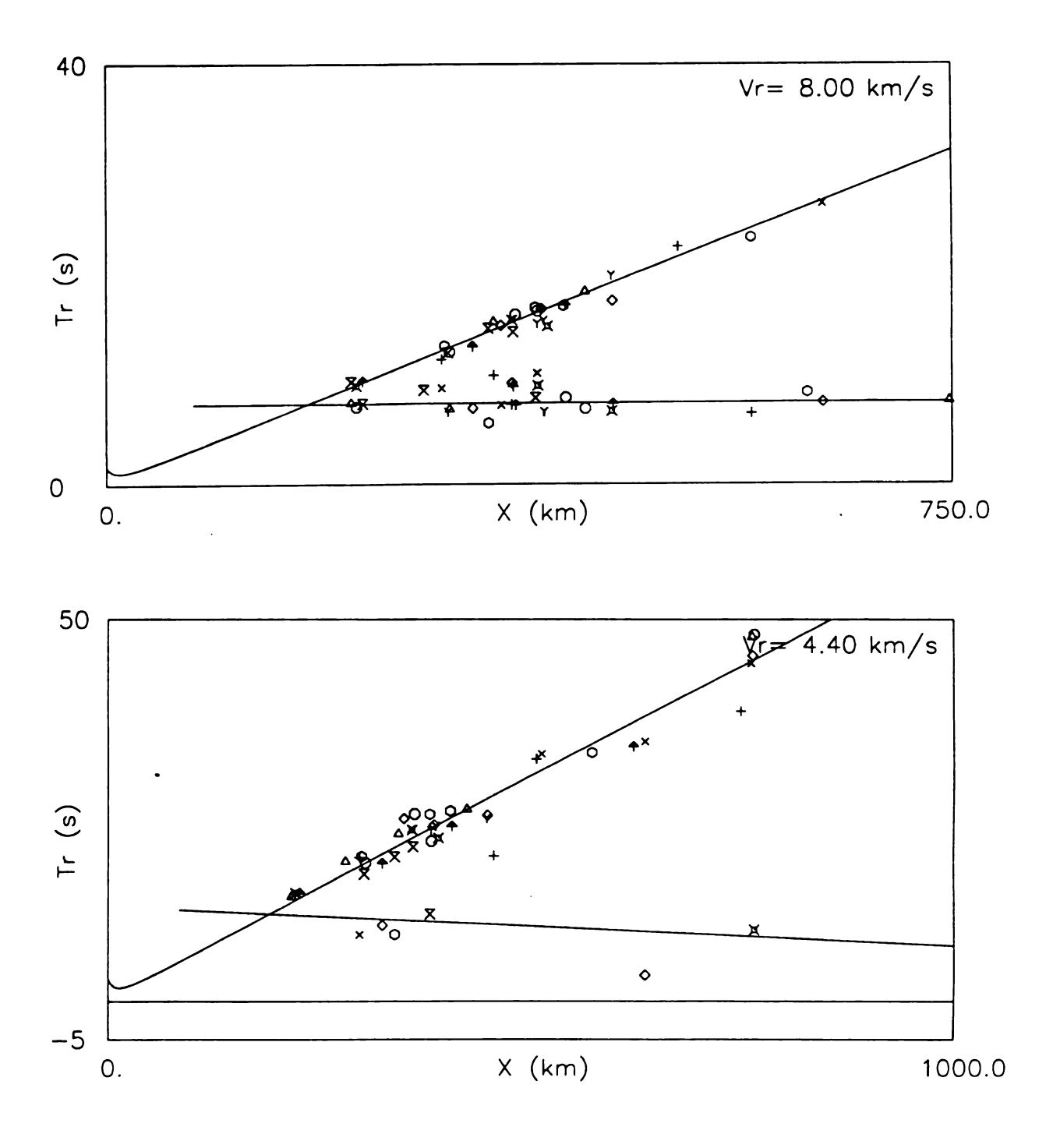


Figure 47. Nezhdaninskoe station reduced traveltime curves and crustal model. Pg velocity 5.98 km/sec, Pn velocity 7.98 km/sec, and crustal thickness 39 km. Sg velocity 3.50 km/sec. Conventions as in Figure 22.

F

d

p

S

0

(N

no

ve]

results. Suvorov and Kornilova (1986) indicate a crustal thickness of 44 km at Khandyga, 40 km at Nezhdaninskoe, and 37 km at Yakutsk. However, data from their study indicate somewhat higher Pn velocities. Neustroev and Parfenov (1985) have also calculated crustal thicknesses for the eastern Siberian platform, indicating 42 km for Khandyga and Yakutsk, and 40 km for Nezhdaninskoe. Bulin (1989) indicates a crustal thickness of 37 km for Nezhdaninskoe.

Evensk, on Shelikhov Bay, is located on the Avekova terrane. The Avekova terrane is composed of Proterozoic gneiss, crystalline schist, and metamorphosed carbonates. Younger units are primarily marine, with minor volcanics (Nokleberg et al., 1994). Evensk data indicate a normal crustal thickness of 37 km, but slightly elevated Pg and Pn velocities at 6.01 km/sec and 8.07 km/sec (Fig. 48). Sn velocities are slightly below normal at 3.48 km/sec. Crustal thickness for Evensk is within 3 km of all other determinations, falling near the center of the field of previous values. There are no other published velocities for Evensk, thus it is not possible to verify the slightly increased velocities.

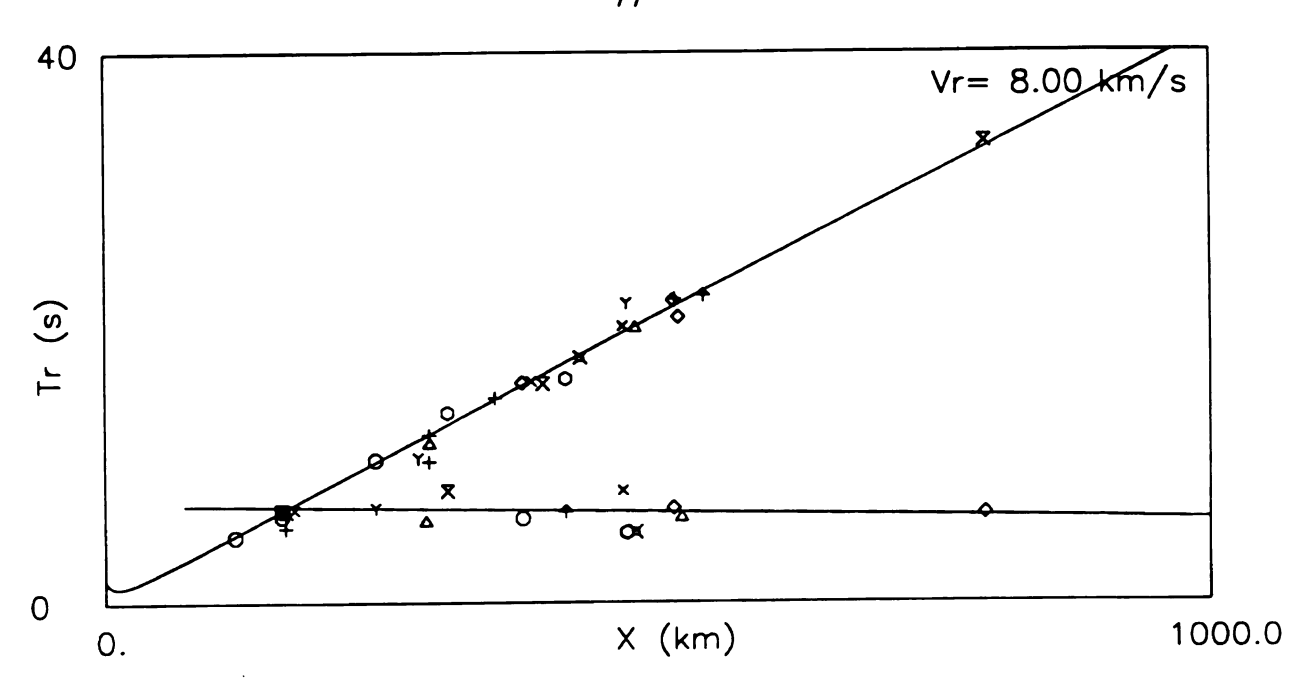
Omolon is located north of Evensk, near the center of the Kolyma-Omolon superterrane (Nokleberg et al., 1994). Station Omolon lies on the Omolon block of the Kolyma-Omolon superterrane. In this study, aside from stations on the Siberian Platform, Omolon is probably the only station which lies on ancient Precambrian continental crust (Nokleberg et al., 1994). Crustal data for Omolon are well constrained and indicated a normal crustal thickness of 37 km, but slightly reduced P velocities (Fig. 49). A Pg velocity of 5.98 km/sec and Pn velocity of 7.98 fit the data well. A slightly reduced Sg

results. Suvorov and Kornilova (1986) indicate a crustal thickness of 44 km at Khandyga, 40 km at Nezhdaninskoe, and 37 km at Yakutsk. However, data from their study indicate somewhat higher Pn velocities. Neustroev and Parfenov (1985) have also calculated crustal thicknesses for the eastern Siberian platform, indicating 42 km for Khandyga and Yakutsk, and 40 km for Nezhdaninskoe. Bulin (1989) indicates a crustal thickness of 37 km for Nezhdaninskoe.

Evensk, on Shelikhov Bay, is located on the Avekova terrane. The Avekova terrane is composed of Proterozoic gneiss, crystalline schist, and metamorphosed carbonates. Younger units are primarily marine, with minor volcanics (Nokleberg et al., 1994). Evensk data indicate a normal crustal thickness of 37 km, but slightly elevated Pg and Pn velocities at 6.01 km/sec and 8.07 km/sec (Fig. 48). Sn velocities are slightly below normal at 3.48 km/sec. Crustal thickness for Evensk is within 3 km of all other determinations, falling near the center of the field of previous values. There are no other published velocities for Evensk, thus it is not possible to verify the slightly increased velocities.

Omolon is located north of Evensk, near the center of the Kolyma-Omolon superterrane (Nokleberg et al., 1994). Station Omolon lies on the Omolon block of the Kolyma-Omolon superterrane. In this study, aside from stations on the Siberian Platform, Omolon is probably the only station which lies on ancient Precambrian continental crust (Nokleberg et al., 1994). Crustal data for Omolon are well constrained and indicated a normal crustal thickness of 37 km, but slightly reduced P velocities (Fig. 49). A Pg velocity of 5.98 km/sec and Pn velocity of 7.98 fit the data well. A slightly reduced Sg





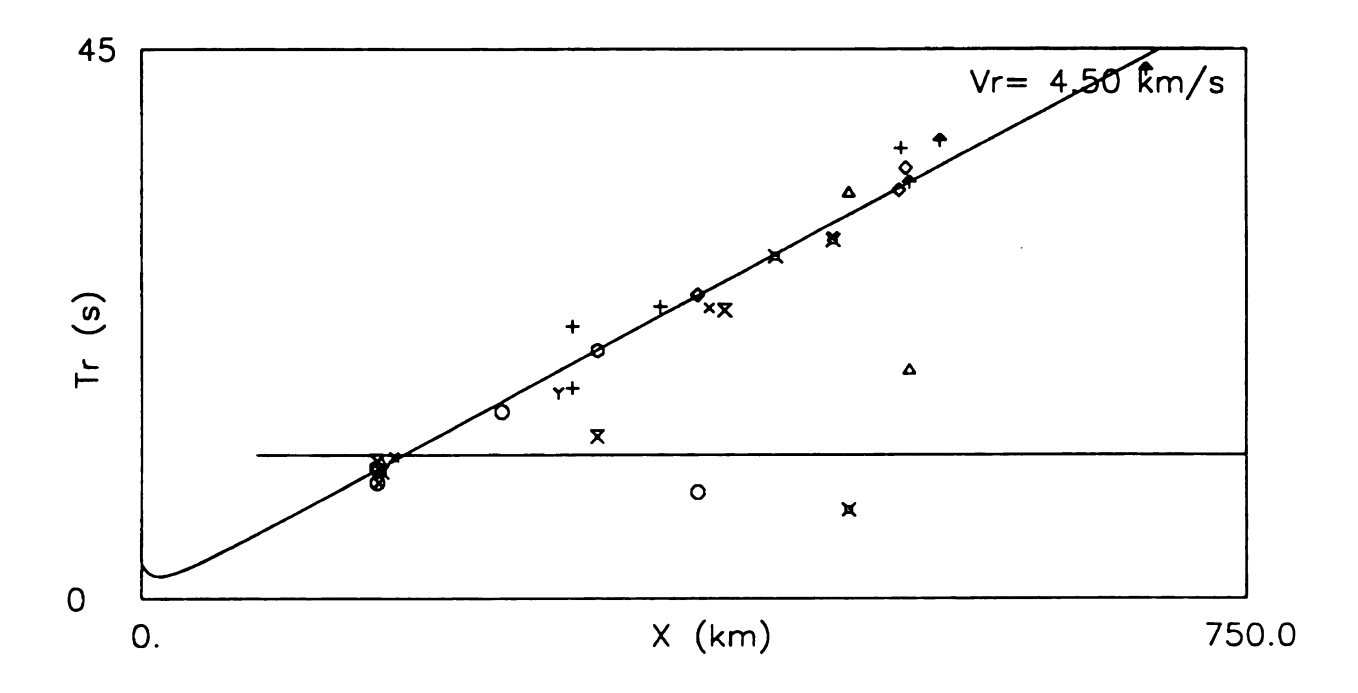


Figure 48. Evensk station reduced traveltime curves and crustal model. Pg velocity 6.01 km/sec, Pn velocity 8.07 km/sec, and crustal thickness 37 km. Sg velocity 3.48 km/sec. Conventions as in Figure 22.

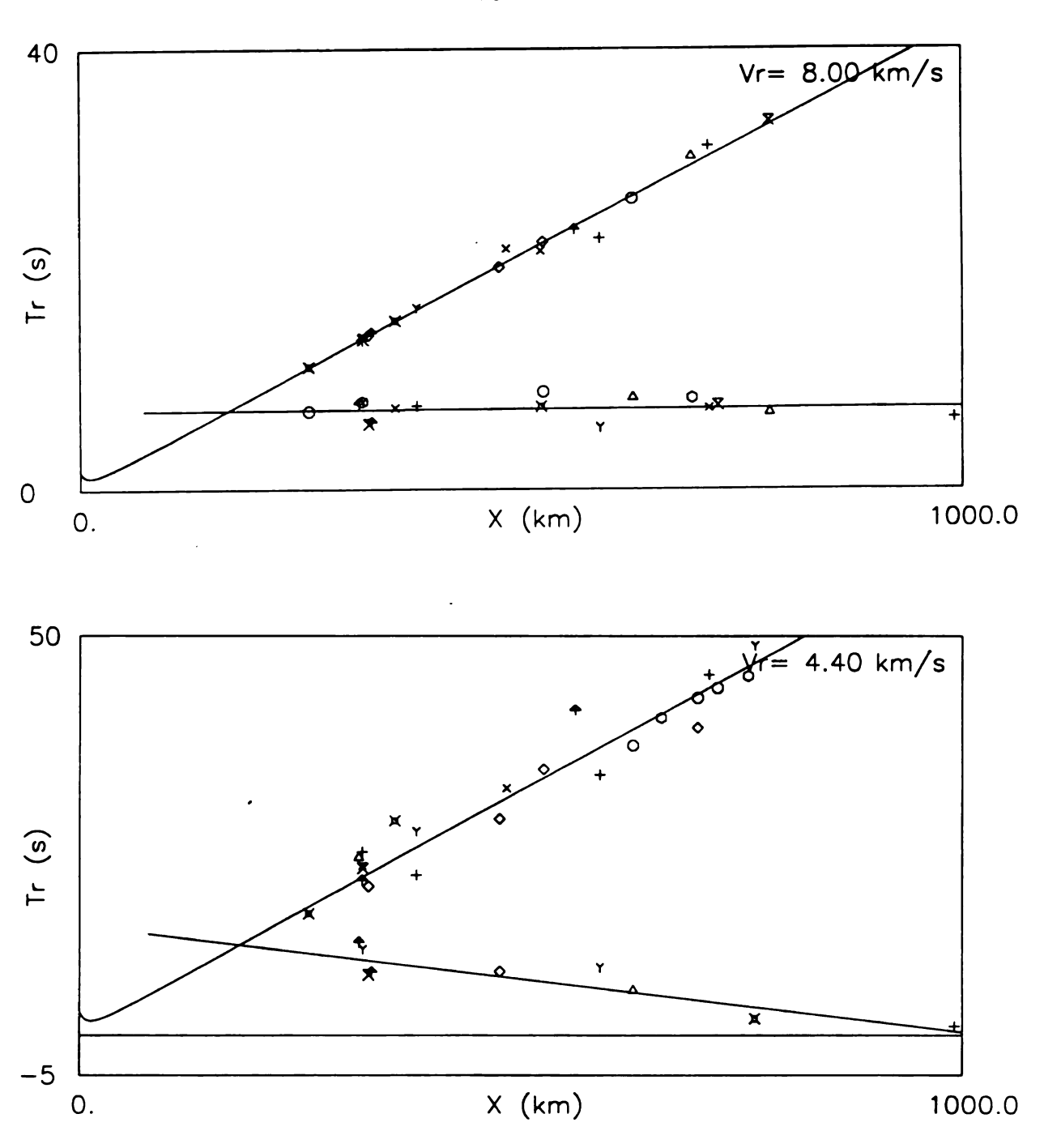


Figure 49. Omolon station reduced traveltime curves and crustal model. Pg velocity 5.98 km/sec, Pn velocity 7.98 km/sec, and crustal thickness 37 km. Sg velocity 3.47 km/sec. Conventions as in Figure 22.

velocity of 3.47 km/sec is also observed for Omolon. Crustal thickness for Omolon is in agreement with previous studies, where values of 38-40 km have been determined.

All crustal thickness values determined in this study are plotted and contoured in figure 50. As a consequence of these results, it is apparent that additional data is necessary for some stations, while for other stations additional work to eliminate spurious and misidentified phases would be beneficial. For all stations, it will be necessary in the future to obtain better quantitative fits to the data. However, this method does appear to be able to resolve variations in crustal and upper mantle velocities and crustal thicknesses.

Discussion

The Pn and Pg velocities obtained herein generally indicate a thicker crust and lower velocity upper mantle than the results of the Magadan-Ust' Srednikan refraction line (Davydova et al., 1968; Ansimov et al., 1967; Belyaevsky, 1974). In comparison with the analysis of Suvorov and Kornilova (1986; Fig. 6), an interesting pattern develops. For individual stations, results are either in good agreement with Suvorov and Kornilova (1986), within 2 km, or not, being 6 km to 10 km greater. All stations where crustal thicknesses determined in this study are 6 km or greater than those of Suvorov and Kornilova (1986) fall along a north-west-north trend from Magadan. Results for stations to the northeast of this trend (Omsukchan, Seimchan, and Susuman) are in excellent agreement with Suvorov and Kornilova (1986). To the southwest, stations Yakutsk, Khandyga, and Nezhdaninskoe, are also in good agreement with values by Suvorov and Kornilova (1986). In general, the trend follows the region where the crust is thinnest in

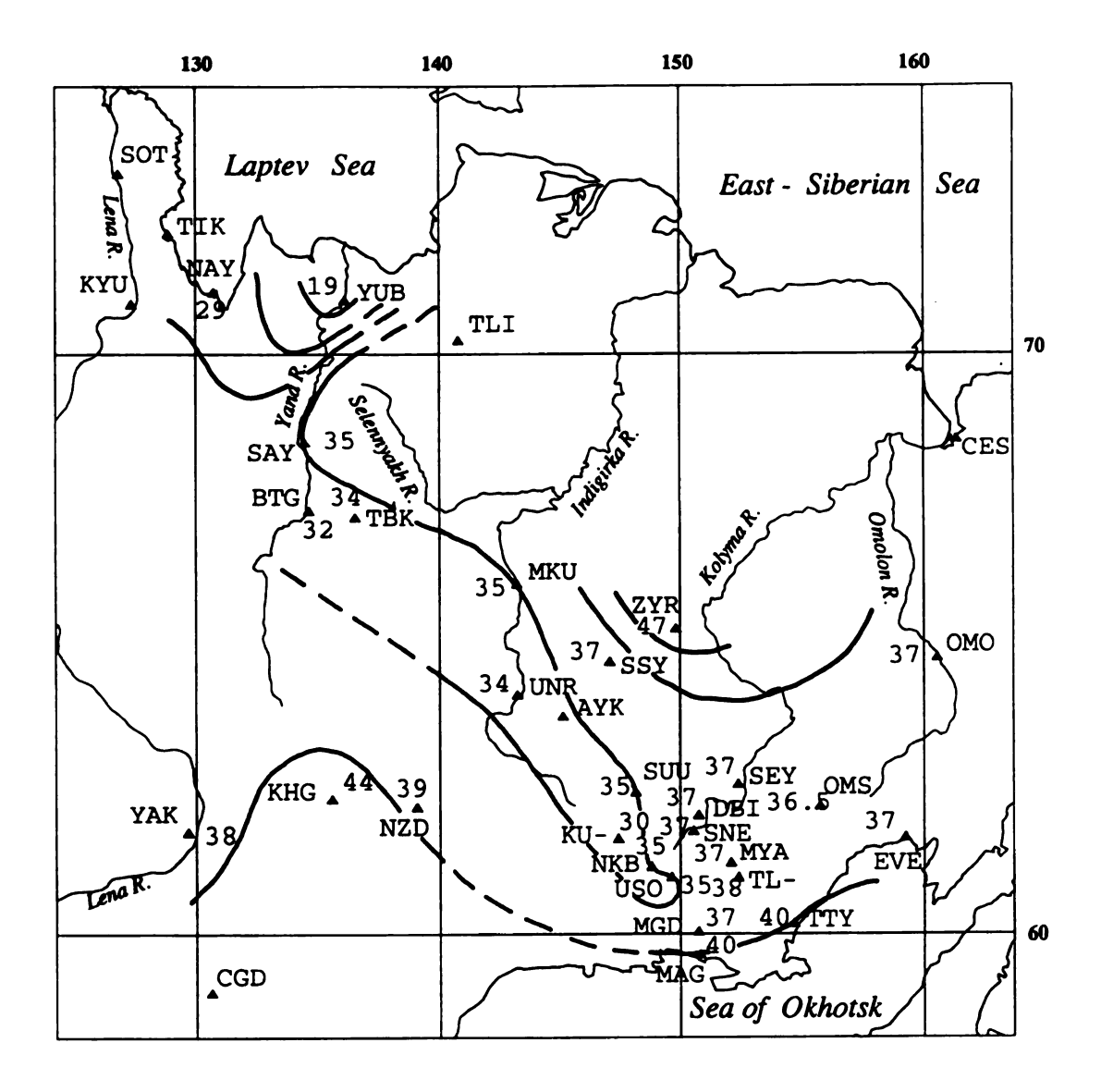


Figure 50. Summary of crustal thickness determinations for the study area. Contour interval = 5 km. Note the generally thinner crust extending northwest from station Ust' Omchug (USO). This region of thinner crust corresponds to the seismically active region and boundary between the North American and Eurasian plates. The thinned crust in this region may have resulted from a Cenozoic rifting episode. Station codes as in figure 7.

both studies. This trend is likely the result of the systematically mislocated epicenters used by Suvorov and Kornilova (1986). The associated errors appear to be about half that of Suvorov and Kornilova (1986). In addition, Suvorov and Kornilova (1986) assumed the thickness at Magadan using the refraction line, however as noted above, this result should be applied at Stekolnyi. Upper mantle velocities are generally slightly less, but are in agreement between this study and Suvorov and Kornilova (1986). Specifically, the highest Pn velocity determined in both studies study was at Khandyga (Table 1). The crustal thicknesses also agree fairly well with those reported by Belyaevsky and Borisov (1974) for Stekolnyi, Magadan, Omolon, and Omsukchan. Their value for Magadan lends some support for a thicker crust in the Okhotsk-Chukotka volcanic belt. Overall, Khandyga, Nezhdaninsk, Yakutsk, and perhaps Omolon show the most consistent agreement among multiple studies. Thus, the degree of confidence for stations in older platform regions is high.

The major differences between the various determinations are for Ust' Nera, Magadan, and Nelkoba. Nelkoba data indicates a thickness 4 km to 6 km thinner than that determined by P-Ps conversions (Mishin and Dareshkina, 1966; Belyaevsky and Borisov, 1974; Vaschilov, 1989). Nelkoba and Magadan both have a high degree of scatter in the Pn data, thus it is possible to vary the crustal structure model to conform with other studies and still maintain a reasonable fit to the data. The situation at Ust' Nera is more problematic. There is a great difference in the crustal thickness reported at Ust' Nera by Suvorov and Kornilova (1986), 24 km, and by Bulin (1989), 40 km. Our results fall somewhat in between at 34 km. Although there is some scatter in the Pn data,

a crust significantly thicker or thinner can not be supported. Thus, the author is inclined to disagree with the results of Suvorov and Kornilova (1986), and Bulin (1989). Gravity analysis by Norton et al. (1994) also suggest a crustal thickness near Ust' Nera of 35-36 km, supporting a slightly thinned crust relative to the regional average.

The overall general trend for crustal thicknesses determined in this study support a slightly thinner crust throughout the central Chersky seismic belt (Fig 50). Throughout most of the Chersky seismic belt, the crustal thickness variations are generally less than 4 km. This may imply that the effects of the Moma rift are less than envisioned by Parfenov et al. (1988) and Lander (1984). This study does indicates significant crustal thinning in the southern portions of the Laptev Sea rift. The basic trend is identical to that identified by Suvorov and Kornilova (1986), except lesser in degree. Converted wave studies are not clearly supportive of this trend.

Gravimetric data are available for the central and northern portion of the study area (Fig. 51; Parfenov et al., 1988; Crumley and Parfenov, 1994). The central portion of the study area shows some correlation with the gravity data. The region of thinned crust corresponds roughly with large negative anomalies, although crustal thickness contours here are constrained by only a few data points. Large negative anomalies do not correlate well with the thinned crust in the northern Laptev Sea rift portion on the study area. The lack of good correlation between gravity anomalies and crustal thickness attests to the difficulty of determining crustal thickness solely with gravity data as in studies by Vaschilov (1984), and Bobrobnikov and Izmailov (1989).

The locations of elevated heat flow levels (Fig. 52) are generally consistent with

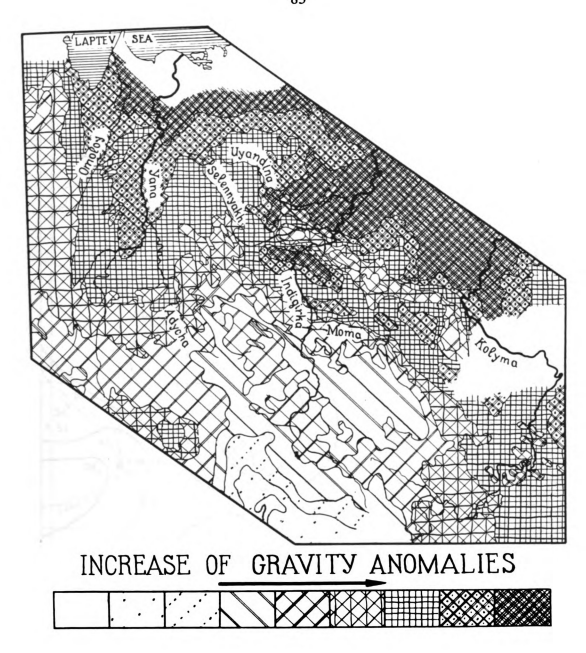


Figure 51. Map of relative gravity anomalies for the northern and central portion of the study area. From Parfenov et al.(1988).

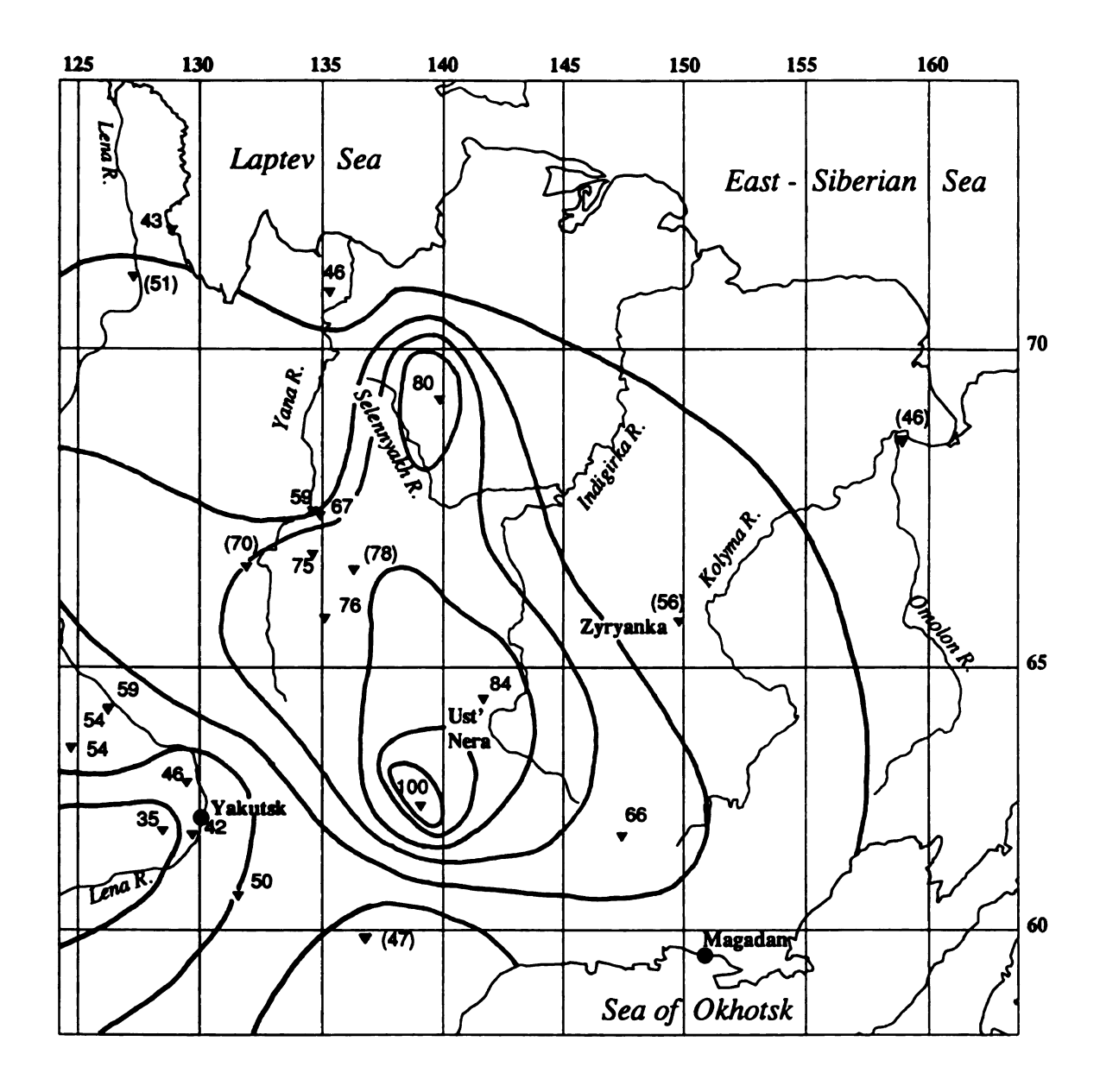


Figure 52. Map of heat flow levels in the study area. Triangles represent borehole locations with values in mW/m². Values in brackets were interpolated from contours on other maps.

the region of thinned crust. Within the thinned crust region, heat flow reaches a maximum of 84 mW/m² at Ust' Nera (Melnikov et al., 1976). At Zyryanka, to the northeast of Ust'Nera, heat flow drops to 56 mW/m² (Duchkov et al., 1982; Duchkov and Sokolova, 1985). To the southwest, there is a slight increase in heat flow to 100 mW/m² at Nezhdaninskoe (Parfenov, 1988), and then a rapid decline to 42 mW/m² near Yakutsk and less than 30 mW/m² just beyond (Duchkov et al., 1982; Koz'min et al., 1994). The regions of elevated heat flow are likely remnants of the extensional episode which formed the Moma rift. However, it is puzzling that heat flow values in the Laptev Sea rift region, on an active rift, do not appear elevated as would be expected. Reported heat flow measurements may be affected by extremely thick permafrost layers (>500m), which in some cases is as deep as the boreholes used in the heat flow measurements penetrate (Melnikov et al., 1976). It should be noted that the actual boundaries of the elevated heat flow region are difficult to constrain with the available data.

Conclusions

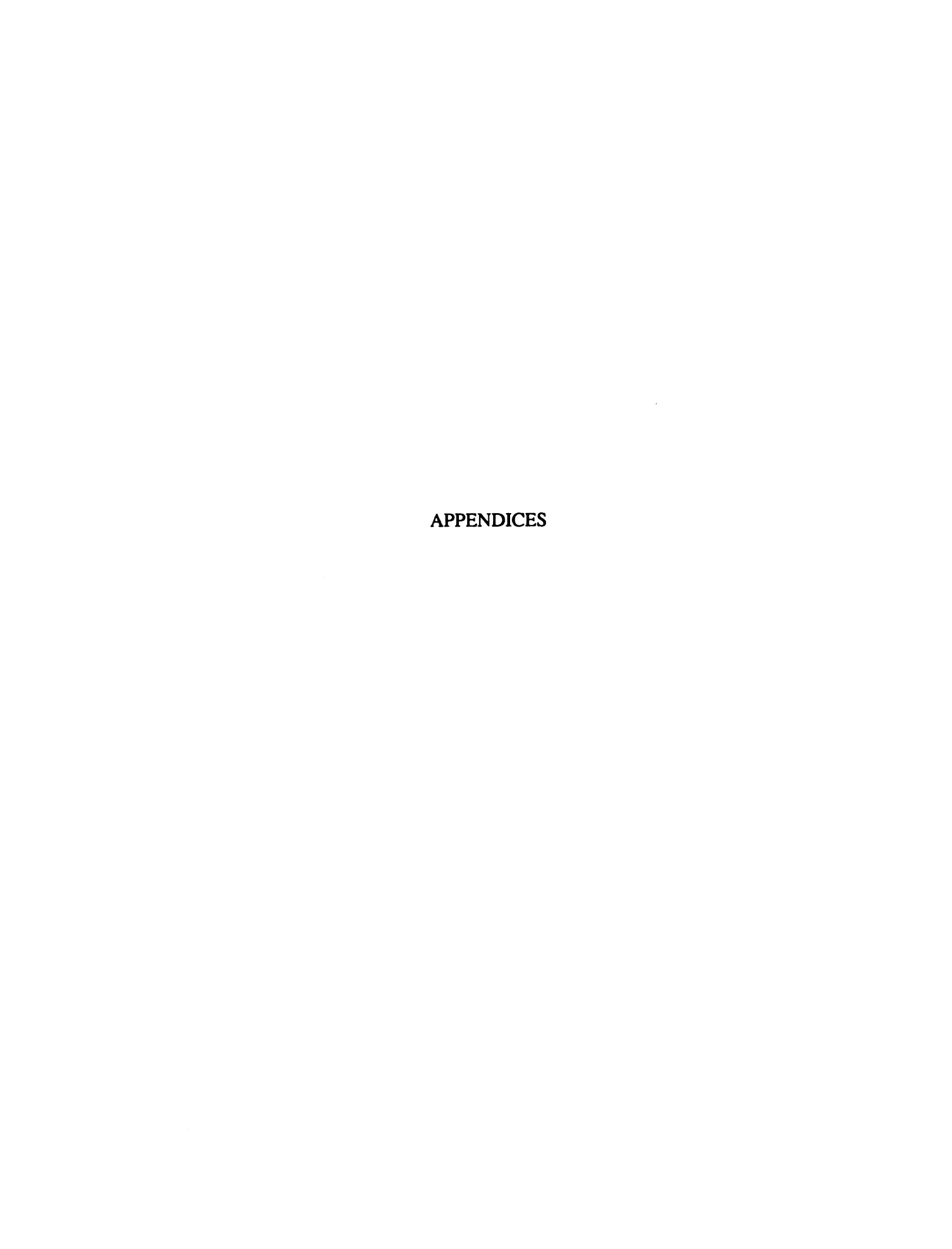
The method of Ruff et al. (1994) allows one to obtain corrections in origin time and timing errors and allows rapid identification of spurious arrivals reported in the Russian bulletins. Combined with relocations of epicenters, this method has allowed the refining of the first-order crustal structure of northeast Russia using available phase data and the investigation of crustal thickness and upper mantle velocities at individual stations. This work confirms that a simple crustal model is a superior method of locating

the region of thinned crust. Within the thinned crust region, heat flow reaches a maximum of 84 mW/m² at Ust' Nera (Melnikov et al., 1976). At Zyryanka, to the northeast of Ust'Nera, heat flow drops to 56 mW/m² (Duchkov et al., 1982; Duchkov and Sokolova, 1985). To the southwest, there is a slight increase in heat flow to 100 mW/m² at Nezhdaninskoe (Parfenov, 1988), and then a rapid decline to 42 mW/m² near Yakutsk and less than 30 mW/m² just beyond (Duchkov et al., 1982; Koz'min et al., 1994). The regions of elevated heat flow are likely remnants of the extensional episode which formed the Moma rift. However, it is puzzling that heat flow values in the Laptev Sea rift region, on an active rift, do not appear elevated as would be expected. Reported heat flow measurements may be affected by extremely thick permafrost layers (>500m), which in some cases is as deep as the boreholes used in the heat flow measurements penetrate (Melnikov et al., 1976). It should be noted that the actual boundaries of the elevated heat flow region are difficult to constrain with the available data.

Conclusions

The method of Ruff et al. (1994) allows one to obtain corrections in origin time and timing errors and allows rapid identification of spurious arrivals reported in the Russian bulletins. Combined with relocations of epicenters, this method has allowed the refining of the first-order crustal structure of northeast Russia using available phase data and the investigation of crustal thickness and upper mantle velocities at individual stations. This work confirms that a simple crustal model is a superior method of locating

earthquakes in the region; new earthquake relocations show the original Russian locations contain systematic errors resulting from the use of a travel time curve with excessive velocities. This study has resolved a slightly thinner crust in portions of the Chersky Seismic Belt, which likely reflect the extensional episode associated with the Moma rift and present Laptev Sea rift systems. This study has also demonstrated the applicability of the 'SQUINT' program to a geographically large area with sparse station coverage. For future works, data from the Yakut network for Magadan region events (and vice versa) will improve the existing data set, and allow determinations of crustal thickness at additional stations, particularly in the northern Sakha Republic (Yakutia) and Chukotka. I also plan to combine data from Alaska and Magadan to study the Bering strait region and to research the possible existence of a Bering Sea block. The extension of this study will also provide additional constraints on the tectonics and evolution of this highly complex region.



APPENDIX A

Earthquake data for events shown in Figure 7 and Figure 11. Events preceded by an asterisk were used in the determination of crustal structure. Bulletin data is from *Materialy Po Seismichnosti Sibiri*, except as noted. All events were relocated using only Pg arrivals and using only first arrivals (primarily Pn). Epicenters and new origin times were determined with high residual stations removed. Dashed lines indicate where insufficient data were available for relocation, or where the relocation was unstable.

APPENDIX A

DATE	BULLETIN	LOCAT	ION	PG RE	LOCATION	1st ARRI	VAL RELOCATION	
	ORIGIN TIME	EPI	CENTER	ORIGIN TIME	EPICENTER	ORIGIN TIM	E EPICENTER	NO-
YR MO DY	HR MIN SE.C	LAT	LONG	HR MON SE.C	LAT LONG	HR MIN SE.C	LAT LONG	TES
76-01-21	06 01 55.0	67.8	140.20	06 01 55.4	66.661 138.390	06 01 47.2	67.765 140.276	
76-02-07	22 58 01.	72.2	132.40					
76-02-11 76-04-08	04 00 59. 04 21 00.	72.1 67.1	131.20 139.70					
76-04-18	07 38 07.	60.8	154.40	07 38 04.8	60.662 154.570			
76-04-26	20 12 19.	61.7	156.30	20 12 19.0	61.657 156.206		(0.00(150.707	
76-05-08 76-06-2 4	11 39 26.6 09 52 20.	60.06 60.2	152.7 4 157.20	11 39 25.5	60.088 152.726	11 39 25.7	60.006 152.787	
76-06-24	17 58 05.	59.8	157.40	17 57 52.5	59.532 158.879			
76-07-01	13 42 05.	72.0	133.70					
76-07-0 4 76-07-16	23 23 35. 07 53 4 2.	65.7 69.6	135.00 138.60					
76-07-24	18 47 42.	72.2	137.80					
76-08-03	16 21 31.	60.4	147.00 125.00	16 21 28.0	60.218 146.876			
76-08-22 76- 08-22	20 02 33. 20 03 52.	72.8 72.8	125.00					
76-08-22	23 43 40.	74.3	141.20					
76-08-26	22 49 50.	72.6	129.00					
76-08-29 76-09-07	01 39 49 20 04 31.	60.9 61.3	132.60 156.00	20 04 22.5	61.048 156.803			
76-09-29	06 05 50.	61.9	147.00	06 05 46.7	61.744 146.857			
76-09-30	21 05 39.	58.0	147.10					
76-10-03 77-01-11	23 16 08. 09 02 21	63.1 66.5	150.70 141.50					
77-01-24	15 19 57.2	59.04	149.44					
77-02-03	11 13 27.	61.3	156.70	11 13 33.0	61.704 155.894			
77-02-15 77-02-15	06 58 10. 23 35 38.	62.5 75.1	147.00 124.80					
77-02-26	04 39 10.	64.0	157.60					
77-03-09	05 34 37.	60.0	152.80					
77-03-18 77-04-10	09 54 56.8 15 48 41.	60.50 66.1	148.08 142.20					
77-04-13	02 01 10.	58.2	133.90					
77-05-03	11 40 24.	60.6	161.60			11 40 29.2	60.806 160.569	
77-05-13 77-05-1 4	10 52 38. 21 18 58.	59.0 59.0	150.70 150.80	21 18 58.	59.022 150.668	21 18 56.8	58.960 150.367	
77-06-21	06 05 38.	61.7	139.20					
77-06-27 77-09-12	17 4 7 19.8 03 39 00.	63.00	146.41	17 47 15.9 03 39 04.0	62.774 146.185 62.878 154.338	17 47 16.1	62.809 146.287	
77-09-12	07 37 24.	62.9 73.2	155.10 124.80	03 39 04.0	62.878 154.338			
77-10-13	01 57 56.	60.6	153.40					
77-10-29 77-11-06	01 31 07. 04 31 23.	67.8 59. 4	142.00 146.50	04 21 15 6	59.066 146.130			
77-11-06	07 41 03.	61.4	144.70	04 31 15.6 07 41 01.0	59.066 146.130 61.318 144.556			
77-11-18	21 55 42.	60.2	143.40	21 55 35.7	60.125 143.317	21 55 38.1	60.312 143.500	
77-11-18	21 55 39.4	60.05	143.32	21 55 35.7	60.125 143.317	21 55 34.6	60.063 143.179	isc
77-11-27 77-12-06	10 17 03. 20 54 22.	62.4 61.4	153.00 1 4 7.00	10 17 00.9 20 54 20.0	62.418 152.909 61.897 147.046			
77-12-29	18 24 19.2	64.14	145.00					
78-01-03	03 17 36.	68.0	139.70					
78-02-05 78-02-08	21 08 05. 23 38 4 5.	71.0 67.78	131.70 132.65					
78-02-22	23 41 48.	63.3	146.30	23 41 45.8	63.046 145.992			
78-03-20 78-03-28	18 34 36. 18 57 23.	64.8 58.9	148.00	18 34 32.3	64.769 148.030	18 57 06.8	58.836 151.126	
78-05-0 4	19 46 13.	61.3	151.20 122.60	19 46 09.0	61.263 122.677	16 37 00.8	30.030 131.120	
78-05-05	16 06 58.	67.8	139.50					
78-05-26	14 28 12.	71.7	145.20			07 05 46 7	EQ 034 161 E60	
78-06-05 78-06-05	07 05 55. 21 01 39.	60.2 60.0	160.10 159.70			07 05 46.7 21 01 41.0	59.824 161.569 60.279 159.471	
78-06-05	21 01 37.	60.16	160.39			21 01 35.2	60.213 160.390	isc
78-06-22	06 12 38.	63.1	145.50		62.925 145.226			
78-07-17 78-08-22	11 04 04. 17 41 40.	60.6 61.3	158.00 144.60	11 03 34.7 17 41 37.7	59.806 160.660 61.203 144.390	17 41 39.5	61.289 144.417	
78-08-22	18 26 31.	61.2	159.80					
78-09-01	00 22 11.	66.1	142.60					
78-09-03 78-10-12	22 42 26. 03 55 38.	70.2 72.4	141.20 138.40					
78-10-15	17 16 31.	63.8	154.00	17 16 11.7	64.881 154.895	17 16 27.4	63.958 154.184	
78-10-27	06 34 42.	64.6	145.10	06 34 39.5	64.617 145.312	06 34 40.3	64.778 145.217	
78-10-28 78-10-28	09 21 20. 09 21 20.	64.4 64.72	145.20 145.05	09 21 18.1 09 21 18.1	64.526 145.112 64.526 145.112	09 21 19.1 09 21 19.9	64.596 145.065 64.693 145.031	1SC
78-11-13	13 29 13.3	59.59	149.18	13 29 14.5	59.584 149.500			-
78-12-02 78-12-05	15 37 03. 11 19 09.	73.2 67.4	139.80 126.10					
78-12-05	08 20 48.	63.6	144.20	08 20 44.5	64.175 145.575			
79-04-10	02 12 19.	69.7	138.00					

79-04-28	08 55 59.0	59.2	152.20	08 56 05.1	59.476 151.609			
79-05-02 79-05-15	22 10 32.0 23 52 34.0	64.1 63.4	149.30 145.40	22 10 28.8 23 52 32.8	64.201 149.217 63.365 145.131			
79-06-05	13 18 09.	75.4	117.80					
79-06-05 79-06-16	14 38 17. 20 41 52.	75.4 64.8	117.80 1 4 3.60	21 41 47.7	64.910 143.671			
79-06-23	08 22 41.0	58.2	133.70	08 22 33.8	58.111 133.677	08 22 43.3	58.625 133.452	
79-06-27	19 27 28.	61.3	137.00					
79-07-13 79-08-18	15 12 4 7. 19 31 50.	62. 4 60.6	130.00 131.80	19 31 41.4	60.242 131.734			
79-08-19	07 10 08.0	61.6	158.80	07 09 15.7	60.941 164.754	07 09 18.0	60.786 166.109	
79-08-27 79-09-10	02 55 03. 00 15 46.	63.0 60.6	145.70 153.00	02 55 10.7 00 15 43.8	62.690 146.643 60.466 153.153			
79-10-03	01 47 12.8	65.87	144.72					
79-10-07	01 29 30.	64.8	144.20	01 29 25.9	65.064 144.072	01 29 26.0	65.065 144.078	
79-10-09 79-10-26	09 4 2 56.0 00 26 26.0	64.8 62.3	144.10 153.90	09 42 51.8 00 26 25.9	65.015 144.059 62.190 153.841	00 26 26.9	62.326 153.945	
79-10-30	08 04 05.	60.6	131.90					
79-11-03 79-11-11	03 28 56.	72.5	124.00	10 27 26 2	62 202 152 021	10 27 25 6	60 006 160 040	
79-11-11	19 27 38. 08 59 17.0	62.3 62.2	153.80 153.80	19 27 36.2 08 59 15.7	62.282 153.821 62.240 153.802	19 27 35.6 08 59 15.5	62.226 153.843 62.259 153.814	
79-12-09	06 57 54.0	62.2	153.80	06 57 55.7	62.254 153.416	06 57 54.6	62.281 153.298	
79-12-21 79-12-25	08 27 53. 05 36 28.	70.3	132.80	05 36 36 0	60 367 164 310			
79-12-25	04 22 21.0	60.2 61.5	154.40 142.60	05 36 26.8 04 22 16.0	60.267 154.318 61.374 142.694	04 22 20.7	61.742 143.264	
80-01-10	20 57 34.	64.4	148.80	20 57 21.8	64.880 149.777			
80-01-18 80-01-25	18 32 29. 18 4 5 5 0.	72.3 64.0	124.20 145.90	18 45 39.5	64.307 145.250			
80-01-27	18 55 41.0	63.4	150.60	18 55 39.7	63.395 150.571	18 55 40.0	63.443 150.502	
80-01-28	05 11 57.0	63.5	150.60	05 11 56.8	63.506 150.656	05 11 56.7	63.465 150.676	k,1
80-02-01 80-02-01	17 37 27. 19 51 51.	73.3 73.2	122.60 122.40			17 30 16.9	73.226 119.769	
80-02-01	21 32 32.	73.2	122.00					
80-02-01	21 39 02.	73.2	123.10					
80-02-02 80-02-02	03 55 18. 04 58 20.	73.1 73.1	122.50 122.40					
80-02-02	18 28 37.	73.1	122.70					
80-02-03	05 54 11.	73.2	122.50					
80-02-03 80-02-03	07 43 16. 09 21 42.	73.2 73.2	122.60 122.00					
80-02-05	11 10 35.	66.6	146.90					
80-02-10 80-02-12	12 08 46.	73.5	124.30					
80-02-12	14 03 03. 03 49 34.	73.3 72.3	123.70 124.70					
80-02-17	06 15 00.	72.7	135.40					
80-03-11 80-03-12	18 11 23.2 08 20 25.	57.13 73.2	127.65 122.50	18 11 19.3	57.010 127.670	18 11 22.1	56.959 127.694	
80-03-17	08 24 05.	73.8	129.40					
80-03-20	19 08 42.	69.6	125.40					
80-04-03 80-04-22	19 15 13. 19 07 48 .	73.5 65.5	117.30 136.80					
80-05-07	05 04 36.	60.3	152.00	05 04 34.9	60.332 151.944	05 04 34.5	60.301 151.961	
80-05-12	09 09 15.	63.16	147.68	09 09 13.2	63.146 147.648	09 09 13.5	62.997 147.439	
80-05-12 80-05-19	19 30 15. 17 29 50.	63.1 60.0	147.70 144.60	19 30 13.0	63.147 147.667	19 30 14.6	63.386 148.069	
80-06-02	13 15 09.	62.8	145.90	13 15 05.9	62.828 145.765	13 15 07.8	62.973 146.034	
80-06-07 80-06-22	02 04 52.9 00 07 53.	64.33	145.47	02 04 52.5	64.066 145.100	02 04 52.0	64.244 145.148 59.987 146.367	
80-07-09	05 03 53.	60.0 73.3	146.10 122.80	00 07 45.6	59.624 146.011	00 07 52.3	59.987 146.367	
80-07-14	08 30 04.	72.8	131.80					
80-09-19 80-09-2 4	18 28 50. 06 06 57.	63.3 74.3	148.30 125.50	18 28 48.6	63.250 148.172	18 28 50.4	63.125 148.160	
80-09-26	10 29 08.	74.5	132.20					
80-10-16	12 34 54.	71.8	129.10					
80-11-08 80-12-03	15 45 30. 17 58 17.5	62.0 63.58	125.00 152.15		63.809 152.133	17 58 15.6	63.674 152.402	h
80-12-17	08 59 54.3	66.88	130.80					_
80-12-27	02 31 36.	60.1	143.3	20 19 04.3	69.754 139.814	20 19 10.2	69.663 138.490	
80-12-29 80-12-31	20 19 12. 05 00 21.0	69.6 64.0	138.1 1 4 0.70	20 19 04.3	09.754 139.814	05 00 19.4	64.151 140.975	
*81-02-02	19 15 18.	62.4	144.50	19 15 15.5	62.385 144.471	19 15 15.4	62.342 144.434	
81-02-05 81-02-22	12 14 17. 23 06 21.	58.7	132.30	12 13 52.2 23 06 20.0	58.139 134.501 63.176 150.968	23 06 20.3	63.111 150.973	
81-03-01	18 39 37.6	63.2 62.44	151.00 1 4 3.31	18 39 33.8	63.176 150.968 62.216 143.226	18 39 30.7	61.943 142.760	
81-03-15	03 50 32.	69.8	138.00					
*81-05-10 81-05-22	18 08 28. 04 59 21.0	61.6 61.0	157.20 156.7	18 08 25.8 04 59 19.6	61.477 157.220 61.045 156.728	18 08 26.7	61.586 157.228	
81-05-22	04 59 24.5	61.24	156.58	04 59 19.6	61.045 156.728	04 59 23.8	61.361 156.543	isc
81-05-27	05 16 49.	73.7	139.20	02 27 24 5	62 775 151 605			
81-06-19 81-07-03	02 27 28. 06 48 06.	63.7 75.0	151.60 137.00	02 27 24.5	63.775 151.695			
81-07-16	03 45 49.	61.8	144.80	03 45 54.1	61.931 145.968			
81-07-27 81-08-03	22 31 33. 08 16 38.	61.6 70.7	144.5 132.20	22 31 18.9 08 16 35.9	60.968 143.614 70.209 129.172			
81-08-09	19 13 41.	63.4	132.20	19 13 38.4	63.416 146.506		63.326 146.245	
81-08-19	19 17 32.0	67.59	140.45					

				Appendix A	(continu	lea)			
81-08-26	10 45 12.	58.5	140.80	10 45 02.3	58.338	141.057			
81-08-29	22 23 52.	65.4	136.9	22 23 51.4			22 23 49.5	65.389 136.315	,
81-08-29	22 23 51.5	65.49	136.43	22 23 51.4		136.736	22 23 49.2		
81-10-20	14 12 52.	73.4	127.10						
81-10-20	21 23 46.	73.5	127.40						
81-11-03 *81-11-08	03 43 03. 21 56 12.9	70. 4 61.91	140.60 153.56	21 56 08.9	61.822	153.724	21 56 08.3		
81-11-08	21 56 11.	61.8	153.60	21 56 08.9	61.822	153.724	21 56 08.2	61.857 153.615	
81-11-08	22 04 59.	61.7	153.60	22 04 60.0	61.801	153.687			
81-11-09	00 33 22.	61.8	153.70	00 33 20.1	61.840	153.722	00 33 21.9	61.918 153.737	
81-11-10	10 07 52.7	63.99	148.75	10 07 46.5	64.327	148.978	10 07 50.6	64.018 148.711	
81-11-10	10 07 52.	64.0	148.90	10 07 46.5	64.327	148.978	10 07 50.7		
*81-11-10 *81-11-11	10 54 18. 14 22 21.	63.9 61.8	148.80 153.60	10 54 15.5 14 22 18.5	63.914 61.856	148.675 153.674	14 22 18.0	63.901 148.588 61.918 153.629	
81-11-11	15 29 49.5	61.80	153.62	15 29 47.8	61.767	153.724	14 22 16.0	01.910 155.029	
81-11-28	05 14 40.5	62.14	154.14	05 14 37.6	62.201	154.270			
81-12-03	14 41 27.	64.0	148.70	14 41 24.9	63.871	148.372	14 41 26.8	63.867 148.820	1
*81-12-08	10 57 22.	61.8	153.70	10 57 20.6	61.798	153.662	10 57 21.4	61.833 153.548	1
82-03-12	23 23 20.	59.6	148.10	23 23 15.7	59.401	148.058	00 41 14 6	61 007 152 623	
82-04-05 *82-04-06	09 41 16.4 14 41 13.9	61.94 61.79	153.60 153.61	14 41 13.3	61.791	153.669	09 41 14.6 14 41 14.3	61.807 153.631 61.818 153.515	
82-06-23	08 04 37.	60.7	137.60	08 04 26.1	60.275	138.221	08 04 27.4		
82-07-24	08 39 04.	63.6	146.20	08 39 01.8	63.563	146.219	08 39 04.3		
*82-08-04	20 17 05.9	62.48	146.93	20 17 03.5	62.370	146.957	20 17 03.9	62.413 147.027	
82-09-03	07 29 31.8	67.04	133.91	07 29 26.5	66.989	133.414	07 29 22.3		
82-09-08	01 47 44.8	58.9	126.40						
82-09-09	11 42 38.8	62.61	151.10	11 42 37.3		151.037			
82-09-19 82-09-22	12 51 06. 07 23 4 7.	70.0 59.5	129.00 152.00	07 23 46.1	59.425				
82-10-04	15 57 17.	59.9	141.50	15 57 08.8	59.684				
82-12-22	12 10 05.	64.1	156.90	12 10 04.6	63.885		12 10 00.8		
*82-12-22	15 47 03.0	59.22	152.70	15 47 03.6	59.201	152.693	15 47 04.3	59.195 152.658	
82-12-29	04 37 41.2	67.05	140.10						
83-01-04	07 17 16.4	62.19	143.72	07 17 13.6		143.655	07 17 15.6	62.250 143.772	
83-03-04	18 03 02.	69.7	138.10				11 55 12 2	(4.242	
*83-03-12 83-03-12	11 55 14. 18 43 07.	64.2 64.3	141.00 140.80	11 55 11.7 18 4 3 05.2	64.275 64.216	140.871 141.027	11 55 12.2	64.342 140.893	
83-03-12	14 45 07.3	62.98	155.70	14 45 05.5	63.046	155.746	14 45 04.0	63.046 156.214	
*83-03-25	10 36 57.	63.63	149.74	10 36 55.1	63.560	149.797	10 36 55.7	63.609 149.807	
83-03-25	10 36 54.	63.6	149.80	10 36 55.1	63.560	149.797		63.543 149.933	
83-04-04	14 37 36.	67.0	140.20	14 37 34.6	66.942	140.073	14 37 34.4		
*83-05-09	16 48 05.	63.3	146.20	16 48 05.3	63.282	146.227	16 48 03.2	63.377 145.777	d
83-05-10	05 27 25.	64.2	150.80	05 27 24.4	64.193	150.838			
83-05-28 83-05-28	01 10 26. 02 57 58.	74.2 62.1	134.70 150.20	02 57 57.0	61.991	150.358	02 57 57.6	61.006 150.352	h
83-06-08	18 29 46.	59.6	148.20	18 29 43.0	59.465	148.088	18 29 45.1	59.527 148.188	
83-06-10	02 13 23.2	75.53	122.75	02 13 25.	75.035	134.995	02 13 24.5	73.439 122.138	
83-06-10	02 13 25.	75.4	122.50	02 13 25.		134.995	02 13 58.0	73.429 128.102	
83-06-26	05 44 02.	71.4	130.10						
83-10-12	16 07 25.0	60.0	150.00	16 07 23.7		149.772	16 07 25.4	59.965 150.048	
83-10-12	16 09 18.	60.0	150.00	16 09 17.9		149.904	10 45 01 2	60 145 153 056	
*83-10-25 83-11-07	19 44 58. 14 21 04.	60. 0 65.6	153.10 136.50	19 44 59.9 14 20 59.9	60.03 4 65.537	153.031 136.343	19 45 01.3 14 20 58.3	60.145 152.850 65.385 136.508	
84-04-01	22 43 51.4	59.58	146.80	22 43 41.5	59.142		14 20 30.3		
84-04-11	20 50 42.0	59.45	148.24	20 50 40.6	59.419		20 50 42.2	59.490 148.123	
84-07-14	23 32 00.	72.4	136.90						
84-07-19	01 52 36.3	68.94	132.39						
84-08-02	21 25 44.	61.0	144.7	21 25 32.1		145.244		61.750 143.902	
84-08-02	21 25 37.8 22 34 10.6	60.89 63.15	144.7 152.90	21 25 32.1		145.244	21 25 40.8	60.843 144.703	
84-08-08 84-08-12	15 27 08.	74.8	136.60						
84-08-12	15 28 03.	74.17	135.10				15 28 03.1	74.094 134.579	1sc
84-08-12	18 34 32.	74.5	137.60						
84-08-12	21 29 29.	74.8	137.70						
*84-08-21	17 41 04.3	60.90	153.79	17 41 02.7		153.842	17 41 04.3	60.983 153.770	
84-09-03	18 40 23.7	61.16	136.74	18 40 20.9	61.145	136.623	18 40 22.3	61.162 136.660	1
84-09-12	20 10 43.3	59.38	138.59	11 26 22:7	63.393	145 626	11 36 33.1	63.393 145.750	
84-09-19 84-10-29	11 36 35.2 14 06 14.	63.48 62.1	145.76 163.50	11 36 32.7 14 06 11.9	61.876	145.635 163.794	14 06 14.7	62.408 163.551	
84-11-21	08 08 17.0	61.33	156.52	08 08 14.4	61.230	156.433	14 00 14.7	02.400 103.331	
84-11-22	13 53 06.	68.6	140.50	13 52 55.8	68.320	141.169	13 52 56.1	68.492 140.875	
84-11-27	09 05 19.	58.8	140.90						
*84-12-02	08 35 47.	63.3	150.70	08 35 45.1		150.560	08 35 44.7	63.418 150.534	
*84-12-02	18 17 53.6	63.37	150.51	18 17 54.9	63.321	150.579	18 17 54.1	63.339 150.366	
85-01-13	07 31 04.0	60.06	153.05	07 31 03.3	60.025	153.184	07 31 04.2	59.997 153.156	
85-01-15 85-01-16	02 08 32.4 23 44 43.3	65.01 71.07	141.81 123.75	02 08 32.7	65.007	141.723			
*85-01-16	18 03 51.0	60.80	155.20	18 03 50.4	60.782	155.319	18 03 51.0	60.759 155.303	
*85-01-24	20 26 34.	66.9	133.30	20 26 33.2	66.900	132.840		66.871 132.799	
85-01-29	00 36 05.6	64.16	145.82	00 36 06.2	64.116	145.801	00 36 07.6	64.205 145.852	q
*85-01-29	00 36 09.4	64.29	145.7	00 36 06.2	64.116	145.801	00 36 07.5	64.242 145.857	q,ısc
85-01-29	09 45 51.0	64.1	145.80	09 45 52.7	64.200	145.878	00 31 46 4	62 011 127 453	
85-02-01 85-02-01	08 31 55. 08 31 44 .0	62.5	127.90 127. 4	08 31 44.0	62.855	127.144	08 31 46.4 08 31 46.3	63.011 127.452 63.016 127.540	
85-02-01 85-02-01	10 20 52.6	62.84 62.63	127.4	08 31 44.0		127.144	08 31 46.3	03.016 127.540	
85-02-01	21 53 18.3	64.25	145.70						

				Appendix A	(continued)		
81-08-26	10 45 12.	58.5	140.80	10 45 02.3	58.338 141.057		
81-08-29	22 23 52.	65.4	136.9		65.356 136.736		65.389 136.315
81-08-29	22 23 51.5	65.49	136.43	22 23 51.4	65.356 136.736		65.374 136.469 isc
81-10-20	14 12 52.	73.4	127.10				
81-10-20	21 23 46.	73.5	127.40				
81-11-03	03 43 03.	70.4	140.60				
*81-11-08	21 56 12.9	61.91	153.56	21 56 08.9	61.822 153.724		61.885 153.616 c.isc
81-11-08	21 56 11.	61.8	153.60	21 56 08.9	61.822 153.724	21 56 08.2	61.857 153.615 c
81-11-08	22 04 59.	61.7	153.60	22 04 60.0	61.801 153.687		(1 010 150 707
81-11-09	00 33 22.	61.8	153.70	00 33 20.1	61.840 153.722	00 33 21.9	61.918 153.737
81-11-10 81-11-10	10 07 52.7 10 07 52.	63.99 64.0	148.75 148.90	10 07 46.5 10 07 46.5	64.327 148.978 64.327 148.978	10 07 50.6 10 07 50.7	
*81-11-10	10 54 18.	63.9	148.80	10 54 15.5	63.914 148.675		63.901 148.588
*81-11-11	14 22 21.	61.8	153.60	14 22 18.5	61.856 153.674	14 22 18.0	
81-11-11	15 29 49.5	61.80	153.62	15 29 47.8	61.767 153.724		
81-11-28	05 14 40.5	62.14	154.14	05 14 37.6	62.201 154.270		
81-12-03	14 41 27.	64.0	148.70	14 41 24.9	63.871 148.372	14 41 26.8	63.867 148.820
*81-12-08	10 57 22.	61.8	153.70	10 57 20.6	61.798 153.662	10 57 21.4	61.833 153.548
82-03-12	23 23 20.	59.6	148.10	23 23 15.7	59.401 148.058	*********	
82-04-05	09 41 16.4	61.94	153.60		(1. 201 . 152 . (6	09 41 14.6	61.807 153.631 isc
*82-04-06	14 41 13.9	61.79	153.61	14 41 13.3	61.791 153.669		61.818 153.515
82-06-23 82-07-2 4	08 04 37. 08 39 04.	60.7 63.6	137.60 146.20	08 04 26.1 08 39 01.8	60.275 138.221 63.563 146.219		60.252 138.615 63.563 146.537
*82-08-04	20 17 05.9	62.48	146.20	20 17 03.5	62.370 146.957		62.413 147.027 e
82-09-03	07 29 31.8	67.04	133.91	07 29 26.5	66.989 133.414		66.883 132.813
82-09-08	01 47 44.8	58.9	126.40				
82-09-09	11 42 38.8	62.61	151.10	11 42 37.3	62.562 151.037		
82-09-19	12 51 06.	70.0	129.00				
82-09-22	07 23 4 7.	59.5	152.00	07 23 46.1	59.425 152.022		
82-10-04	15 57 17.	59.9	141.50	15 57 08.8	59.684 141.313		
82-12-22	12 10 05.	64.1	156.90	12 10 04.6	63.885 156.648		64.135 156.929 f
*82-12-22	15 47 03.0	59.22	152.70	15 47 03.6	59.201 152.693	15 47 04.3	59.195 152.658 f
82-12-29	04 37 41.2	67.05	140.10	07 17 13.6	62.155 143.655	07 17 15 6	62.250 143.772
83-01-0 4 83-03-0 4	07 17 16.4 18 03 02.	62.19 69.7	143.72 138.10	0/ 1/ 13.6	02.155 145.055	07 17 15.6	02.230 143.772
*83-03-12	11 55 14.	64.2	141.00	11 55 11.7	64.275 140.871	11 55 12.2	64.342 140.893
83-03-12	18 43 07.	64.3	140.80	18 43 05.2	64.216 141.027		
83-03-23	14 45 07.3	62.98	155.70	14 45 05.5	63.046 155.746	14 45 04.0	63.046 156.214 g,s
*83-03-25	10 36 57.	63.63	149.74	10 36 55.1	63.560 149.797	10 36 55.7	
83-03-25	10 36 54.	63.6	149.80	10 36 55.1	63.560 149.797	10 36 56.8	
83-04-04	14 37 36.	67.0	140.20	14 37 34.6	66.942 140.073		67.005 140.107
*83-05-09	16 48 05.	63.3	146.20	16 48 05.3	63.282 146.227	16 48 03.2	
83-05-10	05 27 25.	64.2	150.80	05 27 24.4	64.193 150.838		
83-05-28	01 10 26.	74.2	134.70	00 57 57 0	(1 001 150 250	00 57 57 6	(1 00/ 150 252 }
83-05-28	02 57 58.	62.1	150.20	02 57 57.0	61.991 150.358		61.006 150.352 h
83-06-08	18 29 46. 02 13 23.2	59.6	148.20	18 29 4 3.0 02 13 25.	59.465 148.088 75.035 134.995	18 29 45.1 02 13 24.5	59.527 148.188 73.439 122.138 isc
83-06-10 83-06-10	02 13 25.2	75. 53 75. 4	122.75 122.50	02 13 25.	75.035 134.995 75.035 134.995	02 13 24.5	73.429 128.102
83-06-26	05 44 02.	71.4	130.10				
83-10-12	16 07 25.0	60.0	150.00	16 07 23.7	60.026 149.772	16 07 25.4	59.965 150.048
83-10-12	16 09 18.	60.0	150.00	16 09 17.9	60.001 149.904		
*83-10-25	19 44 58.	60.0	153.10	19 44 59.9	60.034 153.031	19 45 01.3	
83-11-07	14 21 04.	65.6	136.50	14 20 59.9	65.537 136.343		
84-04-01	22 43 51.4	59.58	146.80	22 43 41.5	59.142 146.190		
84-04-11	20 50 42.0	59.45	148.24	20 50 40.6	59.419 148.080	20 50 42.2	59.490 148.123
84-07-14 84-07-19	23 32 00. 01 52 36.3	72.4 68.94	136.90 132.39				
84-08-02	21 25 44.	61.0	144.7	21 25 32.1	60.612 145.244		
84-08-02	21 25 37.8	60.89	144.7	21 25 32.1			
84-08-08	22 34 10.6						
84-08-12	15 27 08.	74.8	136.60				
84-08-12	15 28 03.	74.17	135.10			15 28 03.1	74.094 134.579 isc
84-08-12	18 34 32.	74.5	137.60				
84-08-12	21 29 29.	74.8	137.70				(0.002.152.770
*84-08-21	17 41 04.3 18 40 23.7	60.90 61.16	153.79		60.893 153.842	18 40 22.3	60.983 153.770
84-09-03 84-09-12	20 10 43.3	59.38	136.74 138.59	18 40 20.9	61.145 136.623	18 40 22.3	61.162 136.660
84-09-19	11 36 35.2	63.48	145.76	11 36 32.7	63.393 145.635		63.393 145.750
84-10-29	14 06 14.	62.1	163.50	14 06 11.9	61.876 163.794		
84-11-21	08 08 17.0	61.33	156.52	08 08 14.4	61.230 156.433		
84-11-22	13 53 06.	68.6	140.50	13 52 55.8	68.320 141.169	13 52 56.1	68.492 140.875
84-11-27	09 05 19.	58.8	140.90				
*84-12-02	08 35 47.	63.3	150.70	08 35 45.1	63.376 150.560		63.418 150.534
*84-12-02	18 17 53.6	63.37	150.51	18 17 54.9	63.321 150.579		
85-01-13	07 31 04.0	60.06	153.05	07 31 03.3	60.025 153.184	07 31 04.2	59.997 153.156
85-01-15 85-01-16	02 08 32.4 23 44 43.3	65.01 71.07	141.81 123.75	02 08 32.7	65.007 141.723		
*85-01-16	18 03 51.0	60.80	155.20	18 03 50.4	60.782 155.319		
*85-01-24	20 26 34.	66.9	133.20	20 26 33.2	66.900 132.840	20 26 33.0	66.871 132.799
85-01-29	00 36 05.6	64.16	145.82	00 36 06.2	64.116 145.801		64.205 145.852 q
*85-01-29	00 36 09.4	64.29	145.7	00 36 06.2	64.116 145.801	00 36 07.5	64.242 145.857 q,1sc
85-01-29	09 45 51.0	64.1	145.80	09 45 52.7	64.200 145.878		
85-02-01	08 31 55.	62.5	127.90	08 31 44.0	62.855 127.144		
85-02-01	08 31 44.0	62.84	127.4	08 31 44.0	62.855 127.144		63.016 127.540 isc
85-02-01 85-02-01	10 20 52.6 21 53 18.3	62.63 64.25	127.66 1 4 5.70				
03-02-01	21 .5 10.5	04.23	145.70				

05 02 02	11 20 45 3	٠. ٥.	122.05	11 20 44 0	(5 024 126 000			
85-02-02 85-02-18	11 28 4 5.3 12 51 35.	65.85	137.05 136.50	11 28 44.9 12 51 31.3	65.834 136.990 65.557 136.457	12 51 22 7	66 663 126 652	
*85-03-08	22 24 38.0	59.35	151.96	22 24 37.8	65.557 136.457 59.356 152.162	22 24 34.7	65.662 136.653 59.119 152.197	
85-04-10	11 27 46.6	70.43	141.03	11 27 45.1	70.329 141.424			
85-04-12	09 22 16.	62.4	124.10					
85-04-17	20 37 21.8	65.36	142.96	20 37 19.8	65.406 142.946			
85-04-20	22 29 19.6	59.28	141.72					
85-05-22 85-06-02	18 28 48.6	61.02	157.88	18 28 47.3	60.952 157.850	04 08 09.9	64 073 344 040	
*85-06-02	04 08 08.9 04 08 12.8	64.83 64.8	144.08 144.0	04 08 08.8 04 08 08.8	64.857 144.044 64.857 144.044	04 08 09.9	64.871 144.060 64.898 144.249	100
85-06-24	03 54 35.	65.2	145.00	03 54 34.2	65.286 144.664		04.070 144.247	150
85-06-24	03 54 32.4	65.25	144.49	03 54 34.2	65.286 144.664	03 54 34.6	65.205 144.346	t.isc
85-08-20	03 41 37.7	62.14	145.64	03 41 37.9	62.237 145.488			
85-08-28	05 04 11.3	59.90	137.36	05 04 09.0	59.956 137.081			
85-09-10	10 53 03.3	62.46	142.98					
85-10-05	22 32 36.8 22 37 04.5	59. 44 59. 4 1	150.23	22 32 36.0	59.465 150.201	22 32 35.8		
85-10-05 85-10-05	22 37 04.5	59.45	150.26 150.22	22 37 00.7 22 37 10.9	59.299 149.987 59.225 150.192			
*85-11-28	08 38 25.	64.9	144.30	08 38 20.5	64.863 144.133	08 38 22.1	64.850 144.422	
86-01-05	00 35 23.	70.2	128.40	00 35 23.9	70.276 128.612			
*86-01-18	13 13 23.3	60.20	153.67	13 13 22.0	60.191 153.761	13 13 24.8	60.255 153.530	
86-01-24	13 25 26.8	60.70	138.49	13 25 23.0	60.616 138.566			
86-01-25	21 02 08.7	64.59	147.47		63 653 656 666			
*86-02-15 *86-03-07	20 30 27.5 23 28 10.0	63.97 63.99	152.89 153.50	20 30 26.3 23 28 08.2	63.973 153.096	20 30 26.8 23 28 07.5	64.001 153.038	
86-03-15	04 02 02.	59.9	144.50	23 26 06.2	64.104 153.511	23 28 07.3	64.106 153.469	
86-04-03	15 38 17.6	59.19	154.20	15 38 15.8	59.135 154.478	15 38 13.0	58.975 154.750	
*86-04-06	01 27 20.6	70.76	130.31	01 27 20.5	70.755 130.200	01 27 20.1	70.748 130.241	
86-04-23	04 29 51.	73.8	114.60					-
86-05-11	17 29 00.1	62.07	154.10	17 28 58.9	62.034 154.151	17 29 00.2	62.157 154.243	
86-06-04	22 43 54.2	61.78	158.92	22 43 53.5	61.871 159.025			
86-06-15	06 55 36.8	72.94	126.53	06 55 36.8	72.883 126.515	06 55 34.7	72.946 125.867	
86-06-15 86-06-15	06 55 35.8 06 57 4 5.3	72.73 72.94	126.3 126.62	06 55 36.8	72.883 126.515	06 55 33.4	72.630 123.975	150
86-07-23	23 28 58.	71.9	128.90					
86-07-27	11 25 41.8	64.65	147.09	11 25 40.6	64.634 147.058	11 25 41.3	64.569 147.062	
86-07-27	21 08 42.0	61.96	160.96					
86-08-10	11 11 59.0	63.74	147.88				63.500 147.731	
86-11-09	07 15 36.	75.0	139.40					
86-12-05	15 50 12. 20 07 24.1	74.6	125.00					
86-12-08 86-12-11	00 15 55.	71.32 7 4. 0	140.39 119.60					
86-12-11	01 47 09.	74.0	119.70					
86-12-18	18 04 17.2	61.37	143.53	18 04 11.2	61.177 143.634	18 03 58.9	60.361 145.102	
*86-12-18	18 04 10.2	61.31	143.7	18 04 11.2	61.177 143.634	18 04 09.3	61.135 143.533	isc
86-12-22	02 18 09.4	73.80	119.77					
*86-12-26	03 21 04.9	61.42	149.48	03 21 04.5	61.375 149.426	03 21 03.6	61.403 149.465	
87-01-09	04 29 45.0	60.02	153.01	04 29 44.0	59.974 153.039	04 29 32.7	59.262 154.152	
87-01-09 87-01-16	13 14 18.6 23 53 20.0	67.23 58.59	140.17 125.09	13 14 14.6 23 53 15.1	67.162 140.135 58.644 125.067	23 53 18.3	58.618 124.947	
87-01-19	09 50 36.	74.2	116.80		36.044 123.007	23 33 10.3	30.010 124.947	
87-02-11	00 58 20.8	62.79	156.90	00 58 19.8	62.868 156.909	00 58 19.9	62.826 156.871	
*87-02-11	00 58 24.	62.88	156.70	00 58 19.8	62.868 156.909	00 58 19.7	62.860 156.856	isc
*87-02-11	01 03 07.7	62.82	156.78	01 03 08.0	62.840 156.867	01 03 07.5	62.836 156.850	
*87-02-11	01 09 51.1	62.84	156.76	01 09 50.8	62.859 156.804	01 09 51.5	62.741 156.777	
*87-02-11 87-02-11	06 19 15.4 06 23 02.5	62.84 62.86	156.74 156.80	06 19 16.3	62.812 156.721	06 19 15.6	62.809 156.847	
87-02-11	06 23 06.4	62.99	156.34					
*87-02-11	07 28 17.5	62.77	156.78		62.851 156.849	07 28 18.6	62.823 156.856	
87-02-11	07 29 00.8	62.74	156.64	07 29 06.5	62.656 156.060	07 29 11.9		
*87-02-11	11 36 16.7	62.81	156.80	11 36 16.1	62.846 156.811		62.825 156.814	
*87-03-04	00 09 28.2	61.21	148.50	00 09 28.0	61.116 148.472	00 09 28.3	61.128 148.374	
87-03-08 87-03-16	06 47 31.4 20 58 53.	62.17 64.0	143.62 167.20	20 58 53.5	64.106 167.266	20 58 55.7	64.204 167.313	
*87-04-13	21 20 11.3	66.12	143.11	21 20 12.8	66.207 143.085	20 38 33.7	04.204 107.313	
87-04-15	23 09 22.7	58.52	121.67	23 09 18.3	58.633 121.561	23 09 17.8	58.670 121.649	
87-04-22	03 38 21.1	72.24	129.69	03 38 20.0	72.211 129.863	03 38 20.3	72.195 129.668	
87-07-03	13 23 10.9	59.50	148.84	13 23 09.0	59.394 148.709	13 23 10.3	59.401 148.827	
87-07-05	00 09 01.	61.3	144.60	00 08 55.8	61.31€ 144.483	00 09 00.3	61.680 144.692	
87-07-17	03 43 43.	73.7	118.30	03 43 43.	73.653 118.581	03 43 43.	73.706 118.087	
87-07-21	05 02 32.7	58.97	149.75	05 02 33.6	58.942 149.728	05 02 02.6	56.749 149.651	
*87-09-09 87-09-27	04 43 23.2 13 16 36.8	60.15 61.20	150.28 160.82	04 43 22.8 13 16 32.0	60.149 150.386 61.061 161.183	04 43 22.8 13 16 34.6	60.121 150.454 61.039 161.273	
87-10-06	07 08 43.	73.8	119.00	15 16 52.0	61.061 101.163	15 16 54.6	01.039 101.273	
87-10-08	06 19 18.	73.9	119.30			06 19 18.0	73.693 118.566	
87-11-25	17 28 01.	73.8	118.90			17 28 04.2	73.763 119.695	0
87-11-26	16 11 20.	73.9	119.20	16 11 35.3	73.202 121.342	16 11 20.0	73.788 118.661	
87-11-29 87-12-07	06 15 42.	73.9	119.50	06 16 01.5	72.907 121.943	06 15 42.0	73.730 119.238	
87-12-07 87-12-30	10 51 00.0 12 34 31.8	63.77 73.76	145.65 118.90	10 50 59.5	63.795 145.669	10 50 59.4	63.716 145.630	Ţ
88-01-01	14 36 13.	74.6	130.90	14 36 15.8	74.405 131.060	14 36 08.9	74.682 130.977	
88-01-01	14 36 09.8	74.65	130.90	14 36 15.8	74.405 131.060	14 36 09.6	74.584 130.687	isc
88-01-13	11 56 31.9	71.45	129.14	11 56 31.5	71.451 128.982	11 56 31.3	71.449 129.227	
88-01-19	10 35 32.8	63.76	145.74	10 35 31.6	63.663 145.512			
88-01-30	14 19 22.	73.5	117.80	00 04 04 0	64 210 140 521	00 04 04.9	64 235 140 554	
*88-02-19	00 04 04.8	64.34	148.60	00 04 04.0	64.318 148.521	00 04 04.9	64.335 148.554	

85-02-02 85-02-18 *85-03-18 85-04-10 85-04-17 85-04-20 85-05-22 85-06-02 *85-06-24 85-08-20 85-08-20 85-08-20 85-09-10 85-10-05 85-10-05	11 28 45.3 12 51 35. 22 24 38.0 11 27 46.6 09 22 16. 20 37 21.8 22 29 19.6 18 28 48.6 04 08 08.9 04 08 12.8 03 54 35. 03 54 32.4 03 41 37.7 05 04 11.3 10 53 33.3 22 32 36.8 22 37 04.5 22 37 04.5 22 37 13.6	65.6 59.35 70.43 62.4 65.36 59.28 61.02 64.83 64.8	137.05 136.50 151.96 141.03 124.10 142.96 141.72 157.88 144.08 145.00 145.64 137.36 142.98 150.23 150.23	11 28 44.9 12 51 31.3 22 24 37.8 11 27 45.1 20 37 19.8 	65.834 136.990 65.557 136.457 59.356 152.162 70.329 141.424 65.406 142.946 60.952 157.850 64.857 144.044 65.286 144.664 65.286 144.664 62.237 145.488 59.956 137.081 59.465 150.201 59.299 149.987 59.225 150.192	12 51 32.7 22 24 34.7 	59.119 152.197 64.871 144.060 64.898 144.249 65.205 144.346	isc t,isc
*85-11-28 86-01-05 *86-01-18 86-01-24 86-01-25 *86-02-15 *86-03-07	08 38 25. 00 35 23. 13 13 23.3 13 25 26.8 21 02 08.7 20 30 27.5 23 28 10.0	60.70 64.59 63.97 63.99	144.30 128.40 153.67 138.49 147.47 152.89 153.50	08 38 20.5 00 35 23.9 13 13 22.0 13 25 23.0 	64.863 144.133 70.276 128.612 60.191 153.761 60.616 138.566 	13 13 24.8 	64.850 144.422 60.255 153.530 64.001 153.038 64.106 153.469	
86-03-15 86-04-03 *86-04-06 86-04-23 86-05-11 86-06-04 86-06-15	04 02 02. 15 38 17.6 01 27 20.6 04 29 51. 17 29 00.1 22 43 54.2 06 55 36.8	59.9 59.19 70.76 73.8 62.07 61.78 72.94	144.50 154.20 130.31 114.60 154.10 158.92 126.53	15 38 15.8 01 27 20.5 17 28 58.9 22 43 53.5 06 55 36.8	59.135 154.478 70.755 130.200 	15 38 13.0 01 27 20.1 17 29 00.2 06 55 34.7	58.975 154.750 70.748 130.241 62.157 154.243 72.946 125.867	-
86-06-15 86-06-15 86-07-23 86-07-27 86-08-10 86-11-09 86-12-05	06 55 35.8 06 57 45.3 23 28 58. 11 25 41.8 21 08 42.0 11 11 59.0 07 15 36. 15 50 12.	72.73 72.94 71.9 64.65 61.96 63.74 75.0 74.6	126.3 126.62 128.90 147.09 160.96 147.88 139.40 125.00	11 25 40.6 			72.630 123.975 64.569 147.062 63.500 147.731	
86-12-08 86-12-11 86-12-11 86-12-18 *86-12-18 86-12-22 *86-12-26	20 07 24.1 00 15 55. 01 47 09. 18 04 17.2 18 04 10.2 02 18 09.4 03 21 04.9		140.39 119.60 119.70 143.53 143.7 119.77 149.48	18 04 11.2 18 04 11.2 18 04 11.2				isc
87-01-09 87-01-09 87-01-16 87-01-19 87-02-11 *87-02-11	04 29 45.0 13 14 18.6 23 53 20.0 09 50 36. 00 58 20.8 00 58 24. 01 03 07.7	60.02 67.23 58.59 74.2 62.79 62.88 62.82	153.01 140.17 125.09 116.80 156.90 156.70 156.78	04 29 44.0 13 14 14.6 23 53 15.1 00 58 19.8 00 58 19.8 01 03 08.0	59.974 153.039 67.162 140.135 58.644 125.067 62.868 156.909 62.868 156.909 62.840 156.867	04 29 32.7 23 53 18.3 00 58 19.9 00 58 19.7 01 03 07.5	59.262 154.152 58.618 124.947 62.826 156.871 62.860 156.856 62.836 156.850	
*87-02-11 *87-02-11 87-02-11 87-02-11 *87-02-11 *87-02-11 *87-02-11	01 09 51.1 06 19 15.4 06 23 02.5 06 23 06.4 07 28 17.5 07 29 00.8 11 36 16.7 00 09 28.2	62.84 62.84 62.86 62.99 62.77 62.74 62.81	156.76 156.74 156.80 156.34 156.78 156.64 156.80 148.50	01 09 50.8 06 19 16.3 	62.859 156.804 62.812 156.721 62.851 156.849 62.656 156.060 62.846 156.811 61.116 148.472	01 09 51.5 06 19 15.6 	62.823 156.847 62.823 156.856 62.823 155.096 62.825 156.814 61.128 148.374	
87-03-08 87-03-16 •87-04-13 87-04-15 87-04-22 87-07-03 87-07-05 87-07-21 •87-09-09	06 47 31.4 20 58 53. 21 20 11.3 23 09 22.7 03 38 21.1 13 23 10.9 00 09 01. 03 43 43. 05 02 32.7 04 43 23.2	62.17 64.0 66.12 58.52 72.24 59.50 61.3 73.7 58.97 60.15	143.62 167.20 143.11 121.67 129.69 148.84 144.60 118.30 149.75 150.28	20 58 53.5 21 20 12.8 23 09 18.3 03 38 20.0 13 23 09.0 00 08 55.8 03 43 43.6 05 02 33.6 04 43 22.8	64.106 167.266 66.207 143.085 58.633 121.561 72.211 129.863 59.394 148.709 61.316 144.483 73.653 118.581 58.942 149.728 60.149 150.386	20 58 55.7 23 09 17.8 03 38 20.3 13 23 10.3 00 09 00.3 03 43 43. 05 02 02.6 04 43 22.8	64.204 167.313 58.670 121.649 72.195 129.668 59.401 148.827 61.680 144.692 73.706 118.087 56.749 149.651 60.121 150.454	
87-09-27 87-10-08 87-11-25 87-11-26 87-11-29 87-12-07 87-12-30 88-01-01	13 16 36.8 07 08 43. 06 19 18. 17 28 01. 16 11 20. 06 15 42. 10 51 00.0 12 34 31.8 14 36 13. 14 36 09.8	61.20 73.8 73.9 73.8 73.9 73.9 63.77 73.76 74.6	160.82 119.00 119.30 118.90 119.20 119.50 145.65 118.90 130.90	13 16 32.0 	73.202 121.342 72.907 121.943 63.795 145.669 74.405 131.060 74.405 131.060	13 16 34.6 06 19 18.0 17 28 04.2 16 11 20.0 06 15 42.0 10 50 59.4 	61.039 161.273 73.693 118.566 73.763 119.695 73.788 118.661 73.730 119.238 63.716 145.630 74.682 130.977 74.584 130.687	p r
88-01-01 88-01-13 88-01-19 88-01-30 *88-02-19	14 36 09.8 11 56 31.9 10 35 32.8 14 19 22. 00 04 04.8	71.45 63.76 73.5 64.34	129.14 145.74 117.80 148.60	14 36 15.8 11 56 31.5 10 35 31.6 	71.451 128.982 63.663 145.512 	14 36 09.6	74.584 130.687 71.449 129.227 	150

85-02-02 85-02-18 *85-03-08 85-04-10 85-04-12 85-04-20 85-05-22 85-06-02 *85-06-02 *85-06-24 85-08-20 85-08-28 85-09-10 85-10-05 85-10-05 *85-11-28 86-01-05 *86-01-18 86-01-25 *86-03-07 *86-03-15	11 28 45.3 12 51 35.0 11 27 46.6 09 22 16. 20 37 21.8 22 29 19.6 16 28 48.6 04 08 08.9 04 08 12.8 03 54 35. 03 68 22 37 04.5 22 37 13.6 08 38 25. 00 35 23. 13 13 23.3 13 25 26.8 21 02 08.7 20 30 27.5 23 28 10.0 04 02 02.	65.85 65.6 59.35 70.43 62.4 65.28 61.02 64.8 65.2 65.21 62.14 59.90 62.46 59.41 59.41 59.45 64.9 65.9 66.9 66.9 67.9 68.9 69.9	137.05 136.50 151.96 141.03 124.10 142.96 141.72 157.88 144.00 145.00 145.00 144.49 150.22 150.22 144.30 150.22 144.30 150.22 144.30 150.22 144.30 150.22 144.30 150.25	11 28 44.9 12 51 31.3 22 24 37.8 11 27 45.1 	65.834 136.990 65.557 136.457 59.356 152.162 70.329 141.424 	12 51 32.7 22 24 34.7 22 24 34.7 22 24 34.7 24 08 09.9 04 08 09.9 03 54 34.6 22 32 35.8 22 32 35.8 23 28 07.5	65.662 136.653 59.119 152.197 64.871 144.060 64.898 144.249 65.205 144.346 59.430 150.179 64.850 144.422 60.255 153.530 64.001 153.038 64.106 153.469	
86-04-03 *86-04-06 86-04-23 86-05-11 86-06-04 86-06-15 86-06-15 86-07-23 86-07-27 86-07-27 86-07-27 86-08-10 86-11-09 86-12-08	15 38 17.6 01 27 20.6 04 29 51. 17 29 00.1 22 43 54.2 06 55 36.8 06 55 36.8 06 57 45.3 23 28 58. 11 25 41.8 21 08 42.0 01 11 59.0 07 15 36. 15 50 12. 20 07 24.1	59.19 70.76 73.8 62.07 61.78 72.94 72.73 72.94 71.9 61.96 63.74 75.0 71.32	154.20 130.31 114.60 154.10 158.92 126.53 126.3 126.62 128.90 147.09 160.96 147.88 139.40 125.00 140.39	15 38 15.8 01 27 20.5 	59.135 154.478 70.755 130.200 	15 38 13.0 01 27 20.1 17 29 00.2 06 55 34.7 06 55 33.4 11 25 41.3 11 12 00.2	58.975 154.750 70.748 130.241 62.157 154.243 72.946 125.867 72.630 123.975 64.569 147.062	
86-12-11 86-12-11 86-12-18 *86-12-18 86-12-22 *86-12-26 87-01-09 87-01-16 87-01-19 87-02-11 *87-02-11	00 15 55. 01 47 09. 18 04 10.2 02 18 09.4 03 21 04.9 04 29 45.0 13 14 18.6 23 53 20.0 09 50 36. 00 58 26. 01 03 07. 01 03 07. 01 09 51.1	74.0 74.0 61.37 61.31 73.80 61.42 60.02 67.23 58.59 74.2 62.79 62.88 62.88	119.60 119.70 143.53 143.7 119.77 149.48 153.01 140.17 125.09 116.80 156.70 156.70	18 04 11.2 18 04 11.2 	61.177 143.634 61.177 143.634 61.375 149.426 59.974 153.039 67.162 140.135 58.644 125.067 62.868 156.909 62.868 156.909 62.840 156.867 62.859 156.804	18 03 58.9 18 04 09.3 03 21 03.6 04 29 32.7 23 53 18.3 00 58 19.9 00 58 19.7 01 03 07.5 01 09 51.5	60.361 145.102 61.135 143.533 61.403 149.465 59.262 154.152 58.618 124.947 62.826 156.871 62.826 156.856 62.836 156.856 62.741 156.777	
*87-02-11 87-02-11 87-02-11 *87-02-11 *87-02-11 *87-02-11 *87-03-04 87-03-16 *87-04-13 87-04-12 87-07-03 87-07-05 87-07-07 87-07-21 *87-09-09 87-09-27 87-10-06 87-11-25 87-11-25 87-11-25 87-11-25 87-11-25 88-01-01 88-01-01 88-01-13 88-01-13 88-01-3	06 19 15.4 06 23 02.5 06 23 06.4 07 28 17.5 07 29 00.8 11 36 16.7 00 09 28.2 06 47 31.4 20 58 53. 21 20 11.3 23 09 22.7 03 38 21.1 13 23 10.9 00 09 01. 03 43 43. 13 23 23 2. 13 16 36.8 07 08 43. 06 19 18. 17 28 01. 16 11 20. 16 11 20. 17 28 01. 18 12 02. 19 12 02. 10 51 00.0 12 34 31.8 14 36 09.8 11 56 31.9 10 35 32.8 14 19 22.	62.84 62.89 62.77 62.77 62.78 61.21 62.16 62.12 58.52 72.24 59.50 61.3 73.7 73.7 60.15 61.20 73.8 73.9 73.9 73.9 73.7 74.6 74.6 74.6 74.6 73.5	156.74 156.80 156.34 156.64 156.66 148.50 143.62 167.20 143.11 121.67 129.69 148.84 144.60 118.30 119.75 150.28 160.82 119.00 119.30 119.20 119.50 145.65 118.90 119.20 130.90 130.90 130.90 129.14	06 19 16.3	62.812 156.721	06 19 15.6	62.809 156.847	p r

				Appendix A	(continued)				
*88-02-19	23 50 25.8	64.20	145.79	23 50 24.9	64.171 145.827	23 50 25.5	64.187	145.853	
*88-04-03	02 01 29.8	69.47	138.79		69.428 138.694	02 01 27.7			
88-04-03 88-04-05	03 52 30.8 18 25 57.	69.47 75.1	138.67	03 52 29.1	69.502 138.654				
88-04-05	18 25 41.9	76.7	130.70 129.6			18 25 36.5			isc
*88-05-25	16 55 45.3		150.96	16 55 43.7	64.209 150.934	16 55 44.4			
88-06-01	08 29 54.4	61.96	161.14						
*88-06-09 *88-06-14	13 37 32.2 14 44 43.6	63.29 63.33	157.54 149.55	13 37 32.9 14 44 44.1	63.266 157.627 63.356 149.579	13 37 33.5 14 44 44.0			
88-06-29	19 04 28.	75.0	132.50		03.330 143.379				
88-07-01		64.83	145.85	21 37 34.8	64.880 145.689				
88-09-22	23 58 14.8	61.83	160.00	22 58 14.5	61.934 160.047	00 07 50 0	62.060		
*88-10-17 88-10-25	00 27 59.3 10 12 51.6	62.82 62.98	148.84 148.90	00 27 59.2 10 12 52.4	62.824 148.904 62.891 148.867	00 27 59.2 10 12 48.7	62.869 63.197		
88-12-24	02 43 22.3		149.04	02 43 23.1	64.006 148.913	02 43 22.2			
88-12-30	07 16 42.5	61.11	153.65	07 16 43.0	61.118 153.705	07 16 42.7			
89-01-05	17 52 13.	72.6	140.60	17 52 05.7	72.824 141.324	04 53 30 3	62.007		
89-01-1 4 89-01-15	04 53 41. 17 17 32.1	61.9 58.90	143.80 151.27	04 53 36.9 17 17 18.0	61.946 143.800 57.964 150.965	04 53 39.3 17 17 30.0	62.097 58.591		
*89-01-29	23 23 03.8	62.91	144.88	23 23 01.6	62.825 144.936	23 23 02.0			
89-02-17	19 10 16.4	69.79	129.31	19 10 15.6	69.830 129.137	19 10 13.9			
89-02-25 89-03-01	04 56 16.1 17 09 01.	61.72 73.8	157.66 117.00	04 56 16.6	61.715 157.701				
*89-03-21	10 53 07.0		145.13	10 53 05.1	64.920 145.199				
89-04-09	04 16 25.	59.9	145.30	04 16 23.	59.774 145.194	04 16 22.7	59.863		
*89-04-09			145.23	04 16 23.	59.774 145.194	04 16 22.7	59.879		isc
89-04-24 89-05-19	04 45 39.9 19 29 22.8	59.09 62.30	151.86 155.20	04 45 36.4 19 29 23.7	58.904 151.856 62.411 155.229	04 45 29.4 19 29 24.5	58.275 62.483		
89-05-24	09 38 00.6	61.33	144.70		61.217 144.460	09 38 01.5	61.368		
*89-06-16	07 36 09.4	63.59	142.79	07 36 08.5		07 36 08.9	63.609		m,n
89-06-16	19 40 46.2	61.13	145.72	19 40 45.7	61.020 145.457	20 00 01 5	50 202		_
89-06-30 89-07-02	19 59 59.5 23 58 50.1	59.25 59.65	152.60 150.14	20 00 01.3 23 58 4 8.6	59.350 152.686 59.578 150.119	20 00 01.5 22 58 4 8.6	59.302 59.587		I
*89-07-07	10 51 46.3	64.97	141.78	10 51 43.1	64.991 141.596	10 51 42.8	64.999		
*89-07-09	18 11 48.9	59.96	152.62	18 11 49.0	59.924 152.716	18 11 49.0	59.859		
89-07-25 89-08-05	02 02 38. 4 06 56 07.	62.89 75.4	159.21	02 02 39.5 06 56 03.2	62.915 159.171 75.090 133.045	06 55 54.7	75.723		
89-08-05	06 55 50.		133.40 134.54	06 56 03.2	75.090 133.045		75.999		isc
89-08-05	10 49 34.	75.3	131.80	10 49 35.2	75.018 132.375	10 49 37.8			
89-08-05			134.4	10 49 35.2	75.018 132.375	10 49 22.2	76.171		isc
89-08-05 89-08-08	17 56 15. 05 40 41.	75.9 74.8	130.10 117.10	17 56 20.8	75.315 130.353				
89-09-04	23 20 25.4		148.92	23 20 25.5		23 20 26.4	60.839		
89-09-26	00 18 51.	75.8	130.60						
89-09-26 *89-10-04	00 18 50.1 20 56 4 9.5	76.17 64.79	134.4 146.86	20 56 47.2	64.709 146.818	00 18 48.8 20 56 47.3			1SC
89-11-13	18 15 43.1	62.34	143.59	18 15 40.6	62.279 143.569	18 15 40.1			
89-12-14	19 16 12.	74.2	145.60	19 16 10.6	73.985 146.036				
89-12-18	21 00 40.	74.7	141.60	21 00 42.7	74.344 141.495	12 46 24 0	65 504		
89-12-22 90-03-02	12 46 37.2 21 30 34.	65.48 73.8	136.74 115.90	12 46 3 4 .3 21 30 23.1	65.499 136.828 73.934 113.609	12 46 34.9	65.504		
90-03-06	07 18 10.	67.0	125.40	07 18 01.7	66.916 124.749				
90-03-13	00 33 07.	73.2	133.90	00 33 05.5	73.173 134.461	00 33 00.0	73.277		
90-03-13 90-03-1 4	00 32 59.0 01 12 24.	73.33 73.5	134.90 133.60	00 33 05.5 01 12 22.7	73.173 134.461 73.356 134.217	00 32 59.0 01 12 22.4		134.712 134.392	1 SC
90-03-14	04 31 28.	73.5	133.80	04 31 30.2	73.071 133.596	04 31 20.5			
* 90-03-29	20 47 30.8		145.00	20 47 29.7	64.010 145.044	20 47 29.3	63.962	144.842	
90-04-02	15 32 47.1	62.01	138.12	15 32 44.3	61.969 137.944	15 32 46.2			
90-04-11 90-05-05	16 09 42.4 02 44 16.3	61.95 61.30	154.28 153.99	16 09 43.2 02 44 17.4	61.964 154.280 61.321 153.953				
*90-05-30	11 56 46.5	62.93	144.90	11 56 45.1	62.915 144.806	11 56 47.0	62.953	144.919	
90-06-09	18 24 29.	75.5	113.40			18 24 10.7		108.939	
*90-06-25 90-06-28	07 33 57. 22 04 00.	66.8 75.1	130.80 132.00	07 33 51.7 22 03 57.0	66.827 130.342 75.300 132.311	07 33 52.5 22 03 47.7		130.326	
90-06-28	22 03 47.8	76.2	134.10	22 03 57.0	75.299 132.311	22 03 46.8		134.266	150
90-07-06	16 09 10.0	67.17	144.67	16 09 07.5	67.194 144.699	16 09 10.3	67.232	144.664	
90-07-11	09 44 31.	65.5	125.30	00 00 00 0	(2.057152.022	00.00.50.6	62.073		
*90-07-12 90-07-24	02 22 4 9.6 15 17 22.0	62.06 60.2	153.78 142.80	02 22 50.5 15 17 20.3	62.057 153.827 60.332 142.664	02 22 50.8 15 17 16.4		153.845 142.081	
*90-08-24	01 04 43.9	63.01	151.20	01 04 44.6	63.032 151.219	01 04 44.7		151.201	
90-09-11	00 52 54.	74.4	116.50	00 52 50.8	74.465 115.860				
*90-11-01	13 4 2 05.5 06 16 00.2	61.28	156.79	13 42 06.1	61.309 156.763 61.244 157.005	13 42 06.2	61.321	156.935	
90-11-02 *90-11-02	21 54 04.5	61.28 64.81	156.96 146.66	06 16 00.9 21 54 03.2	61.244 157.005 64.733 146.620	21 54 03.7		146.725	i
90-11-02	21 54 06.0	65.01	146.97	21 54 03.2	64.733 146.620	21 54 03.9	64.813	146.755	
90-11-21	01 12 19.7	59.84	153.44	01 12 19.5	59.929 153.414	01 12 18.8		153.604	
90-11-21 *90-11-22	04 04 05. 19 36 24.8	61.6 62.73	142.90 156.72	04 04 03.7 19 36 25.1	61.836 142.953 62.767 156.743	19 36 25.7	62.773	156.835	
90-11-22	08 23 29.9	59.49	152.44	08 23 30.6	59.429 152.484	19 30 23.7			
*90-12-13	21 34 41.7	64.41	140.63	21 34 39.1	64.433 140.518	21 34 40.5		140.457	
*91-02-10 91-02-11	18 16 32.9 10 58 27.1	62.99	145.55	18 16 32.3 10 58 26.0	62.950 145.634 72.577 125.222	18 16 31.7 10 58 25.1		145.461 125.233	
91-02-11	01 57 05.4	72.60 72.22	125.16 126.81	01 57 04.1	72.577 125.222 72.173 126.820	01 57 05.0		125.233	
*91-03-01	01 57 06.	72.15	126.85	01 57 04.1	72.173 126.820	01 57 05.0		127.173	ā.0
01 02 20	17 06 25 5		126 22	17 06 34 0	66 0AE 126 251				isc
91-03-30	17 06 25.5	66.64	126.33	17 06 24.0	66.845 126.251				a

		71 20	130.00	07 21 57.2	71 401	130.094				a
91-04-01	07 21 57.9 07 18 07.7	71.38 73.02	121.43	07 21 37.2		130.034				<u> </u>
91-05-02			139.84	13 43 45.0		139.816				
*91-07-02	13 43 48.7	65.18		13 43 45.0		139.010	02 26 01.5		143.883	
91-07-24	02 26 04.7	62.23	143.68	01 44 02.7	71.980	127.221	01 44 02.6	72.132	127.810	
*91-07-31	01 44 02.5	72.06	127.56			143.127	19 08 06.7	65.460	143.199	
91-08-04	19 08 08.3	65.47	143.32	19 08 05.9	65.495		19 08 06.7	65.449	143.199	
•91-08-04	19 08 07.	65.5	142.9	10 08 05.9	65.495	143.127	19 14 39.7	65.516		
91-08-04	19 14 41.6	65.47	143.33	19 14 40.6	65.498	143.220	19 14 39.7		142.090	
91-08-25	13 51 02.3	70.73	140.90							
*91-08-26	09 35 48.9	63.18	146.00	09 35 49.0	63.390	146.359	09 35 50.0		146.522	
91-10-13	00 36 37.3	61.09	144.93	00 36 33.4	61.112	144.907	00 36 26.5	60.746	145.318	
91-10-28	21 41 31.4	65.18	131.64							
91-12-23	06 04 17.9	62.41	140.89	06 04 16.0	62.454	140.848	06 04 17.0	62.854	140.570	
*92-01-22	06 29 19.4		143.38	06 29 16.1	65.852	143.180	06 29 17.0		143.087	
92-01-22	06 29 17.1	65.8	143.0	06 29 16.1	65.852	143.180	06 29 16.5		143.124	
92-01-28	00 07 28.5	68.16	133.12	00 07 29.6	68.302	133.967	00 07 23.€	68.211	132.319	
•92-02-12	17 14 57.	64.8	152.90	17 14 51.2	64.972	153.224	17 14 52.1	64.908	153.172	a
92-02-15	04 52 10.	75.9	124.20	04 52 36.7	74.227	124.354	04 51 59.5	76.142	124.780	a
92-02-15	04 52 05.1	75.95	125.1	04 52 36.7	74.227	124.354	04 52 04.2	75.800	125.159	a,isc
92-02-22	17 55 21.4	70.14	139.38	17 55 20.9	70.091	139.399	17 55 21.7	70.133	139.589	a
92-02-23	08 21 42.3	70.06	139.45	08 21 41.2	70.031	139.378	08 21 41.4	70.065	139.498	a
92-05-07	23 22 56.5	63.63	133.53				23 22 54.9	63.848	133.988	a
•92-06-28	23 53 20.6	63.79	145.10	23 53 17.4	63.704	145.682	23 53 18.1	63.739	145.720	a
92-08-26	11 02 17.4		133.14	11 02 16.7		133.208	11 02 17.8		133.410	
92-09-09	00 14 37.3		132.07							
92-09-13	21 43 00.4		154.13				21 42 58.9			
92-10-30	14 20 31.3	72.72	123.83				14 20 30.2		123.682	
92-11-14	20 43 15.8		123.24	20 43 15.0	72.997		20 43 14.9		123.300	
*92-11-17	07 55 18.	67.2	128.80	07 55 13.8	67.258	128.590	07 55 14.8		128.597	
93-02-21	17 06 31.3	65.88	149.53	17 06 18.2	65.993	150.971	07 33 14.8			
93-02-21	17 45 26.3	69.54	129.00	17 45 24.6	69.582	128.736	17 45 27.0			
93-02-24	01 43 44.7		145.00	01 43 43.9	63.005	145.527	01 43 43.7		145.679	
*93-03-05	04 21 05.2	63.78	145.67	04 21 05.1	63.793	145.408	04 21 04.8	63.747	145.452	
93-03-05	03 26 30.5	63.74	142.47	03 26 28.3			04 21 04.8		145.452	
					63.791	142.337				
*93-03-22	18 14 05.9		145.67	18 14 06.8	63.041	145.315	18 14 07.4		145.327	
*93-03-24	16 19 08.5	65.34	142.69	16 18 05.9	65.341	142.609	16 19 06.5	65.492	142.633	
93-03-24	22 43 32.4		129.76	22 43 30.3	71.541	130.109	22 43 28.5		130.369	
93-04-29	12 21 32.5		139.68	12 21 30.7	69.161	140.013	12 21 30.9	69.160	139.878	
93-05-04	20 49 03.8	75.71	132.73	20 49 14.8	74.832	132.134	20 48 50.0	76.999	131.502	
93-05-19	08 32 12.5		140.77				08 32 15.3	58.313	139.867	
93-06-15	11 51 15.4	62.23	141.70	11 51 12.9	62.287	141.543	11 51 14.9	62.290	141.492	
93-06-18	19 16 17.6	62.08	146.30	19 16 14.4		146.166	19 16 14.2	62.109	146.255	
•93-08-30	07 56 37.9		145.80	07 56 34.9		145.881	07 56 34.5		145.905	
93-09-26	10 58 27.7	59.81	144.95							
93-10-02	04 04 06.	73.1	116.50							â

- isc Earthquake parameters determined with supplemental information from Bulletin of the international Seismological Center. Bulletin origin time and epicenter also from BIS.
- a Phase data and parameters from B. Koz'min, Yakutsk Science Instisute.
- b For stations Omsukchan and Seimchan, PG arrivals are misidentified in Bulletin as PN arrivals.
- c For stations Stekolnyi, Evensk, Ust' Nera, and Yakutsk, PN arrivals are misidentified in bulletin as PG. Station Seimchan PG arrival misidentified in bulletin as FN.
- d For station Omsukchan, PN arrival is misidentified in bulletin as PG.
- e For station Seimchan, PN arrival is misidentified in bulletin as PG.
- f For station Ust' Nera, PN arrival is misidentified in bulletin as PG.
- g For station Stekolnyi, PG arrival is misidentified in bulletin as PN.
- h For station Zyryanka, PG arrival is misidentified in bulletin as PN.
- i Station Tenkeli is misidentified in Materialy as station Tungurcha. This is likely due to nearly identical appearing russian codes.
- j For station Nezhdaninskoe, PN arrival is misidentified in bulletin as FG.
- k For station Magadan, PN arrival is misidentified in bulletin as PG.
- 1 For station Ust' Omchug, PN arrival is misidentified in bulletin as PG.
- m For station Moma, PN arrival is misidentified in bulletin as PG.
- n For station Khandyga, PN arrival is misidentified in bulletin as FG.
- o For station Yubileinaya, PN arrival is misidentified in bulletin as PG.
- p For station Naiba, PN arrival is misidentified in bulletin as PG.
- q For station Magadan, PG arrival is misidentified in bulletin as PN.
- r For station Nel' Koba, PN arrival is misidentified in bulletin as PG.

- s Station Ust' Nera misidentified in *Materialy* as station Ust'Nyukzha. This is likely due to nearly identical appearing russian codes.
- t For station Omolon, PN arrival is misidentified in bulletin as PG.

APPENDIX B

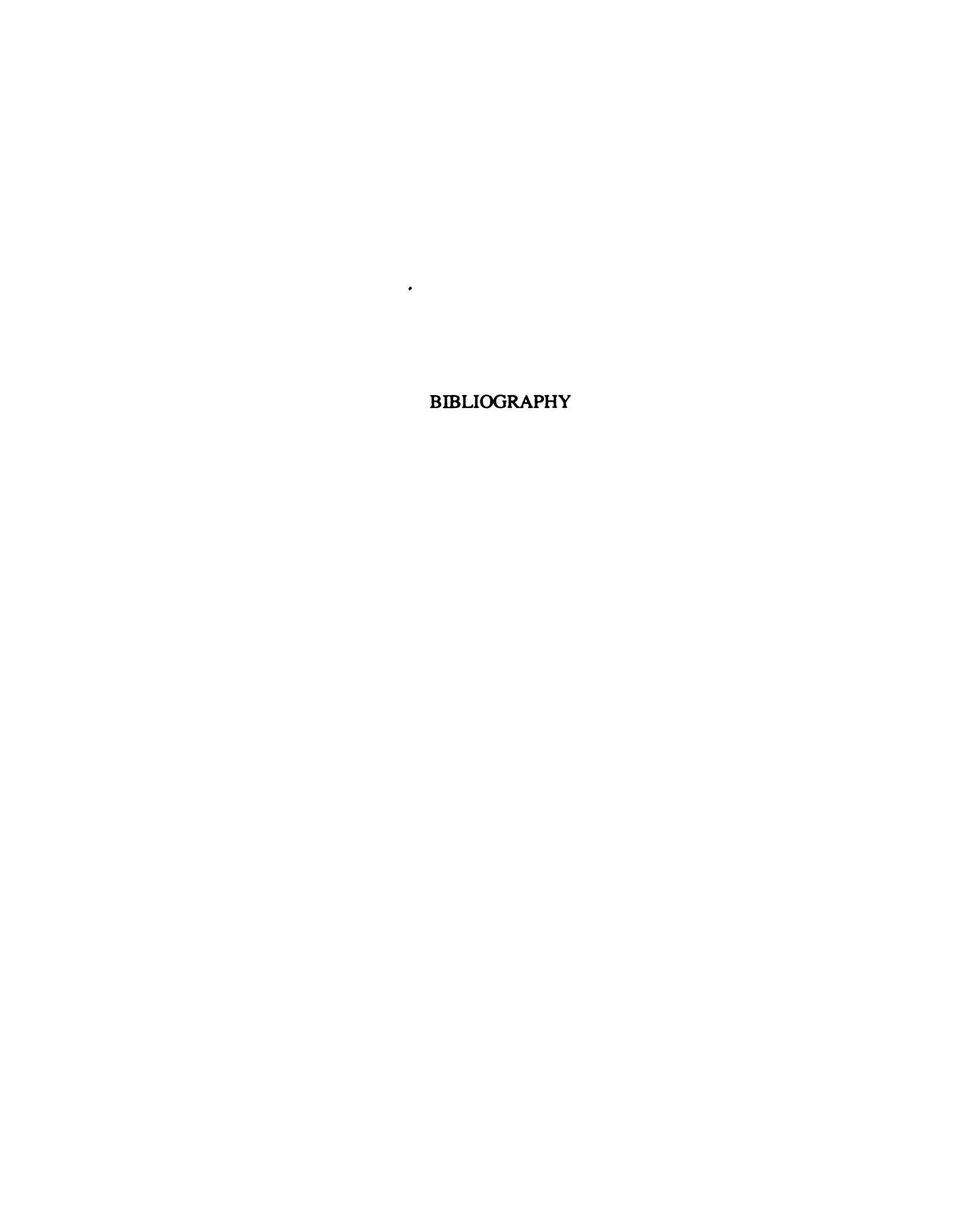
Seismic station coordinates from the Yakut and Magadan networks. Stations outside the study area but listed here were used in earthquake locations.

96

APPENDIX B

Station Name	Code	Elevation (m)	Latitude (N)	Longitude (+E,-W)	Region
Anadyr	ANY	55	64.734	177.496	Magadan
Artyk	AYK	700	64.181	145.133	Yakut
Batagai	BTG	120	67.650	134.625	Yakut
Bilibino	BIL	283	68.058	166.449	Magadan
Chagda	CGD	180	58.750	130.617	Yakut
Cherskii	CES	40	68.750	161.333	Yakut
Chul'man	CLN	600	56.867	124.900	Yakut
Debin	DBI	332	62.339	150.750	Magadan
Dunai	DUY	5	73.900	124.608	Yakut
Egvekinot	EGV	18	66.323	-179.127	Magadan
Evensk	EVE	21	61.921	159.231	Magadan
Iul'tin	ILT	245	67.875	-178.733	Magadan
Khandyga	KHG	125	62.650	135.557	Yakut
Khani	KHN		57.017	121.000	Yakut
Khatystyr	KHY	400	55.680	121.520	Yakut
Kulu	KU-	655	61.892	147.427	Magadan
Kyusyur	KYU	20	70.683	127.367	Yakut
Magadan	MAG	78	59.560	150.803	Magadan
Maiskii	MKI	261	68.975	173.700	Magadan
Markovo	MKN	25	64.684	170.412	Magadan
Moma (Khonu)	MKU	192	66.466	143.216	Yakut
Myakit	MYA	660	61.417	152.083	Magadan
Naiba	NAY	5	70.850	130.733	Yakut
Nelkoba	NKB	531	61.336	148.808	Magadan
Neryungri	NYG	700	56.675	124.650	Yakut
Nezhdaninskoe	NZD	603	62.497	139.058	Yakut
Omolon	OMO	260	65.232	160.535	Magadan
Omsukchan	OMS	527	62.515	155.774	Magadan
Provideniya	PVD	25	64.427	-173.225	Magadan
Saidy	SAY	88	68.700	134.450	Yakut
Sasyr	SSY	580	65.158	147.075	Yakut
Seimchan	SEY	206	62.933	152.382	Magadan
Sinegor'e	SNE	420	62.037	150.523	Magadan
Stekolnyi	MGD	221	60.046	150.730	Magadan
Stolb	SOT	50	72.400	126.825	Yakut
Susuman	SUU	640	62.781	148.149	Magadan
Tabalakh	TBK	200	67.539	136.522	Yakut

Taimylyr	TML	60	72.610	121.917	Yakut
Takhtoyamsk	TTY	11	60.202	154.678	Magadan
Talaya	TLA	730	61.129	152.392	Magadan
Tenkeli	TLI	110	70.183	140.783	Yakut
Tiksi	TIK	30	71.632	128.872	Yakut
Tungurcha	TUG	300	57.317	121.500	Yakut
Ust'Nera	UNR	485	64.569	143.228	Yakut
Ust'Nyukzha	USZ	400	56.561	121.592	Yakut
Ust'Omchug	USO	550	61.133	149.631	Magadan
Ust'Urkima	UUR	600	55.300	123.267	Yakut
Yakutsk	YAK	94	62.015	129.678	Yakut
Zyryanka	ZYR	120	65.717	149.817	Yakut



BIBLIOGRAPHY

- Andreev, T. A., 1984, Calculations using an ECM of parameters of weak earthquakes, in Shilo, H. A., Vaschilov, Y. Y., Linkova, T. I., and Akhlamova, N. N., eds., Seismicheskie Protsessi na Cevero-Vostoke SSSR: Magadan, SKVNII DVNTs AN SSSR, p. 116-127 (in Russian).
- Ansimov, E. M., Sedov, B. M., and Shvarts, D.B., 1967, Seismic exploration in the Northeast USSR, *in* Fotiadi, E. E., ed., Geologicheskie Rezul'taty Geofizicheskikh Issledovanii v Sibiri i na Del'nem Vostoke: Novosibirsk, Nauka, p. 438-442 (in Russian).
- Avetisov, G. P., 1983, Seismologic data on the deep structure of the New Siberian islands and adjacent sea areas: International Geology Review, v. 25, p. 651-660.
- Avetisov, G. P., and Guseva, Y. B., 1991, Deep structure of the Lena Delta region according to seismic data: Sovetskaya Geologiya, n. 4, p. 73-81 (in Russian).
- Belyaevsky, N. A., 1974, The earth's crust within the territory of the USSR: Moskva, Nedra, 278 p (in Russian).
- Belyaevsky, N. A., and Borisov, A. A., 1974, Structure and thickness of the earth's crust in the USSR, in Nalivkin, D. V., ed., Struktura Fundamenta Platformennykh Oblastei SSSR: Leningrad, Nauka, p. 381-393 (in Russian).
- Bobrobnikov, V. A., and Izmailov, L. I., 1989, Present day structure and geodynamics of the earth's crust in the southeastern portion of the Yana-Kolyma system, in Lin'kova, T. I., and Krasnyi, L. L., eds., Geofizicheskie Issledovaniya Pri Reshenii Geologicheskikh Zadach: Magadan, SVKNII DVNTs AN SSSR, p. 5-23 (in Russian).
- Bulin, N. K., 1989, Deep structure of the Verkhoyana-Chukotka folded region according to seismic data: Tikhookeanskaya Geologiya, v. 8(1), p. 77-85 (in Russian).
- Cook, D. B., Fujita, K., and McMullen, C. A., 1986, Present-day plate interactions in northeast Asia: North American, Eurasian, and Okhotsk plates: Journal of Geodynamics, v. 6., p. 33-51.
- Crumley, S. G., and Parfenov, L. M., 1994, Preliminary Gravity Models Around the Kolyma Structural Loop, Sakha Republic, Russia: Eos (Transactions, AGU), v. 75(44) supplement, p. 631.

- Davydova, N. I., Shvarts, Ya. B., and Yaroshevskaya, G. A., 1968, Wave patterns in deep seismic sounding along Magadan-Kolyma profile, in Deep Seismic Sounding of the Earth's Crust in the USSR: International Geology Review Book Section, v. 10, p. 93-102.
- Drachev, S., 1994, Laptev Sea: The NAD drill sites: The Nansen Icebreaker, v. 6, spring, p. 1,7-11.
- Duchkov, A. D., and Sokolova, L. S., 1985, Temperature of the lithosphere of Siberia according to geothermal data: Soviet Geology and Geophysics, v. 26 (12), p. 53-61.
- Duchkov, A. D., Balobaev, V. T., Lysak, S. V., Sokolova, L. S., Devyatkin, V. N., Volod'ko, B. V., and Levchenko, A. N., 1982, The heat flow of Siberia: Soviet Geology and Geophysics, v. 23 (1), p. 34-41.
- Fujita, K., Cambray, F. W., and Velbel, M. A., 1990a, Tectonics of the Laptev Sea and Moma rift systems, northeastern USSR: Marine Geology, v. 98, p. 95-118.
- Fujita, K., Cook, D. B., Hasegawa, H., Forsyth, D., and Wetmiller, R., 1990b, Seismicity and focal mechanisms of the Arctic region and the North American plate boundary in Asia, in Grantz, A., Johnson, L., and Sweeney, J. F., eds., The Arctic Ocean Region; The Geology of North America: The Geological Society of America, v. L, p. 79-100.
- Fujita, K., and Newberry, J. T., 1983, Accretionary terranes and tectonic evolution of northeast Siberia, in Hashimoto, M., and Uyeda, S., eds., Accretion Tectonics in the Circum-Pacific Regions: Tokyo, TERRAPUB, p. 43-57.
- Grachev, A. F., 1973, Moma continental rift (Northeast USSR): Geofizicheskie Metody Razvedki v Arktike, v. 8, p. 56-75 (in Russian).
- Imaev, V. S., Imaeva, L. P., Koz'min, B. M., and Fujita, K., 1994, Active faults and recent geodynamics of Yakutian seismic belts: Geotectonics, v. 28, p. 146-158.
- Kim, B.I., 1986, Structural continuation of the rift valley of Gakkel ridge on the Laptev shelf, in Egiazarov, B. K., and Kazmin, Y. B., eds., Struktura i Istoriya Razvitiya Severnogo Lodovitogo Okeana Sevmorgeologiya, Leningrad, 1986, p. 133-139 (in Russian).
- Kogan, A. L., 1974, Conducting CMRW-DSS seismic work on oceanic ice in the shelves of the arctic seas (Example of work in the Laptev Sea): Geofizicheskie Metody Razvedki v Arktike, v. 9, p. 33-38 (in Russian).
- Koz'min, B. M., Imaev, V. S., Imaeva, L. P., Kornilova, Z. A., 1994, The present-day boundary between the Eurasian and Chinese plates in southern Yakutia: Eos (Transactions, AGU), v. 75(44) supplement, p. 630.

- Koz'min, B. M., 1984, Seismic belts of Yakutia and the focal mechanisms of their earthquakes: Moskva, Nauka, 125 p. (in Russian).
- Lander, A. V., 1984, Anomalous phenomena in surface waves in northeast Eurasia and their relationships to the Moma rift region: Vichislitel'naya Seismologiya, v. 16, p. 127-155 (in Russian).
- Materialy Po Seismichnosti Sibiri, 1976-1990: Irkutsk, Akademiya Nauk SSSR, Sibirskoe Otdelenie, (monthly; in Russian).
- Melnikov, P. I., Balobaev, V. T., Kutasov, I. M., and Devyatkin, V. N., 1976, Heat flow investigations in permafrost regions, in A. Adam, ed., Geoelectric and Geothermal Studies, KAPG Geophysical Monograph: Budapest, Akademiai Kiado, p. 473-480.
- Mishin, S. V., Mishina, L. V., and More, A. G., 1979, Identification of converted waves on seismograms for estimating the position of the base of the earth's crust, in Shilo, N. A., Izmailov, L. I., Linkova, T. I., and Akhlamova, N. N., eds., Geofizicheskie Issledovaniy Strukturi i Geodinamiki Zemnoi Kori i Verkhnei Mantii Severo-Vostok SSSR: Magadan SVKNII DVNTs AN SSSR, p. 128-137 (in Russian).
- Mishin, S. V., and Dareshkina, N. M., 1966, Isolation of converted waves on records of distant earthquakes: Izvestia, Physics of the Solid Earth, v. 2, p. 598-601.
- Naimark, A. A., 1976, Neotectonics of the Moma region, northeastern USSR: Doklady Academy of Sciences of the USSR, Earth Science Sections, v. 229, p. 39-42.
- Neustroev, A. P., and Parfenov, L. M., 1985, Thickness of the earth's crust in the eastern part of the Siberian platform: Soviet Geology and Geophysics, v. 26 (2), p. 126-129.
- Nokleberg, W. J., Parfenov, L. M., Monger, J. W. H., Baranov, B. V., Byalobzhesky, S. G., Bunbtzen, T. K., Feeney, T. D., Fujita, K., Gordey, S. P., Grantz, A., Khanchuk, A. I., Natal'in, B. A., Natapov, L. M., Norton, I. O., Patton, W. W., Jr., Plafker, G., Scholl, D. W., Sokolov, S. D., Sosunov, G. M., Stone, D. B., Tabor, R. W., Tsukanov, N. V., Vallier, T. L., Wakita, K., 1994, Circum-North Pacific tectonostratigraphic terrane map: U. S. Geological Survey Open-File Report 94-714, 221 p., 5 plates.
- Norton, I., Parfenov, L. M., and Prokop'ev, A. V., 1994, Gravity modeling of crustal scale cross sections across the eastern margin of the North Asian craton, northeast Siberia: 2nd International Conference on Arctic Margins, Magadan, Abstracts and Programme: Magadan, SVKNII DVNTs SO ANR.
- Parfenov, L. M., 1991, Tectonics of the Verkhoyansk-Kolyma Mesozoides in the context of plate tectonics: Tectonophysics, v. 199, p. 319-342.

- Parfenov, L. M., Koz'min, B. M., Grinenko, O. V., Imaev, V. S., and Imaeva, L. P., 1988, Geodynamics of the Chersky seismic belt: Journal of Geodynamics, v. 9, p. 15-37.
- Razinkova, M. I., 1987, Methods of studying the earth's crust and upper mantle, *in* Nersasov, I. L., ed., Glubinnoe stroenie slaboseismichnykh regionov SSSR: Moskva, Nauka, p. 6-7 (in Russian).
- Riegel, S. A., 1994, Seismotectonics of Northeast Russia and the Okhotsk plate: M.S. thesis, Michigan State University, 70 p.
- Riegel, S. A., Fujita, K., Koz'min, B. M., Imaev, V. S., and Cook, D. B., 1993, Extrusion tectonics of the Okhotsk plate, Northeast Asia: Geophysical Research Letters, v. 20, p. 607-610.
- Ruff, L., LaForge, R., Thorson, R., Wagner, T., and Goudaen, F., 1994, Geophysical Investigation of the Western Ohio-Indiana Region, Final Report 1986-1992: Washington, U.S. Nuclear Regulatory Commission, NUREG/CR-3145, v. 10, 73 p.
- Sedov, B. M., 1993, Results of deep seismic sounding based on industrial explosions in the In'yali-Debin synclinorium, in Vaschilov, Y. Y., and Romanovskii, N. P., eds., Struktura i Geokinematika Litosfery Vostoka Rossii: SVKNII, Magadan, p. 67-85 (in Russian).
- Sedov, B. M., and Luchina, A. V., 1988, The seismic wave field from near and distant industrial explosions in permafrost rocks, in Vaschilov, Y. Y., and Lin'kova, Y. I., eds., Obemnye modeli struktury zemno kory i verkhnei mantii: Magadan, SVKNII DVNTs AN SSSR, p. 149-163 (in Russian).
- Seismologicheskii Byulleten', 1981-1993, Akademiya Nauk SSSR: Obninsk, Institut Fizika Zemli, (tri-monthly; in Russian).
- Suvorov, V. D., and Kornilova, Z.A., 1986, Thickness of the earth's crust in the southeastern Verkhoyana-Kolyma fold system (according to near earthquakes): Tikhookeanskaya Geologiya, n. 4, p. 32-36 (in Russian).
- Suvorov, V. D., and Kornilova, Z.A., 1985, Deep structure of the Aldan Shield according to near earthquake data: Geology and Geophysics, v. 26 (2), p. 79-84.
- Vashchilov, Y.Y., 1984, Block layer model of the earth's crust and upper mantle: Moskva, Nauka, 237 p. (in Russian).
- Vashchilov, Y.Y., 1979, Seismicity and questions regarding the deep structure of the northeast USSR, in Shilo, N. A., Izmailov, L. I., Linkova, T. I., Akhlamova, I. I., eds., Geofizicheskie issledovaniy strukturi i geodinamiki zemnoi kori i verkhnei mantii severovostok SSSR: Magadan, SVKNII DVNTs AN SSSR, p. 138-157 (in Russian).

Watson, B. F., and Fujita, K., 1985, Tectonic evolution of Kamchatka and the Sea of Okhotsk and implications for the Pacific basin, in: Howell, D. G., ed., Tectonostratigraphic Terranes of the Circum-Pacific Region: Houston, Circum-Pacific Council for Energy and Mineral Resources, p. 333-348.

MICHIGAN STATE UNIV. LIBRARIES
31293014053262